Government of Western Australia

Department of
Mines and Petroleum

REPORT
139

GEOSEQUESTRATION POTENTIAL OF THE CARBONIFEROUS–PERMIAN GRANT GROUP AND PERMIAN POOLE SANDSTONE, NORTHWEST CANNING BASIN, WESTERN AUSTRALIA

by MC Dentith, L Dent, AD George, L Langhi, G Sanchez, Z Seyedmehdi, J Strand, A Vaslin, and R Zaheer

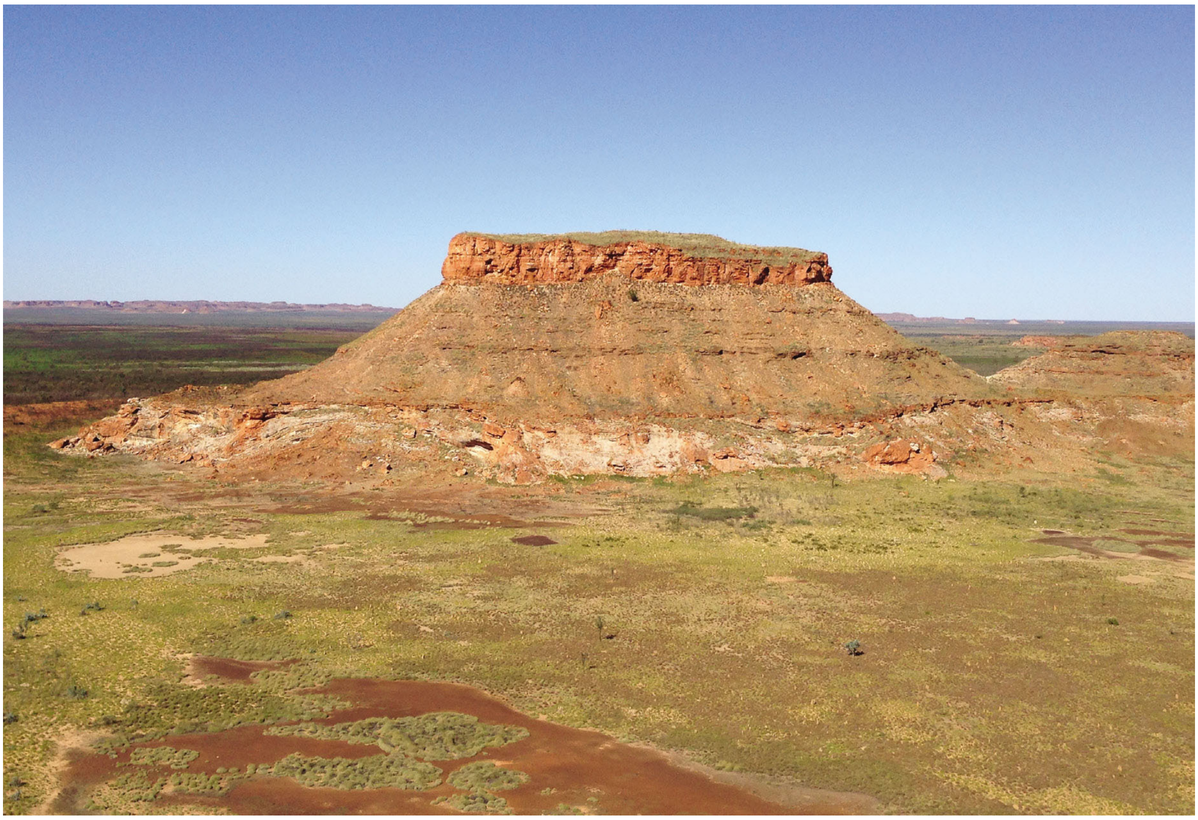

EXPLORATION INCENTIVE SCHEME

The University of Western Australia

CSIRO

Geological Survey of Western Australia

Government of **Western Australia**
Department of **Mines and Petroleum**

REPORT 139

GEOSEQUESTRATION POTENTIAL OF THE CARBONIFEROUS–PERMIAN GRANT GROUP AND PERMIAN POOLE SANDSTONE, NORTHWEST CANNING BASIN, WESTERN AUSTRALIA

by
MC Dentith[1], L Dent[1,2], AD George[1], L Langhi[3], G Sanchez[1], Z Seyedmehdi[1], J Strand[3], A Vaslin[3] and R Zaheer[1]

1 Centre for Energy Geoscience (formerly Centre for Petroleum Geoscience and CO_2 Sequestration), The University of Western Australia, 35 Stirling Highway, Crawley WA 6009

2 Now at the Geological Survey of Western Australia, Department of Mines and Petroleum, 100 Plain Street, East Perth WA 6004

3 CSIRO Energy, Technology Park, 26 Dick Perry Avenue, Kensington WA 6151

Perth 2015

Geological Survey of Western Australia

REFERENCE
The recommended reference for this publication is:
Dentith, MC, Dent, L, George, AD, Langhi, L, Sanchez, G, Seyedmehdi, Z, Strand, J, Vaslin, A and Zaheer, R 2014, Geosequestration potential of the Carboniferous–Permian Grant Group and Permian Poole Sandstone, northwest Canning Basin, Western Australia: Geological Survey of Western Australia, Report 139, 101p.

National Library of Australia Cataloguing-in-Publication entry:

Creator:	Dentith, Mike, author.
Title:	Geosequestration potential of the Carboniferous–Permian Grant Group and Permian Poole Sandstone, northwest Canning Basin, Western Australia / M C Dentith, L, Dent, AD George, L Langhi, G Sanchez, Z Seyedmehdi, J Strand, A Vaslin and R Zaheer.
ISBN:	9781741685794 (ebook)
Subjects:	Geology, Stratigraphic. Carbon sequestration–Western Australia–Canning Basin. Geology–Western Australia–Canning Basin. Canning Basin (W.A.)
Other Authors/Contributors:	Dent, L., author. George, A. D., author. Langhi, L., author. Sanchez G., author. Seyedmehdi, Z., author. Strand, J., author. Vaslin, A., author. Zaheer, R., author. Geological Survey of Western Australia, issuing body.
Series:	Report (Geological Survey of Western Australia) ; 139.
Dewey Decimal Classification:	551.70099411

ISSN 1834–2280

Grid references in this publication refer to the Geocentric Datum of Australia 1994 (GDA94). Locations mentioned in the text are referenced using Map Grid Australia (MGA) coordinates, Zone 51. All locations are quoted to at least the nearest 100 m.

Copy editor: B Striewski
Cartographer: AK Symonds
Desktop publisher: RL Hitchings
Printed by Images on Paper, Perth, Western Australia

Published 2015 by Geological Survey of Western Australia
This Report is published in digital format (PDF) and is available online at <www.dmp.wa.gov.au/GSWApublications>.

Further details of geological publications and maps produced by the Geological Survey of Western Australia are available from:
Information Centre | Department of Mines and Petroleum | 100 Plain Street | EAST PERTH | WESTERN AUSTRALIA 6004
Telephone: +61 8 9222 3459 Facsimile: +61 8 9222 3444 **www.dmp.wa.gov.au/GSWApublications**

Cover photograph: Permian Poole Sandstone unconformably overlies Grant Group sandstone at Mount Hutton (Fitzroy Trough, northern Canning Basin). The unconformity lies at the top of the sandstone package at the base of the hill.

Contents

Appendices

Figures

Tables

Geosequestration potential of the Carboniferous–Permian Grant Group and Permian Poole Sandstone, northwest Canning Basin, Western Australia

by

M C Dentith[1], L Dent[1,2], A D George[1], L Langhi[3], G Sanchez[1], Z Seyedmehdi[1], J Strand[3], A Vaslin[3], and R Zaheer[1]

Abstract

This Report presents the results of an assessment, based on non-proprietary reports and data, of the suitability of the northwestern part of the onshore Canning Basin for the sequestration of by-product CO_2. The study area is within 200 km of James Price Point (JPP).

The Canning Basin, located in the northern Western Australia, has a sedimentary fill that ranges in age from Ordovician to Cretaceous and is up to 17 km thick. Of particular interest in this study is the Carboniferous–Permian stratigraphic interval that contains the Grant Group and Poole Sandstone, potential reservoirs for geosequestration of CO_2, and the likely overlying regional sealing horizon, the Noonkanbah Formation.

Three areas (identified as options A, B, and C) appear to have potential for geosequestration based on available data. Option A is 120 km SE from JPP within the Jurgurra Terrace. Prospective CO_2 storage capacity is estimated to be between 162 and 649 Mt. Option B lies approximately 80 km east of JPP within the Fitzroy Trough. Prospective CO_2 storage capacity is estimated to be between 96 and 383 Mt. Option C is 105 km northeast of JPP within the Fitzroy Trough, close to the Pender Terrace. Prospective CO_2 storage capacity is estimated to be between 71 and 283 Mt. All the traps comprise large fault blocks and as such are critically dependent on the sealing capacity of their bounding faults. In these areas seismic lines are several kilometres apart, and many smaller faults are probably unrecognized. It is likely that individual fault blocks are much smaller due to as yet undetected faults. Also, poor well control means reservoir properties have to be extrapolated over very great distances. Thus, the estimates of potential CO_2 storage are highly speculative.

Fault seal analysis, relying on distant wells, suggests that sealing faults are present in the three proposed geosequestration areas. However, the wells available do not necessarily allow definitive representation of the entire Pennsylvanian–Permian succession as drilling has been restricted to the crests of the anticlines where erosion has removed much of the section. None of the wells intersect the whole succession.

Although data are sparse there is evidence that the faults in the study area are at risk of becoming active, either as a result of natural seismicity or due to changes in the subsurface pressure conditions because of the injection of CO_2.

Detailed sedimentological studies of the Grant Group and Poole Sandstone have been completed. The Grant Group is dominated by thick sandy fluvial facies which have retained good to very good porosity and permeability during burial. A thick intra-Grant Group seal is best developed in the Fitzroy Trough. Fluvial and shallow marine facies of the Poole Sandstone are dominantly heterolithic in the study area. Cored intervals are sparse but suggest that coarse-grained sandy facies are restricted and that overall reservoir quality is likely to be low. The thickness and type of facies of the overlying Noonkanbah Formation suggest a good-quality seal.

There is a significant risk of resource conflict at the proposed sequestration sites and across the whole study area. Hydrocarbon accumulations are possible in the Grant Group and geosequestration would effectively sterilize resources in units at greater depths. The investigated units also constitute important aquifers.

KEYWORDS: Carboniferous, Permian

1 Centre for Energy Geoscience (formerly Centre for Petroleum Geoscience and CO_2 Sequestration), The University of Western Australia, 35 Stirling Highway, Crawley WA 6009

2 Now at the Geological Survey of Western Australia, Department of Mines and Petroleum, 100 Plain Street, East Perth WA 6004

3 CSIRO Energy, Technology Park, 26 Dick Perry Avenue, Kensington WA 6151

Introduction

Gas and condensate fields (Brecknock, Calliance and Torosa) in the offshore Browse Basin (Fig.1) contain a combined contingent volume of 0.42 trillion m^3 (14.9 trillion cubic feet) of dry gas and 69 million m^3 (435.8 million barrels) of condensate (Woodside Energy, 2013). Carbon dioxide (CO_2) content in these fields ranges from 4 to 12%. At the time of writing, possibilities for development of these fields include floating technologies, a pipeline to existing liquefied natural gas (LNG) facilities in the Pilbara and onshore processing at the proposed Browse LNG precinct at JPP, about 50 km north of Broome (Fig.1). This Report describes the results of an assessment, based on non-proprietary reports and data, of the suitability of the northwestern part of the onshore Canning Basin for the sequestration of byproduct CO_2 from these fields. The study area, defined by the Geological Survey of Western Australia (GSWA), is within 200 km of JPP, a distance considered the maximum that liquid CO_2 can be transported economically. Two possible reservoirs were considered: the Poole Sandstone and the Grant Group.

This Report consists of eight sections. Basic aspects of CO_2 geosequestration and the geology of the study area are described first. Next, an integrated structural and stratigraphic interpretation of the study area is presented based on seismic, well, gravity and magnetic data. Three possible geosequestration sites are identified. The next section describes a sedimentological study of the Poole Sandstone and Grant Group to assess reservoir quality. A study of fault seal characteristics and study area seismicity and in situ stress has also been completed.

The limited data available place the emphasis of this study on identification of sites where acquisition of additional data is considered most likely to lead to an improved understanding of the geosequestration potential of study area. Recommendations for further work are described in the final section of the report.

This study was funded by the Western Australian Government's Exploration Incentive Scheme (EIS) and carried out by personnel from the Centre for Petroleum Geoscience and CO_2 Sequestration at The University of Western Australia and CSIRO Energy.

Geosequestration of CO_2

(Raheela Zaheer and Mike Dentith)

Sequestration is the long term of isolation of CO_2 from the atmosphere through physical, chemical, biological, or engineered processes (Friedmann, 2007). Geological storage of CO_2, geosequestration, is an attractive option because the required technologies have already been developed, the potential storage capacity of geological reservoirs is extremely large, and apparently suitable

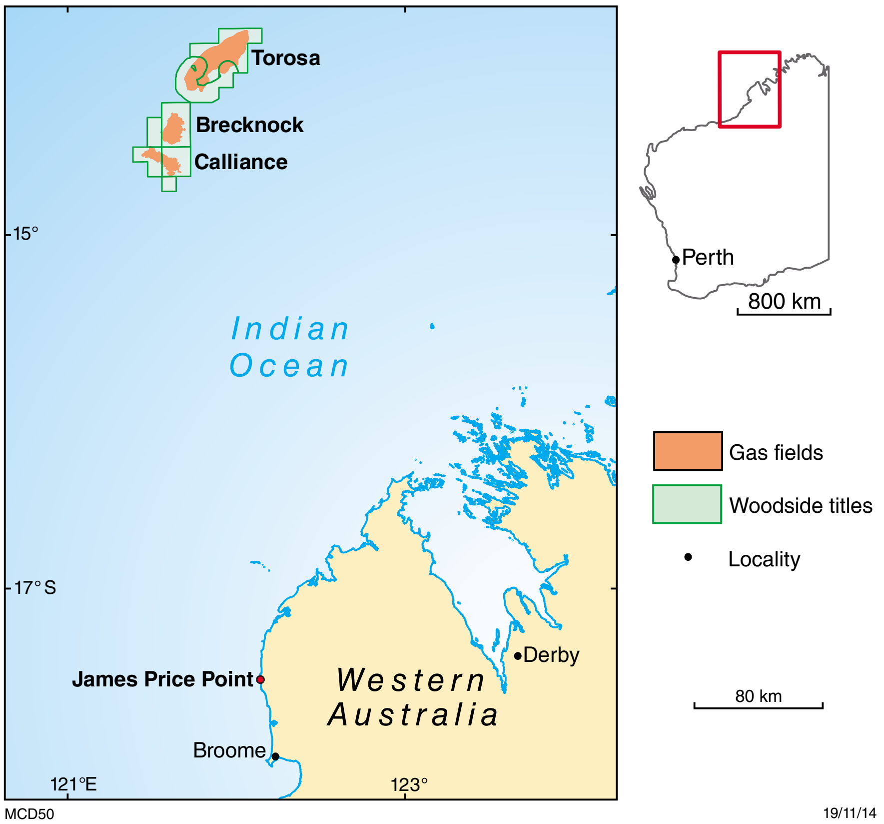

Figure 1. Regional map showing the location of offshore gas fields on the North West Shelf (Browse Basin), James Price Point north of Broome, and the study area

formations are commonly close to the sources of CO_2. Also, the environmental and land use conflict consequences are minimal (Bachu, 2000). Potential reservoirs are porous (storage space) and permeable (CO_2 injectable) formations at sufficient depths such that the CO_2 can be injected as a supercritical phase (see below). Three classes of reservoir are generally recognized: aquifers containing saline water, depleted hydrocarbon fields, and deep coal seams. Saline aquifers are loosely defined as those containing water unsuitable for human consumption or industrial or agricultural use. These represent the only option in the northwest Canning Basin.

There are various semiformal schemes for selecting basins and sites for geosequestration and proposed definitions and terminology used when estimating storage capacity (CSLF, 2007; DOE, 2006; CO2CRC, 2008). None of these schemes is completely appropriate for the northwest Canning Basin study. This is because all of them assume the availability of a considerably greater quantity of relevant data than is the case, in particular the kind needed to calculate the amount of CO_2 that might be stored. Of the schemes, that of CO2CRC (2008) can be adapted for the Canning Basin. There are seven stages in CO2CRC's (2008) site characterization workflow, of which three are based primarily on geoscientific criteria: basin suitability, identification of prospective sites, and detailed site characterization (of preferred sites). In its originally defined form, this work flow is not appropriate for our study, primarily because the study area, the reservoirs and the distance from CO_2 source are preselected. In our study, key variables from CO2CRC's (2008) three geoscientific criteria have been considered. These have been selected primarily because they are perceived to be most significant and because they are assessable with the available data within the project time scale.

Physical trap definition: identification and characterization of subsurface structural and stratigraphic settings that could represent physical trapping sites, and where the reservoirs are expected to be under appropriate temperature (T) and pressure (P) conditions.

Reservoir studies: understanding of geological controls on porosity and permeability based on sedimentology, facies analysis, and stacking patterns of cored intervals and downhole logs.

Temperature–pressure of reservoirs: the T–P conditions in the subsurface determine whether CO_2 can be injected and stored in a supercritical state, which is by far the most efficient state in which to store it.

Trap integrity: faults may represent an escape path and/or may compartmentalize the reservoir, hence their presence is a key variable. Fault seal characteristics can be estimated based on the amount of 'shale' in the succession. Seismicity and the local stress regime is also important because of the risk of catastrophic escape from the reservoir (the study area is in an area of current earthquake activity), and also because it indicates the likelihood of seismicity induced by changes in the subsurface pressure regime due to CO_2 injection and of associated leakage along faults.

A number of key variables could not be assessed because of a lack of suitable data. These include hydrological regime, seal capacity, CO_2-rock–water interactions, and fluid flow simulations.

Physical properties of CO_2

Under normal atmospheric conditions CO_2 is a gas which is denser than air. For ease of transport and greater storage capacity, CO_2 should be injected as a supercritical fluid. The critical point where CO_2 enters the supercritical phase is 31.1°C and 7.38 MPa. In a supercritical state CO_2 behaves like gas, filling all available volume but maintains a 'liquid' density, allowing a greater mass of CO_2 to be stored in a given volume (Fig. 2). It is possible to store CO_2 as a liquid or gas but it is far less efficient to do so. Depending on temperature and pressure, the density of CO_2 varies from 200 to 900 kg/m^3 (Bachu, 2000). Thus, at higher temperature and pressure it has a density approaching, but not exceeding, that of water. Increased density equates with greater storage efficiency.

Based on worldwide average geothermal and hydrostatic pressure conditions (hydrostatic pressure gradient: 1 MPa/100 m; geothermal gradient: 25°C/km), the CO_2 critical point equates to an approximate minimum subsurface depth of 800 m. Below this depth (under normal sedimentary basin conditions), supercritical CO_2 is 30–40% less dense than saline formation water (Ennis-King and Paterson, 2002).

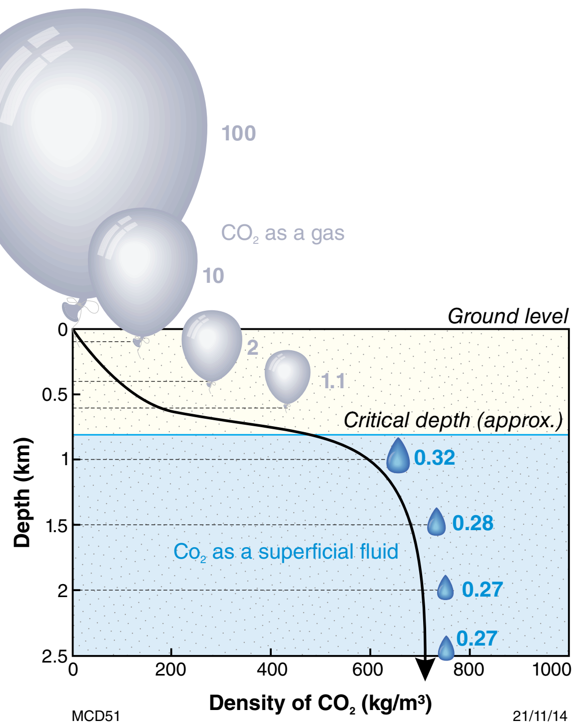

Figure 2. Schematic illustration of increased storage efficiency due to volume change of CO_2 from gaseous to supercritical liquid phase. Volumetric relationship shown in blue numbers (e.g. 100 m^3 of CO_2 at surface would occupy 0.32 m^3 at a depth of 1 km (Kaldi and Gibson-Poole, 2008). Critical depth assumes 'average' temperature–pressure conditions (see text).

Due to its buoyancy it will therefore tend to move upwards until being captured by one of several possible chemical or physical tapping mechanisms. Injection of CO_2 at conditions close to its critical point will induce changes to the gaseous phase if CO_2 reaches shallower depths. The buoyancy and mobility of the gas increase its chance to escape to the atmosphere. Supercritical CO_2 in typical injection conditions is immiscible with water. It is less viscous than water, leading to only parts of the formation water being displaced during injection. A typical CO_2 saturation is within the range of 30–60% (Benson and Cole, 2008).

CO2CRC (2008) considered the maximum practical CO_2 injection depth to be approximately 3500 m. At greater depths the cost of drilling is too high and burial depth-related reduction in reservoir porosity and permeability is too great.

Trapping mechanisms in saline aquifers

Figure 3 summarizes the main CO_2 trapping mechanisms in saline aquifers and the time scales on which they operate. Typically trapping involves a combination of the following mechanisms.

Structural and stratigraphic (physical) trapping of CO_2 in a porous and permeable reservoir unit below a low permeability seal unit is analogous to a hydrocarbon field. Sedimentary basins have two basic types of traps: structural and stratigraphic traps. Structural traps are formed by folding and faulting of the basin fill. Stratigraphic traps, on the other hand, are formed by lateral facies changes such as pinch-outs, reefs, and channel fills where porous and permeable units are juxtaposed against relatively impermeable units. Unconformities where impermeable facies overlie porous and permeable facies are also important stratigraphic traps. Both trap types are suitable for CO_2 storage. Structural and stratigraphic trapping is the most significant trapping mechanism for immiscible CO_2 within a reservoir as CO_2, being more buoyant than other liquids present in pore spaces, will move upwards until trapped by a sealing formation.

Hydrodynamic trapping of CO_2 has two components. On injection up to ~30% of the CO_2 will dissolve in the formation water; this is known as solubility trapping. The solubility of CO_2 decreases with increasing formation water salinity and temperature, but increases with increasing pressure. Aided by convective mixing, total dissolution of injected CO_2 into the formation waters is predicted to take place over hundreds to thousands of years (Ennis-King and Paterson, 2002). CO_2 in solution is no longer buoyant, thus reducing the leakage risk. Both the dissolved and immiscible CO_2 is affected by the flow of the formation waters. In many deep aquifers flow rates are extremely slow, ranging within the order of centimetres per year. Where the reservoir seal extends over hundreds of kilometres from the deep injection site, the time scale for fluid to reach the surface from the deep basin can be millions of years (Bachu et al., 1994; IPCC, 2005). Importantly, suitable trap sites are not necessarily structural or stratigraphic traps.

Residual trapping defines a geological setting where immiscible CO_2 becomes trapped in the pore spaces by capillary pressure forces (Ennis-King and Paterson, 2001) and over time dissolves in the formation water.

Mineral trapping (storage of CO_2 as solid phase) takes place when reactions between the CO_2 and the minerals within the reservoir lead to precipitation of stable carbonate minerals. Carbon dioxide dissolved in water forms a weak acid that reacts with silicate/calcium minerals to form bicarbonate ions. Some of these minerals are stable over a geological time scale (Oelkers and Schott, 2005). The time scale for reactions is within the order of tens to thousands of years, but once precipitation has taken place this represents an effectively permanent entrapment of the CO_2. The reactivity of the reservoir rock depends on its composition, nature of the formation waters, temperature and pressure conditions, pore geometry (i.e. surface area available for reactions), and formation fluid flow rates. Reservoirs comprising 'clean' sandstone tend to be least reactive.

Estimating CO_2 storage capacity

There are inherent uncertainties in estimating subsurface storage volumes even when detailed information on subsurface structure and physical properties is available, such as for a producing hydrocarbon field. In this study relevant data are not available. It precludes detailed calculation of storage estimates and hence only broad estimates can be presented.

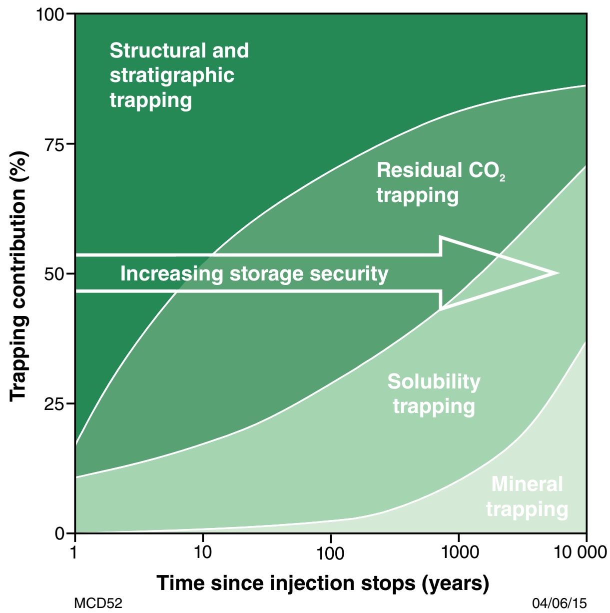

Figure 3. Physical and chemical trapping mechanisms controlling CO_2 storage in saline aquifers (IPCC, 2005)

Key variables are the density of the CO_2 under expected reservoir conditions, the amount of interconnected pore space, and the nature of formation fluids. Even if a pore volume can be calculated, only a fraction of it will be available for CO_2 storage. Also, calculations should ideally account for residual, dissolution, and mineral trapping, which take much longer than the injection and displacement of pore fluids.

Here we restrict our estimates of potential CO_2 storage mass to approximate calculations based on its expected density under reservoir conditions and estimated average porosity and reservoir thickness over the geographic area of the sequestration zone (see section on *Potential sites for geosequestration of* CO_2).

Canning Basin

(Mike Dentith and Annette George)

The Canning Basin is located in northern Western Australia (Figs 4 and 5). The basin covers approximately 640 000 km^2 of which about 530 000 km^2 are onshore. The sedimentary fill ranges in age from Ordovician to Cretaceous and is up to 17 km thick (Forman and Wales, 1981; Towner and Gibson, 1983; Brown et al., 1984; Yeates et al., 1984; Kennard et al., 1994; Shaw et al., 1994). Several major depositional phases are represented in the basin fill, each recording extensional tectonic phases during basin evolution (Fig. 6). Of particular interest in this study is the Carboniferous–Permian stratigraphic interval that contains the reservoir units (Grant Group and Poole Sandstone) and the likely overlying regional sealing horizon (Noonkanbah Formation). The post-Permian tectonic events that potentially created structural traps and compartmentalizing faults are also significant. The Mesozoic succession and tectonic history are also relevant because locally these rocks unconformably overlie the reservoir units and the tectonic events that affected the potential reservoir and seal units.

The Canning Basin originated as an intracratonic sag in the Early Ordovician and its geological history is long and complex. The basin comprises four main depocentres: the Fitzroy Trough and Gregory Sub-basin to the northeast, and the Willara and Kidson Sub-basins to the southwest (Fig. 4). The major basin bounding structures trend northwest. The Fitzroy Trough and Gregory Sub-basin are estimated to contain up to 17 km of strata. Two platforms, the Broome and Crossland Platforms, separate the major depocentres. Shallow terraces flank the sub-basins. The Fitzroy Trough is flanked by the Lennard Shelf and Pender Terrace to the northeast and the Jurgurra and Mowla Terraces to the southwest. The study area comprises mostly the Fitzroy Trough and its flanking terraces, and the Broome Platform (Fig. 4).

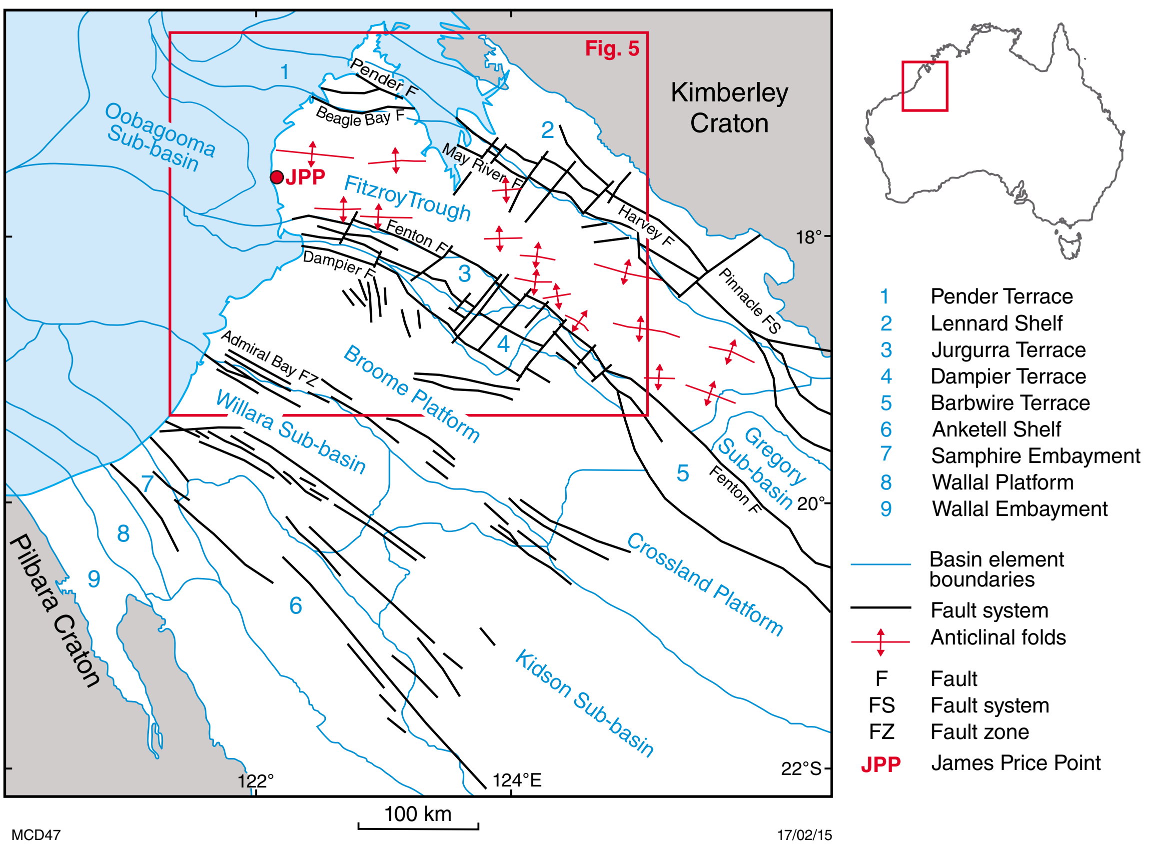

Figure 4. Map of the major structures and regions in the Canning Basin. JPP – James Price Point (Parra-Garcia, 2014)

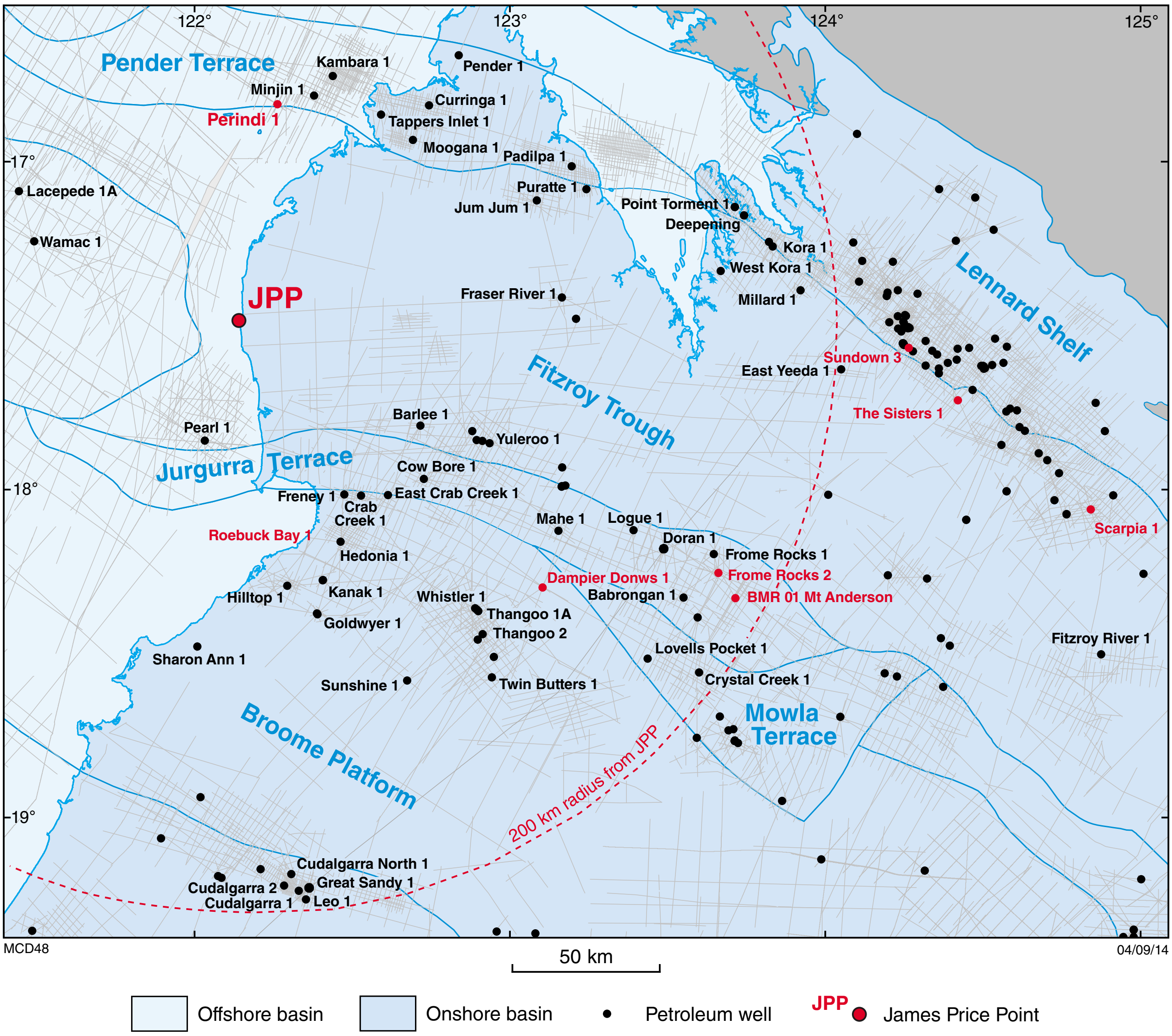

Figure 5. Map of the northwestern Canning Basin, showing the main tectonic elements and the positions of seismic lines and wells used in this study. The red dashed line delineates the radius of the study area, i.e. 200 km from James Price Point (JPP). Wells in red have cores intersecting the Poole Sandstone and/or Noonkanbah Formation and were used for detailed sedimentological examinations via core logging.

Figure 7 shows a regional cross-section across the Fitzroy Trough and part of the Broome Platform. The difference in sedimentary thickness is apparent, as is variation in intensity of deformation. The Broome Platform features broadly subhorizontal, mildly deformed strata. In contrast, within the Fitzroy Trough deformation is much more intense with large-scale folds and numerous faults. Many of these faults display a complex history of reactivation. The prominent unconformity at the base of the Mesozoic succession is also clearly seen where largely undeformed Mesozoic rocks overlie deformed Palaeozoic strata. There is some faulting within the Mesozoic succession but it is a predominantly flat-lying and undeformed part of the basin fill.

The tectonostratigraphic record of the Canning Basin can be divided into four unconformity-bounded megasequences (first-order stratal packages), reflecting the major phases of subsidence and deposition (Kennard et al., 1994; Romine et al., 1994). The megasequences are Ordovician–Silurian, Devonian–Mississippian (Carboniferous), Late Mississippian – Triassic, and Jurassic – Early Cretaceous (Fig. 6). This Report follows the chronostratigraphic nomenclature of Kennard et al. (1994) when referring to depositional ages of stratigraphic units as ‘early’ or ‘late’. Selected surfaces have been mapped on seismic data at a basin-scale in the accompanying Report to this study (Parra-Garcia et al., 2014). Of particular relevance in this context are the surfaces S4 (base Grant Group and Reeves Formation), S5 (base Jurassic), and S6 (base Cretaceous; Fig. 6).

Late Paleozoic deposition was mostly associated with active extension, typically transtensional, and the creation of deep fault-controlled sub-basins on the northern margin of the Canning Basin (Pillara extension, Fig. 6).

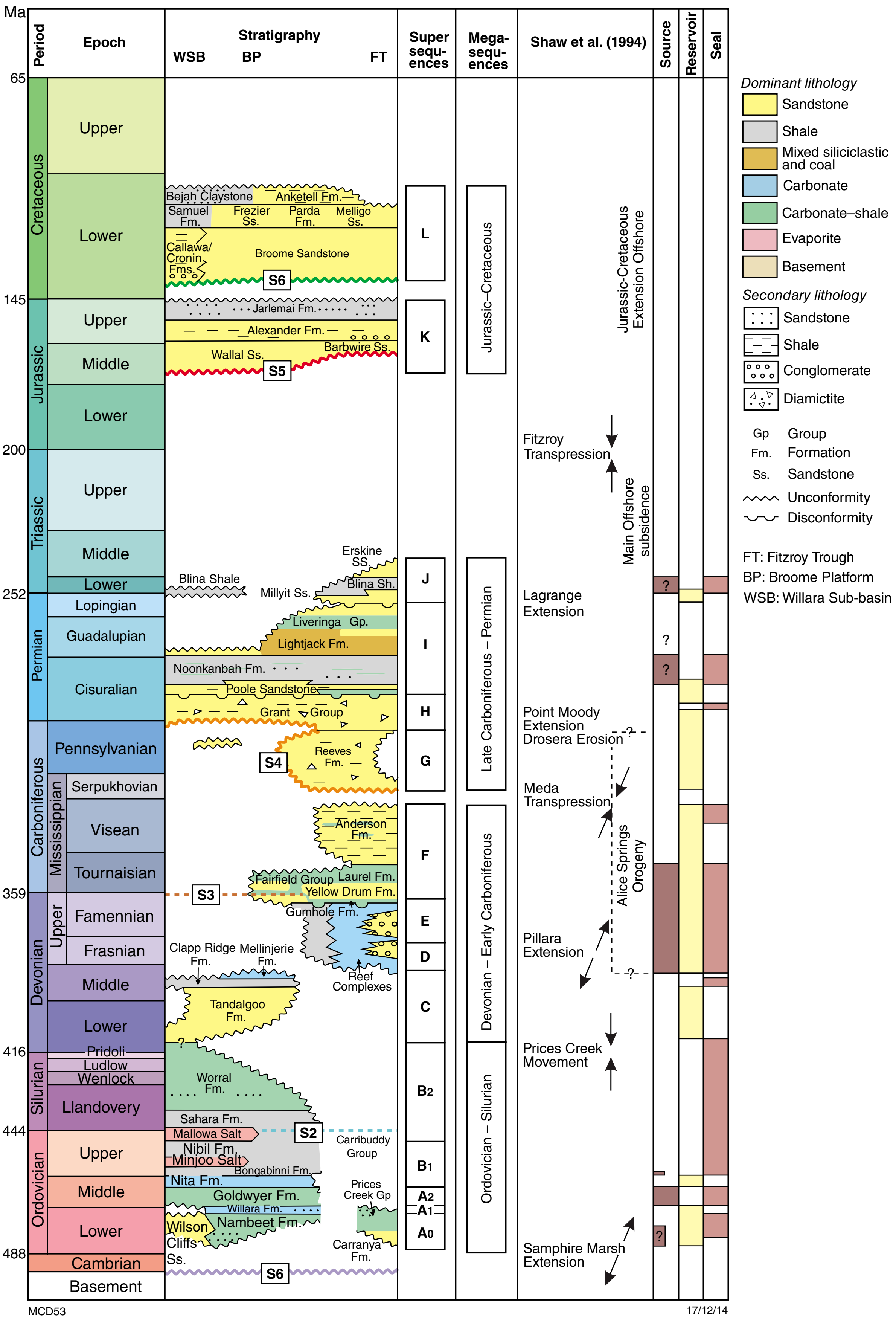

Figure 6. **Stratigraphic column of the Canning Basin, showing main lithostratigraphic units, mega- and supersequences (Kennard et al. 1994; Haines 2009; George et al. 2013), main tectonic events according to Shaw et al. (1994), key stratal surfaces from Parra et al. (2014), and elements of the petroleum system. Modified from Geological Survey of Western Australia (2012).**

Several major compressional events are also recognized and are typically associated with evidence for strike-slip deformation. Of particular importance to this study are the Fitzroy Transpression (Late Triassic; Fig. 6) and the poorly understood Mesozoic tectonic events (within the Canning Basin) associated with the evolution of the passive continental margin to the north and west of the Canning Basin.

Late Mississippian (Carboniferous) – Triassic megasequence

The Late Mississippian to Triassic megasequence in the Canning Basin is up to 4 km thick and is laterally the most extensive megasequence. It is subdivided into four unconformity-bounded supersequences (second-order stratal packages) designated G–J (Kennard et al., 1994). The Reeves Formation, formerly known as the Lower Grant Group and amended by Apak and Backhouse (1998, 1999), comprises supersequence G, the Grant Group includes supersequence H and the Poole Sandstone and Noonkanbah Formation (and overlying Liveringa Group) make up supersequence I. Lower Triassic formations constitute supersequence J. The base and top of this supersequence are seismic surfaces S4 and S5 of Parra-Garcia et al. (2014) (Fig. 6). The lithostratigraphy and biostratigraphy of this megasequence were summarized by Mory (2010). Mory highlights the limited biostratigraphic control and complex facies variations especially between surface exposures and the subsurface well intersections. These issues also create problems for assessing the geosequestration potential of the Grant Group.

Grant Group

Glacigenic sediments were deposited over the entire Canning Basin in the Late Mississippian and Early Permian. They are assigned to the Reeves Formation and Grant Group in the northern and central Canning Basin, and to the Paterson Formation on southern marginal shelves (Forman and Wales, 1981). Mory's (2010) isopach map shows that in the sub-basins the Grant Group is typically 400–800 m thick and thins to 300–400 m on the Broome Platform. Its maximum thickness in the Fitzroy Trough is 1100 m. In the Fitzroy Trough and Lennard Shelf, the Grant Group comprises three formations predominantly made up of likely fluvio-deltaic cross-bedded sandstone with glacially deposited marine and non-marine facies overlying striated bedding surfaces (O'Brien and Christie-Blick, 1992; Mory, 2010). On the Barbwire Terrace (southern side of the Gregory Sub-basin) the Grant Group is also subdivided into three differently named formations, comprising diamictites, turbidites and mudstone — interpreted to have been deposited in deeper marine conditions — shallowing up to fluvial–shallow marine sandstone (Redfern and Millward, 1994). In this area, the extent of glacial influence during deposition of the lower units has been debated (Eyles and Eyles, 2000; Redfern and Williams, 2002) and reconciliation of the different lithostratigraphic schemes for the Grant Group remains problematic (Mory, 2010). From a geosequestration perspective the Grant Group is important because it is dominated by coarse siliciclastic facies, typically with high porosity and permeability, and intercalated muddy facies. This offers the possibility of CO_2 storage and entrapment within sandstone-dominated sections of the Grant Group sealed by intraformational mudstone.

The sedimentology of the Grant Group is described in the section on *Reservoir sedimentology* and regional-scale structure and thickness variations in the section on *Potential sites for geosequestration of* CO_2.

Poole Sandstone – Noonkanbah Formation

The Poole Sandstone and Noonkanbah Formation represent a potential reservoir–seal pair for geosequestration. The Poole Sandstone extends across much of the Canning Basin and is exposed in the southeastern Fitzroy Trough and Lennard Shelf (Playford and Hocking, 1999). It is up to 160 m thick (Mory, 2010) and interpreted by Kennard et al. (1994) to have been deposited following flooding of a low relief erosion surface. It is potentially absent over the Broome Platform although this is a tentative assessment (Mory, 2010). The Poole Sandstone comprises fluvio-deltaic siliciclastic facies intercalated with a local basal carbonate unit known as the Nura Nura Member.

The Noonkanbah Formation has a distribution similar to the Poole Sandstone (Mory, 2010). In the Fitzroy Trough the formation is up to 540 m thick and thins onto the flanking terraces (Mory, 2010). Lithologically the formation is dominated by siltstone with minor sandstone/heterolithic intervals (Forman and Wales, 1981) and is therefore identified as a potential seal.

The sedimentology of the Poole Sandstone and Noonkanbah Formation is described in detail in in the section on *Reservoir sedimentology* and regional-scale structure and thickness variations are reported in the section on *Potential sites for geosequestration of* CO_2.

Fitzroy Transpression

A prominent regional unconformity underlies the Mesozoic succession in the Canning Basin (Fig. 7). Estimates of erosion associated with formation of this unconformity are up to several kilometres in the centre of the Fitzroy Trough (Horstman, 1984). In a north–south compressional stress regime, the northwest-trending extensional faults that define the Fitzroy Trough and flanking shelves were reactivated resulting in a dextral transpressive deformational event in the Canning Basin (Shaw et al., 1994; Parra-Garcia et al., 2014). Of these, the north-trending normal faults and regional-scale en echelon, NW- to WNW-trending antiformal structures form the largest tectonic structures in the study area. The Fenton Fault, on the southwest margin of the Fitzroy Trough, was the locus for structural inversion and

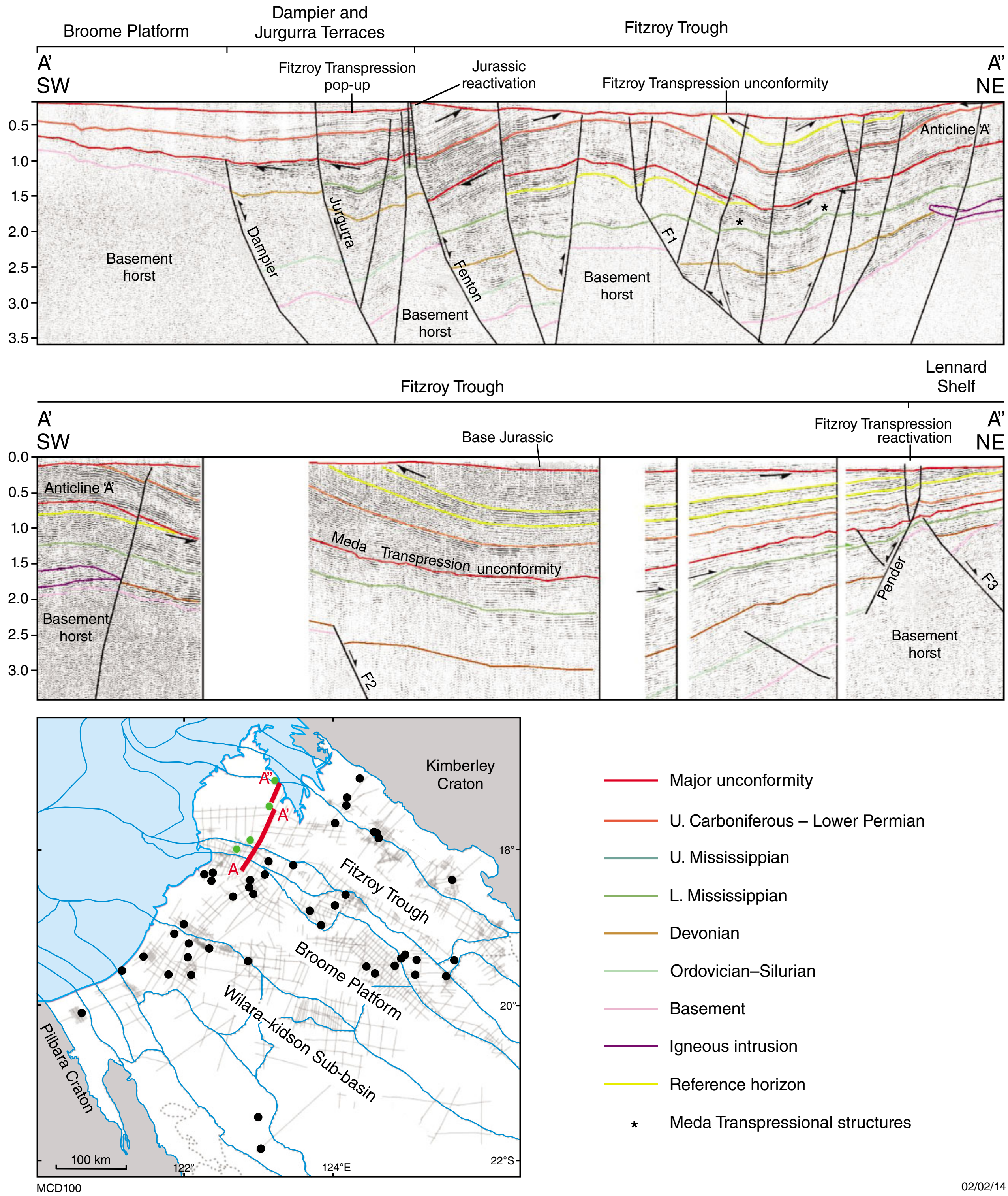

Figure 7. **Regional-scale seismic interpretation across the study area, showing the broad structure, including the relatively undeformed Broome Platform to the southwest and large-scale folding and faulting in the Fitzroy Trough (Parra-Garcia, 2014).**

formation of flower structures. In contrast, the Broome Platform succession shows considerably less deformation. Timing relationships are best seen in offshore seismic data where more complete Triassic successions are present, and from which Smith et al. (1999) identified an early phase of deformation (Middle Triassic) that resulted in flower structures and a subsequent Late Triassic phase that formed the large folds.

Jurassic–Cretaceous megasequence

Jurassic and Cretaceous strata of the onshore Canning Basin represent the feather edge of the North West Shelf passive margin, where the succession is as much as 2500 m thick (Forman and Wales, 1981). The Jurassic section is composed of the Wallal Sandstone and the Alexander, Jarlemai and Jowlaenga Formations, and their correlatives (Forman and Wales, 1981). They correspond to Kennard et al.'s (1994) supersequence K and are bounded by the seismic surfaces S5 and S6 of Parra-Garcia et al. (2014) (Fig. 6). The lower surface, S5, is particularly prominent as a marked angular unconformity on seismic data (Forman and Wales, 1981). The Wallal and Alexander Formations are composed predominantly of sandstone deposited in fluvio-deltaic settings. The siltstone-dominated Jarlemai Formation records widespread marine flooding in the Late Jurassic, with subsequent regression and marine deposition of sandstone of the Jowlaenga Formation. Lower Cretaceous rocks overlying surface S6 (Fig. 6) are dominantly sandstone (Broome Sandstone and correlatives) of shallow marine to fluvio-deltaic affinity (Forman and Wales, 1981) and belong to Kennard et al.'s (1994) supersequence L. Both, the Wallal and Broome Sandstones are important shallow groundwater aquifers in the western Canning Basin.

Mesozoic tectonic events

The Mesozoic tectonic history of the onshore Canning Basin remains poorly understood. There is evidence for broad, open east-trending folds and northwest- and northeast-trending lineaments are apparent on remotely sensed data (SRK Consulting, 1998). Seismic data show some faults displacing Upper Paleozoic strata and terminating at the base-Mesozoic unconformity, whereas other similar structures displace these, and overlying strata, suggesting reactivation of pre-Mesozoic structures. Parra-Garcia et al. (2014) propose that this is a result of deformation concentrated along major faults with reactivation of minor faults in the hanging walls.

Implications for geosequestration

A review of the literature shows that although the large-scale tectonic and stratigraphic history of the Canning Basin is well established, smaller (temporal and spatial) scale aspects remain poorly understood. The following observations are considered important with respect to the geosequestration potential of the study area.

- The study area has experienced significant tectonism during the Fitzroy Transpression but there is limited detailed structural analysis of this event. The creation of large-scale folds and flower structures around major faults suggests potential for structural traps, but deep erosion prior to Mesozoic deposition may indicate that traps are not sealed due to the removal of sealing units (Fig. 8). Also, numerous faults may compartmentalize the reservoir and/or act as leakage paths for CO_2.
- Less deformation on the Broome Platform (and the central part of the Fitzroy Trough) suggests that sequestration may be possible through, for example, hydrodynamic trapping in large relatively undeformed fault blocks.
- Reactivation of older structures is widely documented across the Canning Basin and there are numerous faults in the study area. The likelihood of reactivation of faults under a present-day stress regime and the quality of their sealing capacity needs to be assessed. Siliciclastic facies of the generally flat-lying Jurassic–Cretaceous megasequence are unlikely to form an effective trap in case of a CO_2 escape from Carboniferous–Permian reservoirs. Faults are also less likely to be sealing.
- Understanding the complex stratal architecture of the Grant Group remains problematic. This problem is exacerbated by glacial or glacially influenced paleodepositional environments being among the most difficult to identify, and the least well understood as hydrocarbon reservoirs. Hence, there is an apparent demand to understand the controls on the distribution of porous and permeable facies and potential sealing units in the Grant Group.
- The Poole Sandstone and Noonkanbah Formation are not significant petroleum targets. Although they are often penetrated by petroleum wells directed at deeper targets, there has been limited detailed study on these formations. Notably few seal capacity tests have been undertaken on the Noonkanbah Formation. Basic information on porosity and permeability and geological controls on these aspects is required.

Potential sites for geosequestration of CO_2

(Gilberto Sanchez, Raheela Zaheer and Mike Dentith)

There are no known hydrocarbon fields and no significant coal deposits in the study area. Thus, it has been assumed that geosequestration will be in saline aquifers.

Pressure–temperature conditions

There are limited data on pressure and temperature conditions in the subsurface from petroleum wells in the study area.

The geothermal energy potential of the Canning Basin was assessed in 2009 (Driscoll et al., 2009). This study

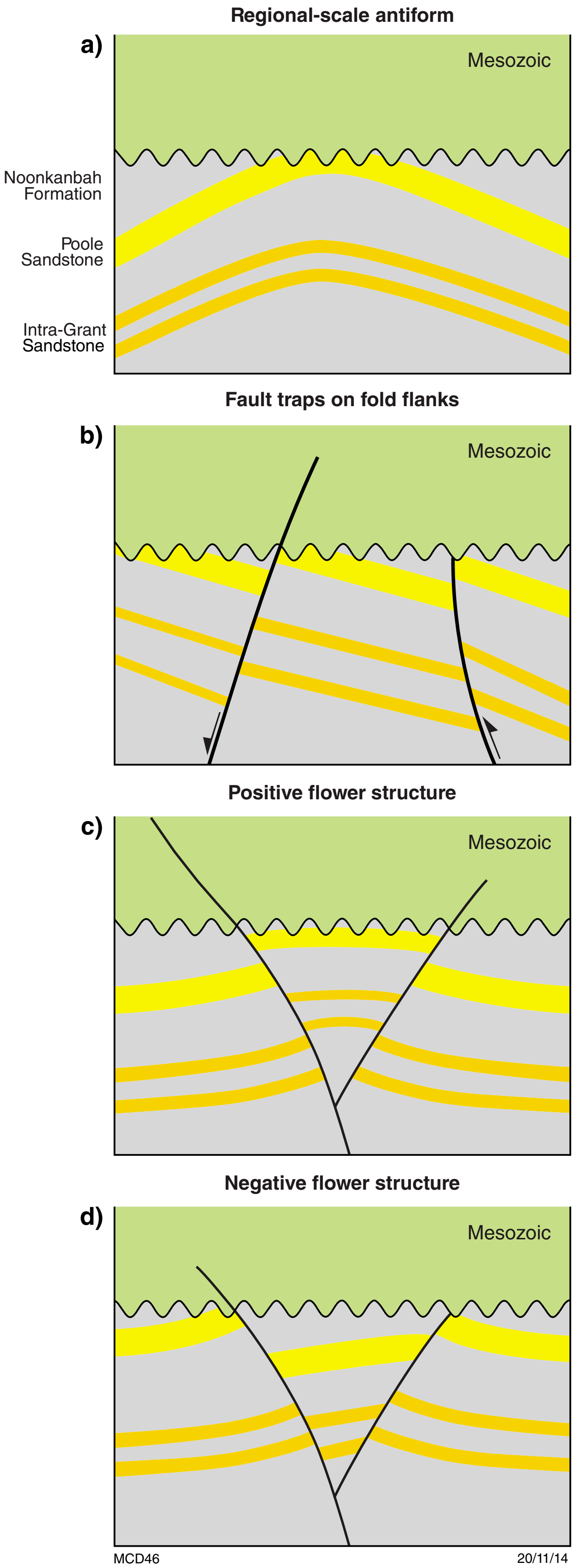

Figure 8. Schematic representation of structural traps relevant to the study area

involved reassessment of public domain downhole temperature data, measurements of thermal conductivity and estimates of geothermal gradients. The study included 28 wells in the area being assessed for geosequestration. Table 1 shows surface temperatures, estimated depth to the 100ºC isotherm, and geothermal gradients. The average surface temperature is 30.3ºC and the average gradient is 31ºC/km. These data show that throughout the study area the required temperature for CO_2 sequestration in a supercritical state will be reached in the top 100 m. This is at a significantly lesser depth than injected CO_2 would be expected to remain trapped in a reservoir.

Pressure information is available from only 11 wells in the study area. Of these data only one measurement is from the Poole Sandstone and six are from the Grant Group/ Reeves Formation. Plotting these data shows a trend that is close to hydrostatic for water with a density of 1080 kg/m^3 (Fig. 9). The three low pressure shallow data points are from Thangoo 2 and appear to be anomalously low.

Geothermal gradients generally vary smoothly across the study area, so the temperatures predicted are probably reliable. This is not necessarily the case with formation pressures, which may be highly variable and discontinuous due to various flow phenomena and permeability barriers. Given the limited available data, the pressure estimates may not be reliable.

The temperature and pressure data have been used to estimate the density of CO_2 as a function of depth in the Canning Basin (Fig. 10). As expected CO_2 will be well within the conditions required for a supercritical state at these depths. The calculated densities have been incorporated in the mass estimates of CO_2 that could potentially be geosequestered at the favoured sites (see section on *Potential geosequestration sites*).

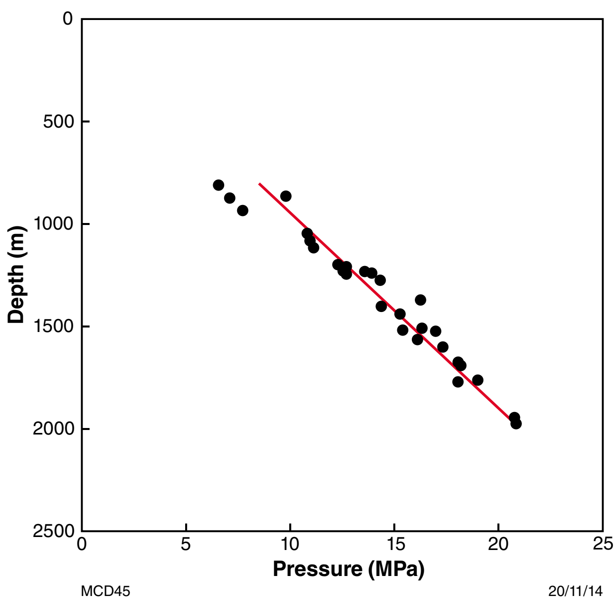

Figure 9. Pressure data from wells in the study area (see also Table 2). Blue symbols denote observed data and the red line shows the increase with depth of the hydrostatic pressure of water with a density of 1080 kg/m^3. The effect of temperature on the calculated hydrostatic data is not taken into account.

Table 1. Temperature data from petroleum wells in the study area. Based on data by Driscoll et al. (2009).

Well	*Distance to JPP (km)*	*Surface temperature (°C)*	*Estimated depth to 100°C isotherm (m)*	*Geothermal gradient (°C/km)*
Crab Creek 1	69	29.7	2656	26.5
Crystal Creek 1	192	31.0	2426	28.4
Cudalgarra 2	189	29.7	1766	39.8
Cudalgarra North 1	185	29.7	1826	38.5
Curringa 1	96	31.2	3304	20.8
Freney 1	66	29.7	2292	30.7
Great Sandy 2	191	29.7	2176	32.3
Hilltop 1	89	29.7	1863	37.7
Jum Jum 1	106	31.2	2573	26.7
Kambara 1	89	30.0	3207	21.8
Kanak 1	100	29.7	1719	40.9
Leo 1	194	29.7	1875	37.5
Lovells Pocket 1	175	31.0	1449	47.6
Mahe 1	125	29.7	1975	35.6
Millard 1	187	31.2	2421	28.4
Minjin 1	81	30.0	2791	25.1
Moogana 1	84	31.2	2822	24.4
Padilpa 1	122	31.2	2150	32.0
Pearl 1	41	30.0	3211	21.8
Pender 1	115	31.2	4592	15.0
Perindi 1	75	30.0	2863	24.4
Point Torment 1 Deepening	171	31.2	1996	34.5
Puratte 1	123	31.2	2383	28.9
Sharon Ann 1	109	29.7	2047	34.3
Sunshine 1	131	29.7	2735	25.7
Tappers Inlet 1	84	31.2		
Twin Buttes 1	139	29.7	1723	40.8
Whistler 1	124	29.7	2222	31.6
	Average	30.3	2410	30.8

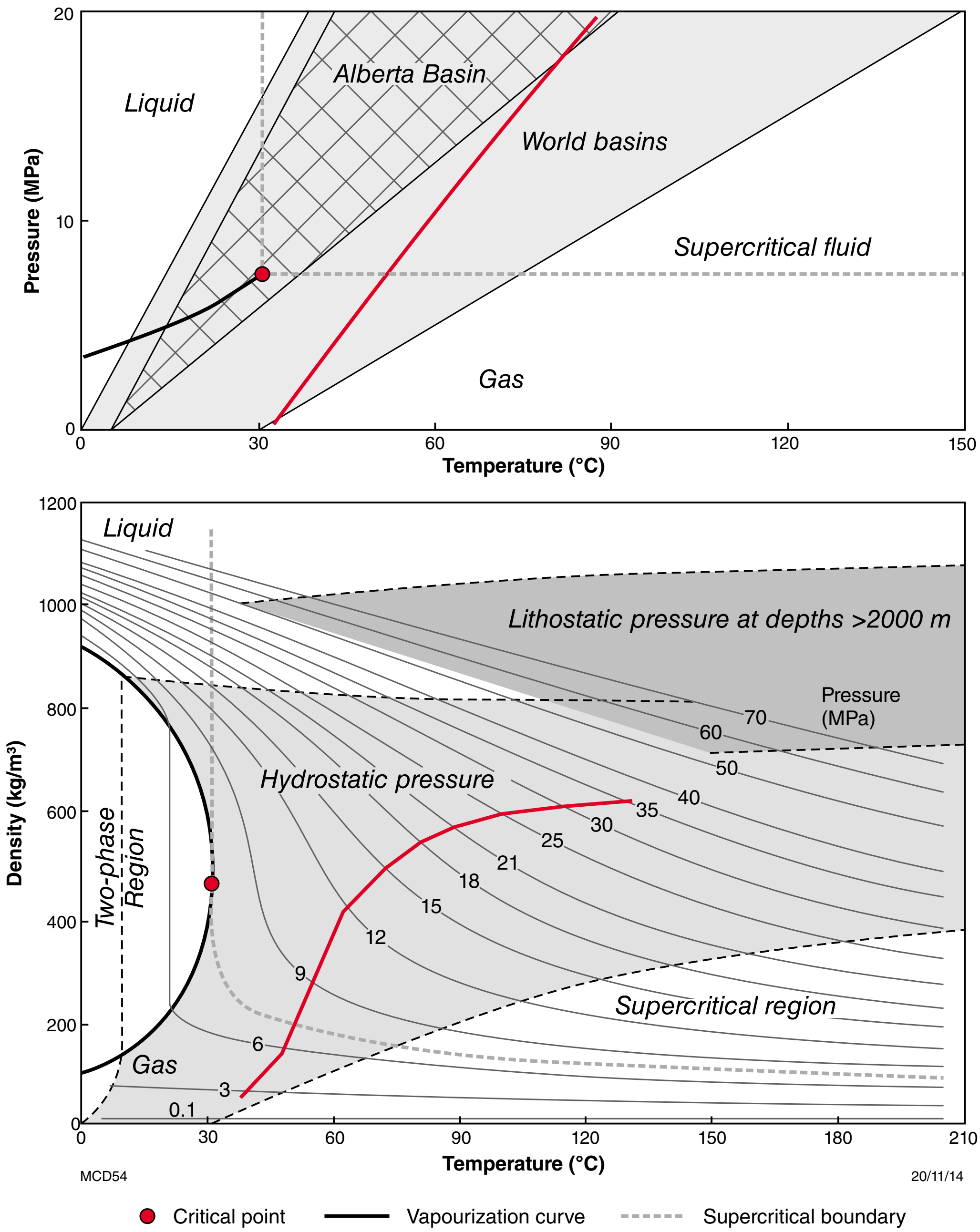

Figure 10. Temperature–pressure conditions (red curves) in the study area plotted relative to the phase behaviour of CO_2 (CO_2 data from Bachu, 2003).

Available data for identifying trap sites

Seismic and well data within 200 km of JPP available for this study are shown in Figure 5. There are 30 seismic surveys with 527 individual 2D lines, ranging in age from 1964 to 1998. There are 40 wells in the study area, however, they are unevenly distributed being mostly at the margins of the Fitzroy Trough. Importantly, an area of ~15 000 km^2 immediately to the east of JPP has no wells and a significant part of this area does not have any seismic data. The available seismic data are of variable quality. Detailed/confident interpretation is not always possible for this reason and unrecognized potential geosequestration sites close to JPP are therefore possible.

Time structure maps have been constructed for the base of the Grant Group (Fig. 11), tops of the Grant Group (Fig. 12), and Poole Sandstone (Fig. 13). A time-interval map of the Noonkanbah Formation (proposed regional seal) was also constructed (Fig. 14). The interpreted base of Grant Group, completed as part of a companion basin-scale study (Parra-Garcia et al., 2014) was also used, although this work is less detailed due to its greater geographical extent. Unfortunately the seismic data are of insufficient quantity and quality to map intra-Grant Group horizons. Together these maps summarize the regional structure and thickness/presence of potential sealing units.

Grant Group

The time structure map of the base of the Grant Group (Fig. 11) confirms the general structural setting shown in Figure 7. Unlike the other mapped horizons, the base of the Grant Group is present across almost the entire study area. Outside the Fitzroy Trough and bounding terraces the base of the group is relatively shallow and relatively undeformed. Within the deformed area, the major WNW–SSE trending structures that define the trough and terraces are clear. These faults are long- lived. They were in existence during the Devonian and may even date from the Precambrian (Parra-Garcia et al., 2014). They have a complex history of reactivation, including the period of the Fitzroy Transpression and are typically associated with rotated fault blocks within flower structures. A second NW-trending fault set is also evident. These faults are mostly within the Fitzroy Trough and were active (and potentially formed) during the Fitzroy Transpression. Most structures mapped in the area are located immediately east of JPP but this may reflect the available seismic data. Even in these areas the faults are poorly defined because seismic data are too widely spaced for confident line-to-line correlations. The interpretation of the area draws heavily on aeromagnetic and gravity data. These data suggest a northwesterly structural trend with some anomalies caused by mafic intrusions along fault planes (see Parra-Garcia et al., 2014).

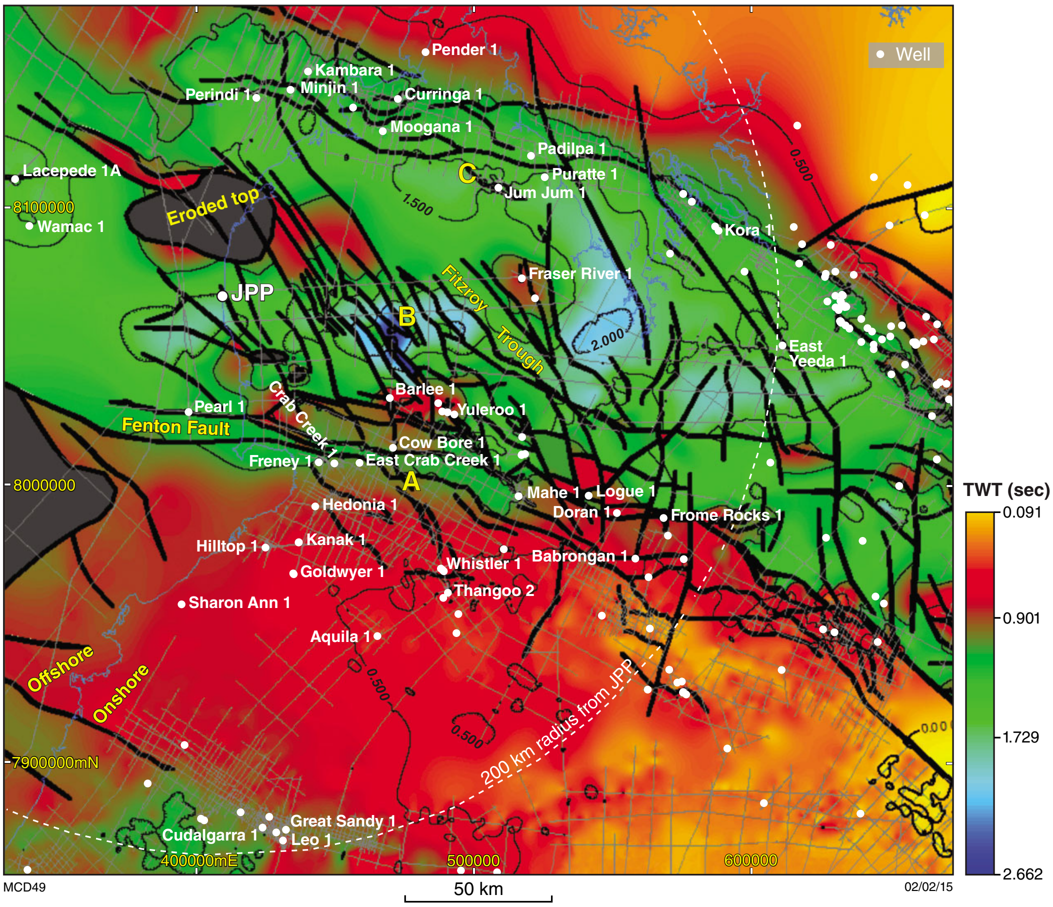

Figure 11. **Time structure map of the base of the Grant Group in the study area. A, B, and C are the three geosequestration options. Faults are shown in black and petroleum wells are represented by white dots.**

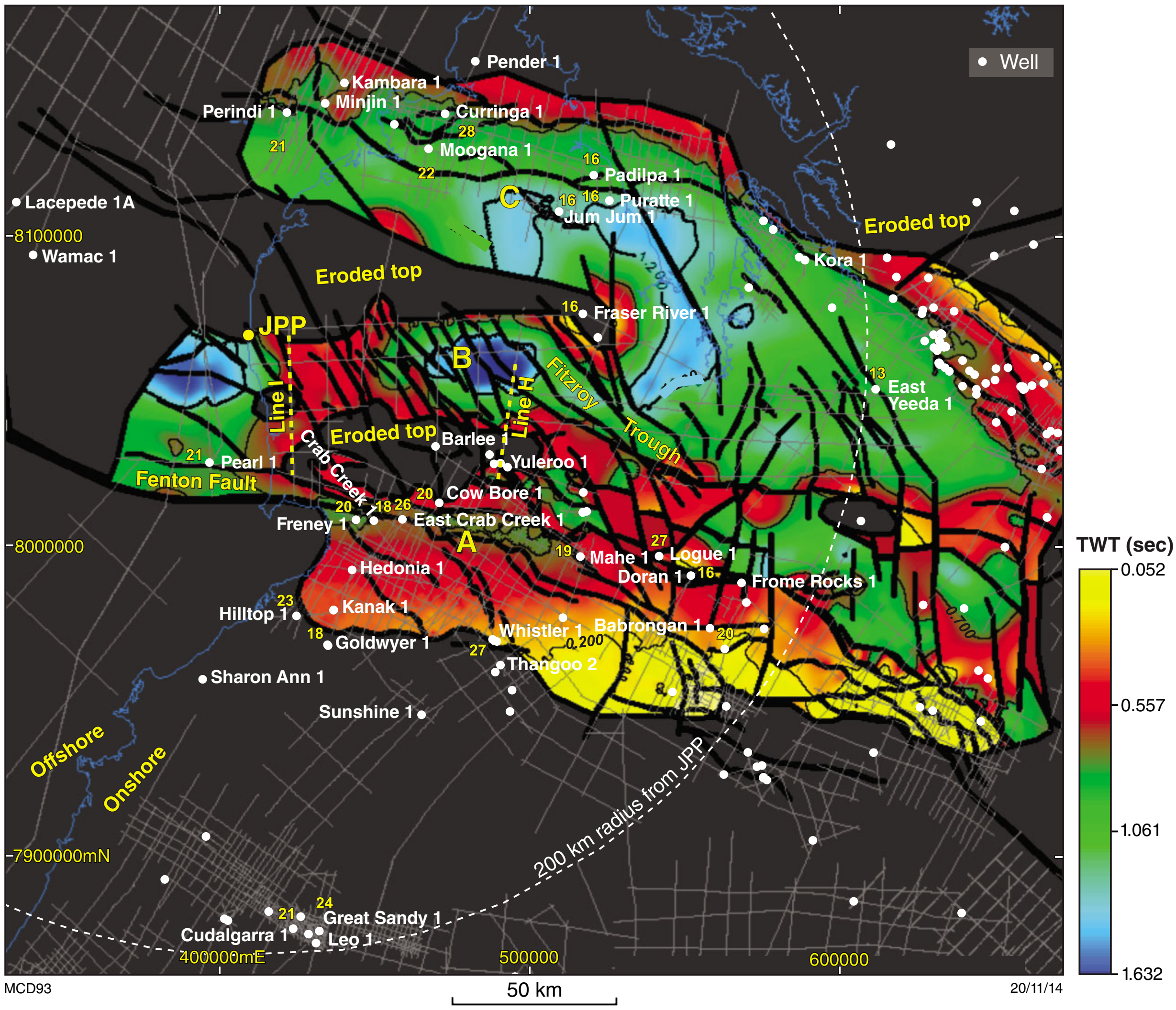

Figure 12. Time structure map of the preserved top of the Grant Group within the study area. A, B, and C are the three geosequestration options. Small yellow numerals denote representative values of porosity from the Grant Group. Faults are shown in black (JPP – James Price Point).

Large-scale folds formed during the Fitzroy Transpression (Fig. 11). A noteworthy feature is a prominent structural high immediately to the east and north of JPP, constituting a potential geosequestration target. However, in appraising these data it is important to consider the shallow depth of the potential reservoirs and the amount of stratigraphic section (including potentially sealing horizons) that has been removed by erosion associated with the base-Mesozoic unconformity (see below). Most importantly, there is only one seismic section in the area (Fig. 7), so the apparent structural closure is not constrained. The proximity of this structure to JPP makes it a potential, although highly speculative, target for further data acquisition. Structural highs near Fraser River 1 and Barlee 1 show that a significant thickness of the Grant Group and overlying Permian units has been removed by Triassic–Jurassic erosion at least in the vicinity of those wells.

The time structure map of the top of the Grant Group (Fig.12) shows a smaller areal distribution compared to the map of its base (Fig. 11) due to the deep erosion that preceded deposition of the Jurassic–Cretaceous megasequence. Importantly, the top of the group is deeply eroded over the crests of major anticlinal structures and large rotated fault blocks in the Fitzroy Trough (Fig. 15). This event has destroyed what otherwise would have been obvious structural traps for the proposed geosequestration reservoirs (Fig. 8). The Grant Group on the margins of the Fitzroy Trough is relatively undeformed (within the constraints of the available data) and located at a depth suitable for geosequestration.

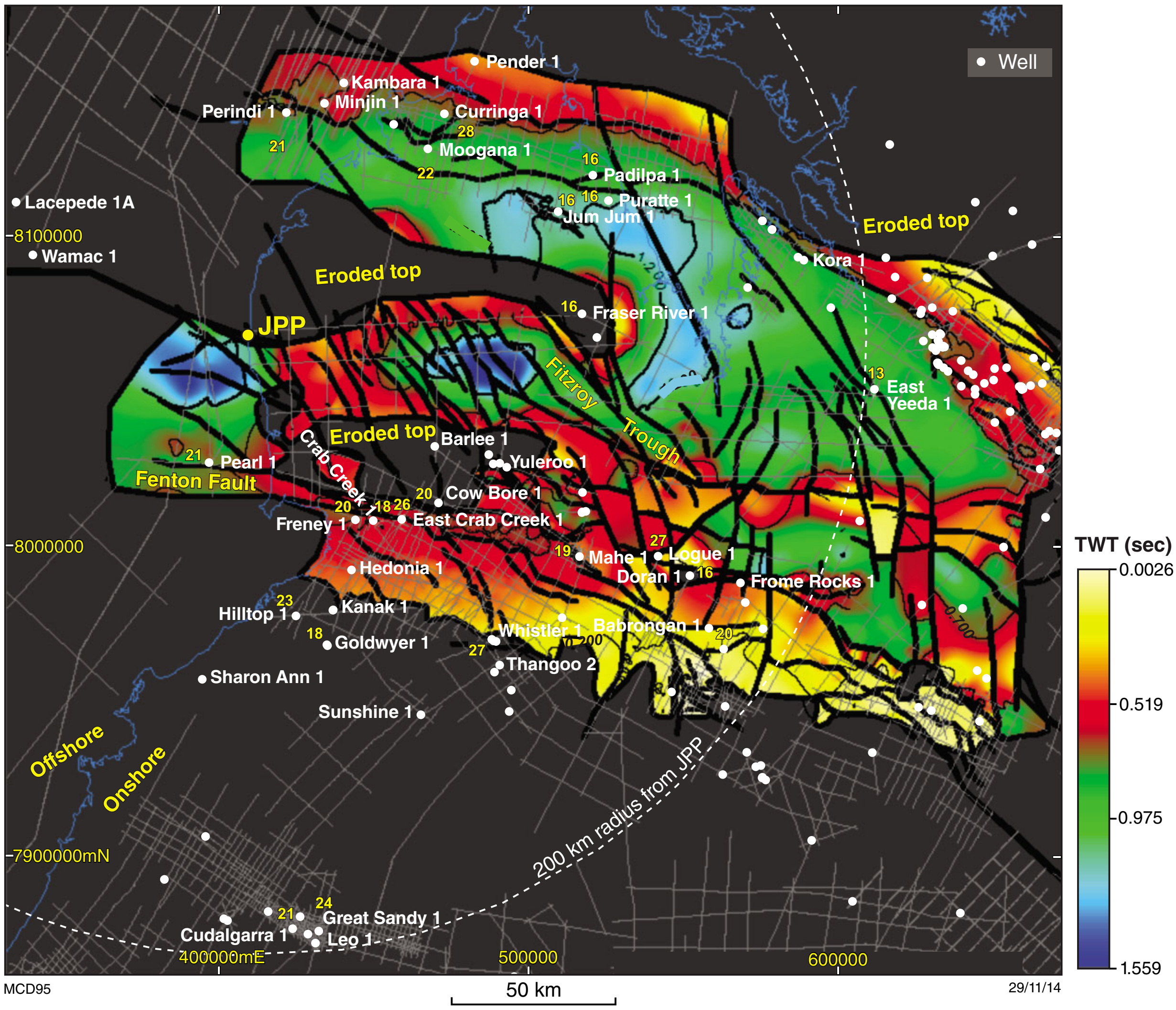

Figure 13. **Time structure map of the preserved top of the Poole Sandstone within the study area. Faults are shown in black (JPP – James Price Point).**

Poole Sandstone and Noonkanbah Formation

In the study area these two units are confined to the Fitzroy Trough and Pender Terrace (Figs 13 and 14). The maps show the large-scale folds and the two dominant sets of faults in the study area. Most significantly, and as expected, erosion associated with the base-Mesozoic unconformity has removed one or both of these units from all the largest folds and from many of the large fault blocks (Fig. 15).

Potential geosequestration sites

Based on the available data three areas (options A, B, and C) appear to have potential for geosequestration (Fig. 11, Table 2). We follow the approach of Varma et al. (2012) in calculating an effective CO_2 storage capacity using the following relationship:

$$GCO_2 = A \times h_g \times \phi TOT \times \rho \times E$$

where 'GCO_2' is the mass estimate of CO_2 storage capacity, 'A' is the geographical area of the region being considered, 'hg' is the gross thickness of reservoir in area 'A', 'ϕTOT' is the average porosity of the reservoir over thickness 'hg', 'ρ' is the density of the CO_2 at the temperature and pressure conditions averaged over the depth range associated with 'hg', and 'E' is the CO_2 storage efficiency factor. The efficiency factor 'E' represents the fraction of the total pore space that is filled by CO_2. This parameter converts gross thickness to net thickness, total area to net area and total porosity to effective, i.e. interconnected porosity. Based on studies in North America Varma et al. (2012) estimated factor 'E' to range between 1 and 4%. The authors follow this approach for calculating prospective storage capacity for these end-member values.

A significant uncertainty in the calculation is estimating the average depth of the reservoir. This is partly because

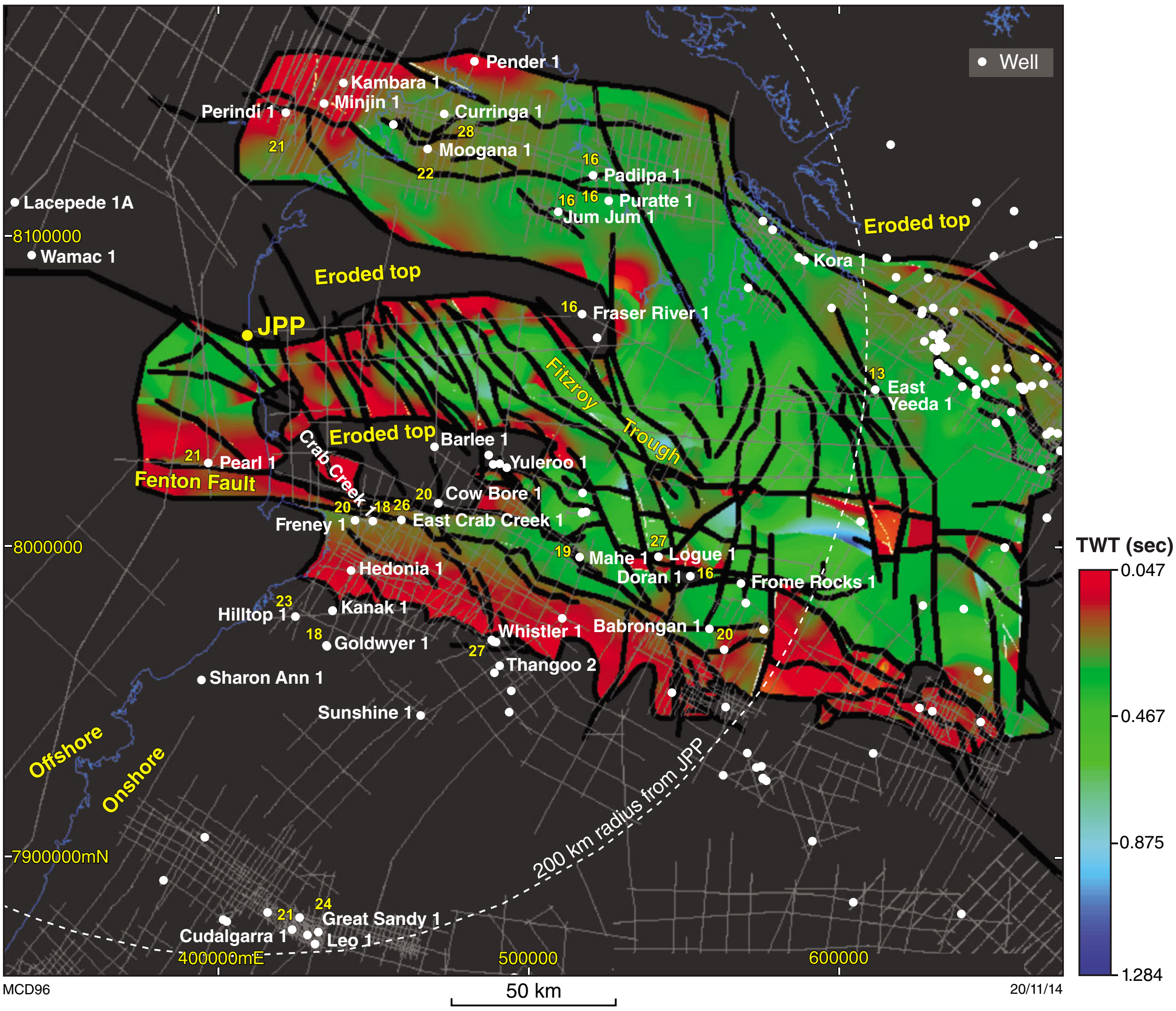

Figure 14. Time interval map of the Noonkanbah Formation in the study area. Faults are shown in black (JPP – James Price Point).

Table 2. Estimated GCO_2 for the three potential geosequestration sites

Option	*Distance to JPP (km)*	*Reservoir*	*Average depth to reservoir (m)*	*Area (m^2)*	*Estimated reservoir thickness (m)*	*Estimated density of CO_2 (kg/m^3)*	*Porosity (%)*	*Prospective storage capacity–GCO_2*	
								E = 1% (Mt)	*E = 4% (Mt)*
A	80–100	Grant GP	1000	548000000	400	370	20	162	649
B	80	Poole Sandstone	1355	113000000	100	480	16	9	35
B	80	Grant GP	1750	113000000	700	550	20	87	348
						Combined		96	383
C	105	Poole Sandstone	1295	96000000	60	470	16	4	17
C	105	Grant Gp	1660	88000000	700	540	20	67	266
						Combined		71	283

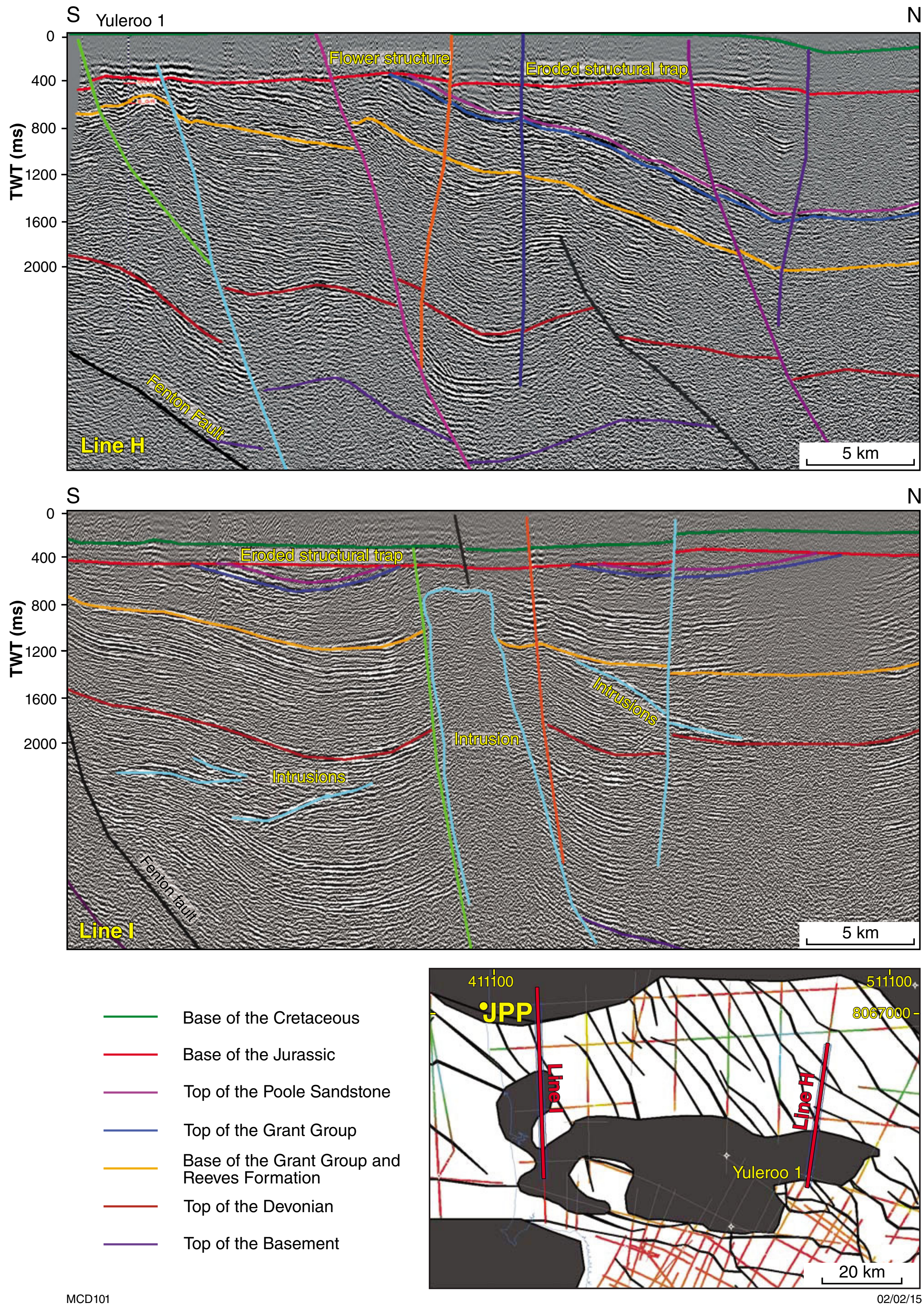

Figure 15. Eroded traps in lines H and I (JPP – James Price Point) [see Figure 12 for location]

the areas selected are very large, but also due to uncertainties in depth conversion. Conversion from time to depth was undertaken using the Kingdom Suite depth conversion function. Using the time–depth charts of the available wells a two-way-time (TWT) to depth conversion factor was determined and interpolated across the study area. Problems with this approach include having to interpolate depth conversion factors over large distances between wells and the results from deeper areas being less reliable due to the tendency to locate wells on structural highs. However, the lack of suitable data renders a more sophisticated approach inappropriate. The uncertainty involved affects the estimated density of CO_2.

Reservoir thickness and porosity was estimated from data averages from wells in the study area. Many of the wells are far from the suggested sequestration sites and reported porosity values are highly variable. This is largely due to changes in rock types and major and complex facies variations in the reservoirs (see section on *Reservoir sedimentology*). The average porosity of the Grant Group is 20%. Very limited data are available from the Poole Sandstone and the authors have used a porosity of 16%. Estimated average porosity is a significant source of uncertainty in the calculation of GCO_2.

Option A: 80% stratigraphic trap and 20% structural trap

Option A is 120 km SE from JPP within the Jurgurra Terrace (Figs 16 and 17). The depth to the top of the Grant Group is estimated to be between 760 and 840 m with an estimated average thickness of 400 m. An average depth of 1000 m to the 'middle' of the Grant Group was used for calculating conditions in the reservoir.

The area comprises a large block of apparently little faulted, subhorizontal strata, which is bounded by the Dampier Fault (South), Fault 1 (North), Fault 2 (West), Fault 3 (East). Both reservoir horizons are preserved, as is a significant thickness of Noonkanbah Formation, however, the Poole Sandstone is too shallow for geosequestration. The same basic structural entity continues for around 100 km in east-southeasterly direction where it shallows and the thickness of the Noonkanbah Formation also decreases. The sealing characteristics of the bounding faults are a key variable in terms of this site's suitability for sequestration of CO_2.

Structurally the proposed trap is a doubly plunging open syncline. Dips on the flanks are around one degree.

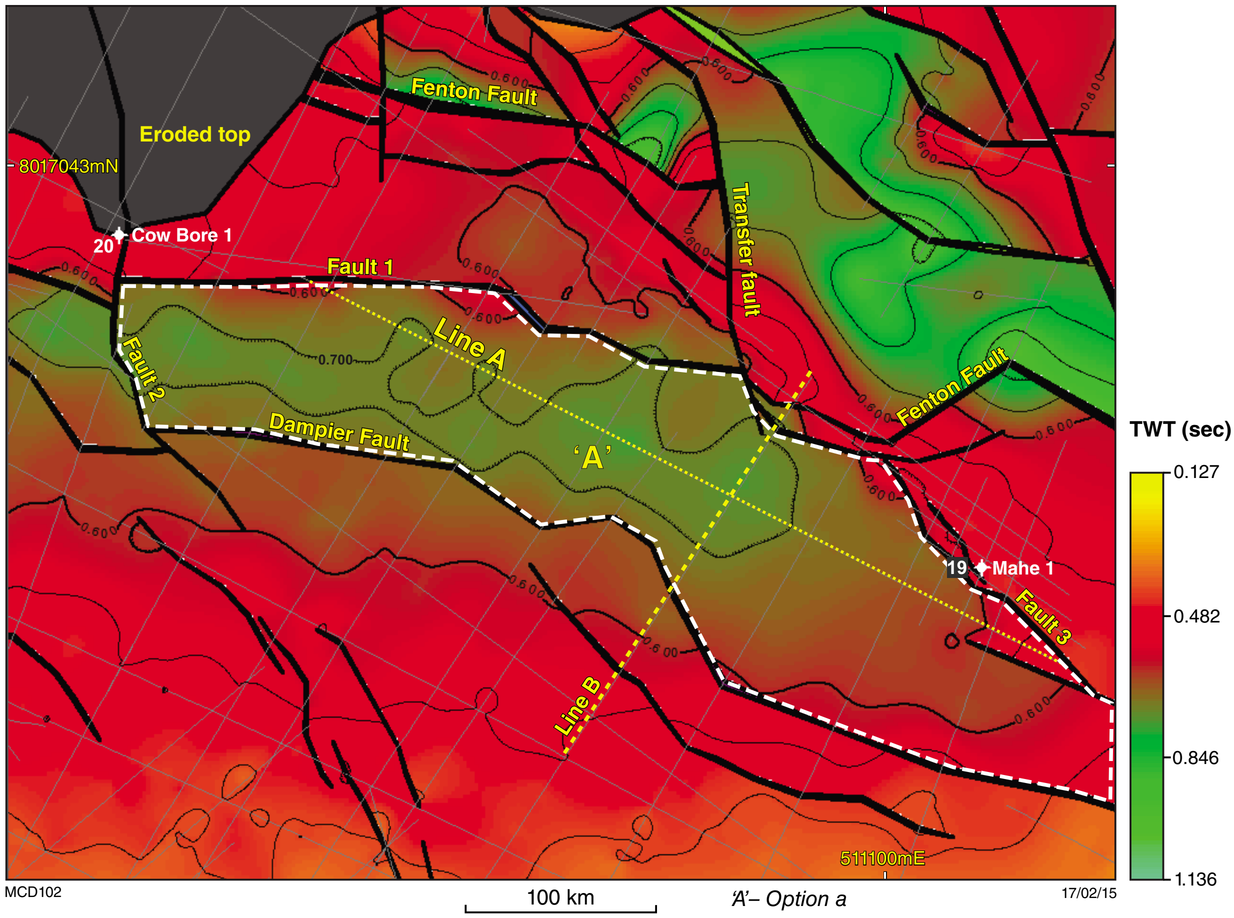

Figure 16. Time structure map of top of the Grant Group in the area of geosequestration Option A. Also shown are the locations of wells Cow Bore 1 and Mahe 1 and the seismic lines presented in Figure 17.

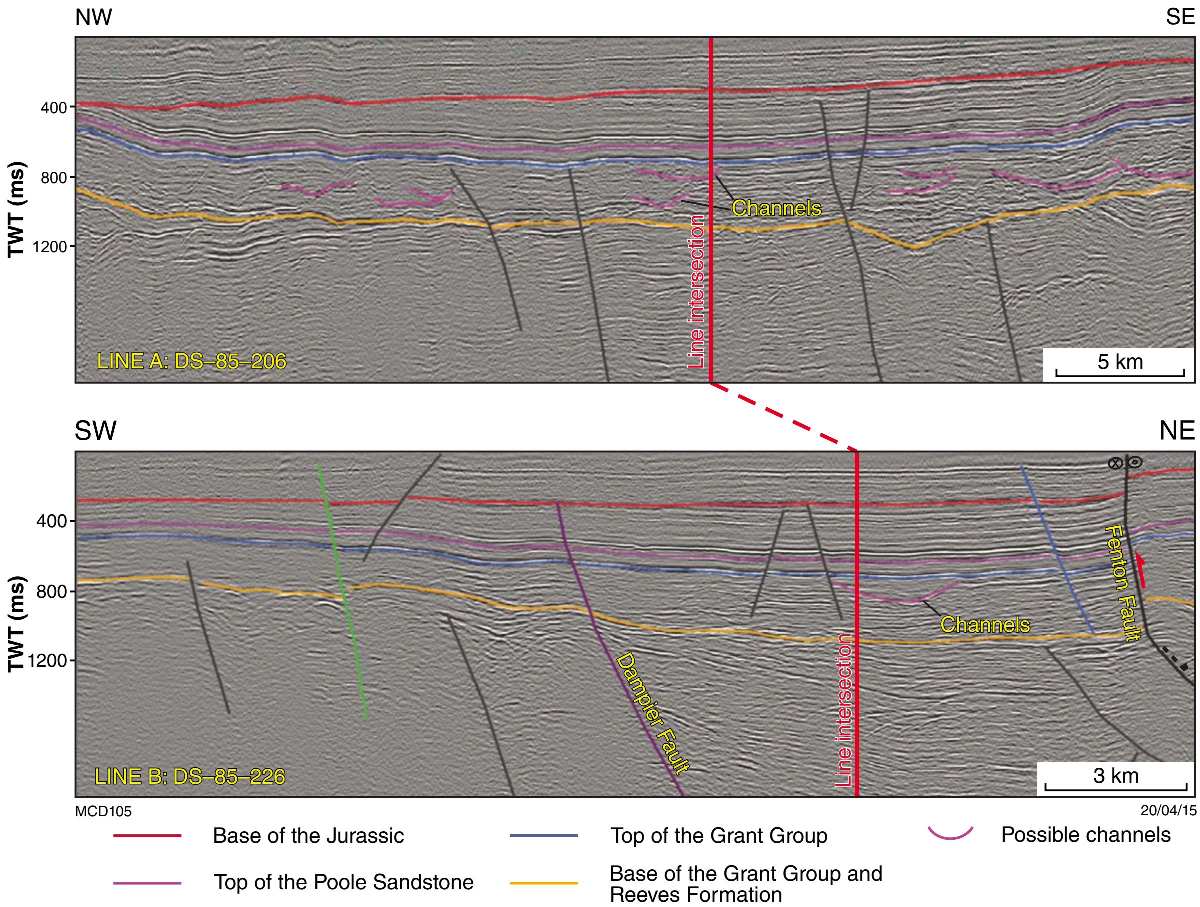

Figure 17. Seismic interpretation across geosequestration Option A, showing some possible channels within the Grant Group (see Figure 16 for locations).

As seen on seismic line B (Fig. 17), the Dampier and Fenton Faults seem to have controlled the thickness of the Carboniferous and Permian sections, implying syndepositional movements. The lithological character of the reservoirs in this region is uncertain because of a lack of wells. There is evidence in the seismic data about what may be channels or valley fills in the Grant Group. This is one of the few areas where details of the internal stratigraphy can be resolved and hence constitute potential targets.

The wells closest to this area are Mahe 1 and Cow Bore 1. The porosity of the Grant Group in these wells ranges from 8 to 46% with an average of about 20%. The large geographical area results in very high estimates of storage potential. In principle, variations in porosity and other key parameters are accounted for in the 'E' factor. Nevertheless, the extremely large area renders it problematic to assign a meaningful 'average' value to any of the parameters involved in the calculation.

Option B: 100% structural trap

Option B lies about 80 km east of JPP within the Fitzroy Trough (Figs 18 and 19). Similar to Option A it comprises a fault block that has not been penetrated by a well. The depth of the top of the Poole Sandstone is between 740 m and 1880 m and for the Grant Group it is 900–1900 m. Both proposed reservoirs are present, as is a significant thickness of Noonkanbah Formation. The depths to the 'middle' of the two reservoirs used to estimate reservoir conditions are 1355 m and 1750 m.

The fault block is bounded by the faults F5, F6, and F7 (Figs 18 and 19). Structurally the area comprises a doubly plunging syncline with very shallow dips on the flanks of only about one degree. The sealing capacity of the faults (F5, F6, and F7) is a crucial variable in this area. The nearest wells, Jum Jum 1, Puratte 1 and East Yeeda 1, are nearly 100 km away and show very large variations in reservoir porosity.

Option C: 100% structural trap

Option C is 105 km northeast of JPP within the Fitzroy Trough, close to the Pender Terrace (Figs 20 and 21). Both potential reservoirs are present, as is a significant thickness of the Noonkanbah Formation. The top of the Poole Sandstone at this locality is situated at a depth between 1220 and 1340 m and the top of the Grant Group between 1240 and 1380 m. The depths to the 'middle' of the two reservoirs, which were used to estimate reservoir conditions, are situated between 1295 m and 1660 m.

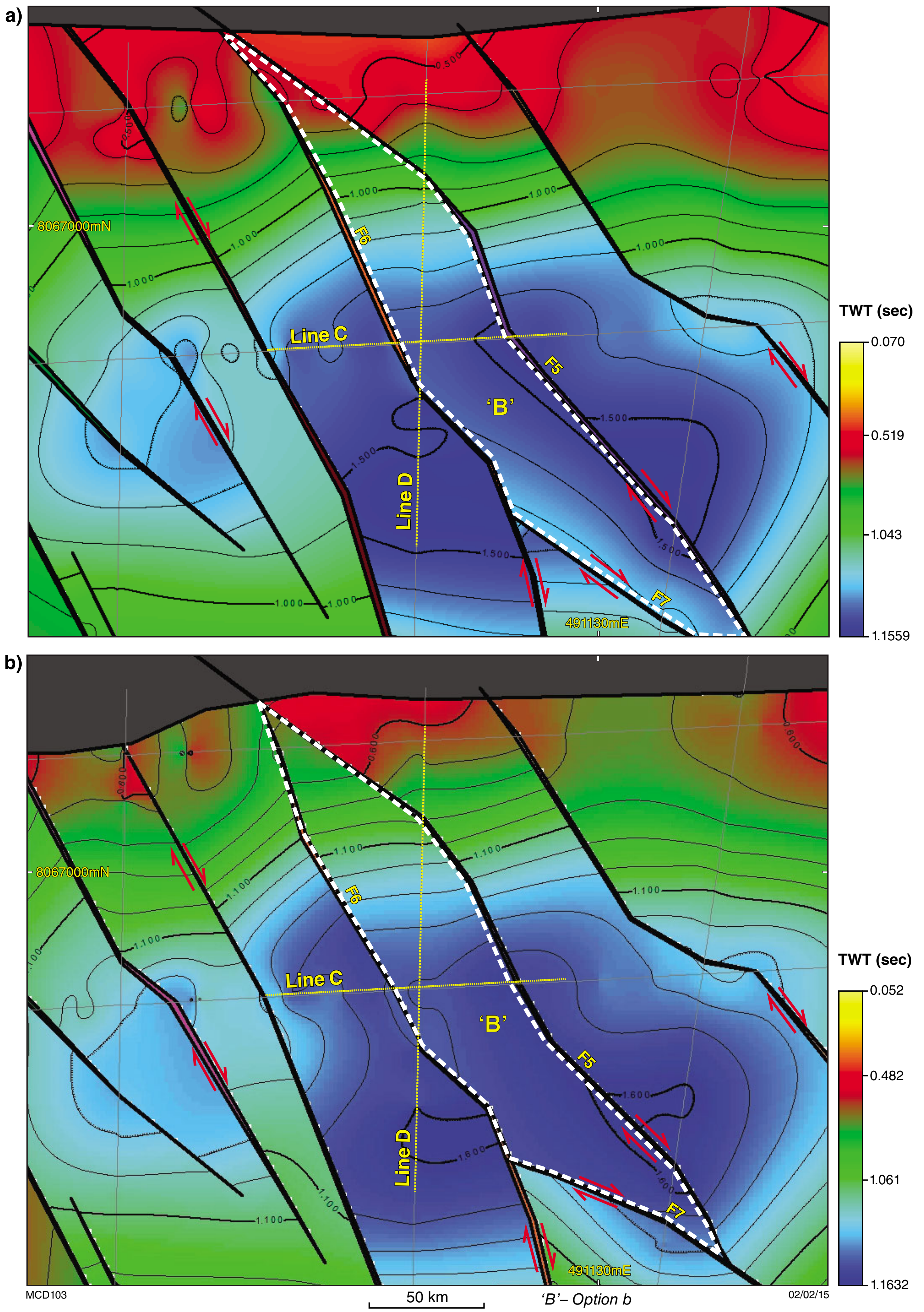

Figure 18. Time structure maps for geosequestration Option B, showing a) top of the Poole Sandstone with contours at 100 msec intervals and b) top of the Grant Group with contours at 100 msec intervals. Also shown are the locations of the seismic lines presented in Figure 19.

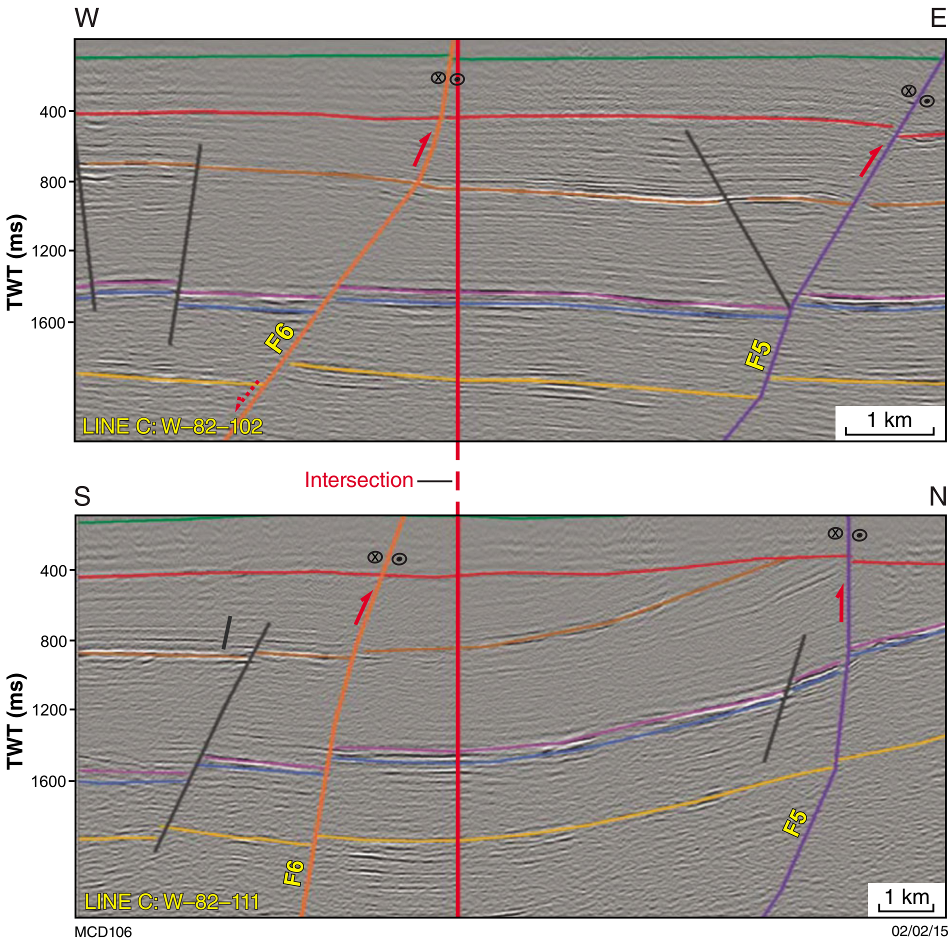

Figure 19. Seismic interpretation in the area of geosequestration Option B (see Figure 18 for location)

Like the other two areas the site comprises a fault block with low stratal dips. To the north the block is bounded by fault F8, (Fig. 20), which is one of the faults associated with the Pinnacle Fault System. Structurally, the proposed trap is on the flank of a syncline with the reservoirs dipping to the south. The sealing capacity of fault F8 plays a critical role for the proposed trap. The structural trap is limited by fault F8 and the 1340 m depth contour for the top of the Poole Sandstone and the 1380 m contour for the top of the Grant Group.

Grant Group reservoir characteristics in this area are variable, differing from east to west. Based on data from Jum Jum 1, Padilpa 1 and Puratte 1in the west average porosity is ~24%, decreasing to ~15% in the east. The 20% value used in the calculations is consistent with these values. The very limited data available from the Poole Sandstone are consistent with the 16% porosity used in the calculation.

Discussion

All the traps comprise large fault blocks and as such are critically dependent on the sealing (or not) characteristics of their bounding faults. Although by Canning Basin standards the seismic coverage is reasonable, the lines are several kilometres apart, and many smaller faults are probably unrecognized. The sealing characteristics of the faults in the northwest Canning Basin are discussed in the section on *Fault sealing characteristics*.

Given the poor well control, reservoir properties have to be extrapolated over very great distances and seismic coverage is also sparse. Thus, the estimates of potential CO_2 storage are highly speculative. The large values are primarily the result of the large geographic extents of the 'fault blocks'. It is likely that individual fault blocks are much smaller due to as yet undetected faults.

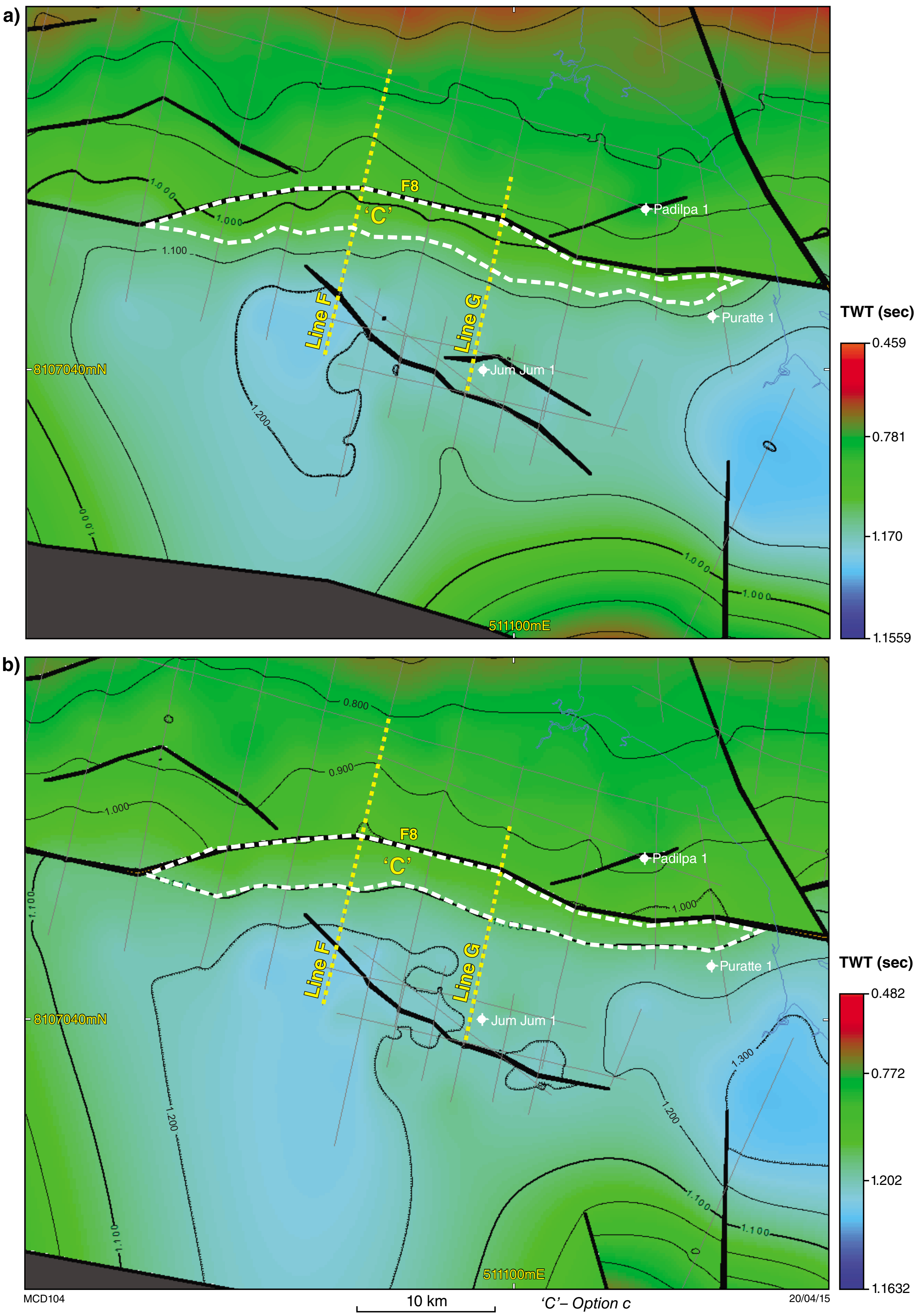

Figure 20. Time structure maps for geosequestration Option C, showing a) top of the Poole Sandstone with contours at 100 msec intervals and b) top of the Grant Group with contours at 100 msec intervals. Also shown are the locations of the seismic lines presented in Figure 21.

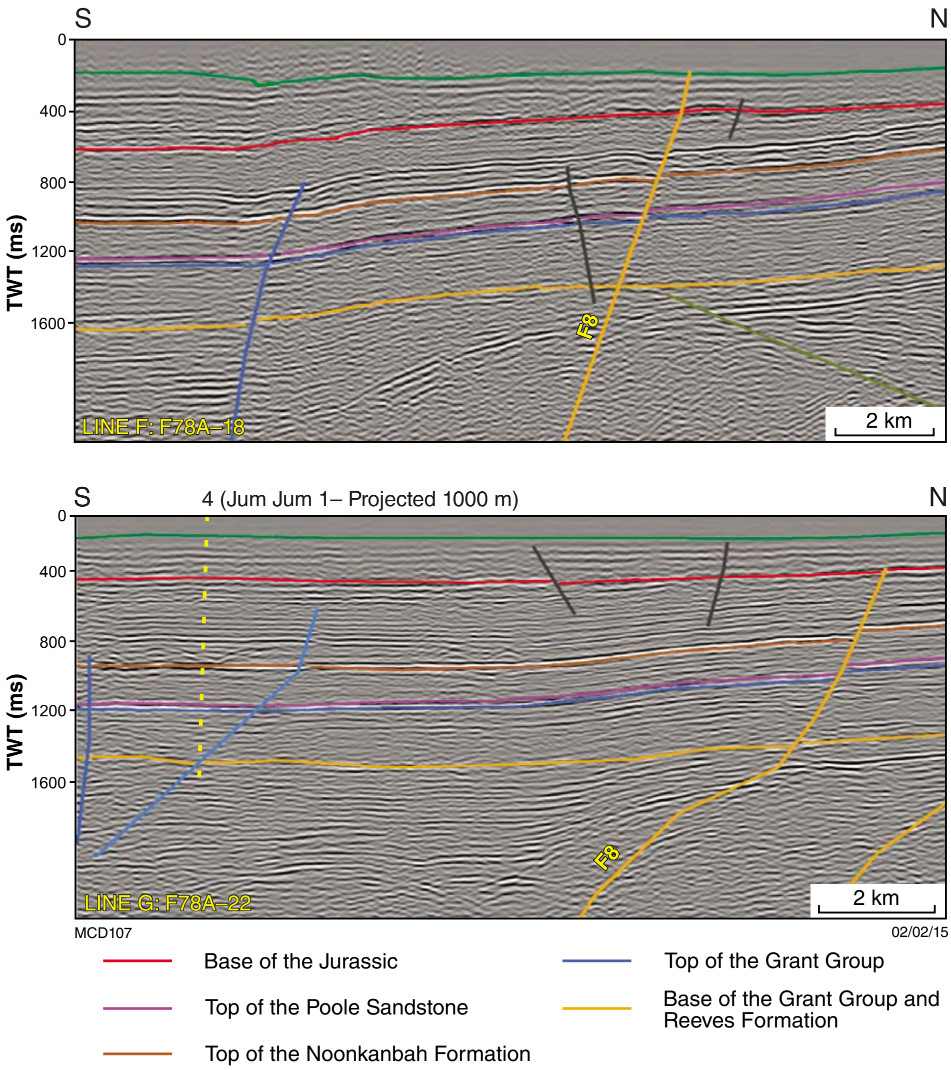

Figure 21. Seismic interpretation in the area of geosequestration Option C. The area to the south of fault F8 comprises the possible sequestration area (see Figure 20 for locations).

Reservoir sedimentology

(Louisa Dent, Annette George and Zahra Seyedmedhi)

Detailed sedimentological studies of two lithostratigraphic units in the Late Mississippian to Triassic megasequence were undertaken to assess their potential as hosts for CO_2 sequestration in the vicinity of JPP. Two independent studies are presented, a regional study on the Poole Sandstone, including the Noonkanbah Formation and locally the Grant Group, and a well-based study of the Grant Group. The regional Poole Sandstone study presented here focuses on paleoenvironmental interpretation of cored intervals. These results are integrated with well logs to assess the distribution of reservoir facies at potential sequestration sites identified on seismic data at appropriate depths and with likely sealing faults (see section on *Potential sites for geosequestration of CO_2*). The Grant Group study is summarized from Dent (2011) and focuses on reservoir quality and sequestration potential using cored intervals from several wells in the study area.

Study 1: Grant Group

Introduction

The sandstone-dominated Grant Group has been proposed as a potential reservoir for CO_2 sequestration. It is a thick unit that underlies the Poole Sandstone and contains mudstone intervals that may be potential seals. Sedimentological examination of the Grant Group was undertaken to assess reservoir quality using cored intervals in wells within a 200 km radius of JPP. The wells are distributed in the Fitzroy Trough, Jurgurra Terrace and northern Broome Platform (Fig. 4).

Lithostratigraphy and age

In the Fitzroy Trough, the Grant Group appears to unconformably overlie the Upper Carboniferous Reeves Formation, which was formerly known as the Lower Grant Group (Apak and Backhouse, 1998, 1999; Mory, 2010). The Grant Group is dominated by sandstone with conglomerate, diamictite, breccia and mudstone (O'Brien et al., 1998; Eyles and Eyles, 2000; Eyles et al., 2001). Thickness is up to two kilometres in the Fitzroy Trough and varies between 200 and 400 metres on the adjacent shelves. The Grant Group was deposited within the *P. confluens* zone to which an Asselian to mid–Sakmarian (Early Permian) age has been assigned (Apak and Backhouse, 1998).

Datasets and methods

Cored intervals in the wells Doran 1, Frome Rocks 2, Fraser River 1 and Thangoo 1A (Fig. 4, Table 3) were logged at 1:100 scale (Appendix 1). Core quality is variable due to the age of some of the core and previous sampling. Core logs for Doran 1, Frome Rocks 2 and Thangoo 1A were drafted in Adobe Illustrator graphic software. Fraser River 1 is presented as a schematic log due to core quality. Facies analysis was undertaken to systematically describe the cored intervals and interpret depositional setting. The limited amount of core means that facies associations can only be broadly defined. Nineteen samples were taken from Doran 1, Frome Rocks 2, Thangoo 1A and Fraser River 1 core to describe detrital composition and diagenetic effects within the facies framework and assess variation in reservoir quality. Samples were prepared as standard thin sections at The University of Western Australia (UWA) and all were etched with hydrofluoric acid and stained for alkali feldspar with sodium cobaltinitrite. Petrographic analysis by conventional polarizing microscopy was carried out to determine detrital composition and diagenetic modification.

Sedimentology

Sixteen siliciclastic facies have been recognized in the core intervals (Appendix 2). Fabric, texture, sedimentary structures, and fossil content/trace fossils were used to identify facies and interpret depositional conditions and processes. Each facies has been given a code representing the grain size and any prominent sedimentary structures. Three facies associations are identified based on common grouping of facies (FA1–FA3, Fig. 22).

Facies Association 1: interbedded sandstone and siltstone

Description: FA1 is characterised by thickly to very thickly bedded, fine- to medium-grained sandstone interbedded with siltstone and heterolithic facies. It is present in all wells except Frome Rocks 2 (Fig. 22). Its thickness varies between wells, with a maximum of 316 m in Fraser River 1. The major facies are massive sandstone (Sm), cross-laminated sandstone (Sxl, Slo) and massive siltstone (F) with minor fine-grained sandstone (Sf) and heterolithic facies (e.g. Sfh). Sedimentary features include common organic matter, deformed/convolute lamination and mudstone rip-up clasts (Fig. 22). Fining-upward arrangements of facies are recognized, however, the overall stacking pattern of FA1 is more broadly aggradational.

Interpretation: The thick sandstone packages and massive sandstone beds indicate high sediment loads and rapid deposition. The fining-upward trends indicate channel-fill deposits with the fine-grained and ripple cross-laminated sandstone and heterolithic facies indicating moderate to low energy conditions at the channel margins (e.g. Miall, 1996). Lack of bioturbation supports a non-marine setting. Massive siltstone indicates periods of deposition in very low energy or standing water conditions (Carling and Dawson, 1996). Mudstone rip-up clasts and abundant organic material indicate inclusion of sediment from muddy areas on channel margins. The overall fine to medium grain size and common channel-margin facies suggest deposition in and at the margins of lower energy fluvial channels.

Table 3. List of Grant Group core in the study area

Well	Location	Thickness of Grant Group (m)	Cored intervals	Core samples	Sample numbers
Doran 1	Jurgurra Terrace	560	C5–12, C14	C12–C15	1–4
Fraser River 1	Fitzroy Trough	1 161[(a)]	C10–73, excluding C13, C16–19, C21, C36, C51[(b)]	C12, C23, C43, C49, C57, C59–60, C64, C66, C70	10–19
Frome Rocks 2	Jurgurra Terrace	441	C6–C8	C6–C8	5–8
Thangoo 1A	Broome Platform	380	C1	C1	9

NOTES: (a) Thickness includes the Reeves Formation which is apparently conformable in the Fitzroy Trough and comprises very similar facies associations as described in this study [see lithostratigraphic assignments for this well in Mory (2010, Appendix 5)]

(b) Missing core

Facies Association 2: thickly bedded sandstone

Description: FA2 is characterized by thick intervals of thickly bedded sandstone (Fig. 22) and is present in all wells except Thangoo 1A. FA2 is thickest in Fraser River 1 (~695 m). Dominant facies are massive sandstone (Sm, Sc), planar- and cross-laminated sandstone (Sl, Sxl) and very fine-grained sandstone (Svf). Grain size ranges from coarse to very fine, but is typically medium. Fining-upward facies arrangements are well developed with intervals of massive sandstone overlain by planar, cross-bedded, and laminated sandstone (Fig. 22). Uppermost very fine grained sandstone may contain abundant mud drapes. Absence of bioturbation supports a non-marine setting. Overall FA2 stacking patterns are aggradational.

Interpretation: The dominance of massive medium- to coarse-grained sandstone indicates rapid deposition of high sedimentary loads in moderate to high energy settings. Ripple cross-lamination and very fine grained sandstone, containing abundant mud drapes suggest periods of lower energy at channel margins (Miall, 1996, 2010). The stacked fining-upward trends are characteristic of channel-fill deposits that are typically associated with phases of channel migration (Miall, 1996). The thick aggradational sandstone and limited channel margin facies suggest deposition in major fluvial channel areas.

Facies Association 3: thick siltstone

Description: FA3 is composed exclusively of massive (F), deformed (Fd), and organic (Fo) siltstone facies present in Fraser River 1 core, forming an interval approximately 100 m thick (Fig. 22). Organic matter defines the laminae in the deformed siltstone. The organic siltstone facies contains fossilised wood fragments and fine sand laminae.

Interpretation: Thick intervals of siltstone indicate prolonged low energy conditions (Miall, 1996, 2010). Lamination indicates some traction current activity consistent with input of fine-grained sand. Lack of bioturbation suggests non-marine deposition. The facies present are potentially consistent with abandoned channels but the thickness of FA3 may indicate a long-lived lake some distance from active channels because there are no thinly bedded sandstone or heterolithic overbank facies.

Depositional setting

The Grant Group facies associations in the studied wells are interpreted as fluvial deposits. The lack of bioturbation, marine fossils, clear wave-formed structures, or other marine indicators such as glauconite, supports a fluvial setting. FA1 and FA2 are dominated by sandstone beds with fining-upward trends, indicating high sedimentary loads and channel deposition. These features, together with dominantly aggradational stacking patterns, are common in sandy fluvial systems with multiple low sinuosity channels (Galloway and Hobday, 1983; Miall, 2010). These depositional systems are dominated by channels that contain large bar complexes formed by lateral and downstream accretion (Miall, 1996). Although these features cannot be defined from the limited cored intervals, based on the main sedimentary features a multi-channelled, sand-dominated, low sinuosity fluvial system is interpreted (Fig. 22). No direct glacial depositional features are recognized, however, the high sediment loads are consistent with glacial outwash. The lack of conglomeratic facies potentially indicates the study area was distal to major sediment input sites.

FA1 and FA2 both show characteristics commonly associated with channel-fill deposits. FA1 is interpreted as having formed in shallow channels with well-developed channel margins. This is because the sandstone facies are typically finer grained than those in FA2 and heterolithic facies and overbank siltstones are common (Fig. 23). Channel migration is indicated by fining-upward trends topped with siltstone. FA2 is interpreted as active channel fills with massive, medium- to coarse-grained sandstone, indicating high energy conditions (Fig. 23). It is highly likely that FA2 and FA1 form large multi-storey channel fill complexes similar to those interpreted from seismic data across the outer Lennard Shelf (O'Brien et al., 1998). FA3 is a very thick (~100 m) interval of siltstone indicating prolonged low energy depositional conditions away from active channels such as an interchannel lake. No obvious marine indicators are recognized in these wells and it is possible that the thick siltstone contains evidence for intermittent marine flooding. Marine-deposited or marine-influenced facies are recognized elsewhere in the region, e.g. in the upper part of the Grant Group in Sundown 3 (see section *Study 2: depositional setting*) and from foraminifera in siltstone of Roebuck Bay 1 (Crespin and Condon, 1956).

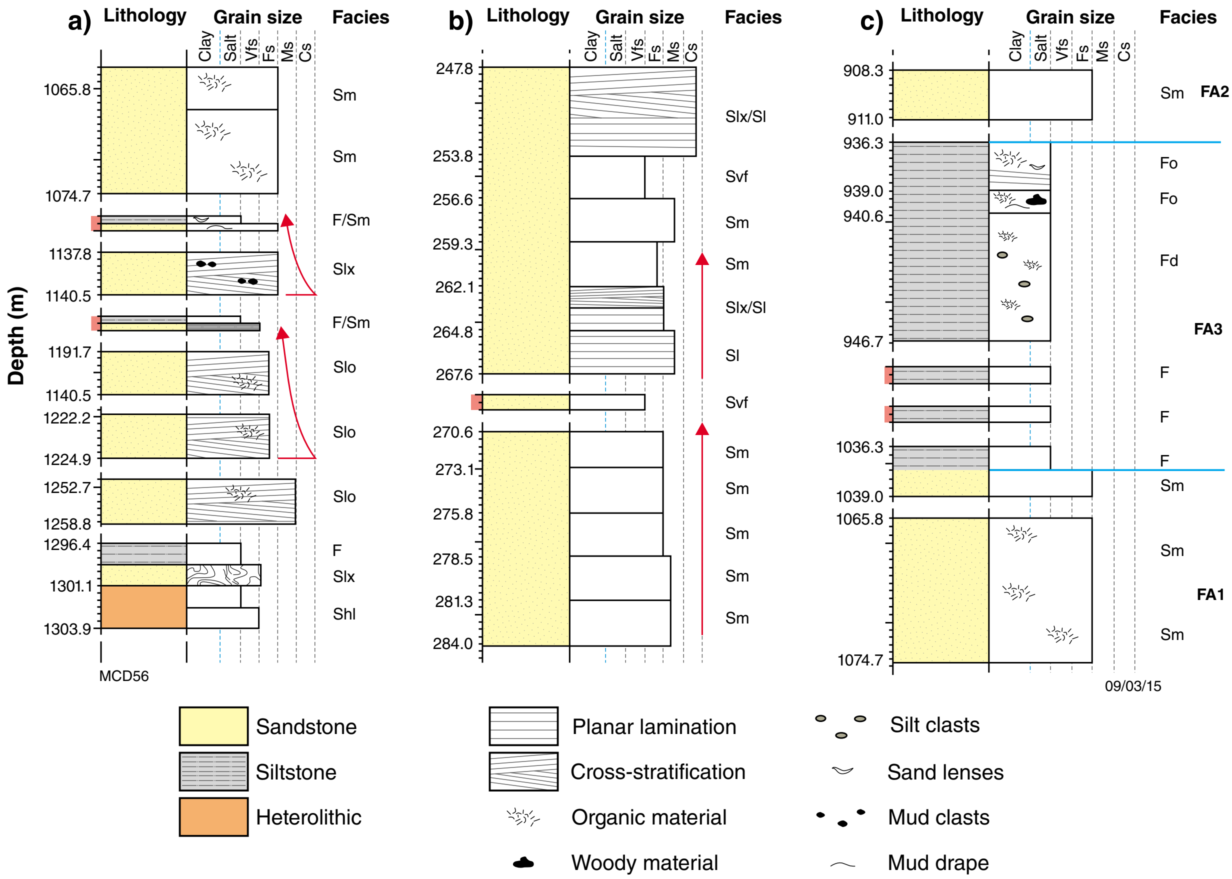

Figure 22. Facies associations (FA) in logged core of the Grant Group in Fraser River 1. Fining-upward trends indicated by red arrows. A) FA1 interbedded sandstone and siltstone. B) FA2 thickly bedded sandstone. C) FA3 thick siltstone interval underlain by FA1 and overlain by FA2. Refer to Appendix 2 for facies codes and descriptions. Grain size abbreviations: Vfs = very fine sand, Fs = fine sand, Ms = medium sand, Cs = coarse sand.

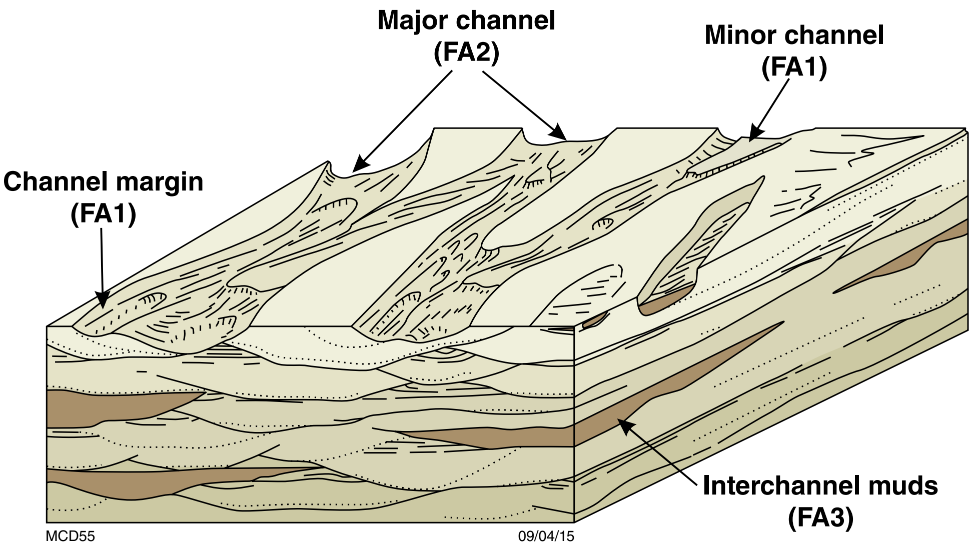

Figure 23. Model of sand-dominated low sinuosity fluvial system showing depositional environments interpreted for facies associations (FA1–3) of the Grant Group identified in this study (modified from Selley, 2000).

Sandstone composition and classification

Detrital composition is dominated by subrounded to subangular, moderately to well-sorted quartz (80–95% of detrital grains). Monocrystalline quartz is most common with up to 4% polycrystalline quartz. Feldspars are present in minor quantities in most samples (up to 8%) with the exception of two Fraser River 1 sandstone samples with no feldspar. Alkali feldspars are the most abundant and comprise 1–6% of the framework with plagioclase up to 3%. Lithic fragments are present in all samples and comprise up to 5% of the framework. Sedimentary and metamorphic varieties are present. Most sedimentary lithic fragments are chert (crypto- to microcrystalline) and metamorphic lithic fragments display distinct foliated textures, e.g. schist. Polycrystalline feldspar is rare. Accessory minerals (<1%) are biotite, muscovite, and rounded zircon.

Dark brown organic material is present in small amounts of up to ~5% (e.g. base of Doran 1 and Fraser River 1). Sandstone beds in the study area are texturally mature and classified as quartzarenites, subfeldsarenites and sublitharenites based on their relative proportions of quartz, feldspar and lithic fragments (Fig. 24).

Diagenetic modification

Grant Group sandstones show modification by several diagenetic processes, including compaction, grain fracturing, cementation, dissolution, and replacement by authigenic phases (Fig. 25). Sandstone samples have clast-supported fabrics that typically display planar or sutured grain contacts, indicating compaction before significant cementation (Fig. 25). Other compaction-related features include deformation of soft grains (e.g. micas) and organic material around harder grains (Figs 25d and e).

Quartz overgrowth cements are commonly developed (Fig. 25f) but only locally significantly fill primary intergranular porosity. They are best developed in clean sandstone where detrital clay does not inhibit their formation. Sandstone from deeper parts of the wells also show sutured grain contacts between quartz overgrowths and adjacent grains, suggesting continued compaction (Fig. 25g). Samples with poikilotopic carbonate cement tend to show dissolution around the majority of quartz grain edges and also around some alkali feldspar grains (Fig. 25a). This cement occludes porosity where it is developed (Figs 25b and 26a) and forms discrete horizons up to ~2.5 m thick in Doran 1 and Frome Rocks 2 core. Samples with poikilotopic carbonate cement tend to show least grain fracturing and other evidence for mechanical compaction suggesting cementation prior to deep burial. Patchy calcite locally overgrows quartz overgrowth cement and is a minor cement in general. Kaolinite is present in all cored intervals and locally replaces detrital grains such as plagioclase. Kaolinite cement overprints poikilotopic calcite and quartz overgrowths and tends to occlude porosity (Fig. 26b). Very minor authigenic phases include sericite and chlorite, which replace plagioclase and lithic fragments, respectively.

Reservoir quality

Measured porosity values for Doran 1 and Fraser River 1 indicate that overall sandstone beds have very good to good porosity, although variable, ranging from 4–28% with an average of ~16% (Table 4). There is no clear pattern with respect to facies identified in this study (Table 4), although the number of observations is limited. In general, compaction and cementation are the main porosity reducing agents in sandstone, as has been observed in the Grant Group. Commonly, sandstone beds show a reduction in porosity with increasing burial depth

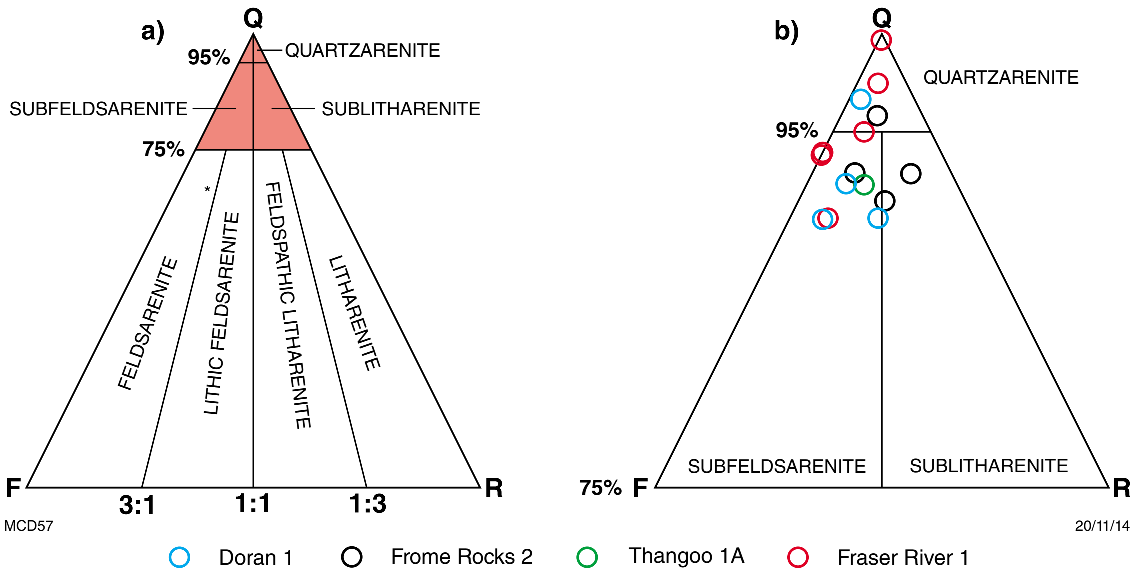

Figure 24. Classification of Grant Group sandstone samples using the QFR plot of Folk et al. (1970), where Q = monocrystalline and polycrystalline quartz, F = total monocrystalline feldspar, R = lithic fragments, including chert. Grant Group data plot in red shaded area in a) are expanded in b).

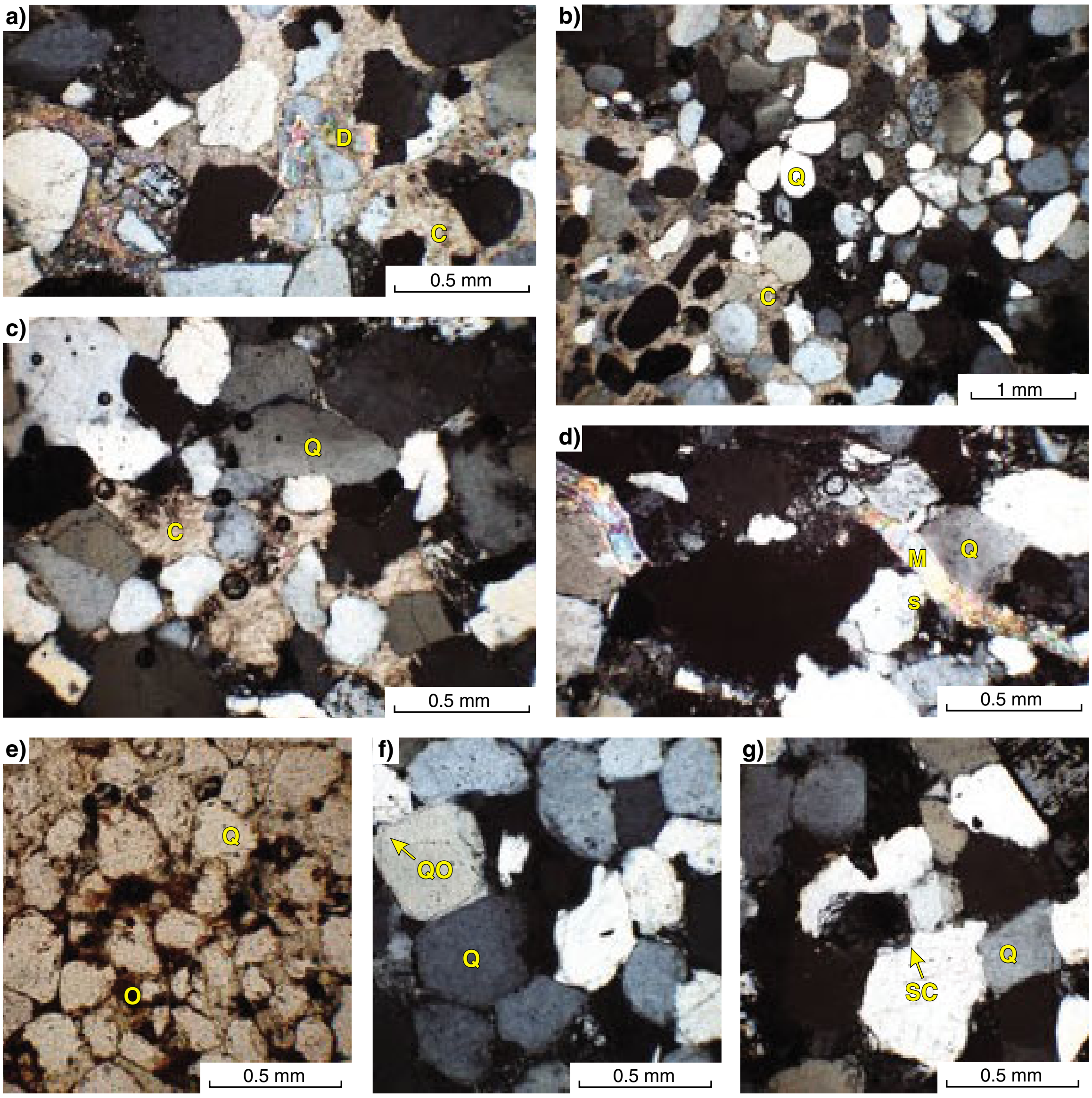

Figure 25. Diagenetic features observed in Grant Group sandstones in the northern Canning Basin. Images taken in cross-polarized light except where stated otherwise. C: calcite cement, D: grain dissolution, M: deformed muscovite, O: organic material, Q: detrital quartz, QO: quartz overgrowth. a) Minor dissolution of quartz and feldspar grains and calcite cement in sandstone (Doran 1, core 10, 499 m), b) poikilotopic carbonate cement composed of coarse crystals (Doran 1, core 10, 499 m), c) patchy carbonate cement occluding primary pore spaces in sandstone (Fraser River 1, core 64, ~1070 m), d) ductile deformation of detrital muscovite flakes in sandstone (Fraser River 1, core 70, ~1255 m), e) detrital organic material deformed around detrital quartz grains (Fraser River 1, core 70, ~1255 m) [plane-polarized light],f) quartz overgrowth cement; original grains visible because of very thin dust coating on detrital grain surface (Fraser River 1, core 12, ~220 m), g) sutured grain contacts (SC) between detrital quartz grains in sandstone (Fraser River 1, core 70, ~1255 m).

(Haszeldine et al., 2000). However, measured values do not conform to this trend and values are variable throughout the two wells examined.

Variation in porosity is most likely related to the type of cement filling intergranular pore space. Poikilotopic calcite has had the largest effect on porosity and, where present, largely occludes pore space as noted above (Fig. 26a). Quartz overgrowths and kaolinite cement abundances are variable. However, where they are common, both significantly reduce porosity (Fig. 26b), although the habit of kaolinite is known to retain microporosity.

Measured permeability values indicate reasonable permeability overall (Table 4). No clear relationship between permeability and depth or porosity is evident that is potentially reflecting the influence of cement distribution. Deformation of detrital grains may block pore throats and reduce permeability. Sandstone facies containing organic matter and detrital clay have among the lowest permeability values which would have been further reduced by compaction (e.g. Fig. 25e).

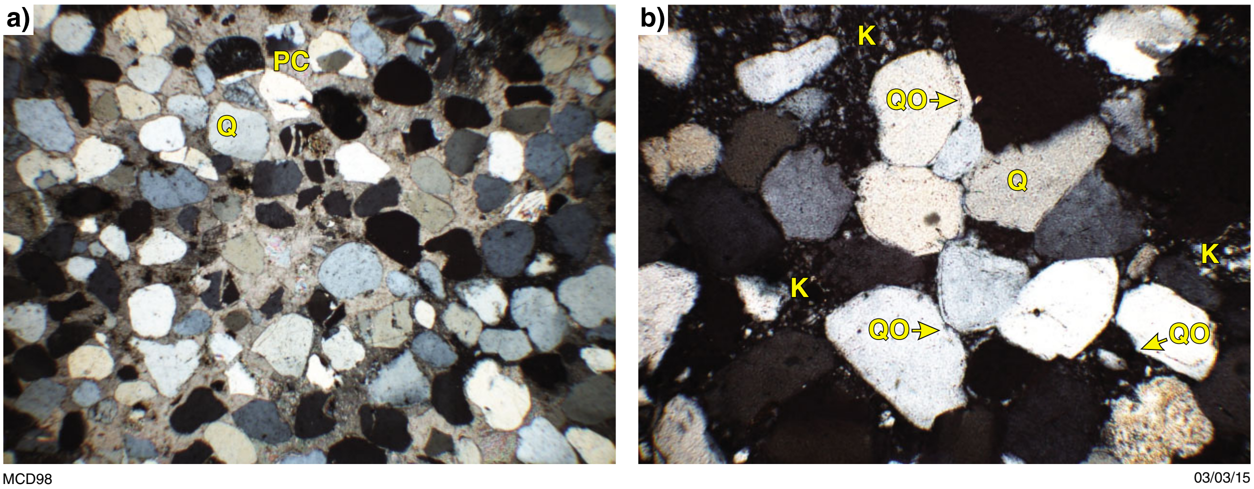

Figure 26. Photomicrographs (cross-polarized light) showing occlusion of pore space by cement. A) poikilotopic calcite cement (PC) in sandstone with marked reduction in porosity and permeability. Q: detrital quartz. Field of view 7 mm). B) quartz overgrowth cement (QO) on rounded quartz grains (Q) and younger kaolinite cement (K). Field of view 3 mm.

Table 4. Porosity and permeability data at various depths and their relationship to facies identified in wells Doran 1 and Fraser River 1, including thin section sample code from the same core section and facies. *Closest facies to measurement depth. Measurements derived from the Western Australia Petroleum and Geothermal Information Management System (WAPIMS) database and other reports.

Well	*Top Depth (m)*	*Base Depth (m)*	*Porosity (%)*	*Permeability (mD)*	*Facies*	*Sample*
Doran 1	457.3		14		Fine sandstone (Sf)	S1
Doran 1	499		5.5		Massive sandstone (Sm)	S2
Doran 1	501.1		4		Massive sandstone (Sm)	-
Doran 1	554.2		15		Laminated or deformed sandstone (Sl–Sd)	-
Doran 1	628.8		24	1256	Planar-laminated sandstone (Slo)	S4
Doran 1	630.1		27	260	Planar-laminated sandstone (Slo)	S4
Doran 1	695.3		17	471	Planar-laminated Sandstone (Slo)*	-
Fraser River 1	247.8	253.9	27.8	564	Planar- or cross-laminated sandstone (Slx/Sl)	S11
Fraser River 1	541.93	548.03	18.7	912	Massive sandstone (Sm)	-
Fraser River 1	1068.63	1074.72	11.2	83	Massive sandstone (Sm)	S17
Fraser River 1	1252.73	1258.82	17.9	1504	Cross-laminated sandstone (Sxo)	S19

Study 2: Poole Sandstone

Introduction

The Lower Permian Poole Sandstone and overlying Noonkanbah Formation are identified as a potential reservoir–seal pair for CO_2 sequestration. Sedimentological examination of the Grant Group, Poole Sandstone, and Noonkanbah Formation was undertaken to assess reservoir quality in the Poole Sandstone, using cored intervals in wells within a 200 km radius of JPP. The wells are distributed along the central Fitzroy Trough, northwestern Lennard Shelf, Jurgurra and Mowla Terraces, and Broome Platform (Fig. 4). The depositional settings of the Poole Sandstone and overlying Noonkanbah Formation have been interpreted from facies analysis of cored intervals. Sandstone facies previously assigned to the Poole Sandstone in Sundown 3 have been reinterpreted as Grant Group in this study. Analysis of wireline log data in these and additional wells was undertaken to establish the distribution and broader facies characteristics in the region.

Lithostratigraphy and age

The ~160 m-thick Poole Sandstone disconformably overlies the Grant Group (Mory, 2010). It has been interpreted to record shallow marine deposition at the termination of glacial conditions (Kennard et al., 1994). The Poole Sandstone locally includes the basal Nura Nura Member that is composed of limestone and calcareous sandstone. In the southeastern Fitzroy Trough, basal limestone facies are absent and the Poole Sandstone is dominated by sandstone facies with common plant fossils and likely to be of fluvio-deltaic origin (Mory, 2010). Coarsening-upward cycles have been recognized in the northwestern and central part of the Fitzroy Trough (Mory, 2010), where the facies overall are finer grained (Forman and Wales, 1981). The overlying Noonkanbah Formation is dominated by fine-grained siliciclastic facies (mudstone and fine sandstone) deposited in a warming, low energy marine environment (Forman and Wales, 1981). The Poole Sandstone lies within the *P. pseudoreticulata* palynological zone and the Noonkanbah Formation coincides with the S. *fusus* and *P. sinuosus* Zones (Mory, 2010).

Datasets and methods

This study used an integrated approach combining core sedimentology, wireline log, and biostratigraphic data. Eight petroleum or stratigraphic wells within the 200 km radius, and just outside this zone, have cored intervals in the Poole Sandstone and/or Noonkanbah Formation (Table 5). The selected wells provide reasonable coverage of tectonic elements across the area (Fig. 4). Sedimentological data generated by examination and logging of core from these wells (at a scale of 1:50) has been summarized as drafted logs using WellCAD software. Some of the core is too disrupted for logging but has been described in this study.

Biostratigraphic, petrophysical, and geophysical data have been used to provide a spatial and temporal framework in which sedimentological data have been placed. These data were also used to establish geometry of depositional packages and tectonic history. Well data including petrophysical logs, paleontological identifications, and formation top depths were extracted from well completion reports and compared with Mory (2010). Gamma-ray (GR) logs were available for the majority of wells and were used to correlate stratal packages in various wells (Appendix 3).

The dominance of sandstone facies in the Poole Sandstone and Grant Group means that it is likely to be difficult to confidently identify these lithostratigraphic units where age data are absent or uncertain. The basal carbonate facies of the Poole Sandstone (Nura Nura Member) can be utilized to separate the Poole Sandstone and Grant Group. Nevertheless, is not present in all wells/areas as outlined above.

The age of most of the wells in the study area creates problems, i.e. five of eight studied wells were drilled in the 1950s. Gamma-ray logs, an important tool for correlation, are absent in two of the wells with cored intervals. It includes the Bureau of Mineral Resources' (BMR) wells Mount Anderson 1 and The Sisters 1 and available spontaneous potential logs are difficult to use in correlation and synthesising data. An additional problem is the discrepancy between core depths in the well completion report and the available core in Frome Rocks 2 (Table 6). The total amount of core is the same in both, so depths recorded on the core have been used in this study.

Sedimentology

Twenty-two siliciclastic facies ranging from conglomerate to mudstone and one carbonate facies have been recognized in core (Appendix 4). Fabric, texture, sedimentary structures, and fossil content/trace fossils were used to identify facies and interpret depositional conditions and processes. Each facies is given a code, indicating the grain size and any prominent sedimentary structures. Nine facies associations are identified based on common grouping of facies FA1–FA9 (Appendix 4).

Three facies associations from the Grant Group in Sundown 3 are described in this study (FA1–FA3). The Poole Sandstone is dominated by heterolithic sandstone and mudstone facies (FA5–6) with some coarser sandstone facies (FA4). The Nura Nura Member [as restricted by Mory (2010) to carbonate facies] is represented by FA7. Two heterolithic sandstone–mudstone facies associations (FA8–FA9) are recognized in the Noonkanbah Formation.

Facies association 1: cross-bedded sandstone

Description: FA1 is composed of cross-bedded, medium-grained sandstone with sharp, locally pebbly bed bases (Figs 27 and 28). Proportions of mud drapes, carbonaceous flakes, and detrital clay are variable and bioturbation is very rare (Fig. 27).

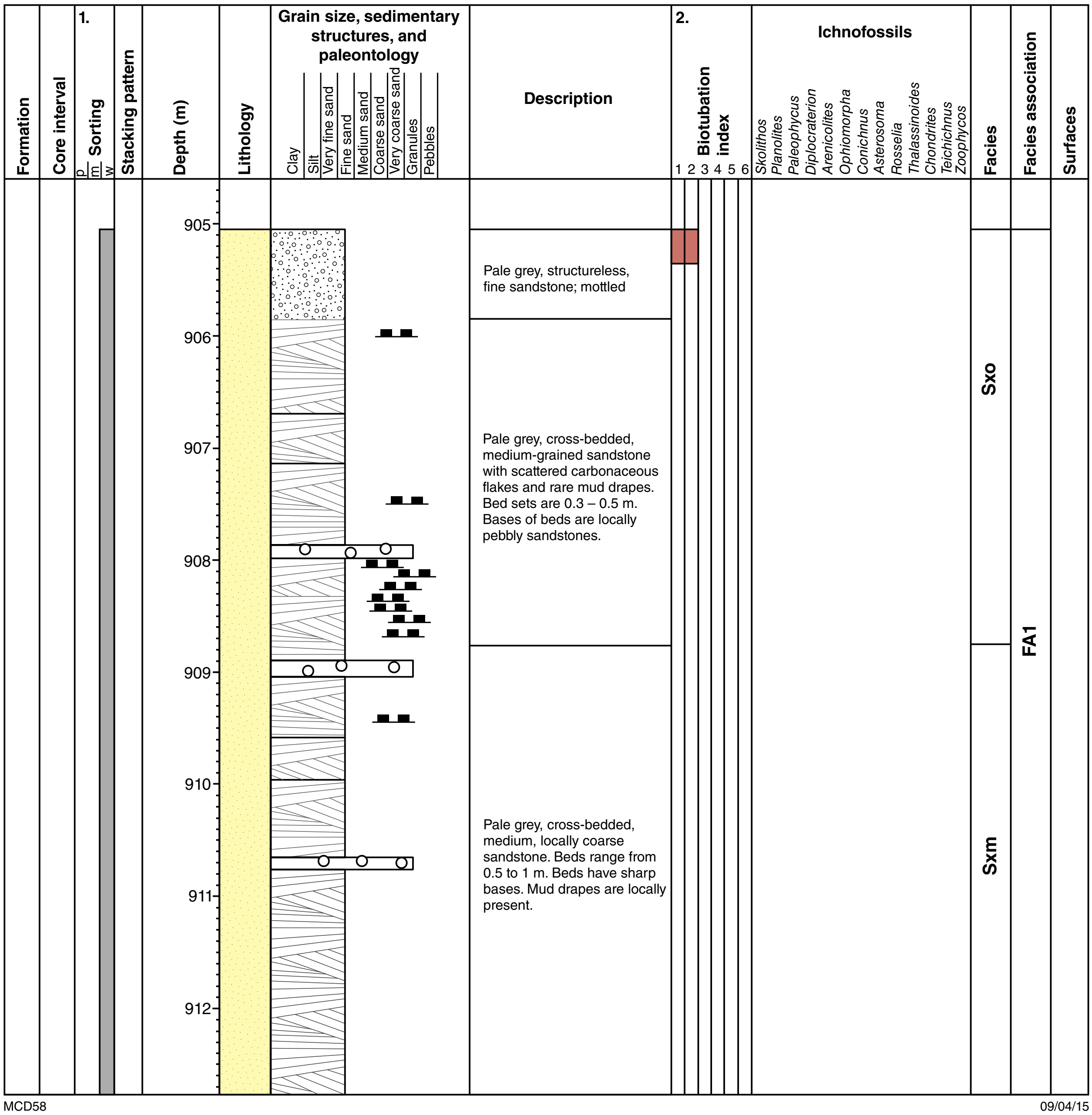

1. Sorting description abbreviations: p = poor, m = moderate, w = well-sorted

2. Bioturbation index follows the scheme presented by Tucker (2011)

Figure 27. Core log of well Sundown 3, core 1 highlighting cross-bedded sandstones (facies Sxm and Sxo) of FA1 assigned to the Grant Group in this study. Facies descriptions are provided in Appendix 4.

Interpretation: FA1 is interpreted as fluvial channel fills based on sharp-based pebbly sandstone and cross-bedding (Miall, 1996). Lack of significant bioturbation in FA1 suggests non-marine conditions.

Facies association 2: lenticular-bedded heterolithic sandstone-siltstone and mudstone

Description: FA2 is characterised by heterolithic facies (Figs 29–31). The basal facies in this association is fine-grained sandstone with double mud drapes (Smh), overlain by lenticular-bedded heterolithic fine-grained sandstone–siltstone (Hm). This facies is weakly to moderately bioturbated with *Planolites* and rare *Teichichnus* (Figs 30–32). The uppermost part is dominated by a thick interval of mudstone that lacks bioturbation (Mh, Fig. 31).

Interpretation: the dominance of fine-grained facies in FA2 suggests deposition in a low-energy environment. Double mud drapes in fine-grained sandstone (Fig. 32) indicate tidal influence and the bioturbation, notably *Teichichnus* burrows, is consistent with a marine influence (Dalrymple, 2010; Pemberton et al., 2001). FA2 is interpreted as muddy tidal flat deposits.

Facies association 3: ripple cross-laminated heterolithic sandstone-mudstone

Description: FA3 is characterised by sharp-based, fine-grained sandstone that displays convolute lamination (Sfc) and ripple cross-lamination (Sfr), overlain by bioturbated mudstone (Figs 29 and 31). Mudstone with no bioturbation (M) is a minor facies. Syneresis cracks and the trace fossils *Teichichnus* and *Chondrites* are common (Figs 31 and 32).

Interpretation: FA3 is interpreted as sandy tidal flat deposits. Double drapes suggest tidal influence and mudstone without bioturbation signifies stressed conditions likely to have been generated by freshwater input. The trace fossils are consistent with a marine to brackish setting (Pemberton et al., 2001). Syneresis cracks also support brackish water conditions with changes in salinity.

Facies association 4: medium- to fine-grained sandstone

Description: FA4 is composed of fining-upward pebbly sandstone (Gs) and medium- to fine-grained sandstone (Sm; Figs 33 and 34). The sandstone is composed of quartz, feldspar, and mica with some organic fragments up to 20 mm long, which are most likely wood fragments (Fig. 35).

Interpretation: the upward arrangement of facies suggests channel deposition. Lack of bioturbation denotes fluvial channel deposition away from marine influence.

Facies association 5: heterolithic sandstone–mudstone with minor conglomerate

Description: FA5 is composed of heterolithic facies composed of fine-grained sandstone with mud laminae or ripple cross-lamination (Sff) and lenticular-bedded to wavy-laminated fine-grained sandstone–mudstone (Hm and Hw; Figs 36 and 37). Locally sharp-based, clast-supported conglomerate with angular mudstone clasts and rounded carbonate mudstone-cored clasts (Gm) form the bases of fining-upward packages. Minor facies are bioturbated sandstone (Sfv) and planar-laminated sandstone (Sfh). Trace fossils are typically vertical burrows such as mud-lined *Ophiomorpha* (Fig. 36).

Interpretation: fine-grained facies with lenticular bedding and wavy lamination suggest deposition in an overall low-energy environment with alternating current energy. Mud drapes and ripple cross-laminated sandstone support a tidal influence. *Ophiomorpha* is a marine to brackish sandy substrate indicator (Pemberton et al., 2001). Fining-upward facies arrangements with sharp bases and basal conglomerates suggests channel fills. FA5 is therefore interpreted as indicating tidal flat environments with minor channels.

Facies association 6: heterolithic sandstone–mudstone with hummocky–swaley cross-stratification and mudstone

Description: FA6 shows a fining-upward arrangement of hummocky(–swaley) cross-laminated sandstones (Sfs), overlain by bioturbated lenticular-bedded sandstone (Sfm) and heterolithic sandstone–siltstone with local bioturbation (Hl; Figs 38 and 39).

Interpretation: FA6 was deposited below fair weather wave base and above storm wave base (offshore transition), reflecting the influence of storms indicated by the hummocky–swaley cross-lamination. Bioturbation supports a marine depositional setting.

Facies association 7: skeletal rudstone–grainstone and mudstone

Description: FA7 is composed of thinly- to very thinly bedded skeletal rudstone–grainstone interbedded with mudstone (Lgs) and overlying laminated siltstone with carbonaceous flakes (Mh; Figs 40 and 41). Elongate skeletal grains, up to 30 mm long and oriented parallel to bedding, include abraded fragments of bryozoans, crinoids, fusulinid foraminifera, and shell fragments. Intraclasts of skeletal packstone–wackestone are locally present. Small scale fining-upward trends are present in facies Lgs.

Interpretation: the fossil taxa, notably crinoids and fusulinids indicate open marine conditions for FA7. Abraded and fragmented shells in conjunction with alternating coarse-grained fossiliferous to fine-grained, non-fossiliferous beds support reworking and deposition by high energy wave activity, for example during waning storm activity. Fine-grained facies record deposition below fair weather wave base between storm events.

Facies association 8: heterolithic sandstone–mudstone

Description: FA8 is a fine-grained association dominated by mudstone (Mh) with heterolithic very fine grained sandstone–mudstone with local lenticular bedding (Hh; Figs 42 and 43). The facies are arranged in fining-upward packages up to 1.5 m thick. Bioturbation is absent.

Interpretation: dominance of mudstone in FA8 suggests deposition in low energy conditions, most likely lower shoreface to offshore. The absence of bioturbation in core suggests locally stressed conditions during deposition.

Facies Association 9: bioturbated, heterolithic sandstone–mudstone

Description: FA9 is composed of heterolithic fine-grained sandstone and mudstone (Hb, Hm) with minor bioturbated or ripple cross-laminated, fine-grained sandstone (Sfb, Sff) stacked in fining-upward packages (Figs 44–47). Trace fossils in fine-grained sandstone beds are commonly subhorizontal burrows such as *Chondrites* and minor *Planolites* (Figs 45 and 46). Sandstones contain rare bivalve fragments.

Interpretation: FA9 was deposited in a marine environment as indicated by common bioturbation, although low diversity and fossil fragments. Abundant mudstone and *Chondrites* in FA9 and suggest deposition in the lower shoreface to offshore transition (Pemberton et al., 2001).

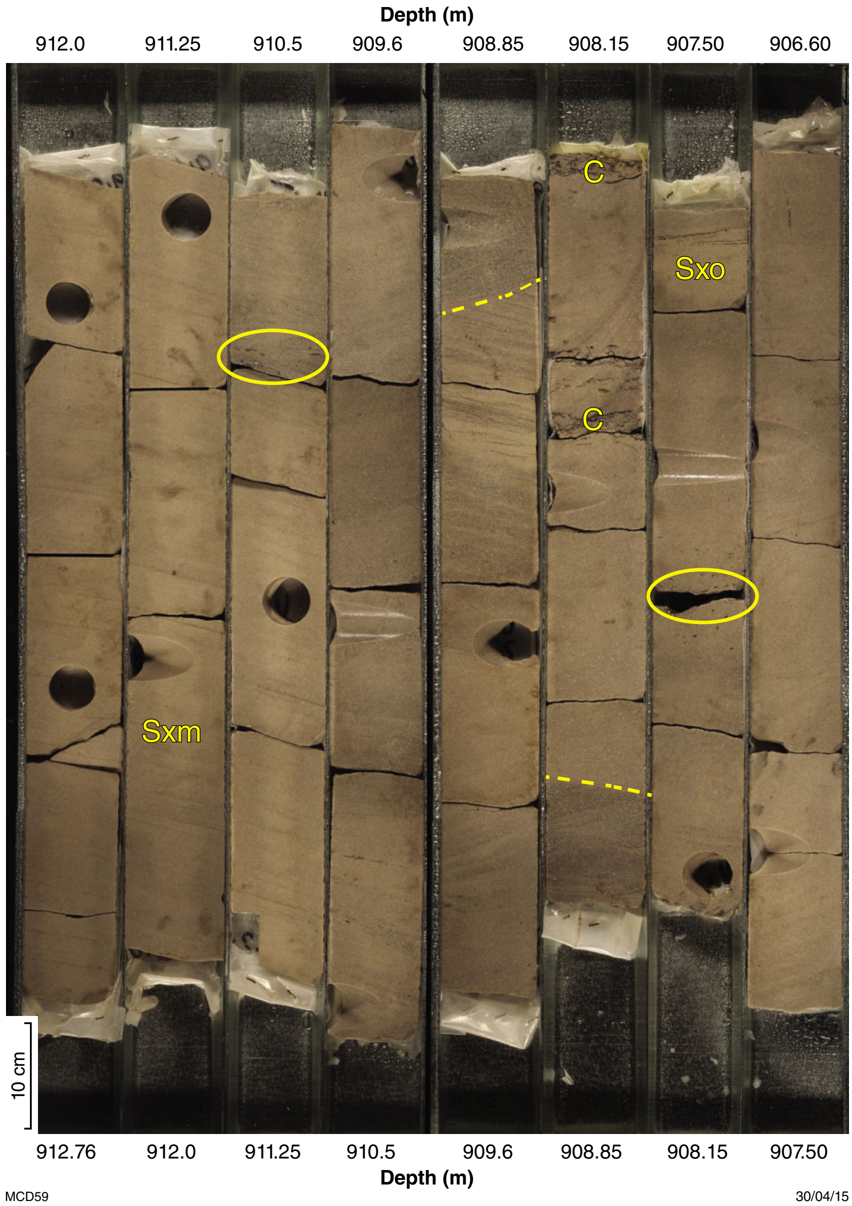

Figure 28. Core photos of well Sundown 3 for the drill section from 906.06 to 912.76 m, showing cross-bedded, fine- to medium-grained sandstones (FA1) with sharp bases (dashed lines) and local pebbly bases (circled). Thick cross-bedded sandstone (Sxm) is overlain by medium to thick cross-bedded sandstone (Sxo) with common carbonaceous flakes (C). Facies descriptions are provided in Appendix 4.

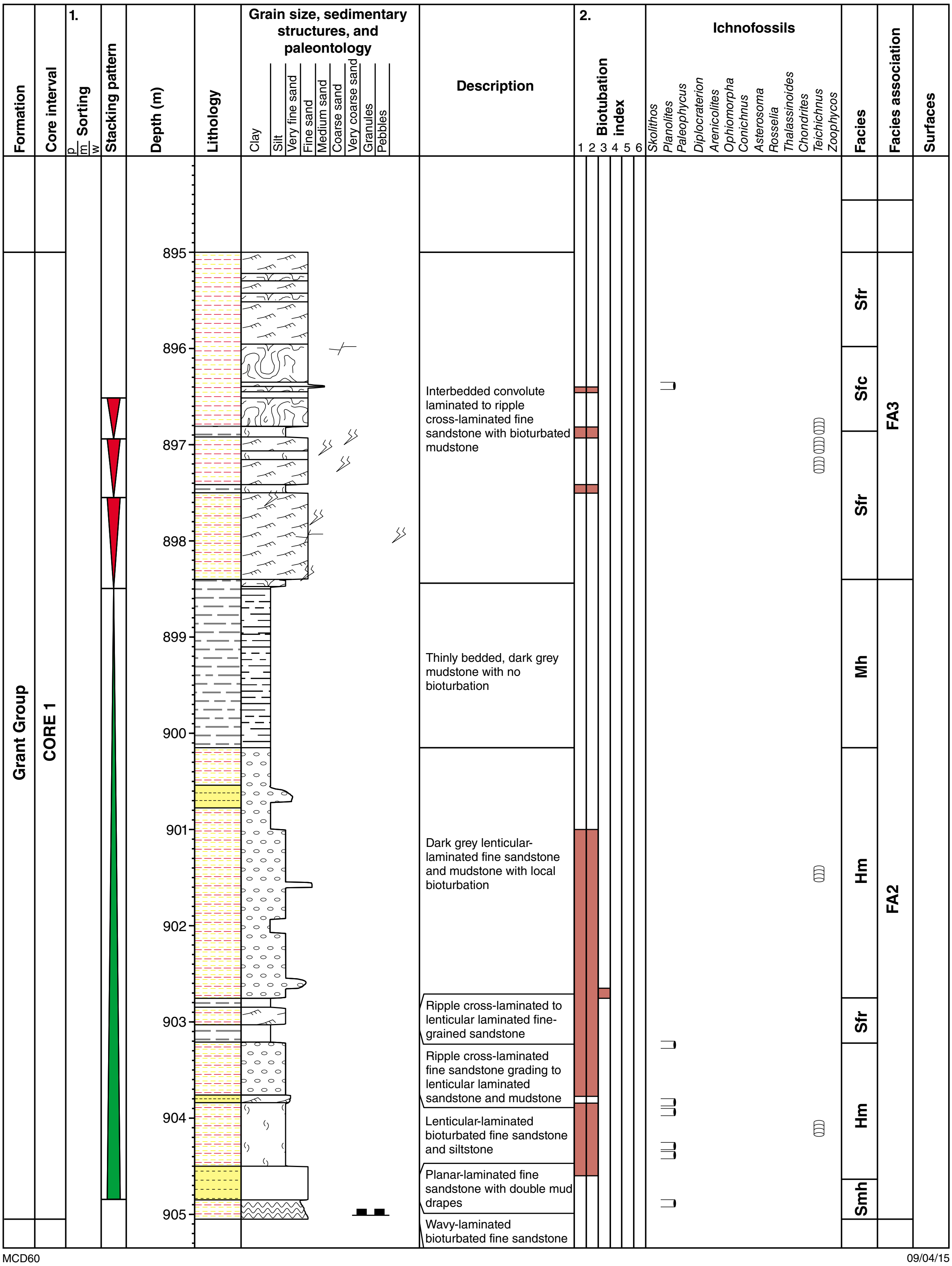

1. Sorting description abbreviations: p = poor, m = moderate, w = well-sorted
2. Bioturbation index follows the scheme presented by Tucker (2011)

Figure 29. Core log of well Sundown 3, core 1, showing arrangement of heterolithic sandstone–mudstone (FA2) and fine-grained sandstone (FA3). The trace fossil *Teichichnus* indicates marine influence. Facies descriptions are provided in Appendix 4.

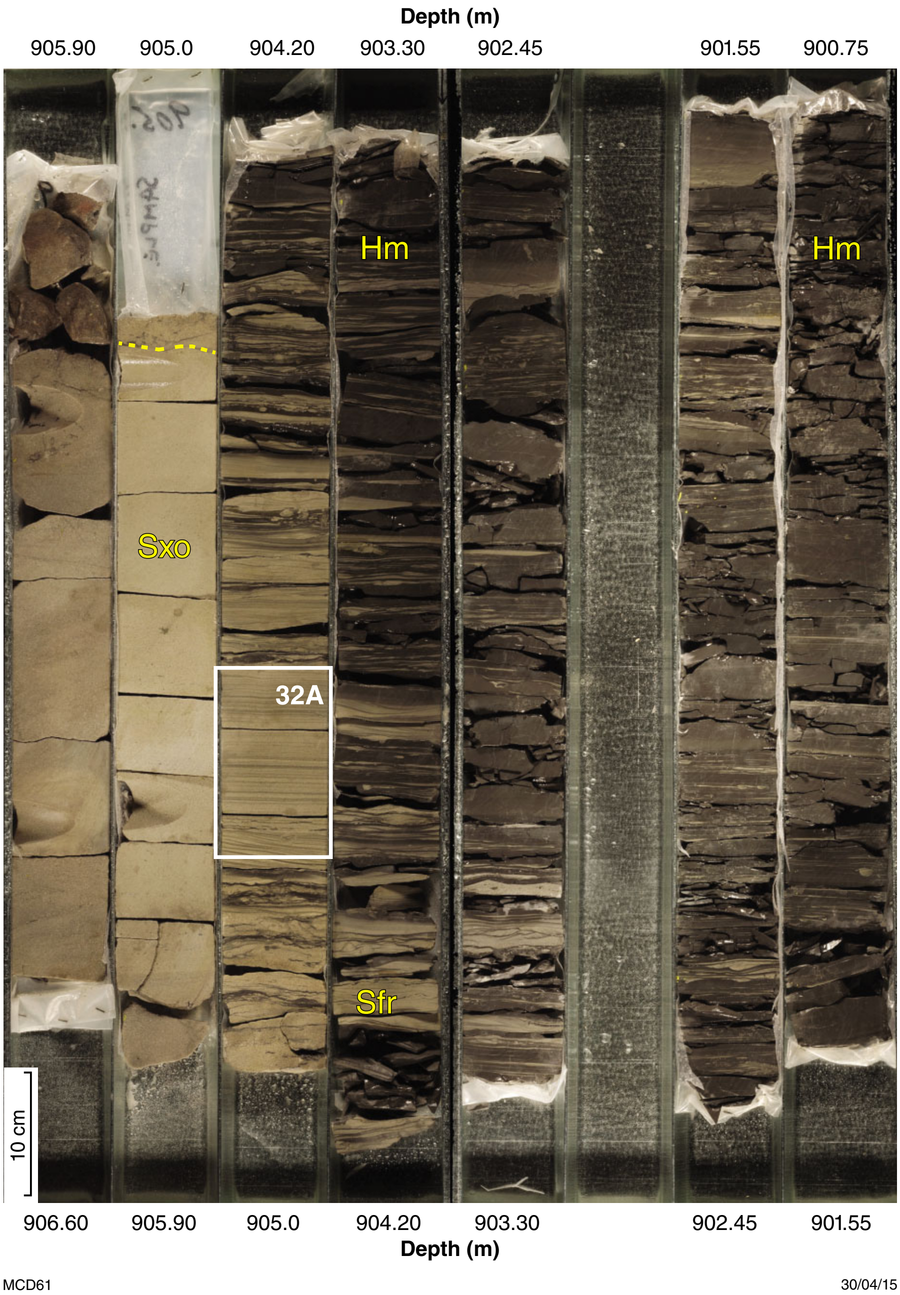

Figure. 30. **Core photos of well Sundown 3 for drill section from 900.75 to 906.06 m, showing heterolithic ripple cross-laminated sandstone–mudstone facies (FA2) overlying cross-bedded sandstone facies (FA1) at 905.05 m. Inset 32A depicts laminated sandstone shown in detail in Figure 32A. Facies descriptions are provided in Appendix 4.**

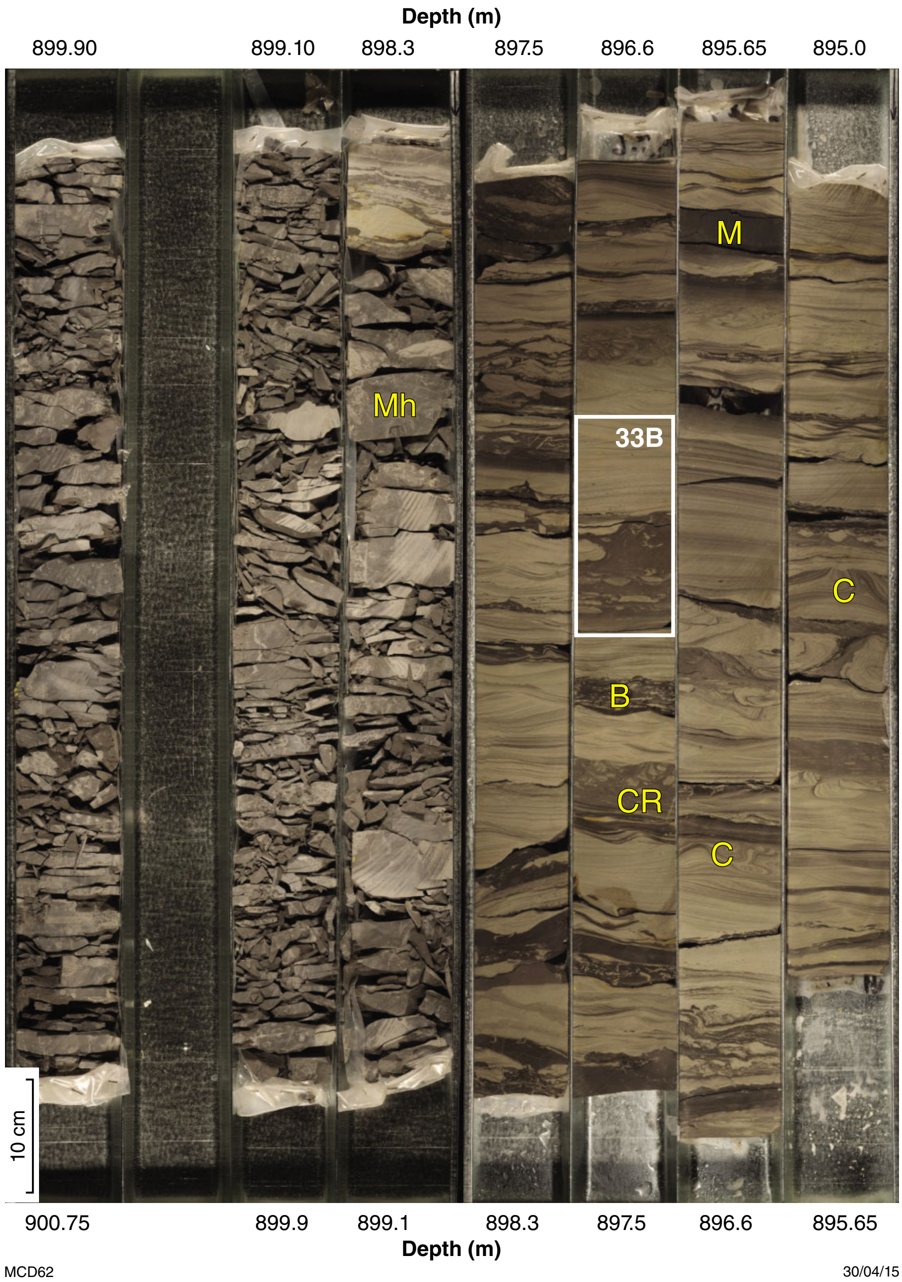

Figure 31. **Core photos of well Sundown 3 for drill section from 895 to 900.75 m, showing heterolithic sandstone–mudstone facies (FA2) and ripple cross-laminated, fine-grained sandstone–mudstone facies (FA3). The upper part is dominated by sandstone with convolute lamination (C, facies Sfc), ripple cross-lamination and climbing ripple cross-lamination (CR, facies Sfr), and bioturbated mudstone (B). Mudstone with no bioturbation (M) is minor. Syneresis cracks are abundant and indicate changes in salinity most likely from freshwater input. The lower part of the core is composed of mudstone with no bioturbation (Mh). Inset 33B depicts a bioturbated core interval shown in detail in Figure 32 b). Facies descriptions are provided in Appendix 4.**

Table 5. List of available cores from Poole Sandstone – Noonkanbah Formation in the study area

Core	*Noonkanbah Formation*	*Poole Sandstone – Noonkanbah Formation*	*Poole Sandstone*	*Nura Nura Member*	*Grant Group*
BMR Mt Anderson 1	C1–C11		C12–C15		
Dampier Downs 1	C14–C18			C19	
Frome Rocks 2	C1–2		C3-C4		
Perindi 1				C1–2	
Roebuck Bay 1	C19–C22			C23–C24	
Scarpia 1			C1		
Sundown 3					C1
The Sisters 1	C1	C2			

Table 6. Depth discrepancies in Frome Rocks 2 Well Completion Report (WCR) and cored intervals

Core	*Top WCR (m)*	*Base WCR (m)*	*Top Core (m)*	*Base Core (m)*
1	212.14	215.19	213.36	216.41
2	334.37	337.41	334.97	338.03
3	456.59	459.64	457.2	460.25
4	631.55	634.59	630.93	633.98

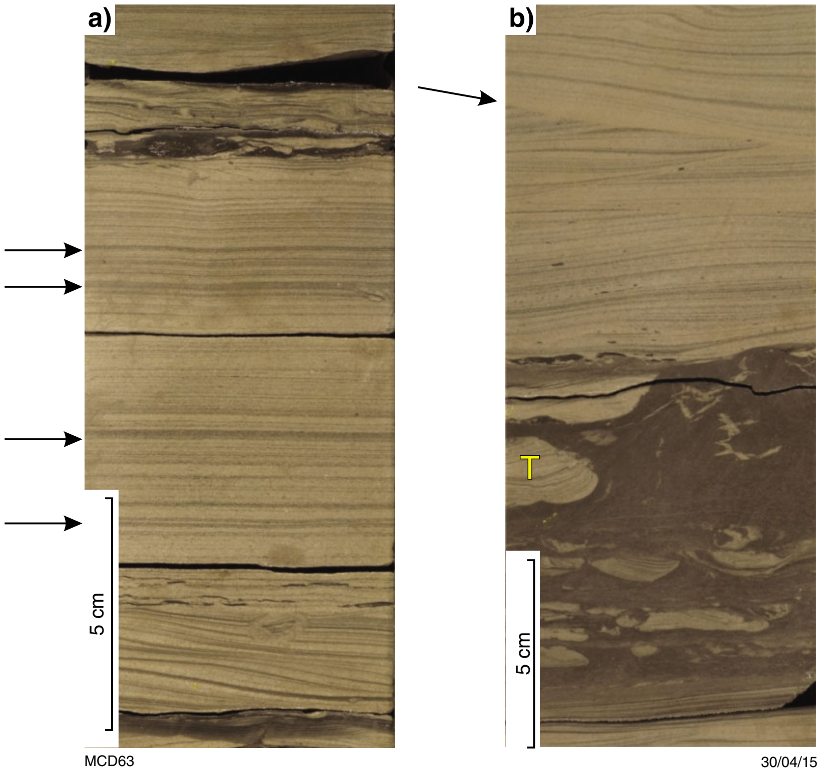

Figure 32. Core photos showing details of heterolithic sandstone–mudstone (Fig. 30) and ripple cross-laminated, fine-grained sandstone (Fig. 31). A) Fine-grained sandstone with double mud drapes suggesting tidal influence. B) Bioturbated mudstone with *Teichichnus* (T) trace fossil is truncated and overlain by fine sandstone with double mud drapes (arrows). A shallower erosion surface (arrow) truncates these strata and is overlain by facies similar to those in Figure 32a).

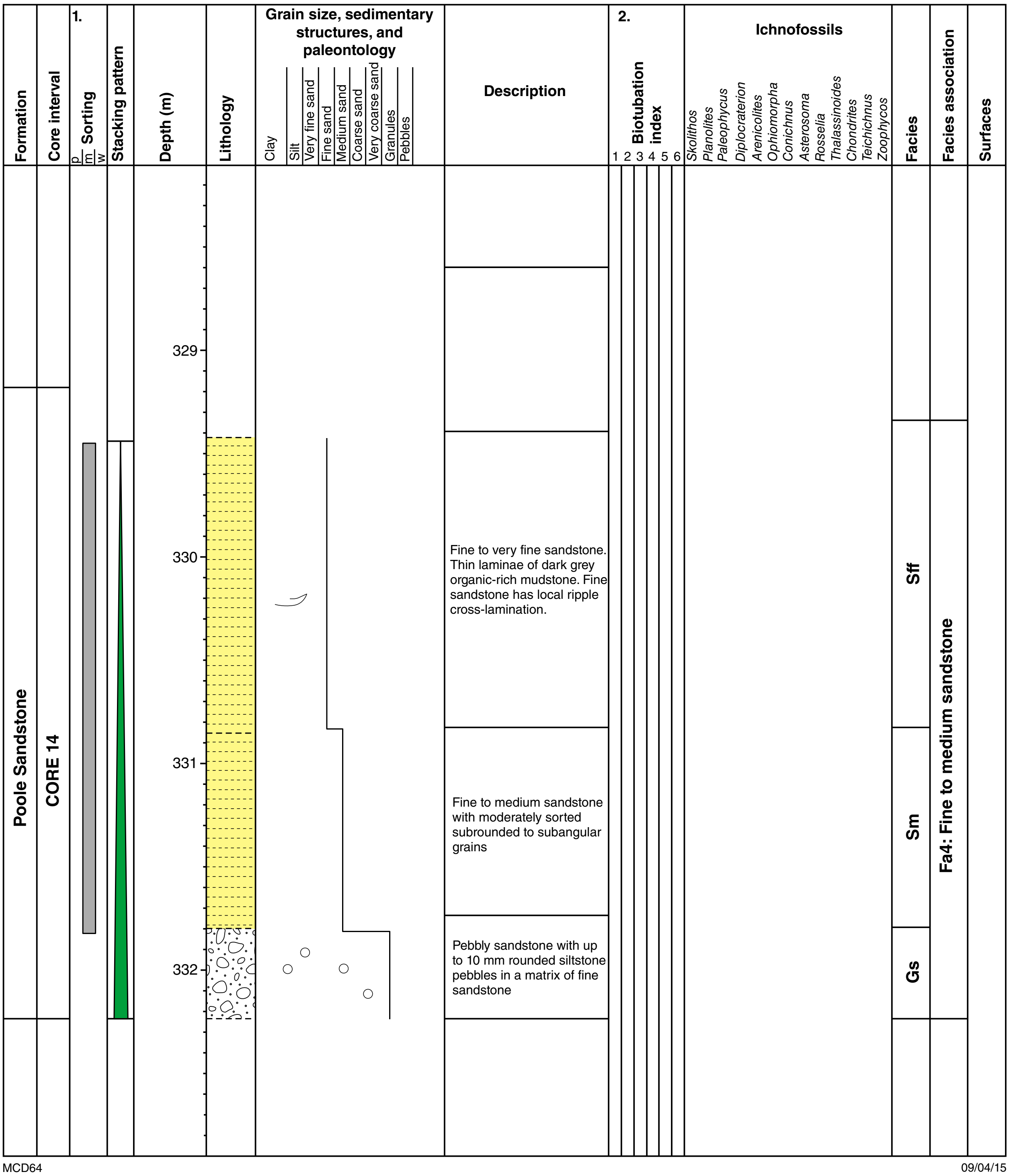

1. Sorting description abbreviations: p = poor, m = moderate, w = well-sorted

2. Bioturbation index follows the scheme presented by Tucker (2011)

Figure 33. Core log of well Dampier Downs 1, core 14, showing the fining-upward arrangement of the conglomeratic and sandstone facies in FA4. Facies descriptions are provided in Appendix 4.

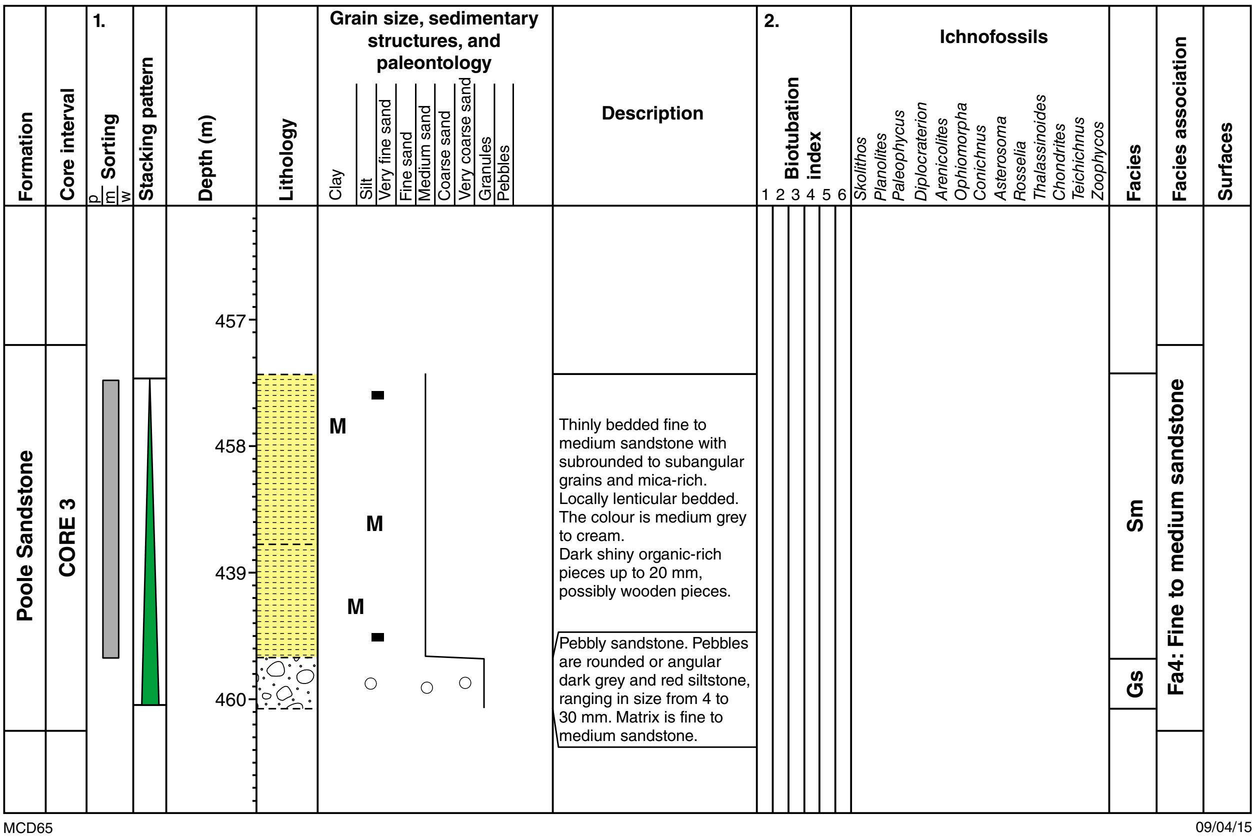

1. Sorting description abbreviations: p = poor, m = moderate, w = well-sorted
2. Bioturbation index follows the scheme presented by Tucker (2011)

Figure 34. Core log of FA4 in well Frome Rocks 2, core 3, showing the fining-upward arrangement of the conglomeratic and sandstone facies in FA4. Facies descriptions are provided in Appendix 4.

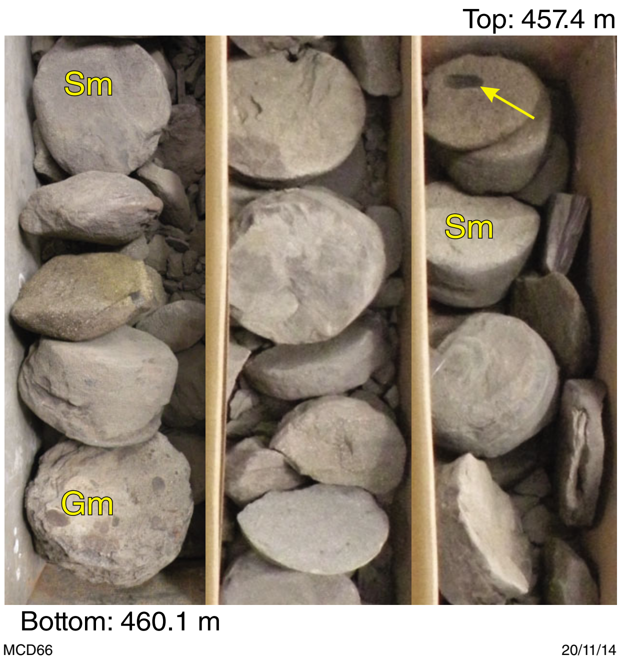

Figure 35. Core photos of well Frome Rocks 2, core 3, showing facies of FA4. Note fragmented organic matter (arrow). Gm and Sm facies descriptions are provided in Appendix 4.

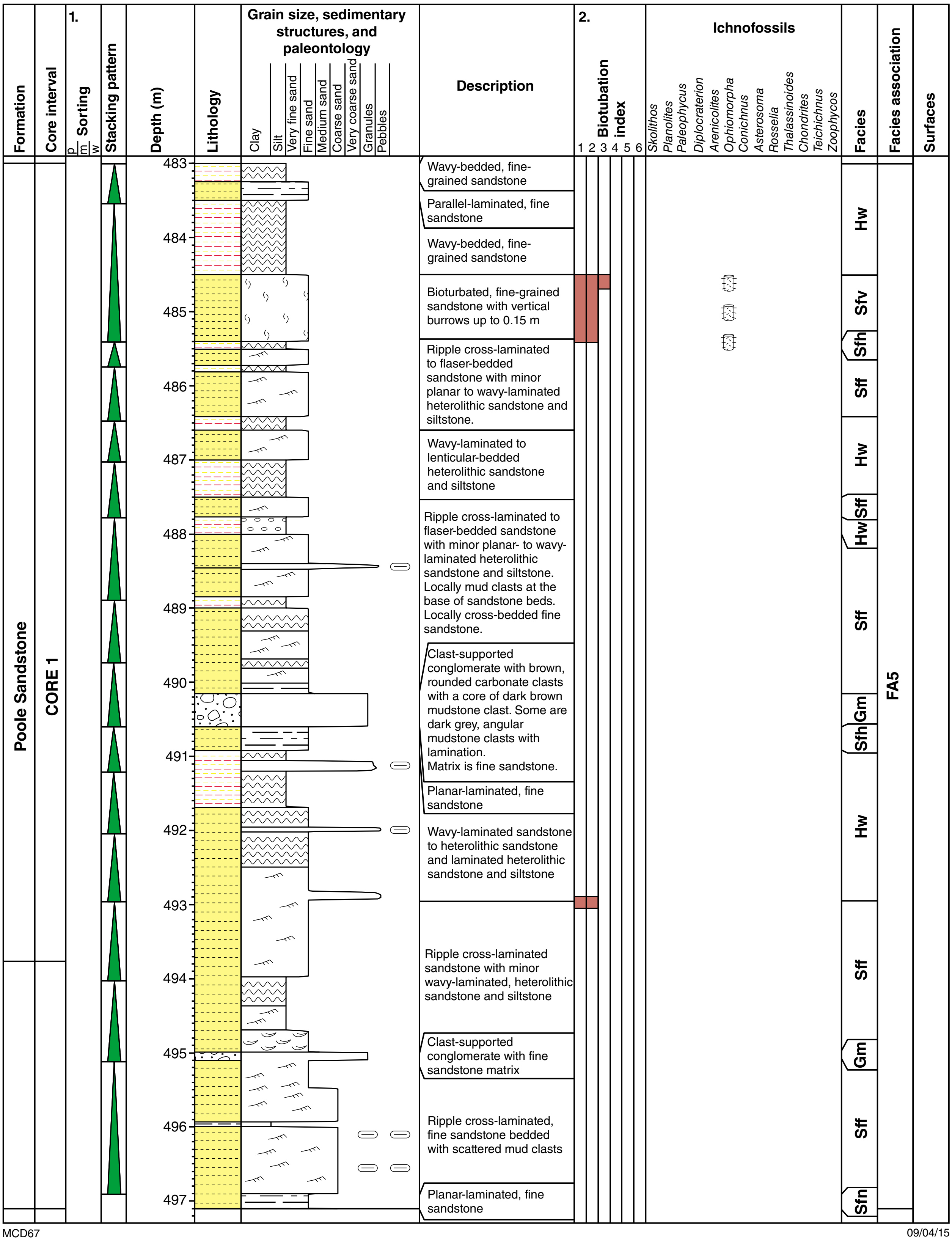

1. Sorting description abbreviations: p = poor, m = moderate, w = well-sorted

2. Bioturbation index follows the scheme presented by Tucker (2011)

Figure 36. Core log of well Scarpia 1, core 1, showing stacked fining-upward facies patterns of the conglomeratic, sandstone and heterolithic facies in FA5. Facies descriptions are provided in Appendix 4.

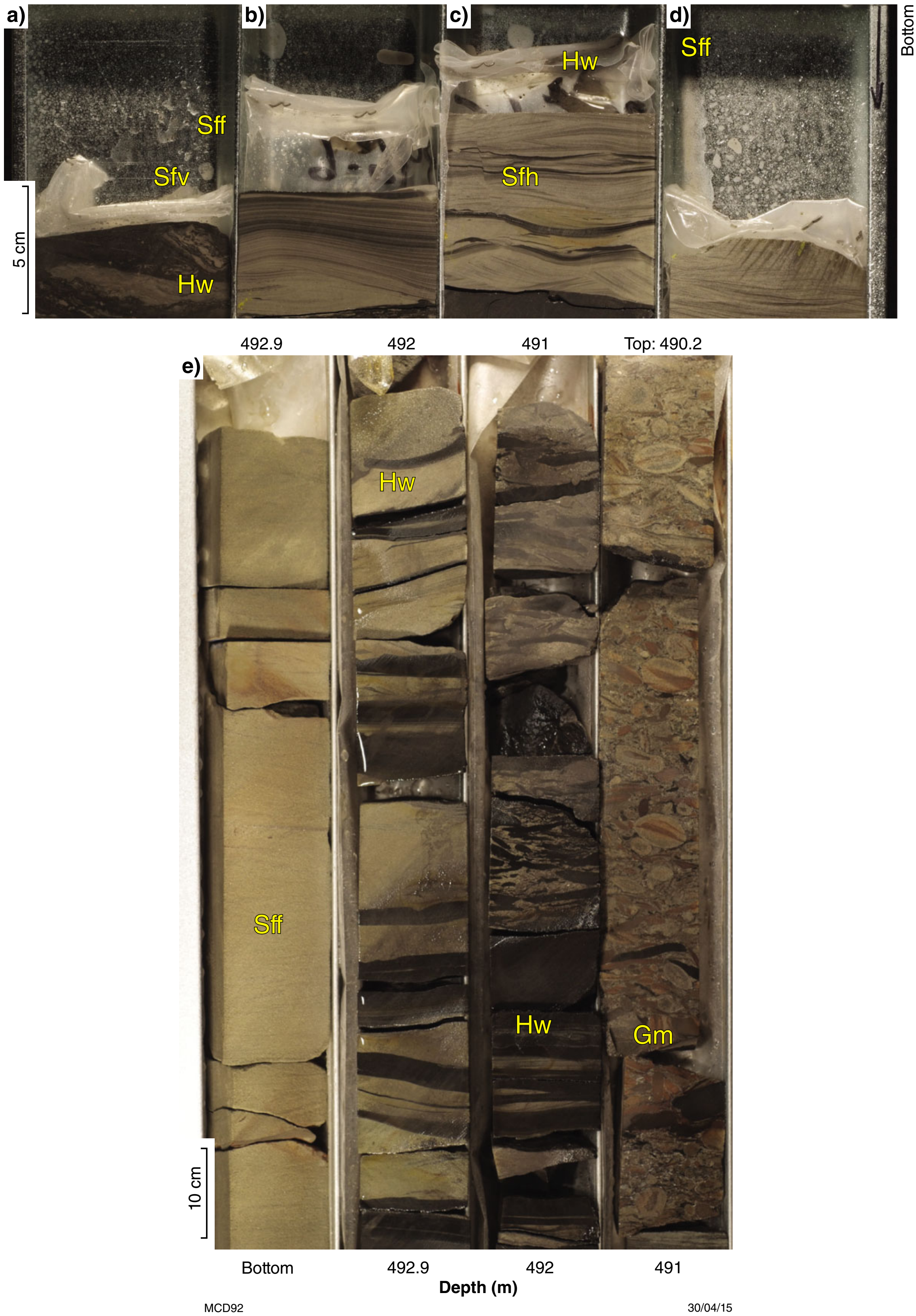

Figure 37. Core photos of well Scarpia 1, core 1, showing various facies in FA5. Conglomeratic facies (Gm) is interpreted as minor channel fill. Heterolithic (Hw) and sandstone facies (Sfh and Sff) suggest deposition on tidal flats. Facies descriptions are provided in Appendix 4.

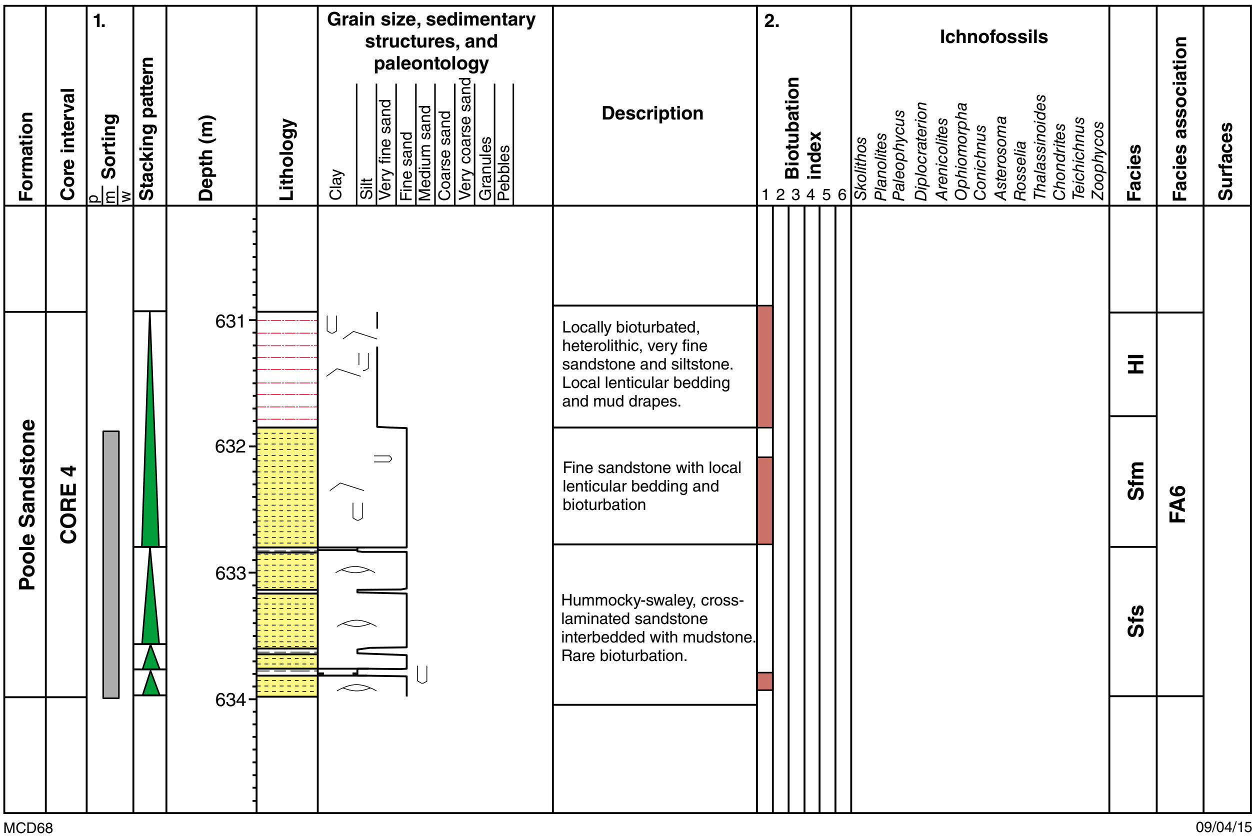

1. Sorting description abbreviations: p = poor, m = moderate, w = well-sorted

2. Bioturbation index follows the scheme presented by Tucker (2011)

Figure 38. Core log of well Frome Rocks 2, core 4, showing fining-upward arrangement of hummocky cross-laminated fine sandstone (Sfs), fine sandstone (Sfm) and heterolithic sandstone–siltstone (Hl) in FA6. Facies descriptions are provided in Appendix 4.

Depositional setting

The three Grant Group facies associations in Sundown 3 are interpreted as fluvial channel fills (FA1) and sandy tidal flat environments with marine influence (FA2 and FA3). In well completion reports, this cored interval was previously included in the Poole Sandstone. However, the proposed unconformity with the underlying Grant Group is not obvious in the core (Fig. 28) and correlation favours its assignment to the Grant Group (Fig. 48). The marine influence in the uppermost Grant Group in Sundown 3 is consistent with marine deposition recognized in the Carolyn Formation on the Lennard Shelf and adjacent Fitzroy Trough (Mory, 2010 and references therein).

Facies associations in the Poole Sandstone are interpreted to represent four major depositional environments and are consistent with fluvio-deltaic systems (e.g. Bhattacharya, 2010). Fluvial channel fills (FA4) are the most proximal environment represented. The second significant environmental setting is tidal flats with minor channels (FA5). Heterolithic sandstone–mudstone with hummocky cross-laminated (FA6) and skeletal rudstone–grainstone (FA7) indicate deposition between fair weather and storm wave base. Evidence for marine deposition is most clearly represented by the carbonate facies of FA7, hummocky, cross-laminated facies of FA6 and tidally influenced facies with bioturbation in FA5.

FA8 and FA9 of the Noonkanbah Formation are heterolithic sandstone–mudstone of the lower shoreface to offshore transition. Where cored, the boundary with the underlying Poole Sandstone is transitional, as seen in The Sisters 1 between FA5 and FA9 (Figs 45 and 47).

Synthesis

Depth and thickness of the Poole Sandstone and Noonkanbah Formation vary across the study area (Table 7) in association with the structural division boundaries in the northwestern Canning Basin (Fig. 48). In wells on the southwestern margin of the Fitzroy Trough (Jurgurra Terrace and Broome Platform), the Noonkanbah Formation and the overlying Upper Permian Liveringa Group were uplifted and eroded. In contrast, the Liveringa Group is present in wells on the Lennard Shelf and Fitzroy Trough (Fig. 48). Hence, much of the significant thickness change in the Noonkanbah Formation is a result of uplift and erosion during Mesozoic transpression. At a depth of 828 m the top of the Poole Sandstone is deepest in well Perindi 1 (offshore) (Table 7).

Figure 39. Core photos of well Frome Rocks 2, core 4, showing sandstone (Sfs, Sfm) and heterolithic (Hl) facies in FA6. Note hummocky cross-lamination at the bottom of the core shown in the inset. Length of core boxes is 1 metre. Facies descriptions are provided in Appendix 4.

Correlation of well logs, with some control provided by facies associations, shows distinctive coarsening-upward facies trends in the Poole Sandstone in all wells (Fig. 48). Cored intervals with fluvial channel fills (FA4) at the top of these coarsening-upward trends and storm-influenced offshore transition facies associations (FA6 and FA8; e.g. in Dampier Downs 1 and Frome Rocks 2) indicate that these trends record delta progradation. This setting is best recorded in the Jurgurra Terrace and Broome Platform wells. It is potentially also present in the Sundown wells on the Lennard Shelf, although these wells were not cored through this interval (Fig. 48).

In contrast, the wells in the Fitzroy Trough close to the Lennard Shelf south of the Sundown Field show more poorly defined coarsening-upward trends dominated by much finer grained facies on well logs (Fig. 48). Heterolithic tidal flat deposition (FA5, lower delta plain) is present in cored intervals, such as in Scarpia 1 and The Sisters 1. In The Sisters 1, the transitional boundary with the overlying offshore facies association (FA9) of the Noonkanbah Formation was cored (Figs 45 and 47). The facies associations of the Noonkanbah Formation (FA8 and FA9) are distributed across all the structural divisions (Fig. 48), indicating widespread marine flooding in the late Early Permian (Fig. 6).

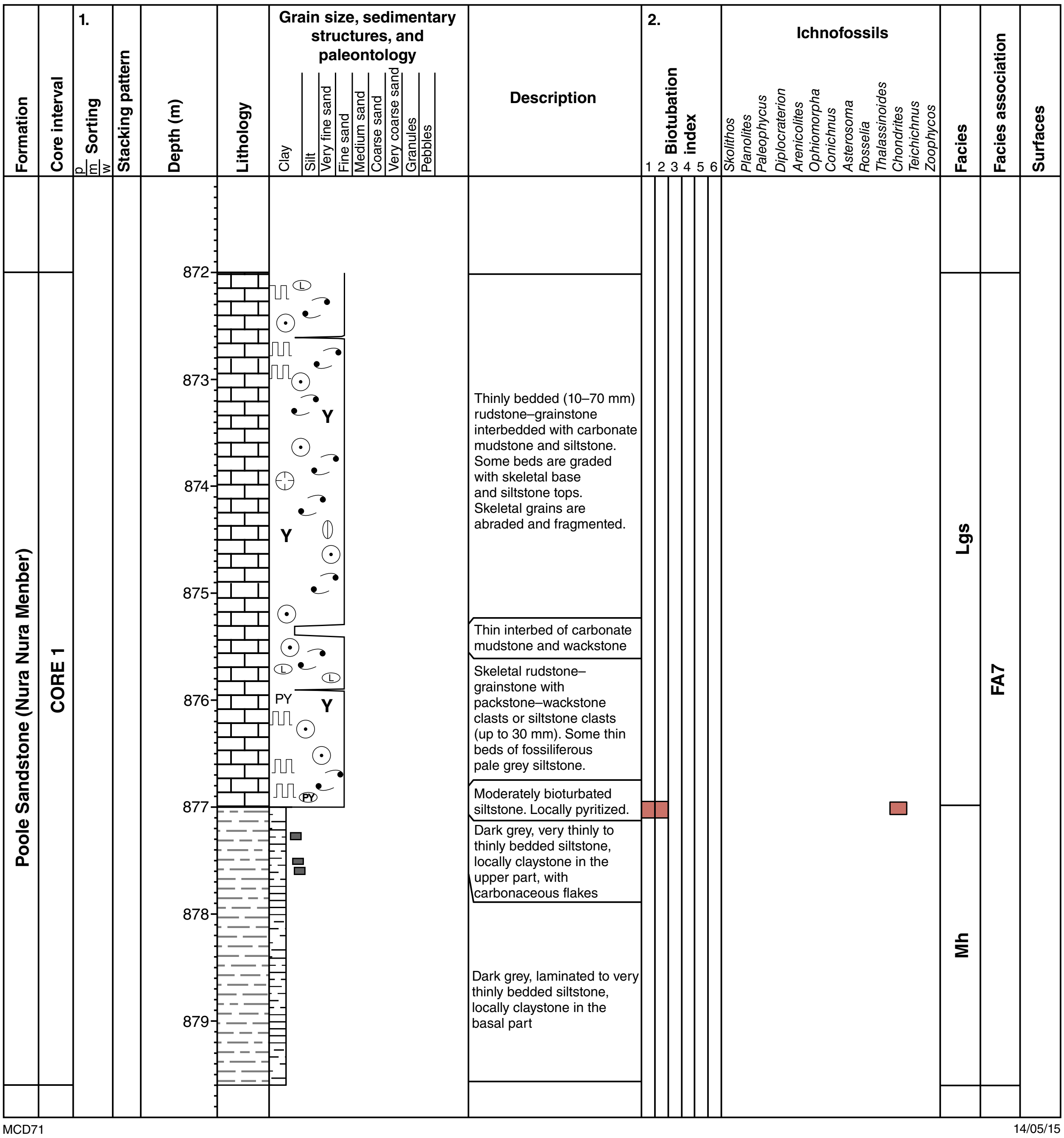

1. Sorting description abbreviations: p = poor, m = moderate, w = well-sorted

2. Bioturbation index follows the scheme presented by Tucker (2011)

Figure 40. Core log of well Perindi 1, core 1, showing arrangement of mudstone (Mh) and limestone (Lgs) facies in FA7. Facies descriptions are provided in Appendix 4.

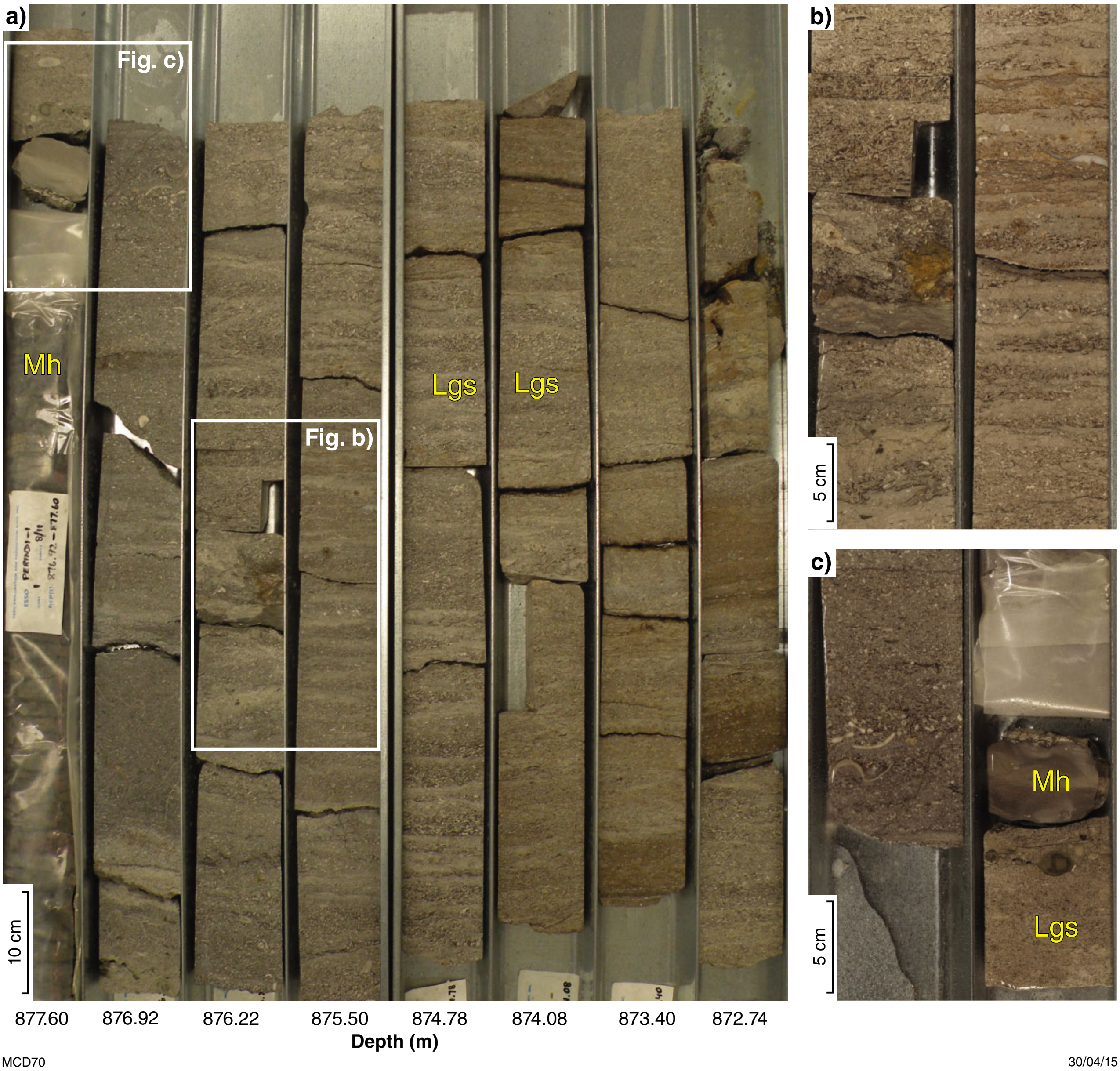

Figure 41. **Core photos of FA7. A) Facies skeletal rudstone–grainstone (Lgs) and siliciclastic mudstone (Mh). Core depths are shown in metres. B) Details of facies Lgs with skeletal grains and thin beds, alternating from fossiliferous to fine-grained non-fossiliferous. C) Facies Mh at the contact with facies Lgs is bioturbated. Facies descriptions are provided in Appendix 4.**

The carbonate-dominated facies of FA8 (Nura Nura Member) were deposited in marine areas away from major siliciclastic supply that were most likely topographic highs at that time, e.g. northern Broome Platform (Roebuck Bay 1) and Pender Terrace (Perindi 1; Fig. 48). In these wells the Poole Sandstone is dominated by fine-grained facies (high GR values; Fig. 48) with only minor sandstone.

Implications for geosequestration

Grant Group

FA1 and FA2 are suitable reservoir units for CO_2 storage because they are composed of massive, planar- and cross-laminated sandstone facies with good to very good overall porosity and permeability despite compaction and several phases of cement precipitation. Both associations form very thick intervals of sandstone that create potential for high capacity storage space. Sandy low sinuosity systems may be extensive and the recognition of similar facies associations across the study area suggests potential for broad lateral distribution of the reservoir units FA1 and FA2. Lateral distribution will play a significant role in determining the region's reservoir capacity and economic suitability for sequestration (Kovscek, 2002). Additionally, in Fraser River 1 intercalated thinner intervals of siltstone and heterolithic facies in FA1 are likely to increase reservoir heterogeneity, which is known to increase lateral distribution of CO_2 in the reservoir and therefore overall capacity (Chadwick et al., 2004; Torp and Gale, 2004).

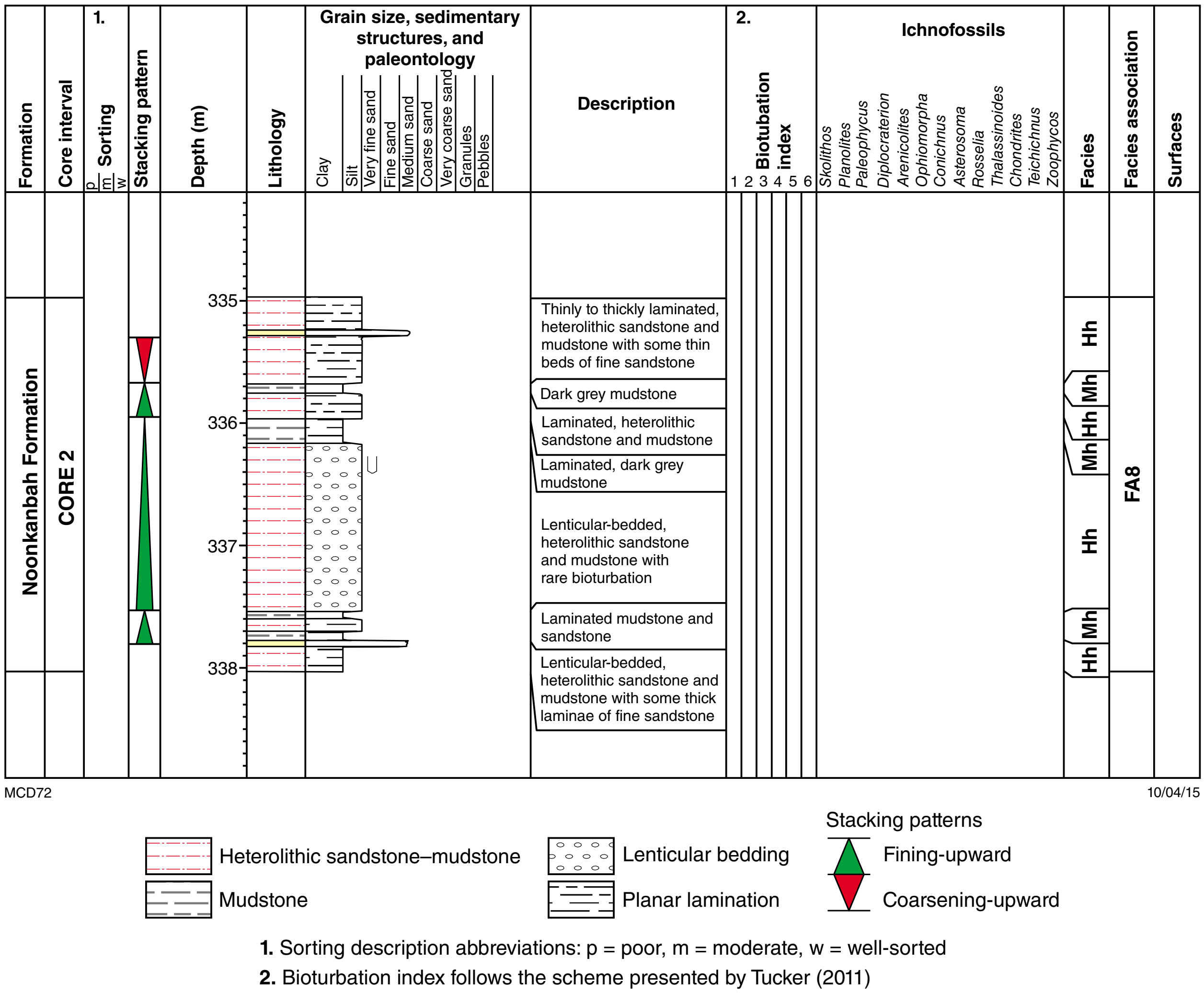

Figure 42. Core log of well Frome Rocks 2, core 2, showing arrangements of heterolithic (Hh) and mudstone (Mh) facies in FA8. Facies descriptions are provided in Appendix 4.

Storage is further constrained by the presence and depth of seals. CO_2 is naturally buoyant and will rise vertically once injected into the reservoir (Wollenweber et al., 2010). Consequently, a seal must overlie the reservoir at or below the supercritical depth. The only well containing a seal (FA3) is Fraser River 1 (between 936 and 1036.7 m). FA3 is entirely composed of mudstone overlying suitable reservoir facies (FA1) below the supercritical depth (Table 6). This is advantageous as both features provide a good barrier against leakage by diffusion, a common concern for caprocks (Li et al. 2006). FA2 that overlies FA3 in Fraser River 1 lacks a seal and extends above the supercritical depth, rendering it unsuitable for storage.

Examination of the Grant Group in wells near Fraser River 1 suggests that similar seals are more widely developed. On the northeastern side of the Fitzroy Trough (Fig. 4), for example, Jum Jum 1 has thick mudstone intervals between 1650 m and 1730 m depth and in Booran 1 mudstone ranges from a depth of 1650 m to 1750 m (Powis, 1986; ESSO, 1982; Fig. 4). Further analyses of the lateral extent and geochemical and geomechanical characteristics of potential seals are required.

In the other wells seals are not cored but potential intervals have been described in well completion reports. In Doran 1 a 58-m-thick mudstone interval is present between 417.5 and 475.4 m (Bird, 1968). In Frome Rocks 2, a 28-m-thick mudstone interval ranges from 830 m to 858 m (Willmott, 1959). Furthermore, a siltstone interval underlies the Poole Sandstone at approximately 608 m to 635 m. This places it above reservoir interval FA2 and below the supercritical depth for this area. The quality and vertical and lateral extent of the mudstone intervals in both wells require further evaluation to determine their suitability as seals.

Poole Sandstone

The most striking feature of the cored intervals through the Poole Sandstone in the study area is the dominance of heterolithic facies with lesser proportions of coarser grained sandstone. This contrasts with Poole Sandstone that crops out to the southeast in the Fitzroy Trough that is considerably more sandstone-dominated (Mory, 2010 and references therein). It suggests that local areas of higher reservoir quality are possible (e.g. FA4 fluvial

Figure 43. Heterolithic sandstone–mudstone (Hh) and mudstone (Mh) facies of FA8 in wells The Sisters 1 (left) and Frome Rocks 2 (right). Depths for top and bottom of each core are shown in metres. Facies descriptions are provided in Appendix 4.

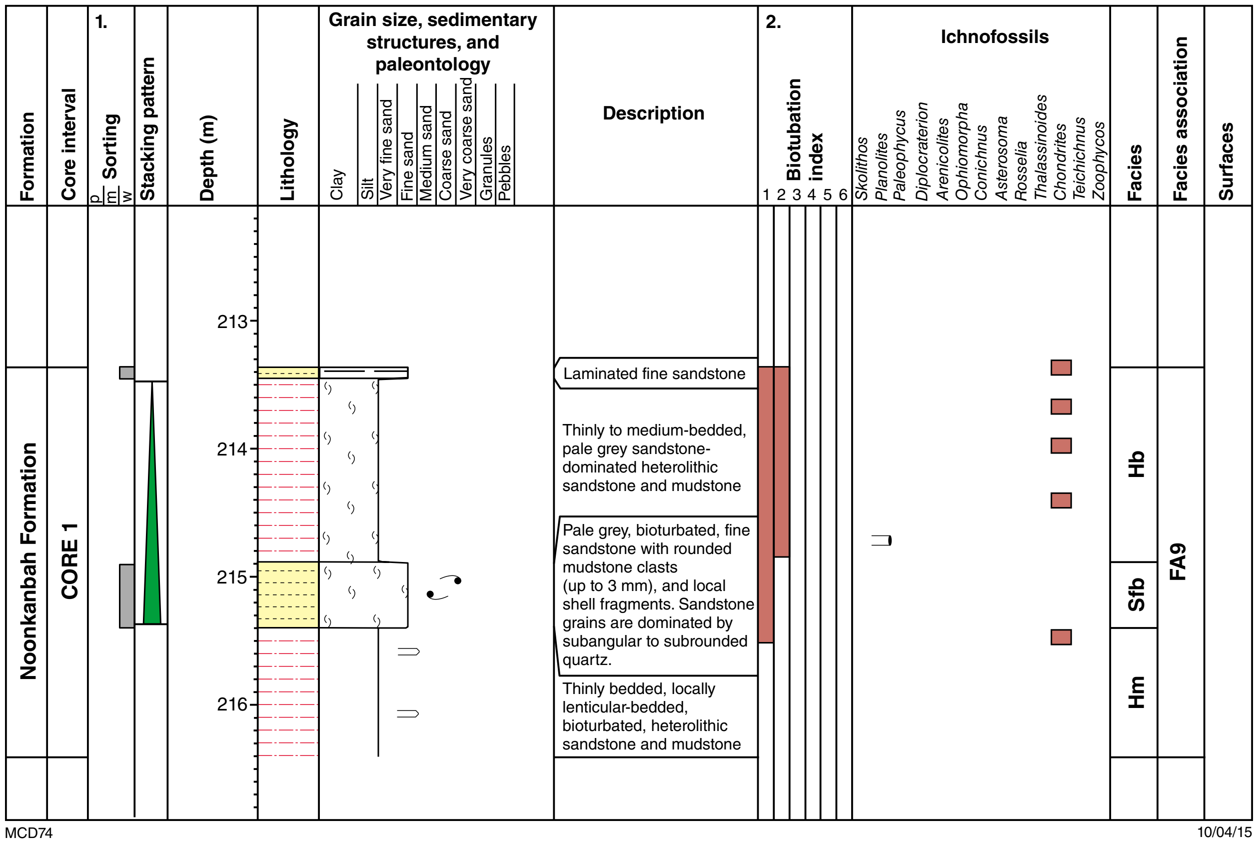

1. Sorting description abbreviations: p = poor, m = moderate, w = well-sorted

2. Bioturbation index follows the scheme presented by Tucker (2011)

Figure 44. Core log of well Frome Rocks 2, core 1, showing fining-upward facies arrangement of sandstone (Sfb) and heterolithic (Hm, Hb) facies in FA9. Facies descriptions are provided in Appendix 4.

channel fills) but that areas with thick heterolithic facies associations are likely to have poor reservoir quality overall. Heterolithic siliciclastic and carbonate facies recording tidal flat deposition on the delta plain (FA5) and offshore storm-influenced deposition (FA6 and FA7) are recognized.

The top of the Poole Sandstone is deepest in Perindi 1 (828 m; Table 7). Nevertheless, as described above, this formation has a muddy carbonate base, as seen in core (Fig. 40) with overlying muddy facies and it appears noticeably thin in the well log (Fig. 48). Roebuck Bay 1 (Jurgurra Terrace) shows a similar facies arrangement although the formation is thicker (Fig. 48). Other areas, including The Sisters 1 where the Poole Sandstone is relatively deep (560 m; Table 7), are likely to have poor reservoir quality based on the dominance of muddy facies as described above. The most prospective area, based on the presence of sandy facies, is the Sundown field where progradational trends to coarser grained facies are sharply overlain by potentially sealing mudstone of the Noonkanbah Formation. However, the lateral extent of these coarser facies appears to be limited to the southeast (Fig. 48).

Conclusions

In the study area the Grant Group is more prospective for CO_2 sequestration than the Poole Sandstone. The dataset available to assess sites is currently limited and additional data, including drillcore, are needed to better define reservoir quality, extent, heterogeneity, and seal characteristics. The Grant Group is largely composed of sandstones, deposited in a low sinuosity fluvial system, that retain good to very good porosity and permeability. Of the four wells with cored intervals examined, Fraser River 1 provides the most prospective sequestration site. The thick sandstone-dominated facies associations (FA1 and FA2) show potential for high reservoir capacity. It is likely that this will be a consistent aspect of the Grant Group in the Fitzroy Trough, given the importance of structural control on thickness. In addition, the prospectivity of this site is enhanced by the thick seal and underlying major reservoir interval, both lying below the supercritical depth for CO_2 sequestration.

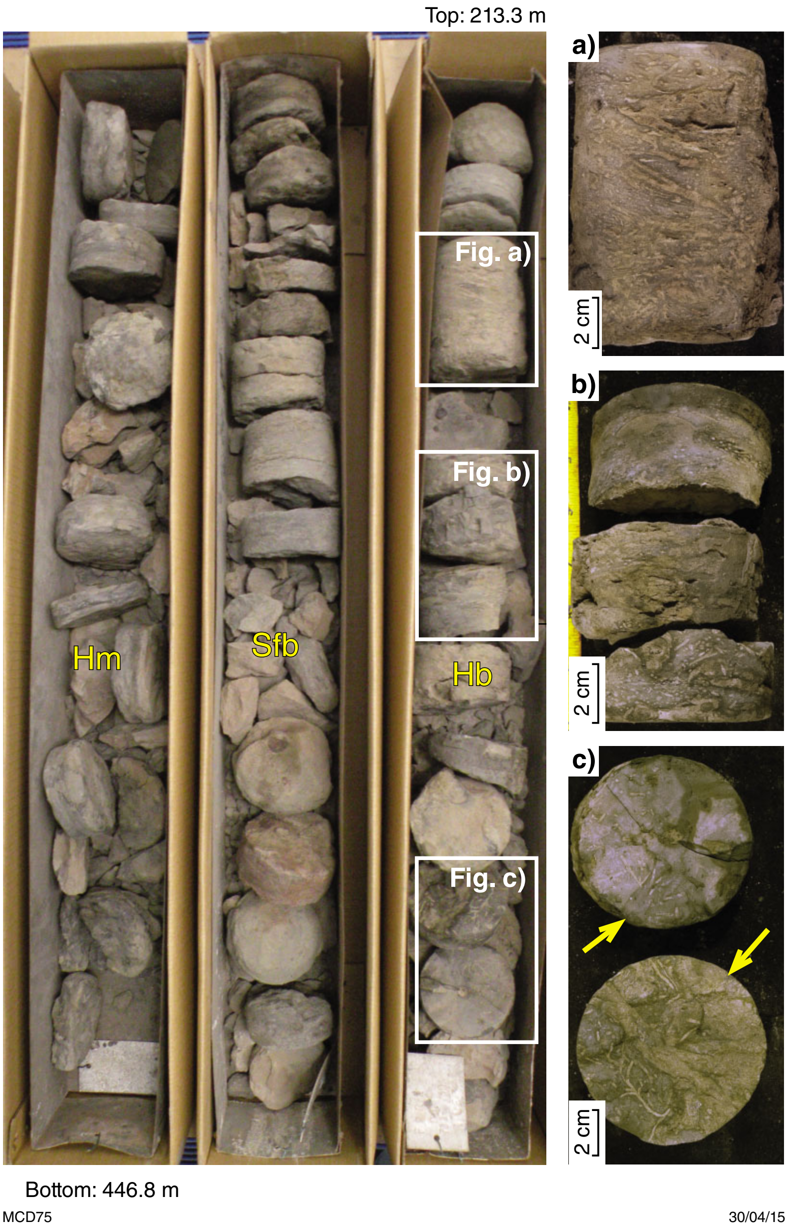

Figure 45. Core photos of Frome Rocks 2, core 1, showing, heterolithic (Hm, Hb) and fine-grained sandstone (Sfb) facies of FA9. The ichnotaxa *Chondrites* shows fine branching tubular burrows (arrow) visible on bedding planes and circular to elliptical shapes in cross-section. Length of core boxes is 1 metre. Depths for top and bottom of core are shown in metres. Facies descriptions are provided in Appendix 4.

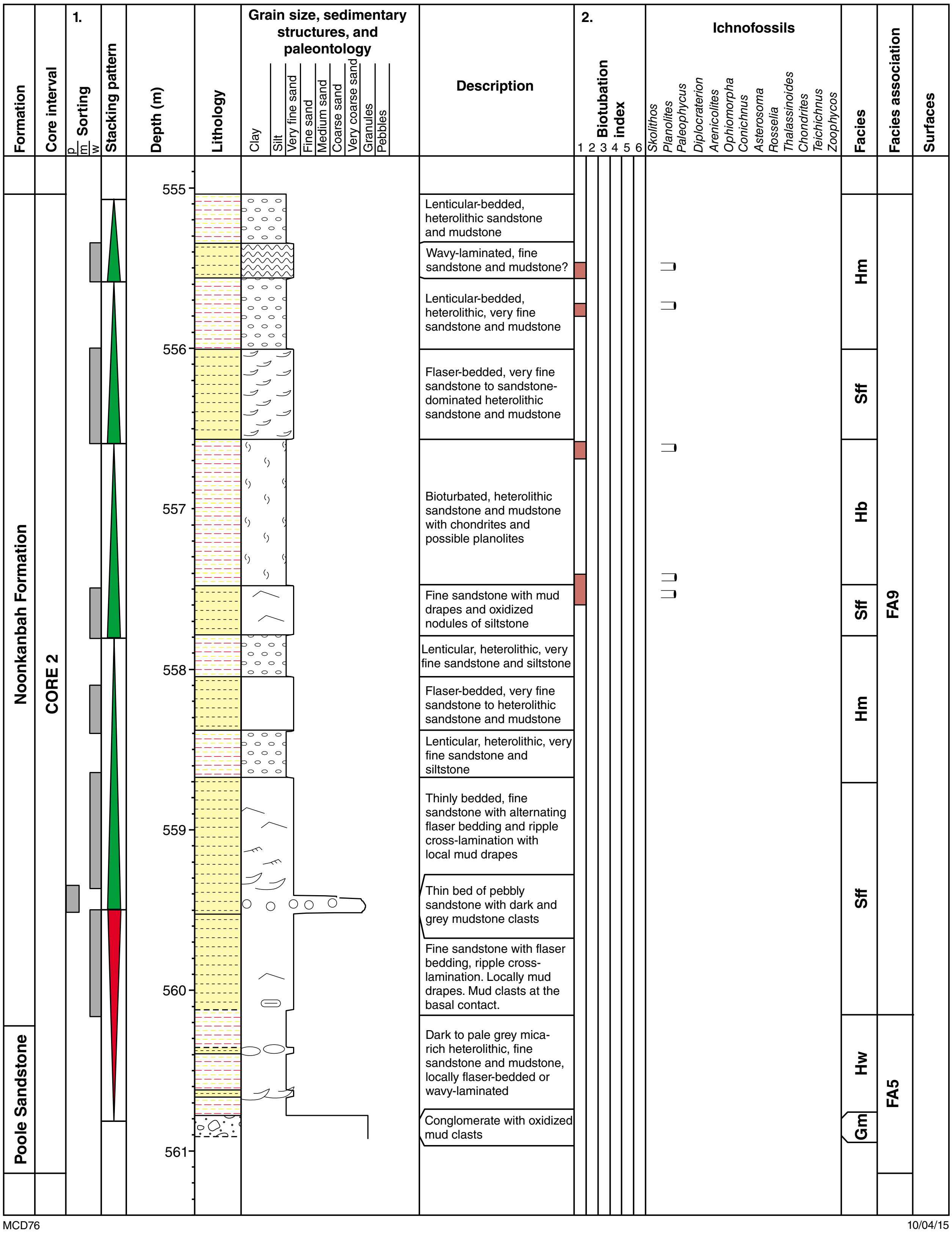

1. Sorting description abbreviations: p = poor, m = moderate, w = well-sorted

2. Bioturbation index follows the scheme presented by Tucker (2011)

Figure 46. Core log of well The Sisters 1, core 2, composed of conglomeratic and heterolithic facies of FA5, gradationally overlain by sandstone and heterolithic facies of FA9. Note predominantly fining-upward arrangements in FA9. Facies descriptions are provided in Appendix 4.

Figure 47. **Core photo of well The Sisters 1, showing heterolithic (Hm and Hb) and fine-grained sandstone (Sff) facies of FA9. FA9 gradationally overlies FA5 composed of conglomeratic (Gm) and heterolithic (Hw) facies. Depths of core top and bottom are shown in metres. Length of core boxes is 1 metre. Facies descriptions are provided in Appendix 4.**

Table 7. Top depths of lithostratigraphic units in examined wells [the upper row was extracted from the WCR of each well and the lower row from Mory (2010)]

Well	*Unconformity at top boundary*	*Overlying unit*	*Noonkanbah Formation (m)*	*Poole Sandstone (m)*		*Grant Group (m)*
				Upper Member	*Nura Nura Member*	
BMR Mount Anderson 1	?	?				
			4	318		427
Dampier Downs 1	Yes	Upper Jurassic Alexander Fm	316.08		468.78	482.19
			316	389	469	482
Frome Rocks 2	No	Lower Permian Liveringa Group	110.64	440.74	635.2	642.82
	Yes		63	539	635.2	462.8
Perindi 1	Yes	Upper Jurassic Alexander Fm	absent	828	868	877
			absent	828	867	877
Roebuck Bay 1	Yes	Upper Jurassic Alexander Fm	477.62		606.25	624.23
			477	538	606	624
Scarpia 1	No	Lower Permian Liveringa Group	158	473.4	519.3	552
			156	473		552
Sundown 3	No	Lower Permian Liveringa Group	438	779	835	904
			444	779		835
The Sisters 1	No	Lower Permian Liveringa Group	337.72	560.22		758.95
			?159	560		617

The sandstone intervals in Frome Rocks 2 also lie below the supercritical depth. However, cored intervals show significant poikilotopic calcite, forming cemented intervals up to 2.5 m thick that reduce intergranular porosity to less than 5%. Extensive cement formation could significantly compromise reservoir quality, although restriction of cements to these thin intervals in an otherwise porous and permeable interval could generate reservoir heterogeneity that serves to increase capacity (Kuuskraa et al., 2009).

The Poole Sandstone is overlain by the regionally extensive mudstone-dominated Noonkanbah Formation. It was initially proposed as a prospective reservoir–seal pair and in some areas its depth is suitable for sequestration. Well logs and cored intervals, however, highlight the dominance of heterolithic facies in the Poole Sandstone in the northwestern Canning Basin. Coarser, sandstone-dominated facies associations representing fluvial channel-fill deposits are present but they appear to be locally distributed. For example, potential coarse sandstone intervals in the Sundown area are laterally equivalent to much muddier facies in nearby well The Sisters 1 (Fig. 4). Shallower structural subdivisions of the area, such as the Jurgurra Terrace, may be more prospective.

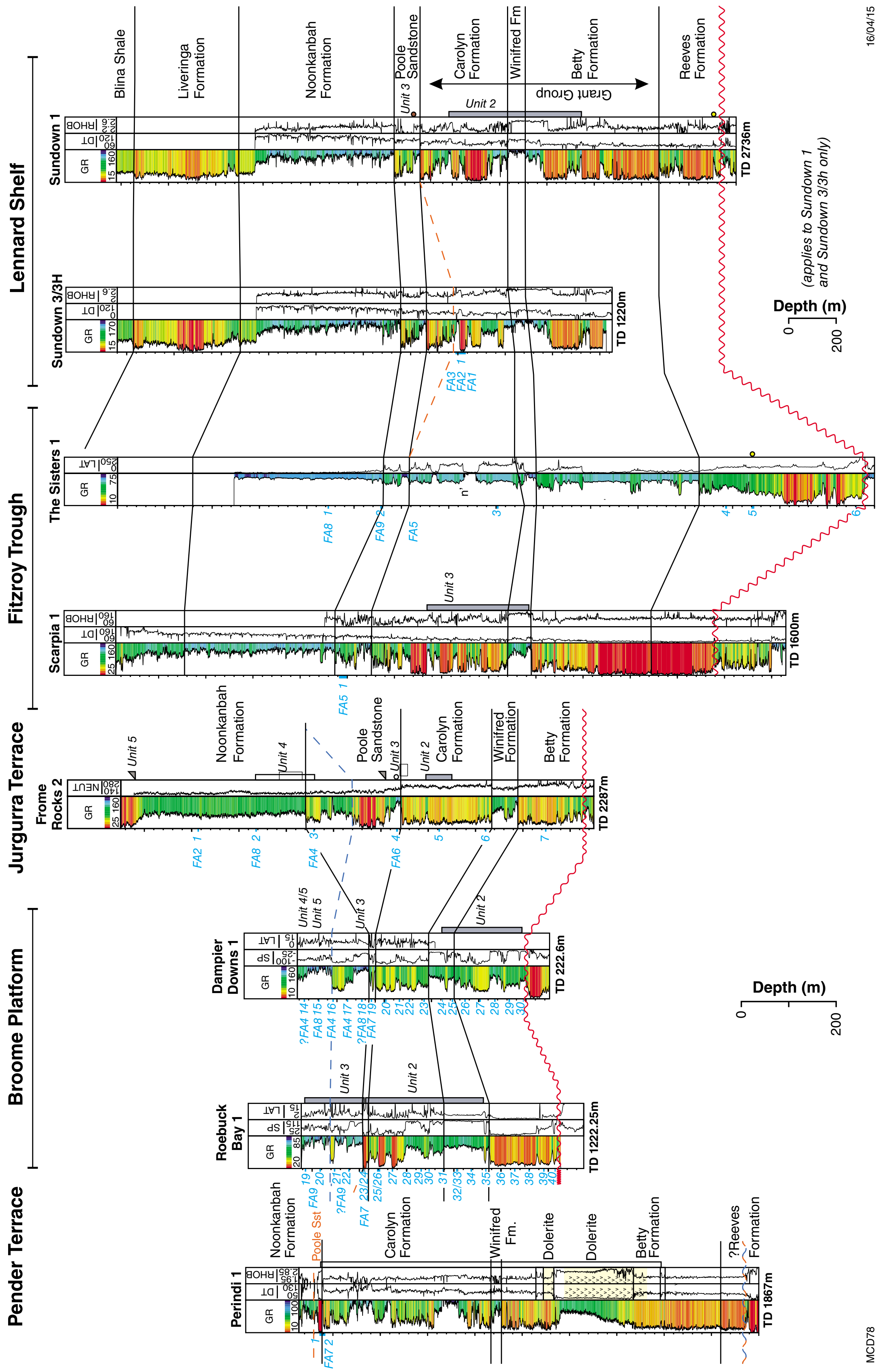

Figure 48. Correlation of well logs and facies associations across the study area using cored wells shown by black lines. Additional orange lines show correlations from well completion reports and the blue lines delineate an alternative correlation from Mory (2010).

Fault sealing characteristics

(Julian Strand, Antoine Vaslin and Laurent Langhi)

The seismic interpretation shows that the study area is heavily faulted. The areas selected as possible potential geosequestration sites comprise large fault blocks. This reduces the likelihood of compartmentalization of the reservoir by faults, at least on the scale identifiable, using the available data. However, the absence of structural closure signifies that it is important to know whether the faults bounding the blocks are likely to seal.

Fault seal prediction in mixed clastic sequences can be derived from knowledge of the clay content of the deposit. Gamma-ray logs for wells in the study area were converted into a shale volume (Vshale) for the sequence intersected by the well, using a methodology derived from Larionov (1969). Note that given the focus of the investigation to identify areas with the best sealing potential the conversion utilised was set with the aim to underestimate Vshale in order to minimize potentially over-optimistic sealing results.

To assess the sealing capacity of sand on sand-faulted juxtapositions, a number of different fault seal algorithms may be utilized. The shale gouge ratio (SGR), described by Fristad et al. (1997), Yielding et al. (1997), and Freeman et al. (1998), is an attempt to predict the proportion of shale incorporated into a fault zone. At each point on the fault, the algorithm calculates the net content of shale/clay in the volume of rock that has slipped past that point on the fault. The implicit assumption in this algorithm is that material is incorporated into the fault gouge in the same proportions as in the wall rocks in the slipped interval (Fig. 49). If this assumption is true, then SGR can provide a direct estimate of the upscaled composition of the fault zone because of the mechanical processes of faulting. A high SGR value corresponds to more phyllosilicate in the fault zone and therefore to higher capillary threshold pressure and lower permeability. Case studies by Yielding (2002), Sperrevik et al. (2002), Dockrill and Shipton (2010), Bretan et al. (2011), and Manzocchi et al. (2010) have shown that there is a general correlation between the measured clay content of a fault zone and the calculated SGR value, with higher SGR values derived from fault zones containing a higher observed clay content. In many basins, in particular the Brent Province (Yielding, 2002), a SGR of >15% corresponds to faults that are sealing hydrocarbon columns (Fig. 50).

Hence, the sealing properties of a sequence can be predicted for various fault displacements. For simple 'layer-cake' stratigraphy, the fault seal potential can be expressed as a variety of standard attributes such as SGR. Triangle, throw, or juxtaposition diagrams are a 1D graphical technique that can be used to quickly evaluate uncertainty in the stratigraphy and the V_{shale} log. The plots are essentially a 'template' on which to visualize the likely

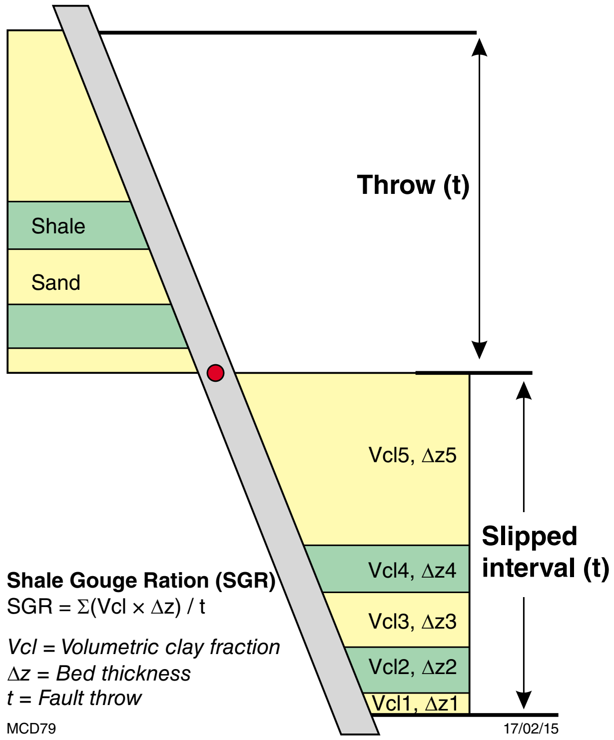

Figure 49. Schematic diagram defining the shale gouge ratio (SGR) after Yielding et al. (1997). At any point on the fault surface, the SGR is equal to the net shale (or clay, Vcl) content of the interval (t) that has slipped past that point (red dot).

juxtaposition relationships at different throws and the kind of fault seal properties that might be generated when a V_{shale} curve and well sequence slips past itself (Fig. 51). Such diagrams are very conducive for a first stage analysis of likely juxtaposition relationships and computed seal attributes for V_{shale} logs at different throws. It is useful for analyzing sparse 2D data or in cases where the structure is not reliably mapped. The technique can also be applied to investigate sensitivity issues arising from 3D fault seal analysis. A 3D structural model is not required for a triangle analysis and the seal potential can be quickly assessed based on different well logs. In hydrocarbon exploration it has become standard procedure to use fluid densities to convert SGR into column height supported (Yielding, 2002). This practice has recently been applied to CO_2 sequestration. For this procedure a density of 475 kg/m^3 for CO_2 in the supercritical state is used (Bretan et al., 2011).

Triangle plot analysis

In several of the 24 wells analyzed the potential reservoir horizons are too shallow for geosequestration. However, the results are still useful as they give an indication of lateral variations in the nature of the reservoir and its sealing properties.

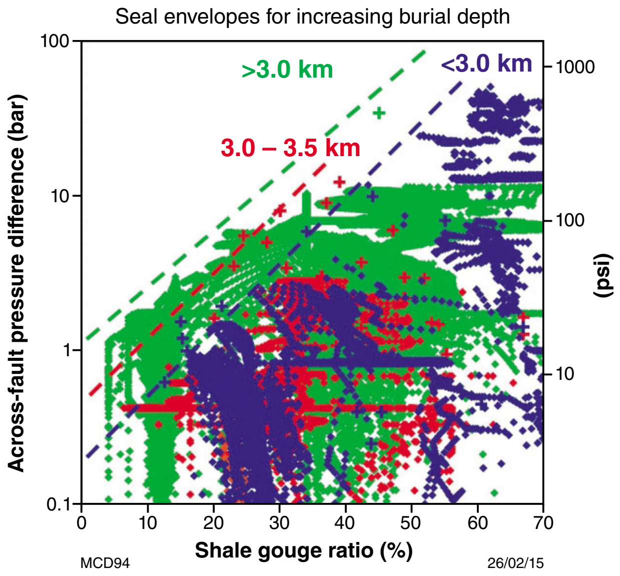

Figure 50. **Empirical approach to fault seal calibration after Yielding (2002), showing the comparison of SGR and in situ across fault pressure difference for faults in a variety of extensional basins. Data points are colour coded by burial depth (blue: <3 km, red: 3–3.5 km, green: 3.5–5.5 km). Dashed lines, i.e. the seal envelopes, represent the maximum across fault pressure that a specific SGR could support without leaking.**

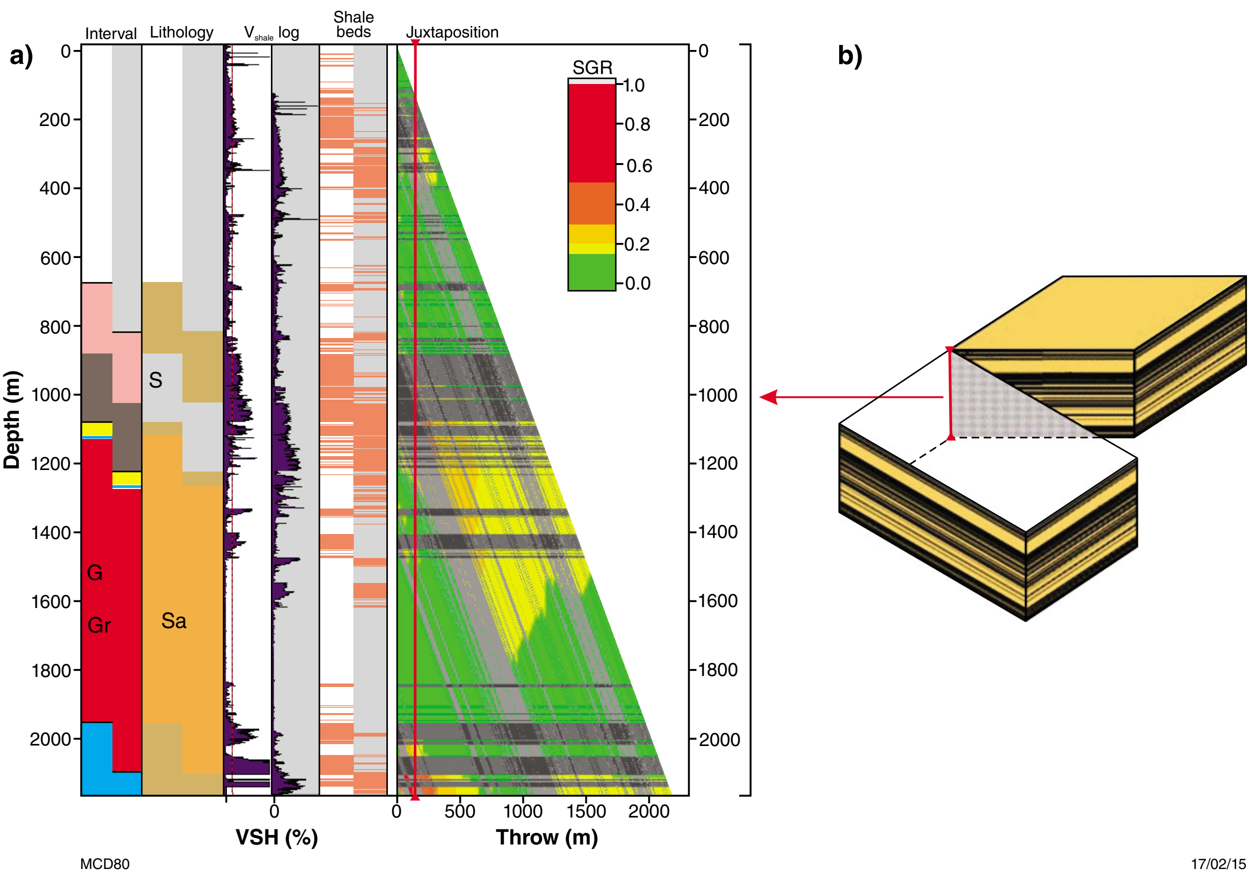

Figure 51. **Analysis of the impact of a simplistic fault on a 'layer-cake' stratigraphy, a) block diagram to illustrate the relative movement of the upthrown and downthrown blocks. The grey area in a) corresponds to the triangle diagram in b). The triangle diagram shows SGR modelled from well Moogana 1 (Pender Terrace) with an offset of 100 m.**

Pender Terrace / Lennard Shelf

Several of the wells closest to JPP are on Pender Terrace and more distant wells are situated on Lennard Shelf (Fig. 5). The wells generally intersect extensive Upper Paleozoic units, including the Noonkanbah Formation and Poole Sandstone. Across the Pender Terrace the Poole Sandstone is relatively clay-rich (commonly 15–20%).

The most westerly of the analyzed wells on Pender Terrace are offshore: Kambara 1, Minjin 1 and Perindi 1 (Fig. 52). The Noonkanbah Formation, where present in this area, is thin with low shale content. The following three wells east, Curringa 1, Moongana 1, and Pender 1, lie immediately onshore, approximately 35 km east of the offshore wells. Curringa 1 and Moongana 1 intersect Noonkanbah Formation and have good potential for top seal. The Poole Sandstone and upper Grant Group have significant shale content and consequently have some potential as a self-juxtaposition fault seal. The Pender 1 section, the most northerly assessed has middle Jurassic units deposited directly on the mid-Grant Group. By comparison to the onshore sequence, the offshore Pender Terrace shows little sealing potential.

The most easterly Pender Terrace wells assessed, Puratte 1 and Padilpa 1, show promising characteristics in terms of top and fault sealing. Both wells intersect thick (300–400 m) Noonkanbah Formation, Poole Sandstone, and Grant Group sections, which contain interbedded clean reservoir and shaley units. Overall, there is good potential for trapping in this succession. Further eastwards, along the Lennard Shelf, the Late Carboniferous – Permian megasequence maintains its potential for top and fault sealing. Wells such as Kora 1 penetrated up to 400 m of Noonkanbah Formation and there are well-developed, intra-formational shale units in the Grant Group interbedded with low Vshale sands. The Poole Sandstone however, is dominantly shaley.

Fitzroy Trough

Wells within the Fitzroy Trough are sparsely distributed. Altogether there are only eight wells in an area covering 50 000 km^2 (Figs 5 and 53). Nevertheless, the wells analyzed form a disparate group. Fitzroy River 1 and Fraser River 1, and Wamac 1 and Lacepede 1 lie along the axis of the Fitzroy Trough, highlighting lateral variations and consistencies along the structure. Whistler 1, Pearl 1, Barlee 1, and the Yulleroo wells are near the southern margin of the Fitzroy Trough. They may therefore potentially be thought of as representing a transitional sequence moving onto the southern terraces.

The Poole Sandstone has not been recorded in any of the wells along the centre of the Fitzroy Trough due to erosion on the crests of antiforms. Fitzroy River 1 is 311 km outside the study area. However, it has been investigated due to its axial position within the Fitzroy Trough, partially in order to assess variations along the trough and also because a number of wells have been drilled in the central parts. Reasonably thick (>100 m), shalier intervals are present within the Upper Carboniferous – Permian sequence in Fitzroy River 1, constituting a minor potential for self-juxtaposition fault sealing. The same sequence is very shallow and has no top seal in Fraser River 1. However, the Grant Group contains shale units exceeding 100 m in thickness, holding the potential for minor, localized sealing.

Wamac 1 and Lacepede 1 in the offshore continuation of the Fitzroy Trough are two of the closest wells to JPP (within about 80 km). The central position of these wells within the Fitzroy Trough is ideal to provide information about the sealing potential of the Upper Carboniferous – Permian succession in the western part of the trough. However, Lacepede 1 only just penetrates the Permian and Wamac 1 terminates in the Jurassic. Note that no significantly shaley units were intersected and there is only minor potential for self-juxtaposition fault sealing in Cretaceous units. The successions indicate that there is little possibility for top sealing. The wells are too shallow to draw any definitive conclusions with regard to seal potential in the deeper parts of the offshore Fitzroy Trough.

Fitzroy Trough southern margin and northern Jurgurra Terrace

Whistler 1, Pearl 1, Barlee 1 and Yulleroo 1 were drilled into the crests of anticlinal structures within 6 km of the southern edge of the Fitzroy Trough (Figs 5 and 54). These wells were chosen to represent the transition from the Fitzroy Trough to the Jurgurra Terrace. Whistler 1 is near the eastern end of the defined Jurgurra Terrace, 210 km from JPP. The other wells are considerably closer, i.e. between 40 and 90 km from JPP.

Whistler 1 and Pearl 1 display similar characteristics to the sections in Fitzroy River 1 and Fraser River 1, which were drilled in the central part of the Fitzroy Trough. These sections lack significant top seals due to erosion associated with the Fitzroy Transpression, but display significantly muddier intervals in Carboniferous–Permian strata. Intraformational shales in both sections suggest some potential for trapping given the presence of suitable structures. The thin Carboniferous–Permian section that remains in Yulleroo 1 shows no evidence for internal sealing potential. However, this interpretation is not diagnostic.

Southern Jurgurra Terrace / Northern Broome Platform

Four wells will be discussed that have been drilled in the transition between the Jurgurra Terrace and the Broome Platform (Figs 5 and 55). The nearest, Freney 1, is 80 km from JPP. These wells form an approximately 25 km-long, east–west-trending transect in which the Noonkanbah Formation shows an increase in thickness and clay content in westerly direction. Additionally, the Poole Sandstone and Grant Groups are also present across the section. The Poole Sandstone varies insignificantly across the area but the Grant Group changes from monotonous clean quartzites in the east to sandstone with thick shaley units in the west.

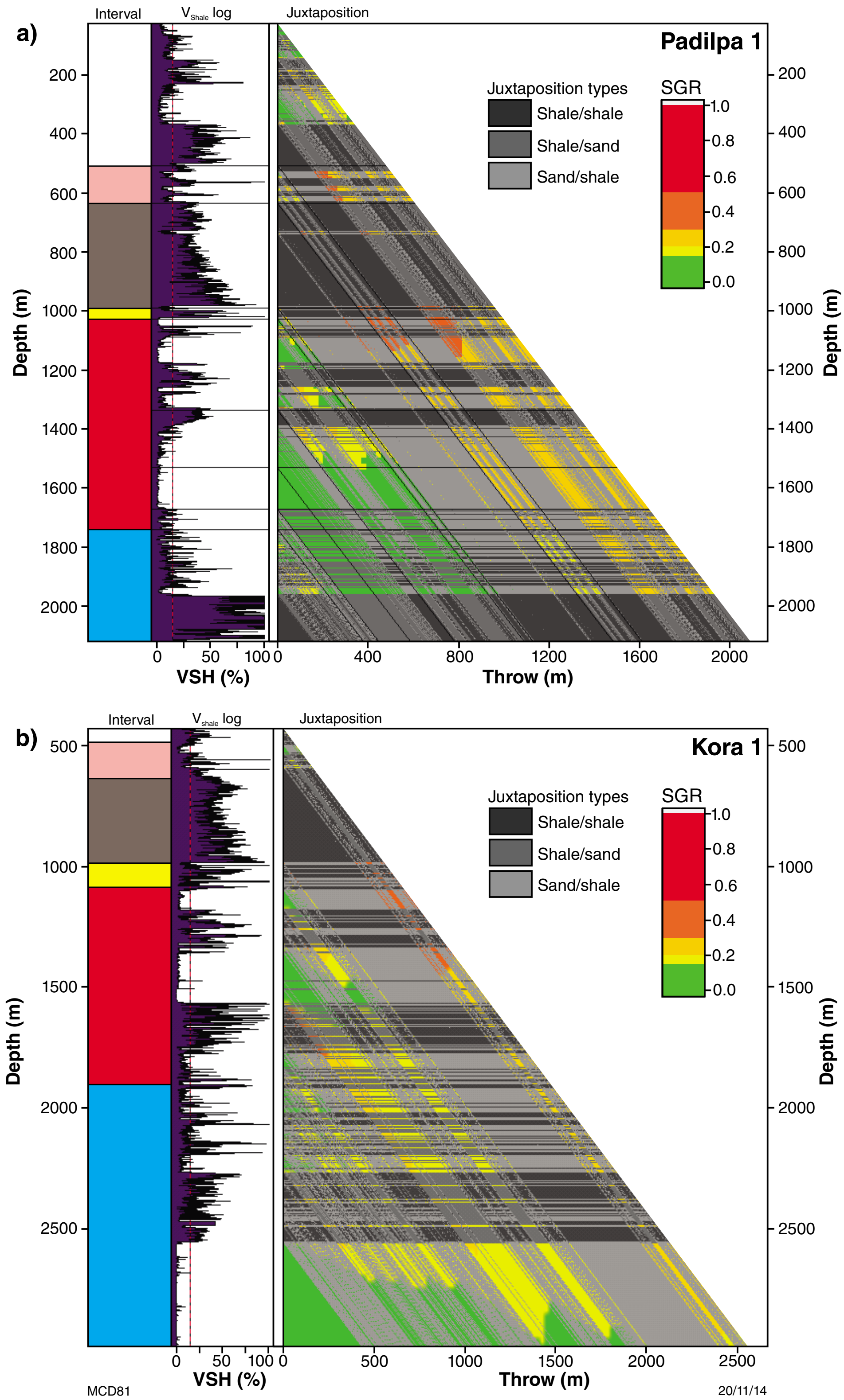

Figure 52. Triangle–juxtaposition plots for wells on the Pender Terrace. In the 'Interval' columns of this and subsequent triangle plots (i.e. Figs 53–57) the Grant Group is represented in red, the Poole Sandstone in yellow, and the Noonkanbah Formation in brown. Significantly the shale content of the succession as a whole and the thickness of the Noonkanbah Formation increases eastward. As a result increasing amounts of orange and red juxtapositions indicate greater SGR and thus fault seal potential. The successions in Padilpa 1 and Kora 1 have excellent potential to act as top and fault seals.

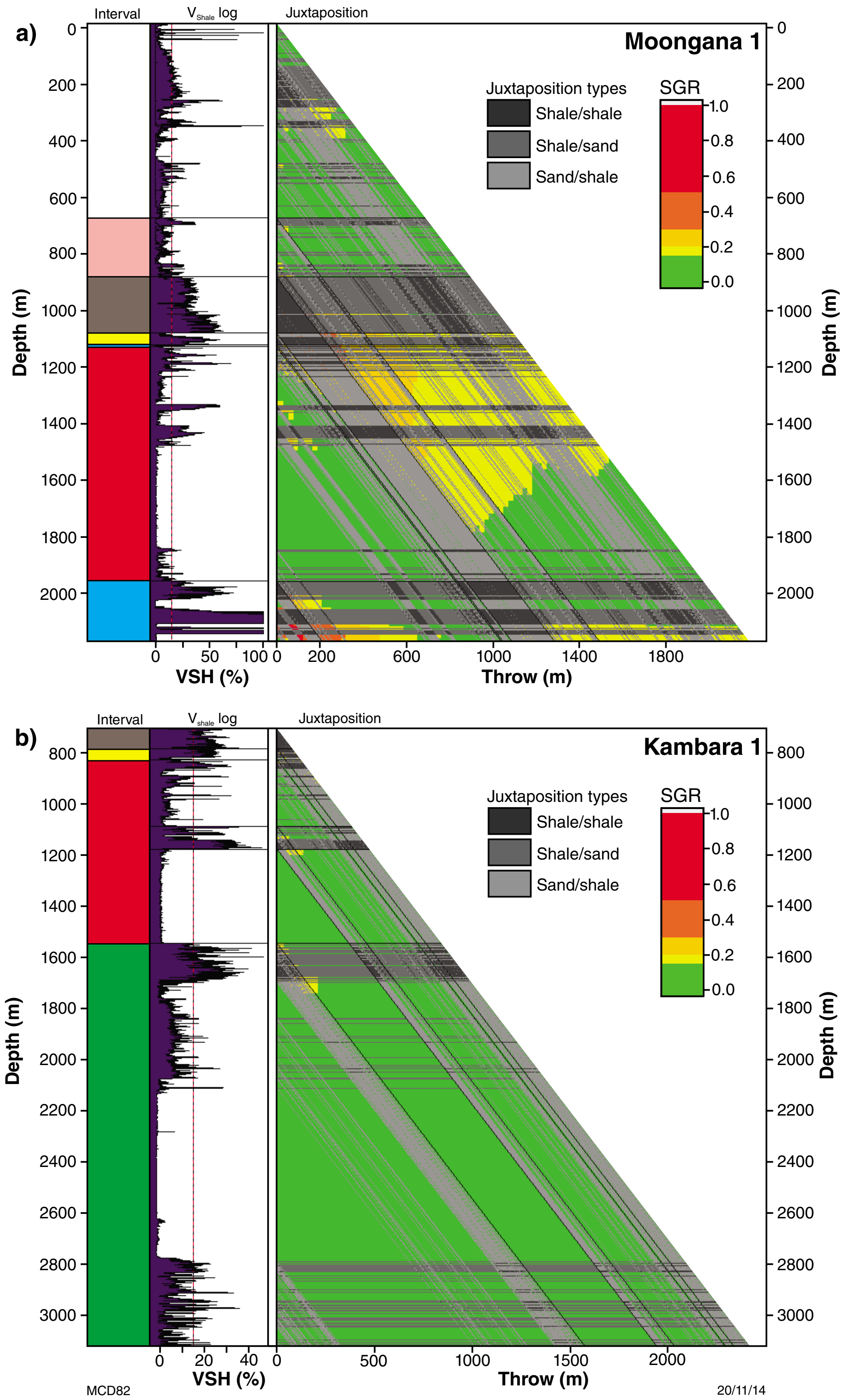

Figure 52. **(continued) Triangle–juxtaposition plots for wells on the Pender Terrace. In the 'Interval' columns of this and subsequent triangle plots (i.e. Figs 53–57) the Grant Group is represented in red, the Poole Sandstone in yellow, and the Noonkanbah Formation in brown. Significantly the shale content of the succession as a whole and the thickness of the Noonkanbah Formation increases eastward. As a result increasing amounts of orange and red juxtapositions indicate greater SGR and thus fault seal potential. The successions in Padilpa 1 and Kora 1 have excellent potential to act as top and fault seals.**

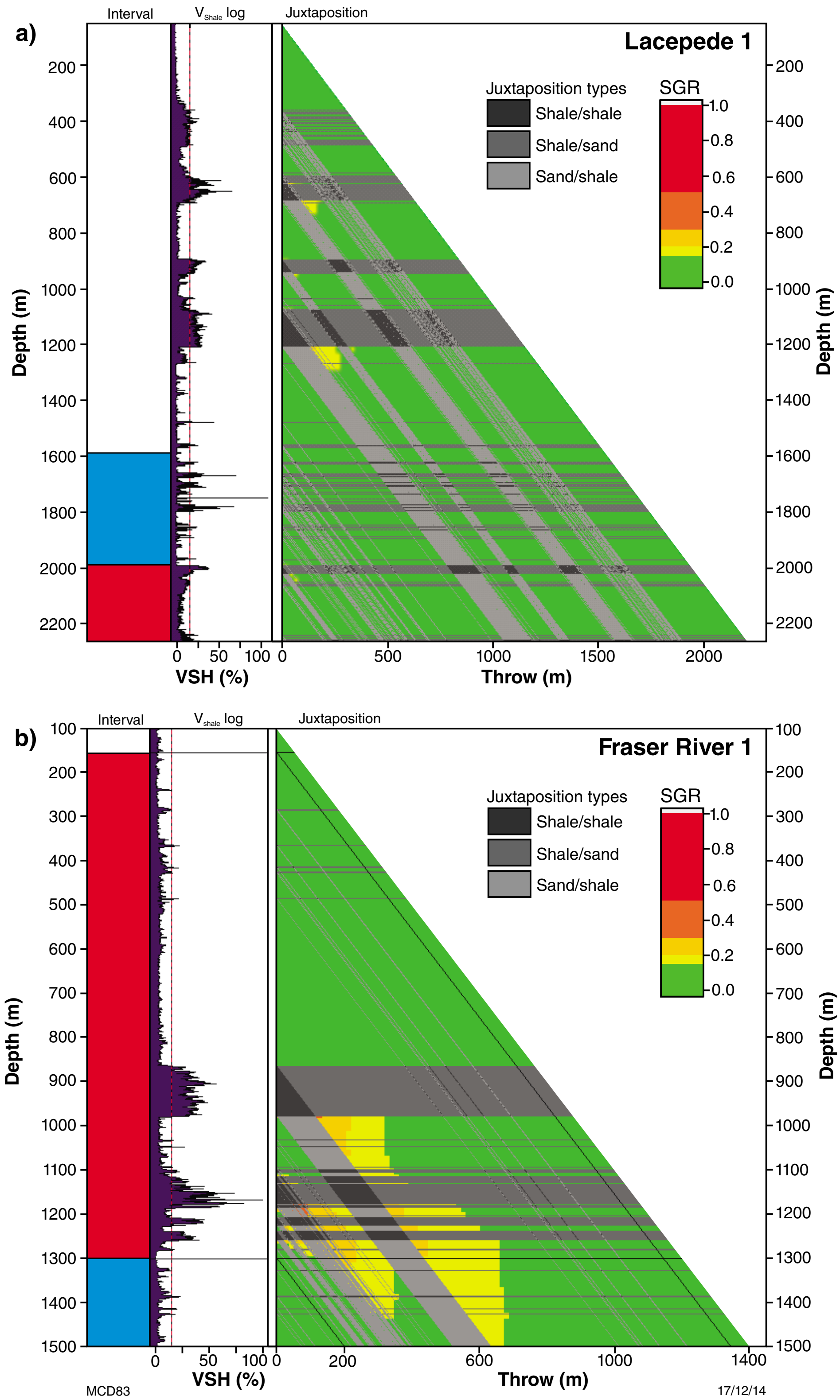

Figure 53. Triangle–juxtaposition plots for wells located near the axis of the Fitzroy Trough. In the 'Interval' column the red section of each triangle plot represents general Carboniferous–Permian units. The red section in well Lacepede 1 is not differentiated beyond 'Upper Permian'. In wells Fraser River 1 and Fitzroy River 1 the red section represent Upper Carboniferous strata. Importantly, the Grant Group contains some significant clay rich units, suggesting some fault seal potential (especially in well Fraser River 1).

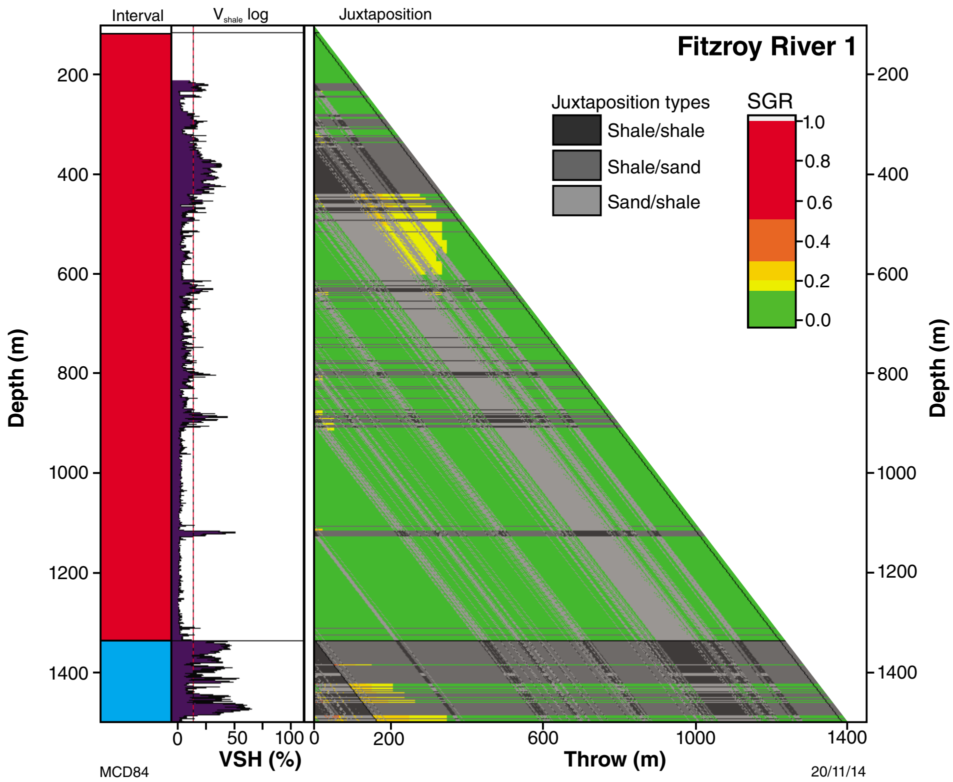

Figure 53. (continued) Triangle–juxtaposition plots for wells located near the axis of the Fitzroy Trough. In the 'Interval' column the red section of each triangle plot represents general Carboniferous–Permian units. The red section in well Lacepede 1 is not differentiated beyond 'Upper Permian'. In wells Fraser River 1 and Fitzroy River 1 the red section represent Upper Carboniferous strata. Importantly, the Grant Group contains some significant clay rich units, suggesting some fault seal potential (especially in well Fraser River 1).

In the vicinity of Cow Bore 1 and East Crab Creek the clean sandy sequence holds no potential for self-juxtaposition fault sealing (Yielding, 2002). The Noonkanbah Formation holds some potential for sealing the Poole Sandstone and Grant Groups. Around Freney 1, however, in addition to 200 m of Noonkanbah Formation top seal, the Carboniferous–Permian sequence with its thick shaley components has very good potential for self-juxtaposition fault seal. Large fault structures (>100 m) cutting this sequence will have potential for sealing traps given suitable top seal geometry.

Broome Platform

On the Broome Platform five wells situated 90 to 110 km south of JPP (Figs 5 and 56) were assessed. In this area the Grant Group generally is unconformably overlain by the Mesozoic. The Poole Sandstone, however, is recorded in Hilltop 1, which is the southeasternmost well. There is no significant top seal above the Permian.

The first three wells, Goldwyer 1, Kanak 1, and Hilltop 1, have very clean Permian sequences, rendering a self-juxtaposition fault seal unlikely. However, the Grant Group in Sharon Ann 1 and Hedonia 1, which are the furthest SW and NE wells, respectively, have a significant shale content, with potential for internal traps given suitable structural geometries. Hedonia 1 is only 12 km from Goldwyer 1, Kanak 1, and Hilltop 1, giving some indication of the localized potential for variation within the Grant Group.

Sunshine 1 is 60 km further inland than any of the other Broome Platform wells. It is located approximately 130 km southeast of JPP and contains a Carboniferous–Permian sequence with thick (>50 m) shaley beds. In this region this sequence lies unconformably between Jurassic and Ordovician sequences.

Discussion

The localities containing Upper Carboniferous – Permian successions showing the highest potential for fault sealing, and hence sequestration, are located on the eastern Pender Terrace (Padilpa 1, Puratte 1, Kora 1, West Kora 1) / Lennard Shelf (>110 km from JPP), on the southern Jurgurra Terrace, and the extreme northern Broome Platform in the vicinity of Freney 1 (80 km southeast of JPP).

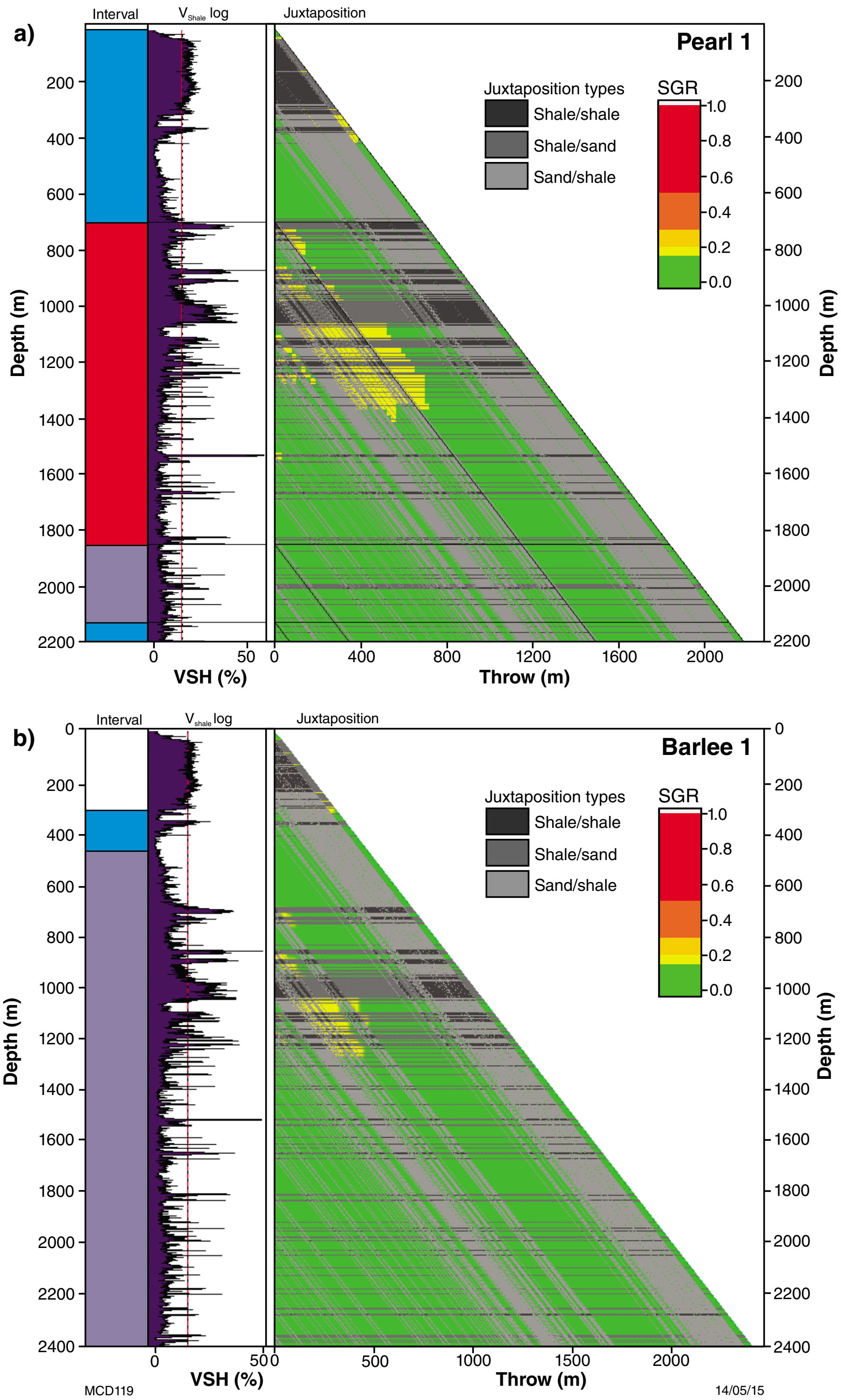

Figure 54. **Triangle–juxtaposition plots for wells on the southern margin of the Fitzroy Trough/outer Jurgurra Terrace, showing wells Pearl 1 (the closest well to JPP, 43 km away), Barlee 1, Yulleroo 1, and Whistler 1. In the 'Interval' column the Carboniferous–Permian units are shown in red. Blue units overlying other units are various Jurassic strata, pink denotes the upper Anderson Formation and blue units below the red unit represent undifferentiated Anderson Formation. The brown unit in well Whistler 1 is Ordovician strata. Wells Pearl 1 and Whistler 1 have well-preserved early Carboniferous–Permian sections with well-developed intraformational shales, especially in well Whistler 1.**

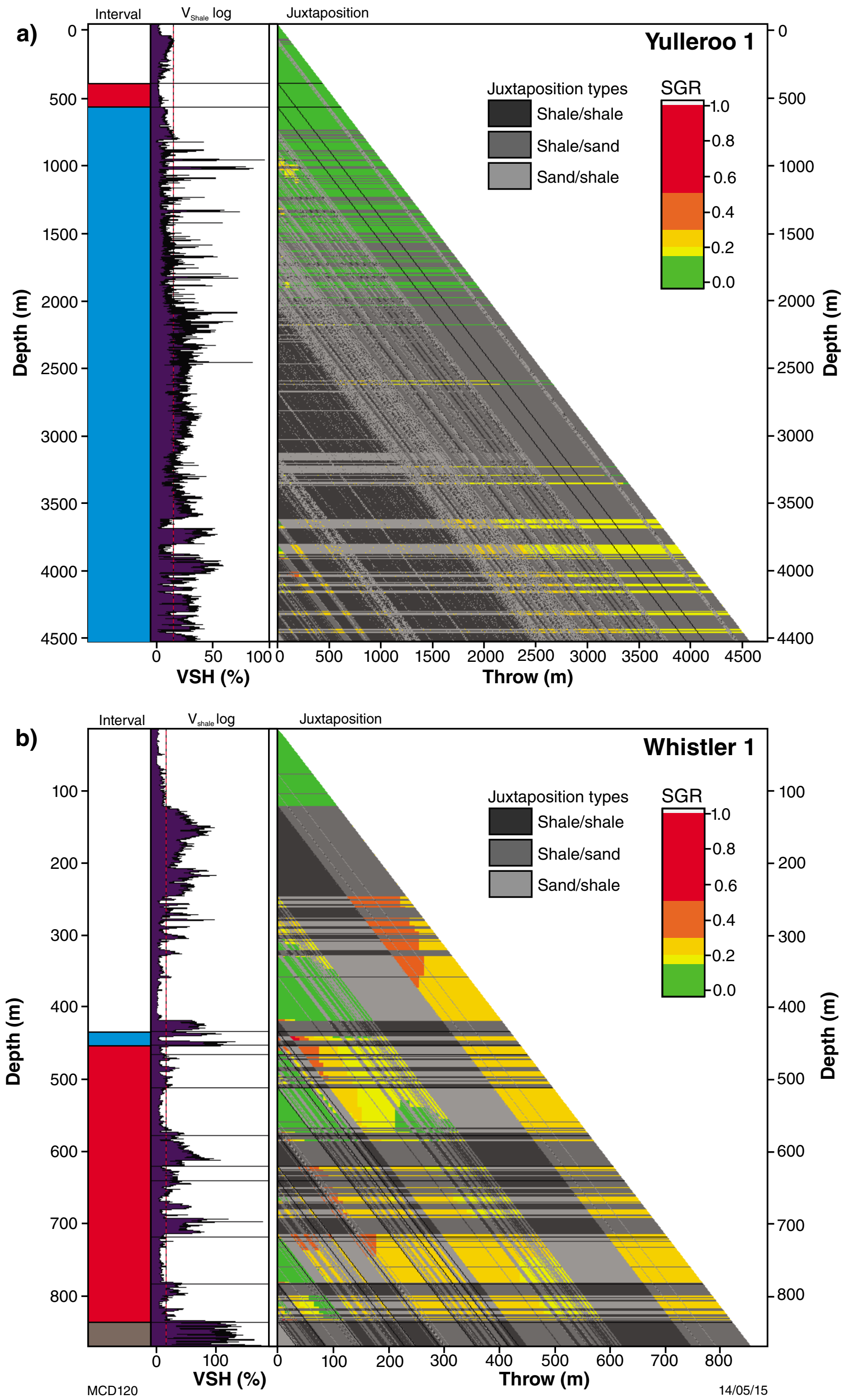

Figure 54. **(continued) Triangle–juxtaposition plots for wells on the southern margin of the Fitzroy Trough/outer Jurgurra Terrace, showing wells Pearl 1 (the closest well to JPP, 43 km away), Barlee 1, Yulleroo 1, and Whistler 1. In the 'Interval' column the Carboniferous–Permian units are shown in red. Blue units overlying other units are various Jurassic strata, pink denotes the upper Anderson Formation and blue units below the red unit represent undifferentiated Anderson Formation. The brown unit in well Whistler 1 is Ordovician strata. Wells Pearl 1 and Whistler 1 have well-preserved early Carboniferous–Permian sections with well-developed intraformational shales, especially in well Whistler 1.**

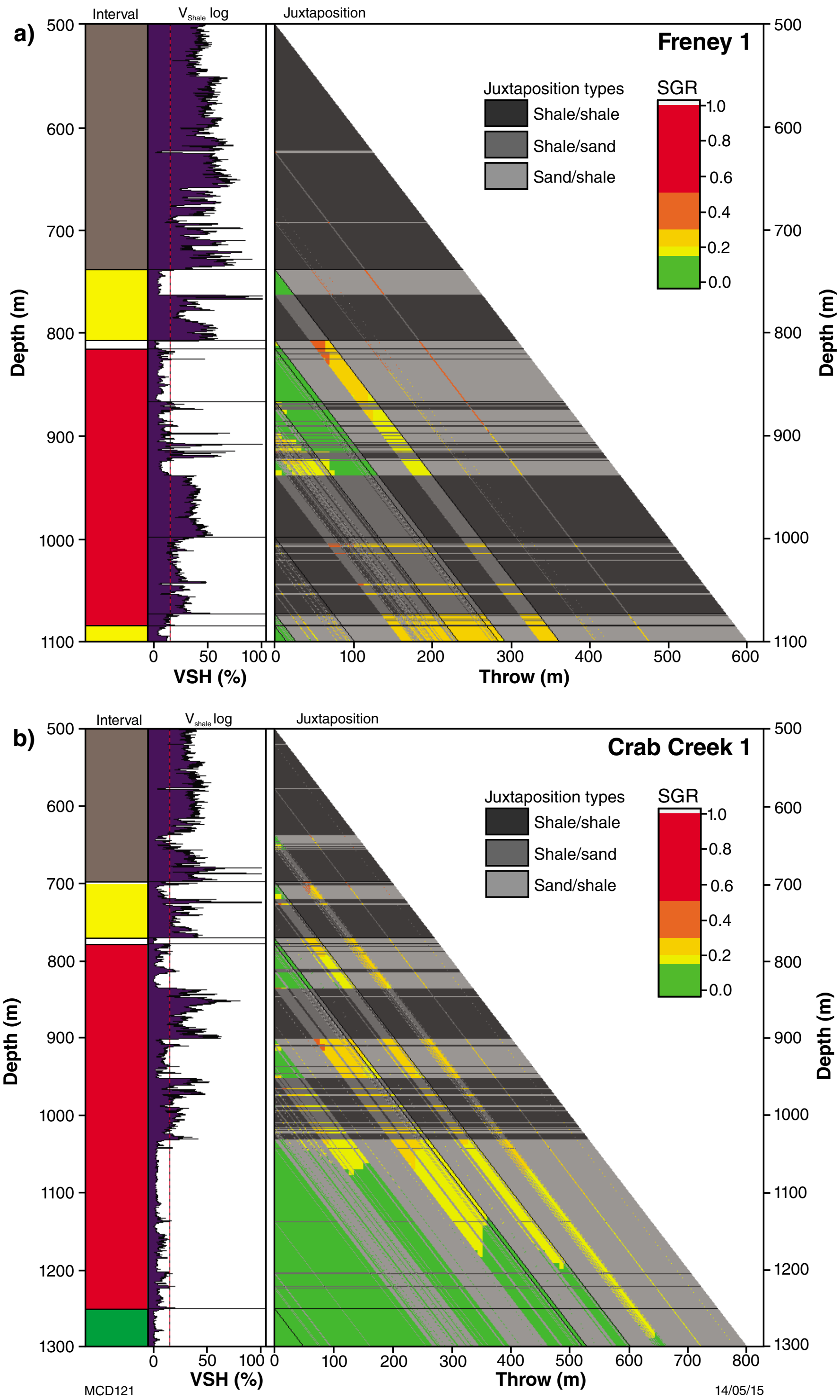

Figure 55. Triangle–juxtaposition plots for the successions in wells Freney 1, Crab Creek 1, East Crab Creek 1, and Cow Bore 1. In the 'Interval' column the Carboniferous–Permian strata are shown red, Poole Sandstone in yellow and the Noonkanbah Formation in brown. In this area the Carboniferous–Permian section is particularly thick, with significant shale content increasing to the west. Wells Freney 1 and Crab Creek 1 show significant top and fault sealing potential.

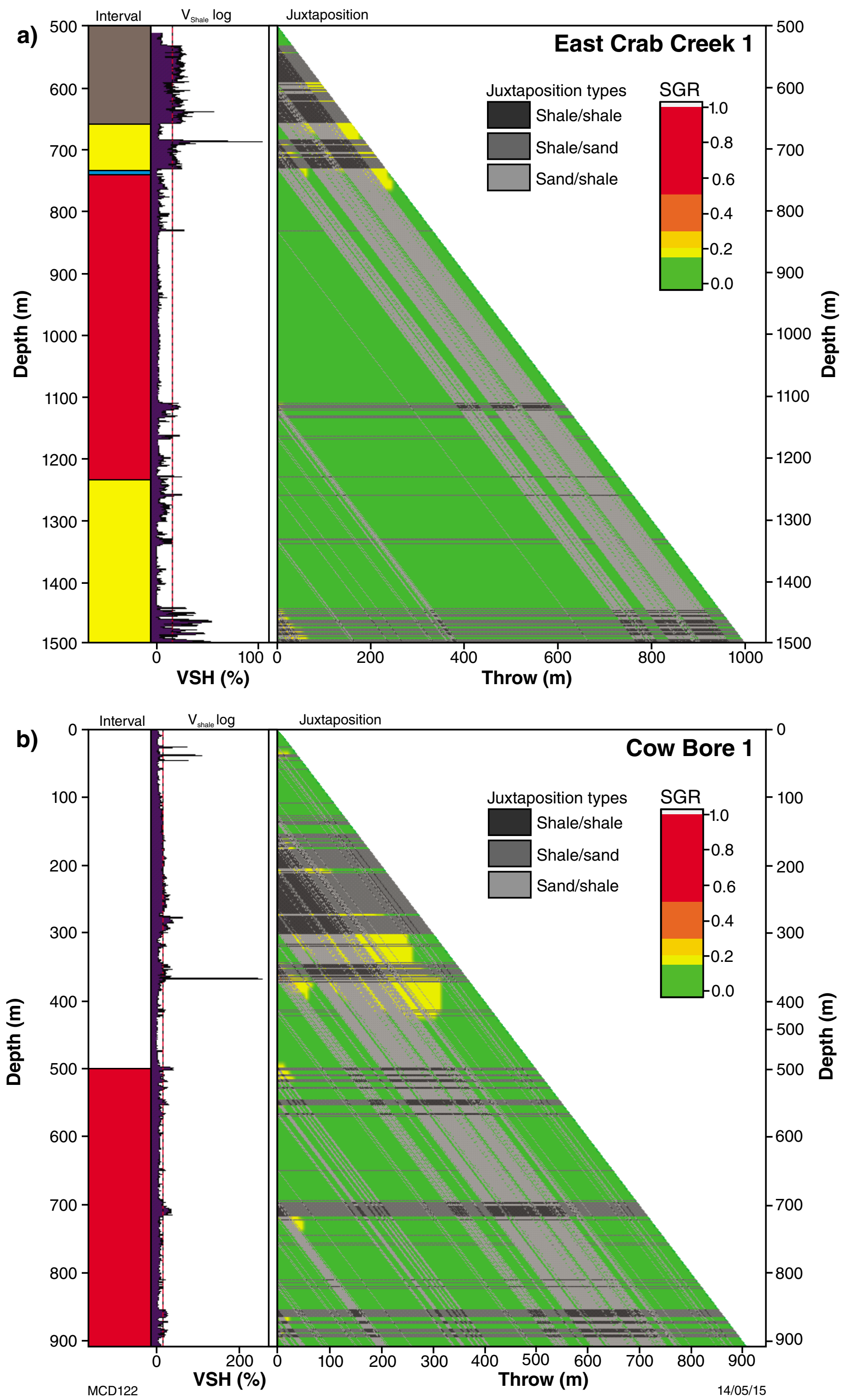

Figure 55. **(continued) Triangle–juxtaposition plots for the successions in wells Freney 1, Crab Creek 1, East Crab Creek 1, and Cow Bore 1. In the 'interval' column the Carboniferous–Permian strata are shown red, Poole Sandstone in yellow and the Noonkanbah Formation in brown. In this area the Carboniferous–Permian section is particularly thick, with significant shale content increasing to the west. Wells Freney 1 and Crab Creek 1 show significant top and fault sealing potential.**

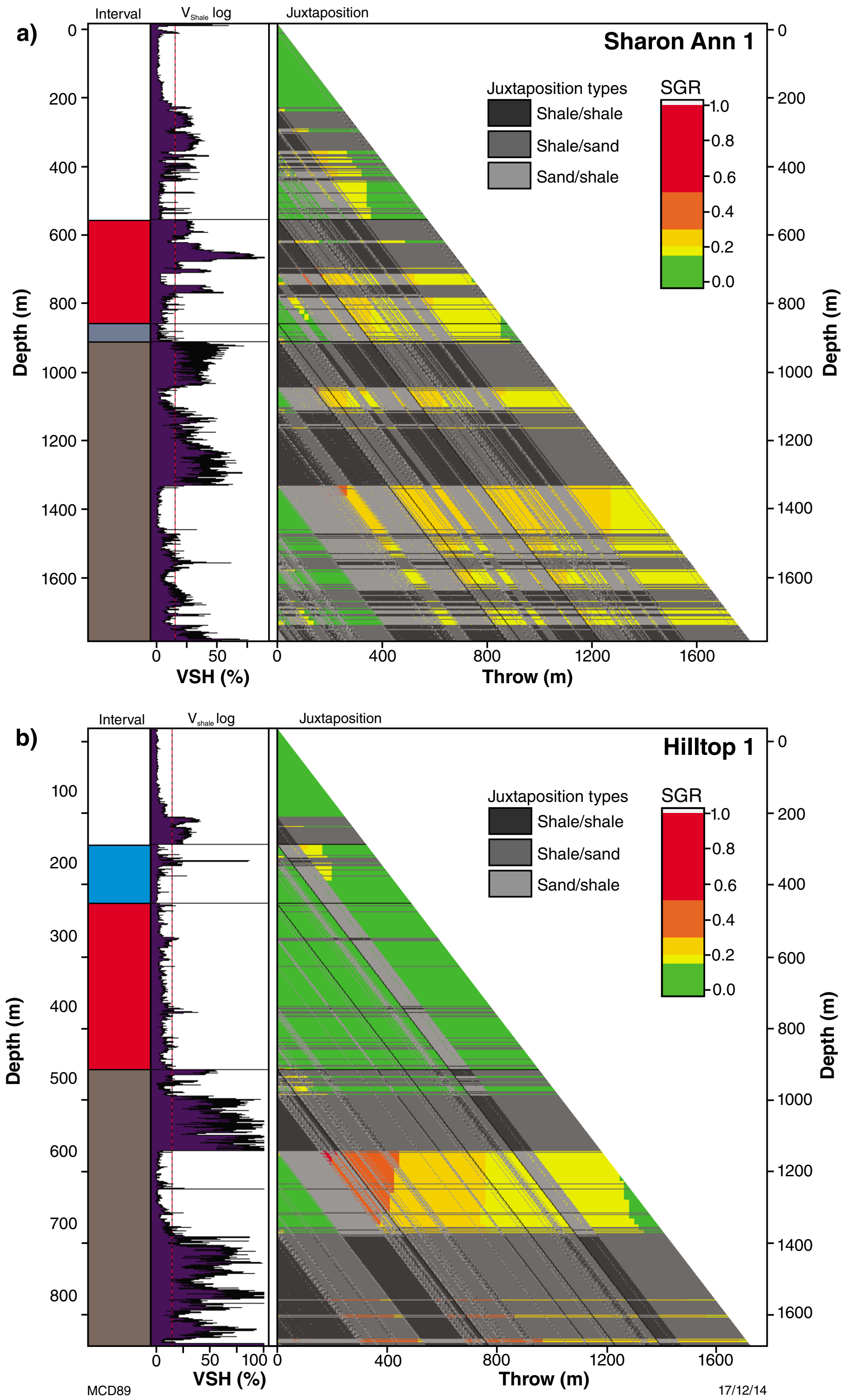

Figure 56. Triangle–juxtaposition plots for wells on the Broome Platform: Hilltop 1, Hedonia 1, Goldwyer 1, Kanak 1, and Sunshine 1. None of the wells have significant Lower Carboniferous Permian Megasequence top seals. Wells Hilltop 1, Kanak 1, and Goldwyer 1 have relatively low shale content Carboniferous–Permian units. However, well Hedonia 1 to the northeast, well Sharon Ann 1 to the southwest, and well Sunshine 1 to the east show a significant quantity of intraformational shale in the Grant Group, which may have some local sealing potential.

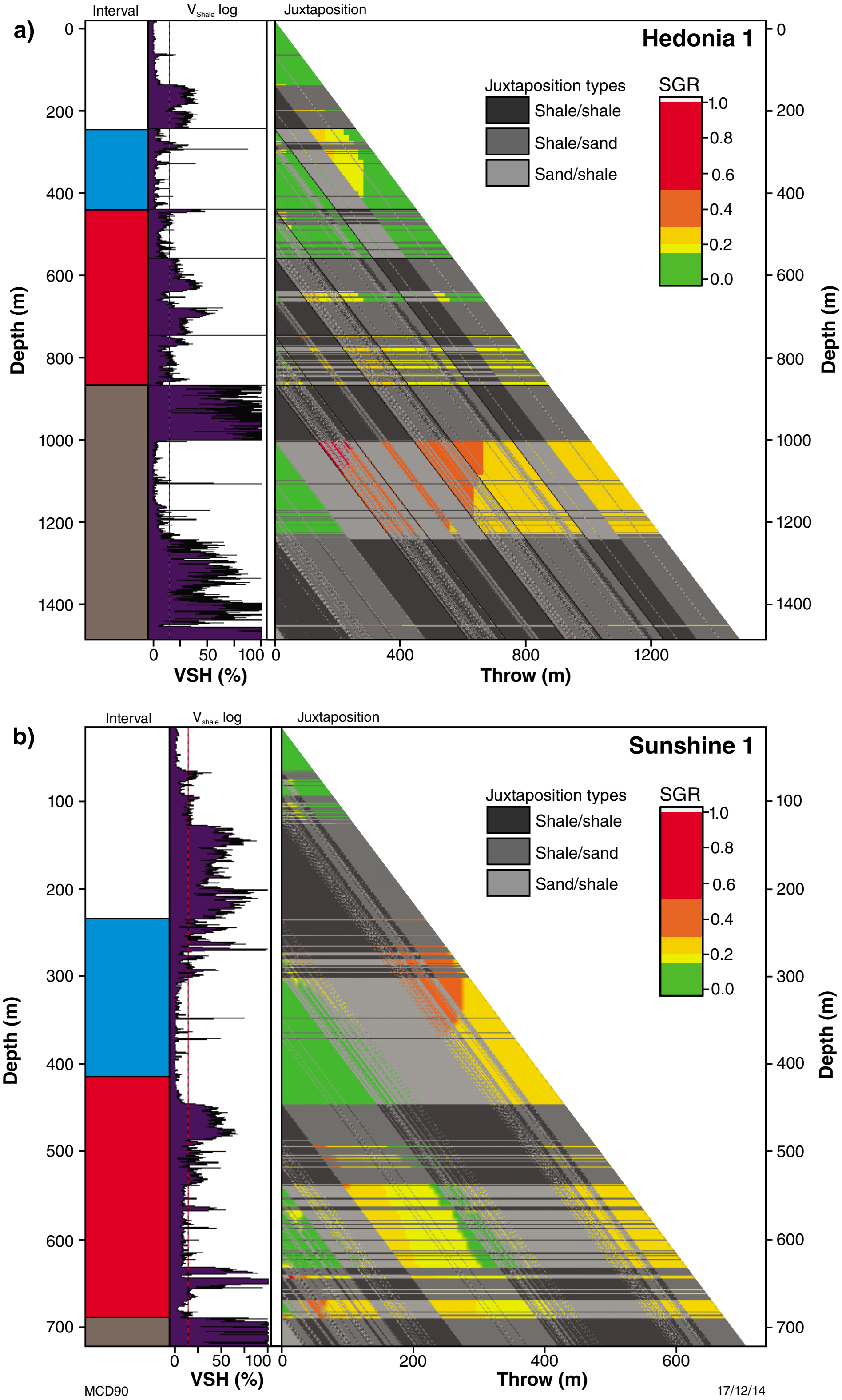

Figure 56. **(continued) Triangle–juxtaposition plots for wells on the Broome Platform: Hilltop 1, Hedonia 1, Goldwyer 1, Kanak 1, and Sunshine 1. None of the wells have significant Lower Carboniferous Permian Megasequence top seals. Wells Hilltop 1, Kanak 1, and Goldwyer 1 have relatively low shale content Carboniferous–Permian units. However, well Hedonia 1 to the northeast, well Sharon Ann 1 to the southwest, and well Sunshine 1 to the east show a significant quantity of intraformational shale in the Grant Group, which may have some local sealing potential.**

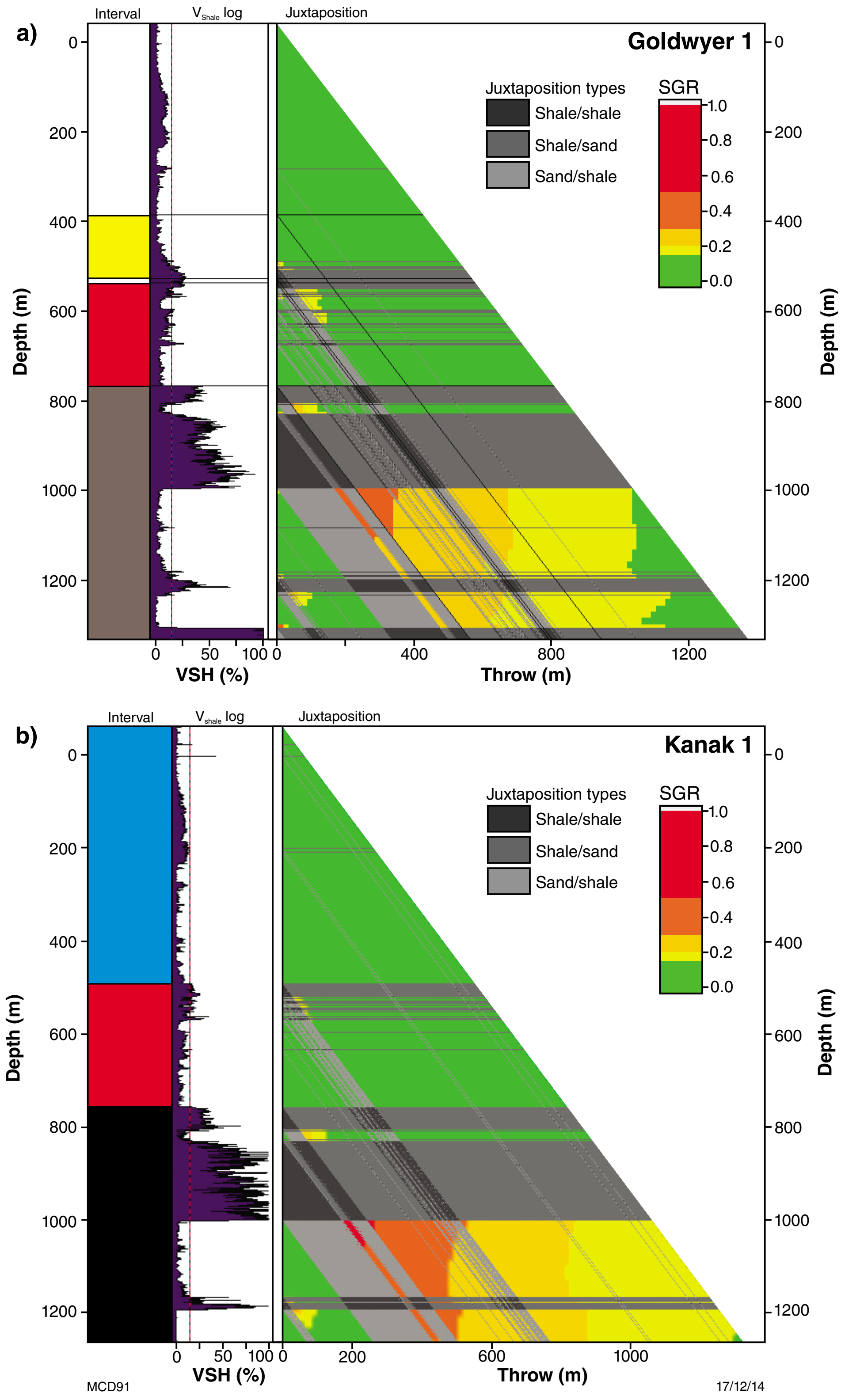

Figure 56. (continued) Triangle–juxtaposition plots for wells on the Broome Platform: Hilltop 1, Hedonia 1, Goldwyer 1, Kanak 1, and Sunshine 1. None of the wells have significant Lower Carboniferous Permian Megasequence top seals. Wells Hilltop 1, Kanak 1, and Goldwyer 1 have relatively low shale content Carboniferous–Permian units. However, well Hedonia 1 to the northeast, well Sharon Ann 1 to the southwest, and well Sunshine 1 to the east show a significant quantity of intraformational shale in the Grant Group, which may have some local sealing potential.

Comparison within groups of wells demonstrates that there is variability within all formations, including variability between the most closely spaced wells. Such local variations should be noted when extrapolating into less explored parts of the Fitzroy Trough.

The Carboniferous–Permian succession on the northern flank of the Willara Sub-basin has a higher mud content than on the Broome Platform. However, those successions analyzed around Great Sandy 1 and Cudalgurra 1 are 170–200 km from JPP.

The wells available for analysis in the Fitzroy Trough do not necessarily allow definitive representation of the entire Upper Carboniferous – Permian succession as drilling has been restricted to the crests of the anticlines, where erosion has removed much of the section. None of the wells intersect the whole succession. In all wells with a significant Carboniferous–Permian succession present, such as Fitzroy River 1, Whistler 1, Fraser River 1, and Pearl 1, clay-rich units within the formations are at least as abundant and as shaley as the most mud-bearing Carboniferous–Permian strata on the terraces flanking the trough. This observation is consistent with the expectation that finer grained facies should typically be more common in the central troughs of basins, with coarser clastic sediments being more abundant on the basin margins. Following this reasoning, Carboniferous–Permian units in the Fitzroy Trough should be more clay-rich than correlative sections on the flanks.

Seismicity and in situ stress

(Mike Dentith and Gilberto Sanchez)

The requirement for sealing faults to preserve the integrity of the recommended sequestration sites means that the local seismicity and in situ stress need to be considered. This is because seismic activity could trigger fault slip and fracture generation. In a worst case scenario it could even cause leakage of geosequestered CO_2. In addition to an obvious relationship with seismicity, the stress regime is important because injection of CO_2 could change the local stress conditions, inducing slip on fault planes and potentially breeching seals. Stresses are also important as they exert a significant influence on fluid flow patterns in fractured rock and so may affect injectivity of CO_2.

Stress regime

The magnitude and directions of crustal stress are often consistent at a regional scale, the ‘far field’ stress regime. At a local scale, heterogeneity of the geology and in particular the faults can cause significant changes in stress conditions. Far field stress conditions are conventionally defined in terms of three orthogonal principal axes of stress. The maximum stress is referred to as S_1 (σ_1), with the intermediate and minimum stresses assigned the subscripts ‘2’ and ‘3’, respectively. The stress regime is often described in terms of ‘Andersonian’ fault theory, where different types of faults, specifically ‘normal’, strike-slip’ and ‘reverse’ faults are explained in terms of the relative magnitudes of a vertical (S_v) and two horizontal (S_H and S_h) stresses. When the intermediate principal stress is vertical the regime is ‘strike-slip’. Ideally, failure is on conjugate strike-slip faults with the maximum principal stress bisecting the angle between them. In practice, failure on a pre-existing faults is more likely than creation of a new fault. However, the approach is a convenient means of identifying which faults are most likely to be active in the contemporary stress regime, i.e. those closest to the ideal orientation for failure. The World Stress Map database contains 11 data points related to stresses in the area encompassed by Figure 57. One data point is based on hydraulic fracture tests, nine are based on the geometry of petroleum wells (borehole breakouts), and the remainder are earthquake focal mechanism solutions. The hydraulic fracture measurements, and to a lesser extent the borehole geometry data, are based on small volumes of rock, whereas the focal mechanism represents an ‘averaging’ of a significant volume. Despite the different scales for these data the maximum principal stress direction is consistently shown to be northeast–southwest. The earthquake data predict a ‘strike-slip’ regime, i.e. the intermediate principal stress is vertical. Also shown on Figure 57 are focal mechanism data from Leonard et al.’s (2002) Australian compilation. Both events have predominantly ‘strike-slip’ mechanisms with the principal stress oriented approximately northeast. The Beagle Bay event is described as having a component of normal faulting. Other focal mechanism solutions have been determined from the region surrounding Figure 57, for example in the eastern Canning Basin and offshore, where focal mechanisms have similar characteristics. It is concluded that the orientation and relative magnitudes of the principal stresses are adequately constrained at the scale of the study area. Note that significant changes in stress conditions are expected at a local scale, especially in the vicinity of faults.

Comparison of the stress field with faults defined by the seismic interpretation described in the section on *Potential sites for Geosequestration of* CO_2 shows that many trend roughly perpendicular to the principal stress direction, and hence are not ideally oriented for reactivation as they have steep dips. Faulting is more likely on the larger west-northwest–east-southeast-trending structures that mostly lie along the margins of the Fitzroy Trough.

Seismicity

The Geoscience Australia earthquake database shows the study area experiences low level, but persistent, seismic activity. The study area lacks seismic recording stations. The nearest is at Fitzroy Crossing (FITZ), about 150 kilometres to the east (Fig. 57). The next closest stations in the Australian national recording network are several hundred kilometres away. As a result many smaller events will not be recorded in the national earthquake database. Hence, the level of seismic activity is almost certainly underestimated. Also, the lack of local seismic stations results in epicentres within the region being poorly located. Depths are unconstrained and lateral uncertainties, when they are estimated, are typically of the order of 10–20 km.

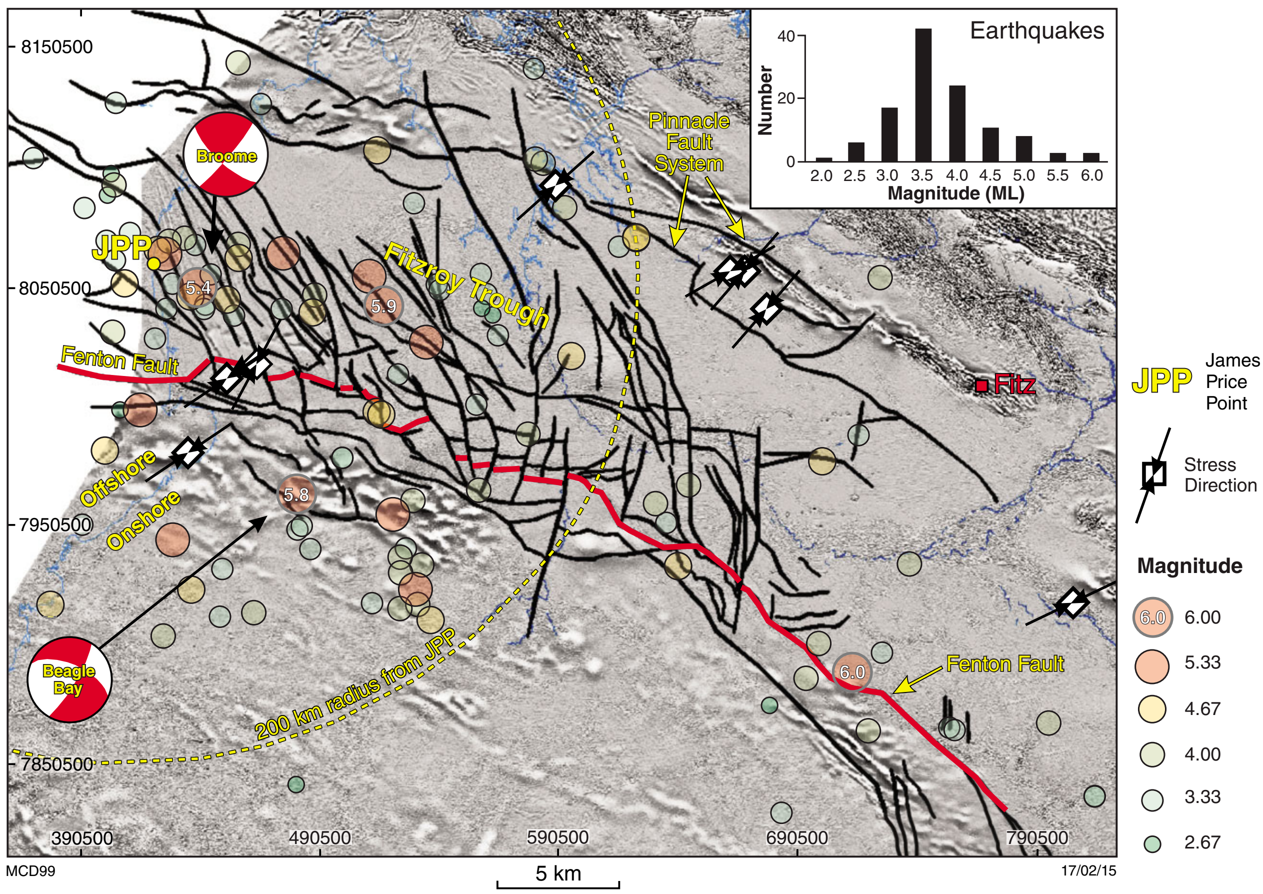

Figure 57. Map of earthquake epicentres superimposed on the main faults defined by seismic interpretation and an image of total magnetic intensity enhanced to emphasize the shallow structure. FITZ – Geoscience Australia permanent seismic station at Fitzroy Crossing.

Figure 57 shows events from the database in the study area plotted on the structural interpretation described in Section 4. There have been 115 events since 1955. Most events have magnitudes (ML) of 3–4, however, events as large as ML 6 have also been recorded. There are seven events with ML of 5 or greater.

Figure 57 demonstrates that there is an apparent correlation between the density of faults defined by the seismic interpretation and the loci of earthquakes. The inaccuracy of the epicentres means that events cannot be confidently assigned to a specific fault. However, the locations of larger events are all near the major northwest-trending faults in the area, for example those defining the southern margin of the Fitzroy Trough. Smaller events are mostly restricted to areas where NW-trending faults are common. All three areas suggested to have the potential for geosequestration experience seismic activity. Despite not being optimally oriented relative to the regional stress direction, it appears that local stress conditions are conducive to fault reactivation.

Other resources

Detailed investigations of groundwater resources in the western part of the Canning Basin (Leech, 1979), the Broome area (Laws, 1991), and the Derby area (Laws and Smith, 1989) have been completed. Laws (1990) identified substantial groundwater potential within sandstone aquifers of Cretaceous, Jurassic, and Permian age. Triassic, Devonian, Carboniferous, and Silurian sandstones and limestones also contain groundwater (Laws, 1990). Groundwater salinity ranges from fresh to brackish in the unconfined aquifers and from fresh to saline in the confined aquifers. Significant thicknesses of the Wallal Sandstone (Jurassic) were intersected by the wells closest to all three proposed geosequestration sites (89–174 m). A significant thickness of the Broome Sandstone is expected at Option C (130–250 m), and lesser thicknesses at the other two locations. Thus, both the potential geosequestration reservoirs and the overlying units constitute significant groundwater resources and are also present at the proposed geosequestration sites.

The Canning Basin has a long history of hydrocarbon exploration (Carlsen and Ghori, 2005). At present there is only one producing oil field (Blina, situated on the Lennard Shelf). Reservoirs for known hydrocarbon accumulations include the Grant Group. For example, oil or gas shows were found Nerrima 1, Crimson Lake 1, Willara 1, and Auld 1. Oil was discovered in the Grant Group in Sundown 1, Boundary 1, and West Terrace 1 (all on the Lennard Shelf, i.e. adjacent to Option C). Jackson et al. (1994) named the Grant Group and Poole Sandstone as possible reservoirs within the 'Gondawanan Petroleum system'. Redfern and Williams (2002) describe the Grant Group as 'a major potential hydrocarbon reservoir target'. Hence, although neither of the studied geosequestration reservoirs has been demonstrated to host economically significant hydrocarbon resources, many authors who have worked in the Canning Basin believe the Grant Group has significant potential.

The geothermal potential of the Canning Basin was assessed by Driscoll et al. (2009). They concluded that the areas of greatest heat-flow were on the Broome Platform, with low values recorded in the Fitzroy Trough. Areas in the central, northern, and western parts of the basin 'may be areas of increased engineered geothermal system prospectivity' (Driscoll et al., 2009). The Jurgurra Terrace, the location of Option A, was one area where 'if a suitable lithology … preserves natural permeability, it may be possible that hot sedimentary aquifer (HAS) geothermal systems can be developed' (Driscoll et al., 2009). The other potential geosequestration sites are not in areas considered to have geothermal potential.

Summary and recommendations for further work

A desktop study of public domain data has identified three potential CO_2 geosequestration sites with very large storage capacities. All three sites are in fault blocks and the sealing characteristics across bounding faults are a crucial variable in their suitability for geosequestration. Fault seal analysis, relying on distant wells, suggests that sealing faults in the three suggested geosequestration areas are present. A major risk in assessing the geosequestration potential of the study area is incorrect mapping of structure and stratigraphy due to limited, or the absence of, seismic and well data. The lack of seismic data means that there may be many more faults in the nominated areas than presently known. It is also likely that the fault blocks suggested as potential geosequestration sites are not structurally coherent entities. This possibility significantly reduces the 'area' of those sites with an associated decrease in potential storage capacity. The preferred sites require comprehensive characterization using more detailed 2D seismic and potentially later 3D seismic and drilling.

The paucity of seismic and well data onshore within about 70 km of JPP precludes identification of potential geosequestration sites in the most attractive region in terms of transport costs. Based on the very limited data, and extrapolation from better characterized areas to the east and southeast, it is likely that there are sites closer to JPP that are equally promising like the ones identified in this study. It is recommended that reconnaissance seismic data be collected closer to JPP to better define the stratigraphy and structure.

Offshore areas were beyond the scope of this study. However, given the expense of obtaining seismic data to define possible geosequestration sites in the vast area to the east of JPP it may be more cost effective to seek identifying geosequestration sites offshore and closer to JPP. An assessment of the geosequestration potential based on available offshore data is recommended.

Although data are sparse there is evidence that the faults in the study area are at risk of becoming active, either as a result of natural seismicity in the area or due to changes in the subsurface pressure conditions because of the injection of CO_2. Given these significant risks of reservoir breach the seismic/stress/geomechanical regime of the study area consequently needs a clearer characterization to reliably determine its suitability for geosequestration.

Fluvial and shallow marine facies of the Poole Sandstone are dominantly heterolithic in the study area. Cored intervals are sparse but suggest that coarse-grained sandy facies are restricted and that overall reservoir quality is likely to be low. The thickness and type of facies of the overlying Noonkanbah Formation suggest a good quality seal. Nevertheless, it is also recommended to quantify the sealing properties of this formation.

The Grant Group is dominated by thick sandy fluvial facies which have retained good to very good porosity and permeability during burial. They represent the best prospective sequestration targets based on reservoir quality. A thick intra-Grant Group seal is best developed in the Fitzroy Trough. However, its sealing properties are not defined and need to be investigated further.

There is a significant risk of resource conflict at the proposed sequestration sites and across the whole study area. Hydrocarbon accumulations are possible in the Grant Group and geosequestration would effectively sterilise resources in units at greater depths. The investigated units constitute important aquifers. A study of the hydrogeology of the possible geosequestration areas is recommended to address two issues. Firstly to assess their importance as a source of groundwater, and secondly to understand the groundwater regime in the Grant Group and Poole Sandstone and its implications for geosequestration.

Acknowledgements

Jeffrey Haworth, Ted Bowen, Alan Millar, Arthur Mory, and Roger Hocking are thanked for their guidance during this work. Thanks are also due to Badley Geoscience Limited for allowing the use of the TrapTester software.

References

Apak, SN and Backhouse, J 1998, Re-interpretation of the Permo–Carboniferous succession, Canning Basin, Western Australia, *in* The sedimentary basins of Western Australia 2 *edited by* PG Purcell and RR Purcell, Proceedings of the Petroleum Exploration Society of Australia Symposium, Perth, Western Australia, p. 683–694.

Apak, SN and Backhouse, J 1999, Stratigraphy and petroleum exploration objectives of the Permian–Carboniferous of the Barbwire Terrace and adjacent areas, northeast Canning Basin: Geological Survey of Western Australia, Report 68, 30p.

Bachu, S 2000, Sequestration of CO_2 in geological media: criteria and approach for site selection in response to climate change: Energy Conversion and Management, v. 41, p. 953–970.

Bachu, S 2003, Screening and ranking of sedimentary basins for sequestration of CO_2 in geological media in response to climate change: Environmental Geology, v. 44, p. 277–289.

Bachu, S, Gunter, WD and Perkins, EH 1994, Aquifer disposal of CO_2: hydrodynamic and mineral trapping: Energy Conversion and Management, v. 35, p. 269–279.

Bhattacharya, J 2010, Deltas, in Facies models 4 edited by NP James and RW Dalrymple: Geological Association of Canada, Geotext 6, p. 233–264.

Bird, KJ 1968, Doran Corehole No. 1. Well completion report. West Australian Petroleum Pty Ltd.

Benson, SM and Cole, DR 2008, CO_2 Sequestration in deep sedimentary formations: Elements, v. 4, p. 325–331.

Bretan, P, Yielding, G, Mathiassen, OM and Thorsnes, T 2011, Fault-seal analysis for CO_2 storage: an example from the Troll area, Norwegian Continental Shelf: Petroleum Geoscience, v. 17, no. 2, p. 181–192.

Brown, SA, Boserio, IM, Jackson, KS and Spence, KW 1984, The geological evolution of the Canning Basin – implications for petroleum exploration, *in* The Canning Basin, WA *edited by* PG Purcell: Proceedings of the Geological Society of Australia and Petroleum Exploration Society of Australia Symposium, Perth, Western Australia, 1984, p. 85–96.

Carling, PA and Dawson, MR 1996, Advances in fluvial dynamics and stratigraphy: John Wiley and Sons Ltd, London, UK, 546p.

Carlsen, G M and Ghori, KAR 2005, Canning Basin and global Palaeozoic petroleum systems — a review: The APPEA Journal 2005, p. 349–364.

Chadwick, RA, Zweigel, P, Gregersen, U, Kirby, GA, Holloway, S and Johanessen, P 2004, Geological reservoir characterisation of a CO_2 storage site: the Utsira Sand, Sleipner, northern North Sea: Energy, v. 29, p. 1371–1381.

CO2CRC 2008, Storage capacity estimation, site selection and characterisation for CO_2 storage projects: Cooperative Research Centre for Greenhouse Gas Technologies, Canberra, CO2CRC Report Number RPT08-1001, 52p.

Crespin, I and Condon, MA 1956, Micropalaeontology and stratigraphy of Roebuck No. 1 Bore, Canning Basin, Western Australia: Bureau of Mineral Resources, Australia, Geology and Geophysics Record 1956/139, 6p.

CSLF 2007, Estimation of CO_2 storage capacity in geological media — Phase II: prepared by the task force on CO_2 storage capacity estimation for the technical group (TG) of the Carbon Sequestration Leadership Forum (CSLF), viewed 16 September 2014, <http://www.cslforum.org/publications/documents/PhaseIIReportStorageCapacityMeasurementTaskForce.pdf>.

Dalrymple, RW 2010, Tidal depositional systems, *in* Facies models 4 *edited by* NP James and RW Dalrymple: Geological Association of Canada, p. 201–232.

Dent, L 2011, Depositional setting and CO_2 sequestration potential of the Early Permian Grant Group, Canning Basin, Western Australia: The University of Western Australia, Perth, Honours thesis (unpublished).

Dockrill, B and Shipton, ZK 2010, Structural controls on leakage from a natural CO_2 geologic storage site: Central Utah, USA, Journal of Structural Geology, v. 32, p. 1768–1782.

DOE 2006, Carbon sequestration atlas of the United States and Canada: appendix A – methodology for development of carbon sequestration capacity estimates, viewed 16 September 2014, <http://www.precaution.org/lib/carbon_sequestration_atlas.070601.pdf>.

Driscoll, JP, Mortimer, L, Waining, B, Cordon, E and Beardsmore, GR 2009, Geothermal energy potential in selected areas of Western Australia (Canning Basin): Hot Dry Rocks Pty Ltd, Report DOIR0681008, 38p.

Ennis-King, J and Paterson, L 2002, Engineering aspects of geological sequestration of carbon dioxide: Society of Petroleum Engineers; SPE Asia Pacific Oil and Gas Conference and Exhibition, 8–10 October, Melbourne, Paper SPE-77809-MS.

Ennis-King, J and Paterson, L 2001, Reservoir engineering issues in the geological disposal of carbon dioxide, *in* Greenhouse gas control technologies *edited by* DJ Williams, RA Durie, P McMullan, CAJ Paulson and AY Smith: CSIRO Publishing; Fifth International Conference on Greenhouse Gas Control Technologies, Cairns, Queensland, 13–16 August 2000, Proceedings, p. 290–295.

ESSO 1982, Booran 1, Well Completion Report: Esso Australia Ltd.

Eyles, CH and Eyles, N 2000, Subaqueous mass flow origin for Lower Permian diamictites and associated facies of the Grant Group, Barbwire Terrace, Canning Basin, Western Australia: Sedimentology, v. 47, p. 343–356.

Eyles, N, Eyles, CH, Apak, SN and Carlsen, GC 2001, Late Paleozoic tectonostratigraphic evolution and petroleum potential of the northern Canning Basin (Barbwire Terrace), Western Australia: American Association of Petroleum Geologists Bulletin, v. 85, p. 989–1006.

Folk, RL, Andrews, PB and Lewis, DW 1970, Detrital sedimentary rock classification and nomenclature for use in New Zealand: New Zealand Journal of Geology and Geophysics, v.13, p. 937–968.

Forman, DJ and Wales, DW 1981, Geological evolution of the Canning Basin, Western Australia: Bureau of Mineral Resources, Canberra, Australian Capital Territory, Bulletin 210, 91p.

Freeman, B, Yielding, G, Needham, DT and Badley, ME 1998, Fault seal prediction: the gouge ratio method, *in* Structural geology in reservoir characterization *edited by* MP Coward, TS Daltaban and H Johnson: Geological Society London Special Publication 127, p. 19–25.

Friedmann, SJ 2007, Geological carbon dioxide sequestration: Elements, v. 3, p. 179–184.

Fristad, T, Groth, A, Yielding, G and Freeman, B 1997, Quantitative fault seal prediction: a case study from Oseberg Syd, *in* Hydrocarbon seals: importance for exploration and production *edited by* P Møller-Pedersen and AG Koestler: Norwegian Petroleum Society Special Publications, v. 7, p. 107–124.

Galloway, WE and Hobday, DK 1983, Terrigenous clastic depositional systems: applications to petroleum, coal, and uranium exploration: Springer-Verlag, New York, USA, 423p.

Geological Survey of Western Australia 2012, Prospectivity of state acreage release areas L12-15 and L12-16, Fitroy Trough and Pender Terrace, Canning Basin, Western Australia: Geological Survey of Western Australia, 6p.

George, AD, Seyedmehdi, Z and Chow, N 2013, Late Devonian–Early Carboniferous tectonostratigraphic framework for northern Canning Basin carbonate platform evolution, West Australian Basins Symposium: Proceedings of the Petroleum Exploration Society of Australia, Perth.

Haines, PW 2009, The Carribuddy Group and Worral Formation, Canning Basin, Western Australia: stratigraphy, sedimentology, and petroleum potential: Geological Survey of Western Australia, Report 105, 60p.

Haszeldine, RS, Macaulay, CI, Marchand, A, Wilkinson, M, Graham, CM, Cavanagh, A, Fallick, AE and Couples, GD 2000, Sandstone cementation and fluids in hydrocarbon basins: Journal of Geochemical Exploration, v. 69, p.195–200.

Horstman, EL 1984, Evidence for post-Permian epeirogenic uplift in the Canning Basin from vitrinite reflectance data, *in* The Canning Basin, WA *edited by* PG Purcell: Proceedings of the Geological Society of Australia and Petroleum Exploration Society of Australia Symposium, Perth, Western Australia, 1984, p. 401–409.

IPCC 2005, Carbon dioxide capture and storage edited by B Metz, O Davidson, H de Coninck, M Loos and L Meyer: Cambridge University Press, UK, 431p.

Jackson, MJ, Kennard, JM, Romine, K, Southgate, PN, Jones, PJ, Nicoll, R, Young, G and Zeilinger, I 1994, Petroleum systems in the Canning Basin: APEA Journal, v. 34, p. 142–155.

Kennard, JM, Jackson, MJ, Romine, KK, Shaw, RD and Southgate, PN 1994, Depositional sequences and associated petroleum systems of the Canning Basin, WA, *in* The sedimentary basins of Western Australia *edited by* PG Purcell and RR Purcell: Petroleum Exploration Society of Australia, WA Branch; West Australian Basins Symposium, Perth, Western Australia, 1994: Proceedings of the Petroleum Exploration Society of Australia Symposium, p. 657–676.

Kovscek, AR 2002, Screening criteria for CO_2 storage in oil reservoirs: Petroleum Science and Technology, v. 20, p. 841–866.

Kuuskraa, VA, Koperna, GJ, Riestenberg, D and Esposito, R 2009, Using reservoir architecture to maximize CO_2 storage capacity, Energy Procedia, v.1, p. 3063–3070.

Li, Z, Dong, M, Li, S and Huang, S 2006, CO_2 sequestration in depleted oil and gas reservoir–caprock characterisation and storage capacity: Energy Conversion and Management, v. 47, p. 1372–1382.

Larionov, VV 1969, Borehole radiometry: Nedra, Moscow, USSR.

Laws, AT 1990, Outline of the groundwater resource potential of the Canning Basin, Western Australia, *in* Proceedings of the International Conference on Groundwater in Large Sedimentary Basins, Western Australia *edited by* H Ventriss: Australian Water Resources Council, Canberra, Conference Series no. 20, Proceedings, p. 319–328.

Laws, AT, 1991, Broome, WA: Geological Survey of Western Australia, 1:250 000 Hydrogeological Series.

Laws, AT and Smith, RA 1989, Derby regional groundwater investigation: Geological Survey of Western Australia, Record 1989/12, 41p.

Leech, REJ, 1979, Geology and groundwater resources of the southwestern Canning Basin, WA, in Annual Report for the year 1978: Geological Survey of Western Australia, p. 66–74.

Leonard, M, Ripper, ID and Yue, L 2002, Australian earthquake fault plane solutions: Geoscience Australia, Record 2002/19.

Manzocchi, T, Childs, C and Walsh, JJ 2010, Faults and fault properties in hydrocarbon flow models: Geofluids, v. 10, no. 1–2, p. 94–113.

Miall, AD 1996, The Geology of Fluvial Deposits, Sedimentary Facies, Basin Analysis and Petroleum Geology: Springer-Verlag, Berlin, Germany, 582p.

Miall, AD 2010, Alluvial deposits, *in* Facies model 4 *edited by* NP James and RW Dalrymple: Geological Association of Canada, p. 105–137.

Mory, AJ 2010, A review of mid-Carboniferous to lower Triassic stratigraphy, Canning Basin, Western Australia: Geological Survey of Western Australia, Report 107, 130p.

O'Brien, PE and Christie-Blick, N 1992, Glacially-grooved surfaces in the Grant Group, Grant Range, Canning Basin and the extent of the late Palaeozoic Pilbara ice sheets: BMR Journal of Australian Geology and Geophysics, v. 13, p. 87–92.

O'Brien, PE, Lindsay, JF, Knauer, K and Sexton, MJ 1998, Sequence stratigraphy of a sandstone-rich Permian glacial succession, Fitzroy Trough, Canning Basin, Western Australia: Australian Journal of Earth Sciences, v. 45, p. 533–545.

Oelkers, E and Schott, J 2005, Geochemical aspects of CO_2 sequestration: Chemical Geology, v. 217, p. 183–186.

Parra-Garcia, M 2014, Tectonic evolution and source rock maturation, Canning Basin, Western Australia: The University of Western Australia, Perth, PhD thesis (unpublished).

Parra-Garcia, M, Sanchez, G, Dentith, MC, and George, AD 2014, A regional-scale structural and stratigraphic study of the Canning Basin, Western Australia: Geological Survey of Western Australia, Report 140, p.215.

Powis, GD 1986, Jum Jum 1, Well completion report: Esso Australia Ltd.

Pemberton, SG, Spila, M, Pulham, AJ, Saunders, T, MacEachern, JA, Robbins, D and Sinclair, IK 2001, Ichnology and sedimentology of shallow to marginal marine systems: Geological Association of Canada Short Course Notes, v. 15, 343p.

Playford, PE and Hocking, RM 1999, Lennard Shelf (1:250 000 scale) *in* Devonian reef complexes of the Canning Basin, Western Australia, *edited by* PE Playford, RM Hocking and AE Cockbain: Geological Survey of Western Australia, Bulletin 145, Plate 7.

Redfern, J and Millward, E 1994, A review of the sedimentology and stratigraphy of the Permian¬–Carboniferous Grant Group, Canning Basin, *in* The sedimentary basins of Western Australia *edited by* PG Purcell and RR Purcell: Petroleum Exploration Society of Australia, WA Branch; West Australian Basins Symposium, Perth, Western Australia, 1994, Proceedings of the Petroleum Exploration Society of Australia Symposium, p. 753–756.

Redfern, J and Williams, BPJ 2002, Canning Basin Grant Group glaciogenic sediments: part of the Gondwanan Permo–Carboniferous hydrocarbon province, *in* The sedimentary basins of Western Australia 3 *edited by* M Keep and SJ Moss: Petroleum Exploration Society of Australia, WA Branch; West Australian Basins Symposium, Perth, Western Australia, 20–23 October 2002, Proceedings of the Petroleum Exploration Society of Australia, p. 851–871.

Romine, KK, Southgate, PN, Kennard, JM and Jackson, MJ 1994, The Ordovician to Silurian phase of the Canning basin, WA: Structure and sequence evolution, *in* The sedimentary basins of Western Australia *edited by* PG Purcell and RR Purcell: Petroleum Exploration Society of Australia, WA Branch; West Australian Basins Symposium, Perth, Western Australia, 14–17 August 1994, Proceedings of the Petroleum Exploration Society of Australia Symposium, p. 677–696.

Selley, RC 2000, Applied sedimentology, 2nd edition: Academic Press, San Diego, USA, 521p.

Shaw, RD, Sexton, MJ and Zeelinger, I 1994, The tectonic framework of the Canning Basin, W.A., including 1:2 million structural elements map of the Canning Basin: Australian Geological Survey Organisation, Record 1994/48, 89p.

Smith, SA, Tingate, PR, Griffiths, CM and Hull, JNF 1999, The structural development and petroleum potential of the Roebuck basin: The APPEA Journal, v. 39, p. 364–385.

Sperrevik, S, Gillespie, PA, Fisher, QJ, Halvorsen, T and Knipe, RJ 2002, Empirical estimation of fault rock properties, *in* Hydrocarbon seal quantification *edited by* AG Koestler and R Hunsdale: Norwegian Petroleum Society (NPF) Special Publication, v. 11, p. 109–125.

SRK Consulting 1998, Canning Basin Project 1998: Geological Survey of Western Australia, Statutory petroleum exploration report, S6353 R1 A5, 124p. (unpublished).

Torp, TA and Gale, J 2004, Demonstrating storage of CO_2 in geological reservoirs: the Sleipner and SACS projects: Energy, v. 29, p. 1361–1369.

Towner, RR and Gibson, DL 1983, Geology of the onshore Canning Basin, Western Australia: Bureau of Mineral Resources, Canberra, Australian Capital Territory, Bulletin 215, 51p.

Tucker, ME 2011, Sedimentary rocks in the field: a practical guide, 4th edition: Wiley-Blackwell, UK, 276p.

Varma, S, Underschultz, J, Giger, SB, Field, B, Roncaglia, LJ Hodgkinson, J and Hilditch, D 2013, CO_2 geosequestration potential in the Northern Perth Basin, Western Australia: Australian Journal of Earth Sciences, v. 60, p. 23–44.

Willmott, SO 1959, Frome Rocks No. 2, Geological completion report: West Australian Petroleum Pty Ltd.

Wollenweber, J, Alles, S, Busch, A, Krooss, BM, Stanjek, J and Littke, R 2010, Experimental investigation of the CO_2 sealing efficiency of caprocks: International Journal of Greenhouse Gas Control, v. 4, p. 231–241.

Woodside Energy 2013, Browse LNG fact sheet, viewed May 2013, <http:/www.woodside.com.au/Our-Business/Browse/documentsBrowse%20LNG%20factsheet.pdf>.

Yeates, AN, Gibson, DL, Towner, RR and Crowe, RWA 1984, Regional geology of the onshore Canning Basin, WA, *in* The Canning Basin, WA *edited by* PG Purcell: Proceedings of the Geological Society of Australia and Petroleum Exploration Society of Australia Symposium, Perth, 1984, p. 23–55.

Yielding, G, Freeman, B and Needham, DT 1997, Quantitative fault seal prediction: American Association of Petroleum Geologists, Bulletin 81, p. 897–917.

Yielding, G 2002, Shale Gouge Ratio — calibration by geohistory, *in* Hydrocarbon seal quantification *edited by* AG Koestler and R Hunsdale: Norwegian Petroleum Society (NPF) Special Publication, v. 11, p. 1–15.

Appendix 1 – Detailed core logs, Grant Group

DORAN 1 CORE 8, 9 and 10

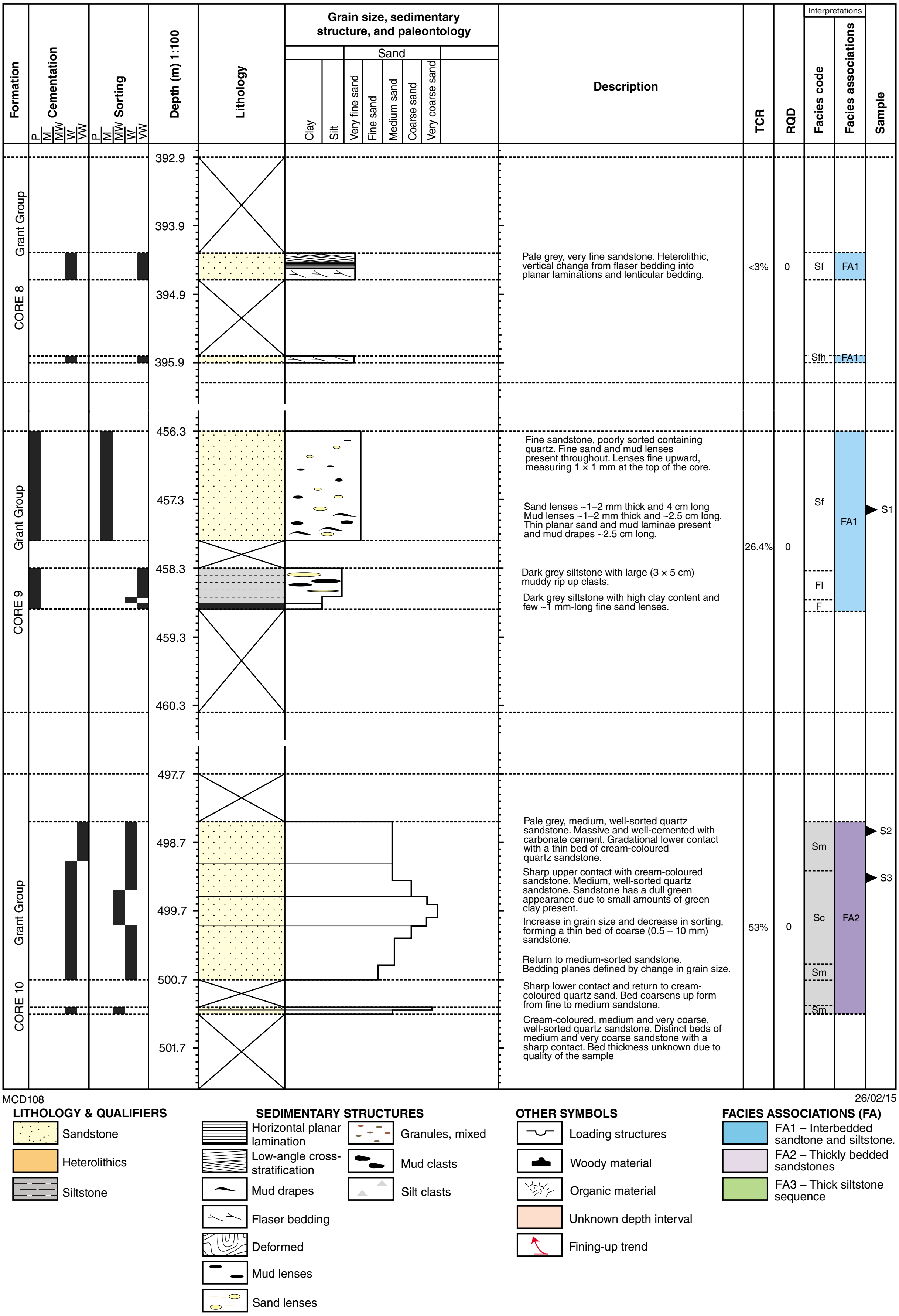

DORAN 1 CORE 11, 12 and 14

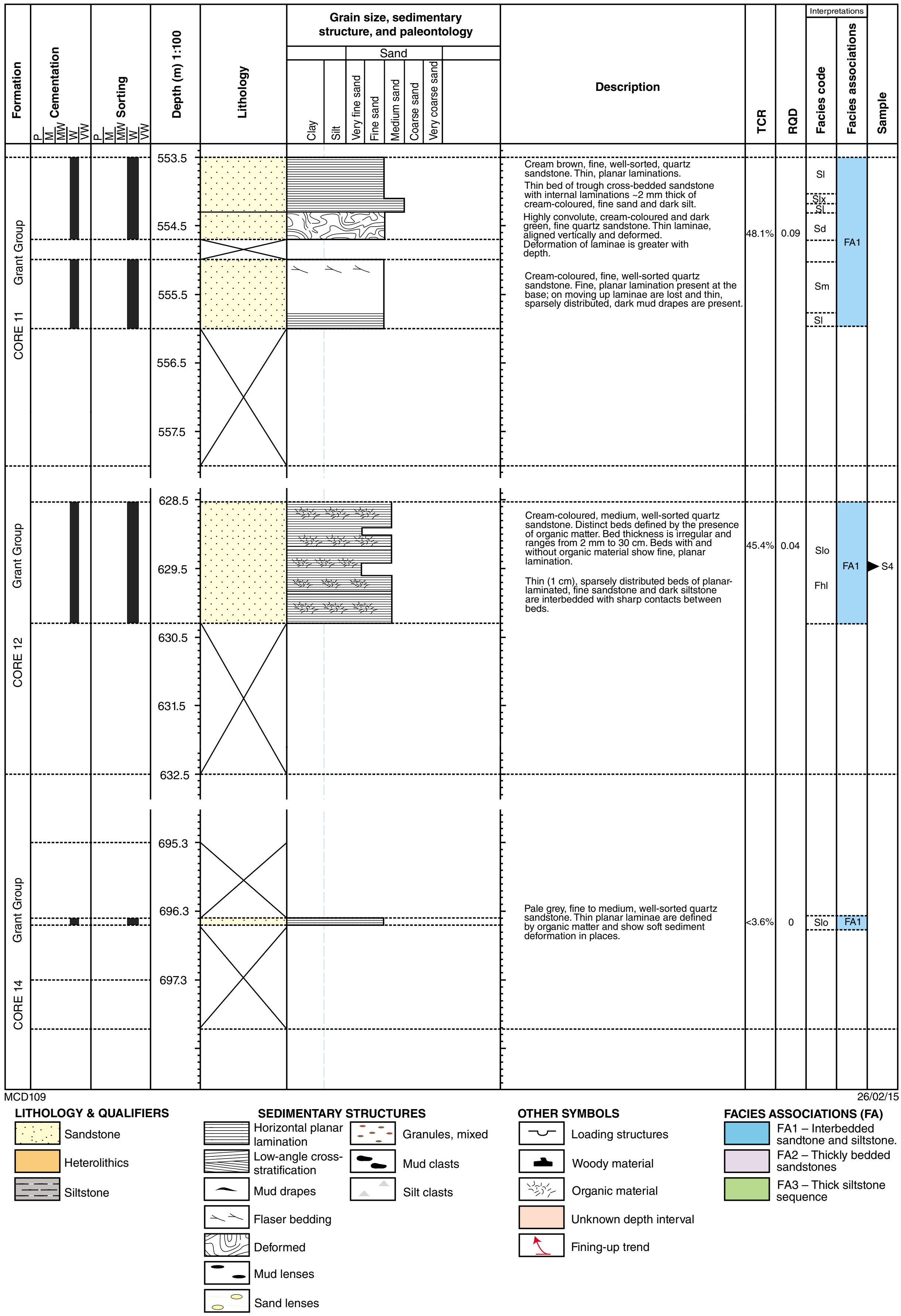

FRASER RIVER 1 CORE 10–34

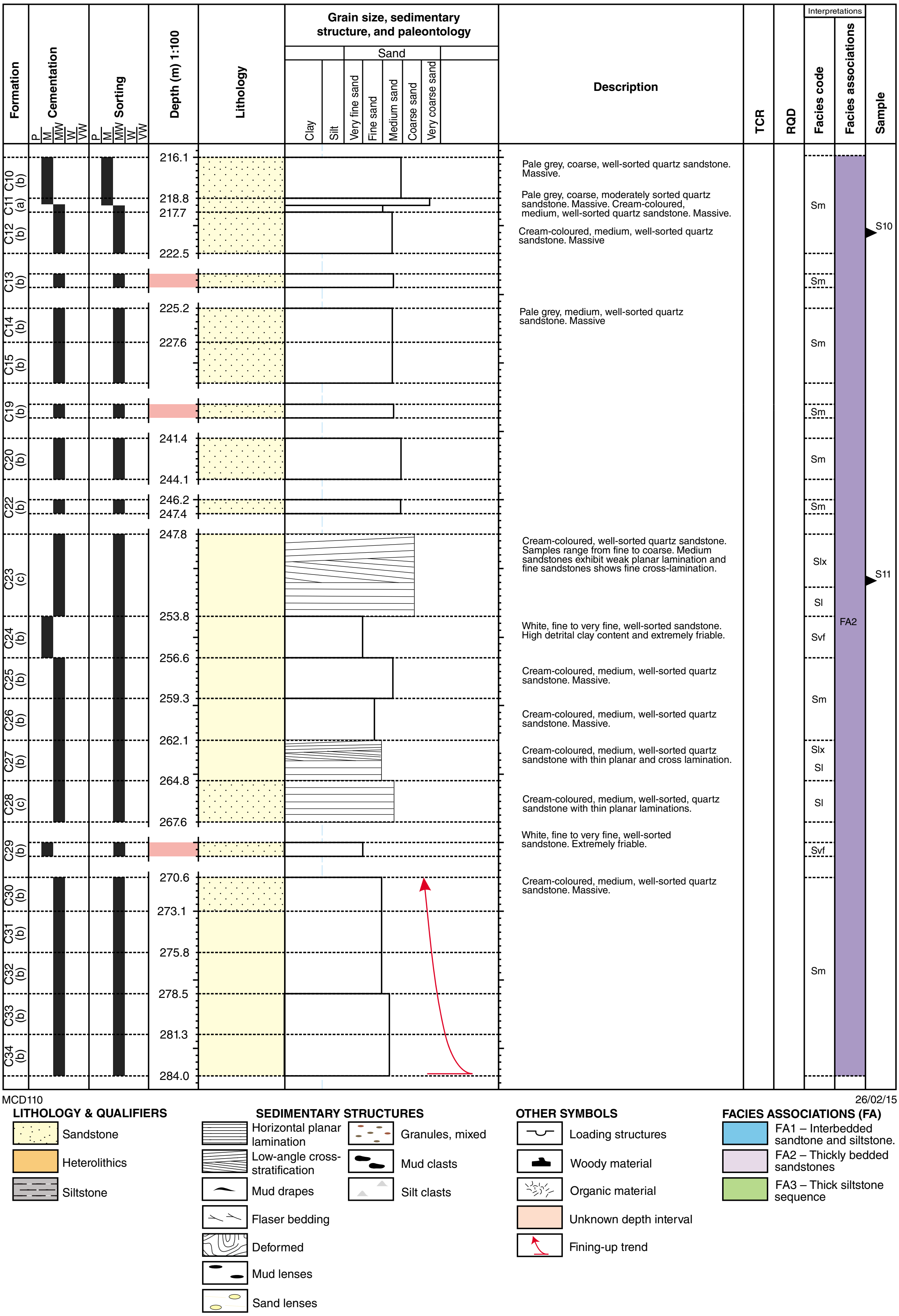

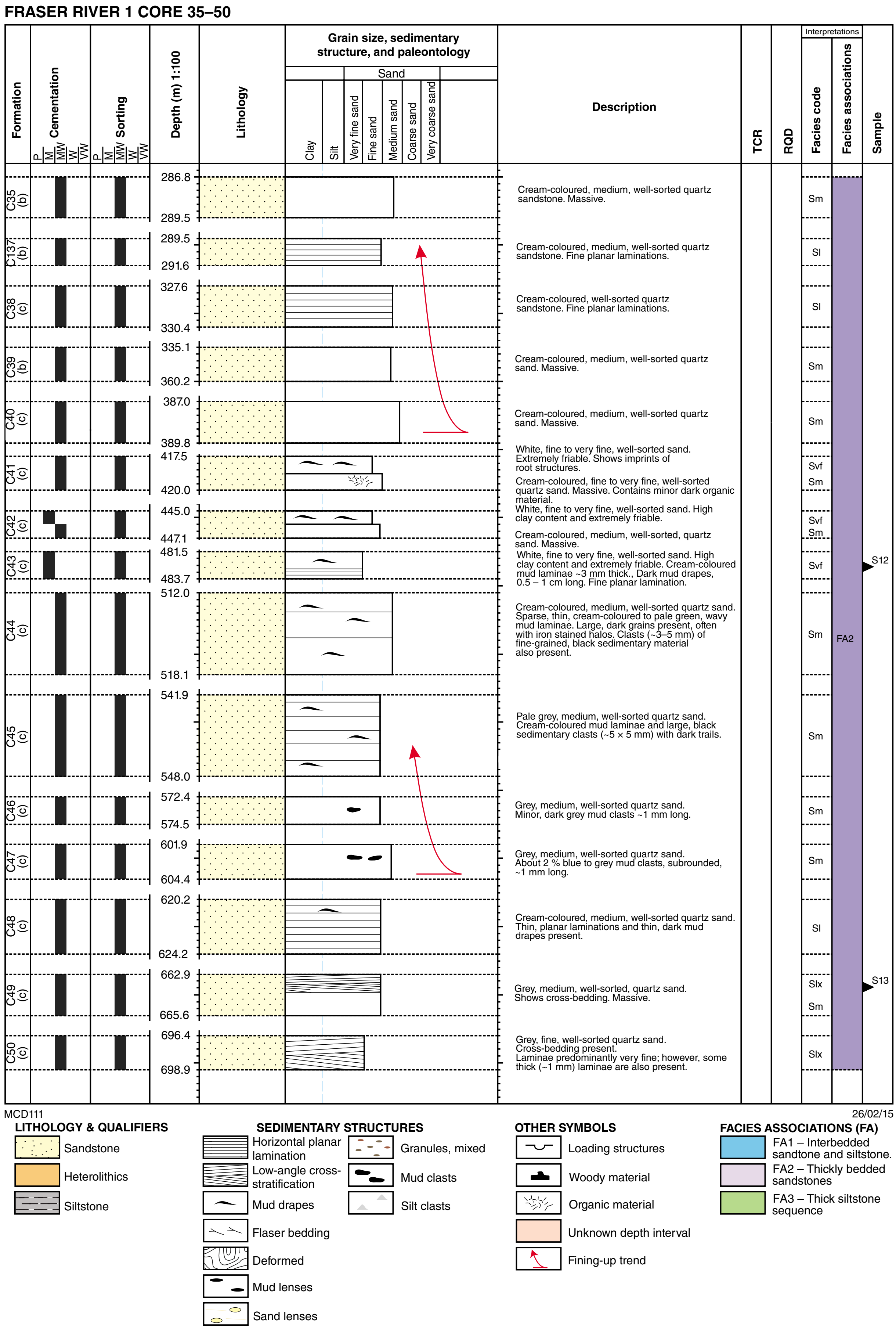
FRASER RIVER 1 CORE 35–50
Formation
Cementation
Sorting
P M MW W VW
Depth (m) 1:100
Lithology
Grain size, sedimentary structure, and paleontology
Sand
Clay
Silt
Very fine sand
Fine sand
Medium sand
Coarse sand
Very coarse sand
Description
TCR
RQD
Interpretations
Facies code
Facies associations
Sample
C35 (b)
286.8
289.5
Cream-coloured, medium, well-sorted quartz sandstone. Massive.
Sm
C137 (b)
289.5
291.6
Cream-coloured, medium, well-sorted quartz sandstone. Fine planar laminations.
Sl
C38 (c)
327.6
330.4
Cream-coloured, well-sorted quartz sandstone. Fine planar laminations.
Sl
C39 (b)
335.1
360.2
Cream-coloured, medium, well-sorted quartz sand. Massive.
Sm
C40 (c)
387.0
389.8
Cream-coloured, medium, well-sorted quartz sand. Massive.
Sm
C41 (c)
417.5
420.0
White, fine to very fine, well-sorted sand. Extremely friable. Shows imprints of root structures.
Svf
Cream-coloured, fine to very fine, well-sorted quartz sand. Massive. Contains minor dark organic material.
Sm
C42 (c)
445.0
447.1
White, fine to very fine, well-sorted sand. High clay content and extremely friable.
Svf
Cream-coloured, medium, well-sorted, quartz sand. Massive.
Sm
C43 (c)
481.5
483.7
White, fine to very fine, well-sorted sand. High clay content and extremely friable. Cream-coloured mud laminae ~3 mm thick., Dark mud drapes, 0.5 – 1 cm long. Fine planar lamination.
Svf
S12
C44 (c)
512.0
518.1
Cream-coloured, medium, well-sorted quartz sand. Sparse, thin, cream-coloured to pale green, wavy mud laminae. Large, dark grains present, often with iron stained halos. Clasts (~3–5 mm) of fine-grained, black sedimentary material also present.
Sm
FA2
C45 (c)
541.9
548.0
Pale grey, medium, well-sorted quartz sand. Cream-coloured mud laminae and large, black sedimentary clasts (~5 × 5 mm) with dark trails.
Sm
C46 (c)
572.4
574.5
Grey, medium, well-sorted quartz sand. Minor, dark grey mud clasts ~1 mm long.
Sm
C47 (c)
601.9
604.4
Grey, medium, well-sorted quartz sand. About 2 % blue to grey mud clasts, subrounded, ~1 mm long.
Sm
C48 (c)
620.2
624.2
Cream-coloured, medium, well-sorted quartz sand. Thin, planar laminations and thin, dark mud drapes present.
Sl
C49 (c)
662.9
665.6
Grey, medium, well-sorted, quartz sand. Shows cross-bedding. Massive.
Slx
Sm
S13
C50 (c)
696.4
698.9
Grey, fine, well-sorted quartz sand. Cross-bedding present. Laminae predominantly very fine; however, some thick (~1 mm) laminae are also present.
Slx
MCD111
26/02/15
LITHOLOGY & QUALIFIERS
Sandstone
Heterolithics
Siltstone
SEDIMENTARY STRUCTURES
Horizontal planar lamination
Low-angle cross-stratification
Mud drapes
Flaser bedding
Deformed
Mud lenses
Sand lenses
Granules, mixed
Mud clasts
Silt clasts
OTHER SYMBOLS
Loading structures
Woody material
Organic material
Unknown depth interval
Fining-up trend
FACIES ASSOCIATIONS (FA)
FA1 – Interbedded sandtone and siltstone.
FA2 – Thickly bedded sandstones
FA3 – Thick siltstone sequence

FRASER RIVER 1 CORE 52–68

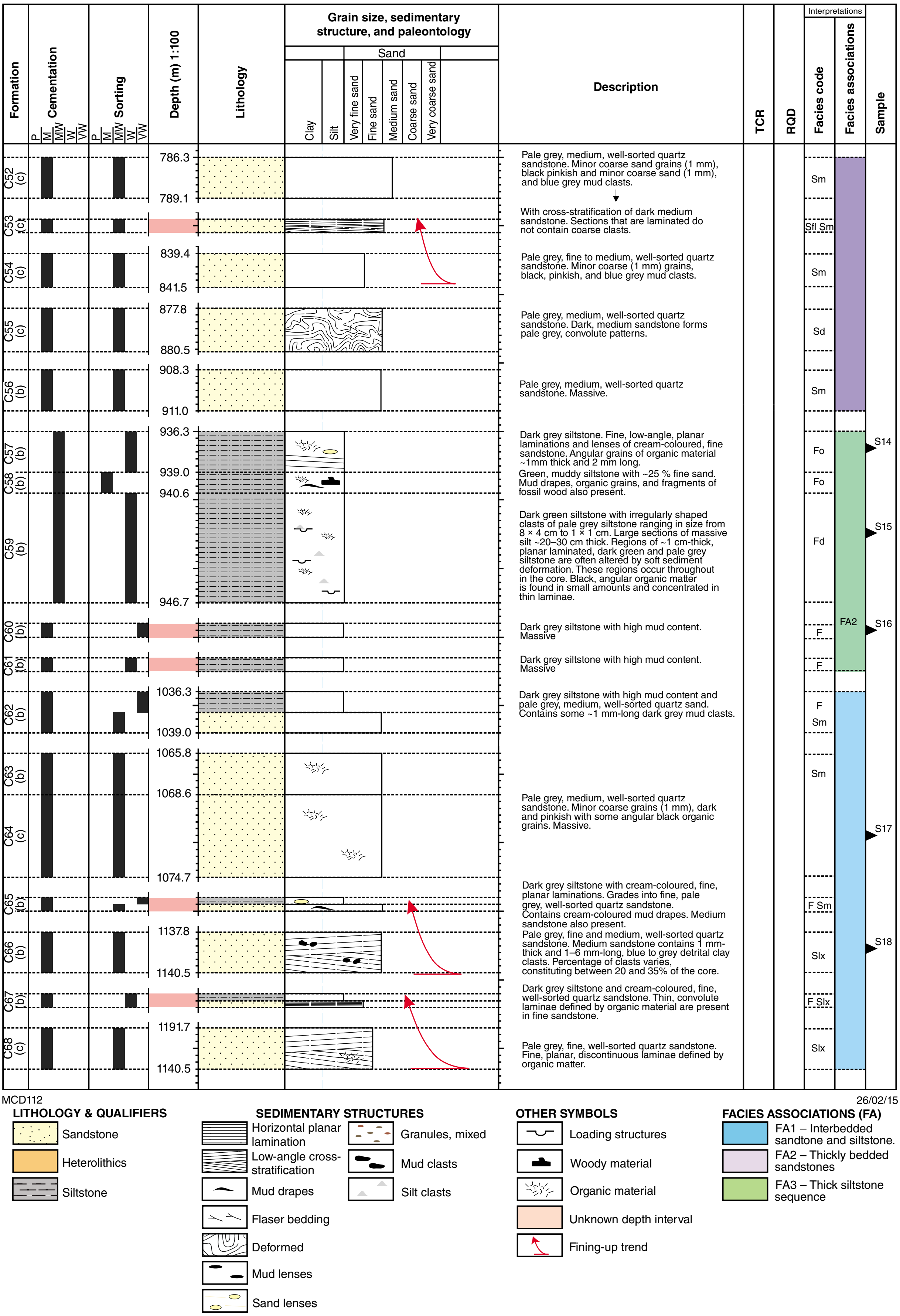

FRASER RIVER 1 CORE 69–73

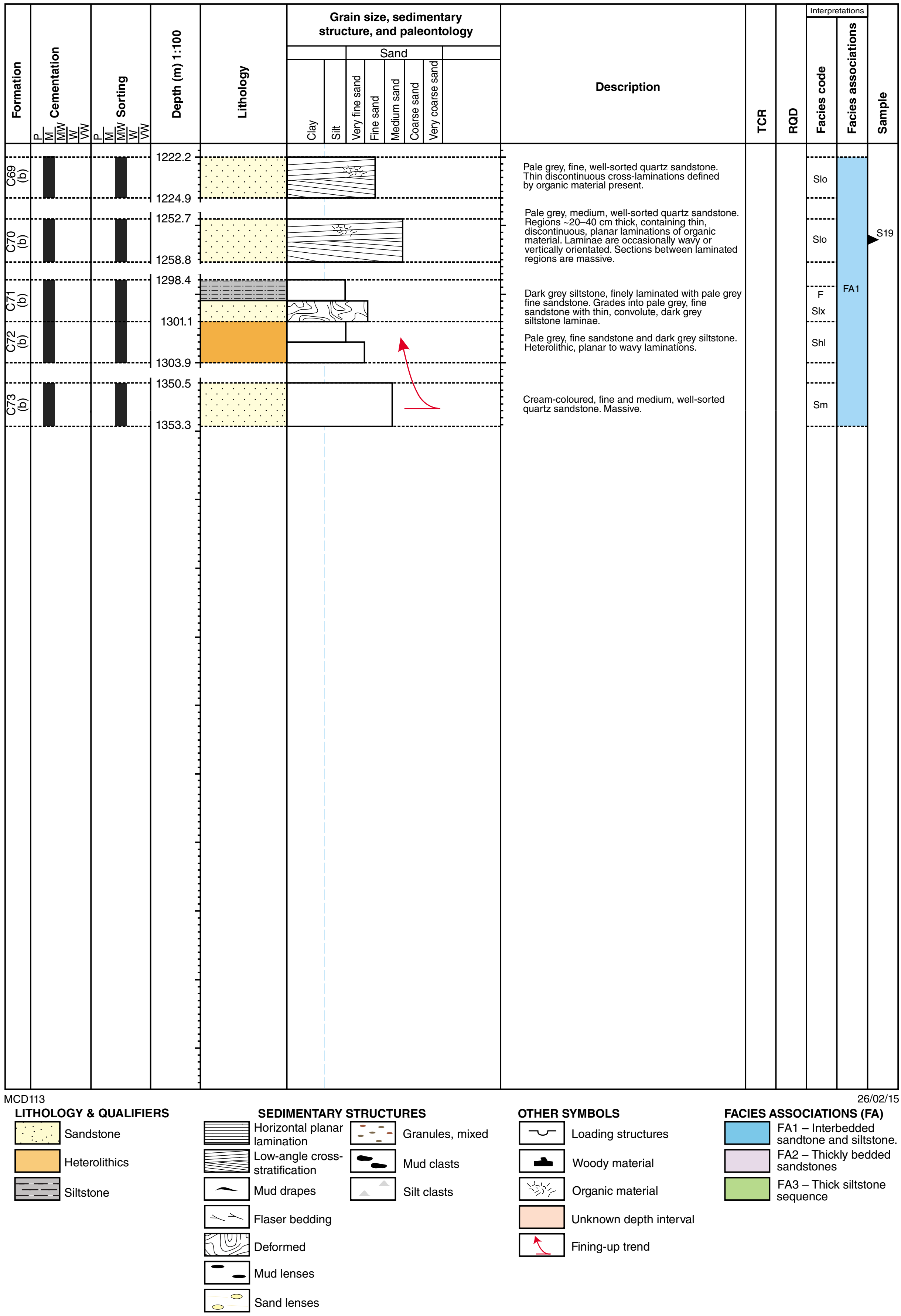

FROME ROCKS 2 CORE 6, 7 and 8

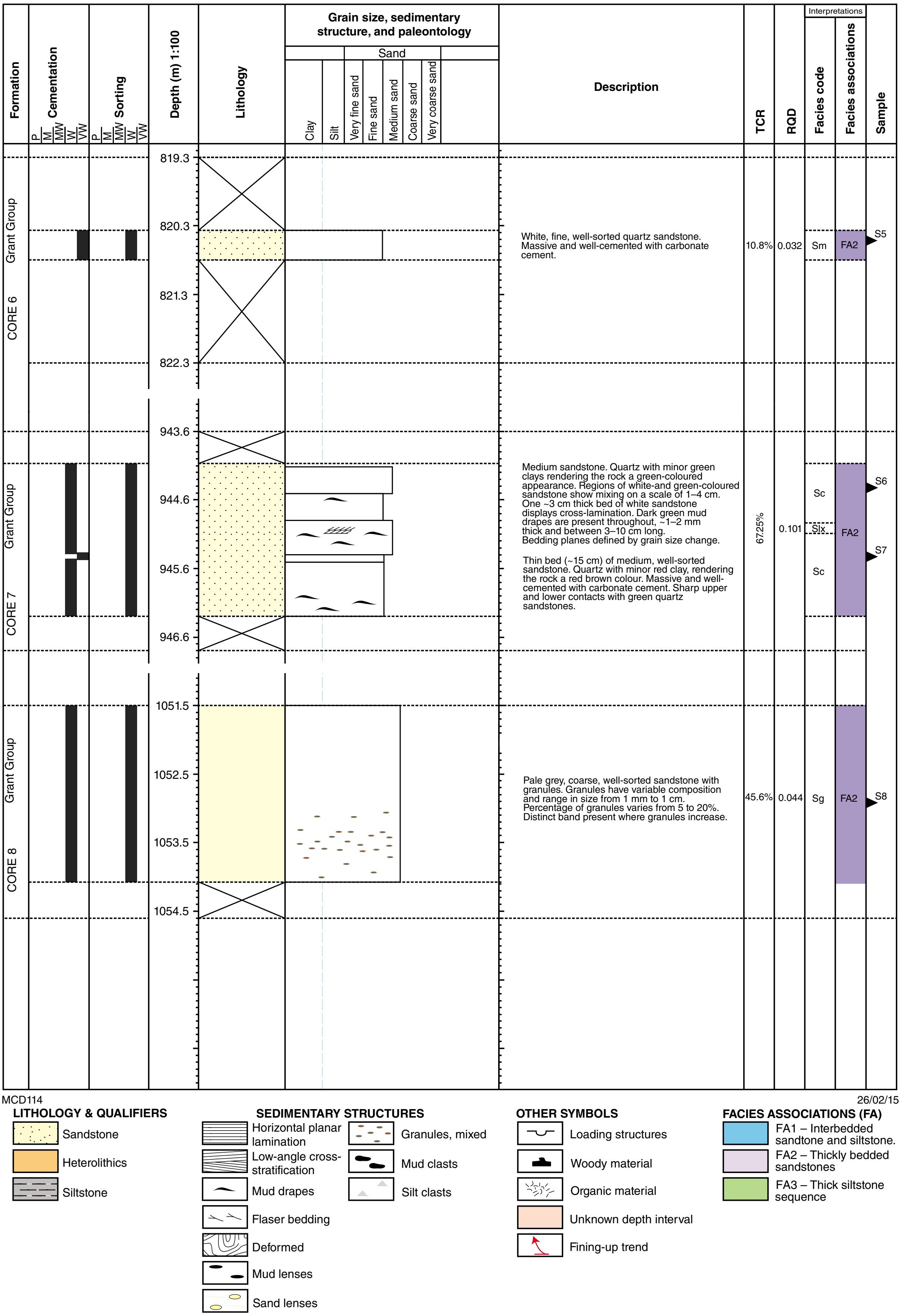

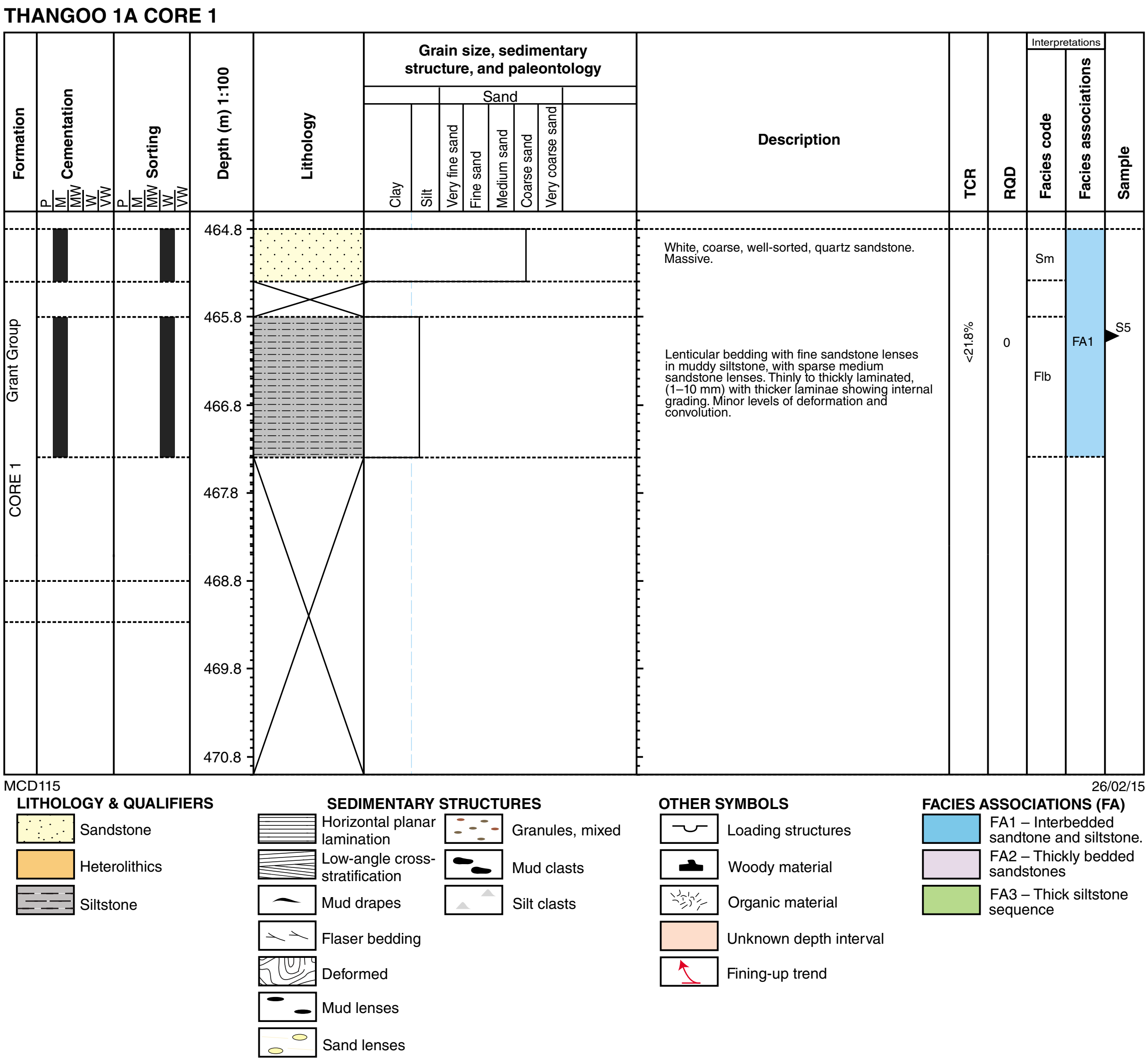
THANGOO 1A CORE 1
Formation
Cementation
Sorting
P M MW W VW
Depth (m) 1:100
Lithology
Grain size, sedimentary structure, and paleontology
Sand
Clay
Silt
Very fine sand
Fine sand
Medium sand
Coarse sand
Very coarse sand
Description
TCR
RQD
Interpretations
Facies code
Facies associations
Sample
Grant Group
CORE 1
464.8
465.8
466.8
467.8
468.8
469.8
470.8
White, coarse, well-sorted, quartz sandstone. Massive.
Lenticular bedding with fine sandstone lenses in muddy siltstone, with sparse medium sandstone lenses. Thinly to thickly laminated, (1–10 mm) with thicker laminae showing internal grading. Minor levels of deformation and convolution.
<21.8%
0
Sm
Flb
FA1
S5
MCD115
26/02/15
LITHOLOGY & QUALIFIERS
Sandstone
Heterolithics
Siltstone
SEDIMENTARY STRUCTURES
Horizontal planar lamination
Low-angle cross-stratification
Mud drapes
Flaser bedding
Deformed
Mud lenses
Sand lenses
Granules, mixed
Mud clasts
Silt clasts
OTHER SYMBOLS
Loading structures
Woody material
Organic material
Unknown depth interval
Fining-up trend
FACIES ASSOCIATIONS (FA)
FA1 – Interbedded sandtone and siltstone.
FA2 – Thickly bedded sandstones
FA3 – Thick siltstone sequence

Appendix 2 – Grant Group facies

APPENDIX 2: GRANT GROUP FACIES

Grant Group facies present in wells Frome Rocks 2, Doran 1, Thangoo 1A and Fraser River 1 from the Northern Canning Basin.
Facies codes: S: sandstone, F: siltstone, c: coarse f: fine, vf: very fine, m: massive, l: laminated x: cross-laminated, o: organic, p: carbonate cement, d: deformed, h: heterolithic

	Code	Name	Bedding	Description	Depositional Conditions
SANDSTONE	Sg	Gritty, coarse sandstone	Thickly bedded	Coarse sand with well-sorted, subrounded grains. Composition is quartz, with minor potassium feldspar and lithic fragments and well-cemented by carbonate cement. Granules of variable composition, ranging from 1 mm to 1 cm in length are present and granule content varies between 5–20%.	Moderate to high energy setting is indicated by the presence of granules. Thick bedding suggests high sediment input (e.g. Carling and Dawson, 1996).
	Sc	Planar-bedded sandstone	Thickly bedded	Medium to coarse sand with well-sorted, subrounded grains. Composed of quartz, with minor potassium feldspar, lithic fragments and detrital clay. Thin to medium planar beds of different grain size with gradational contacts. Minor amounts of green clay mineral give deposit an overall greenish appearance.	Thickly bedded sandstone suggests high sediment input. Bedding indicates traction current deposition.
	Sl	Laminated, medium sandstone	Thickly bedded	Fine to medium sand with well-sorted, subangular grains. Composed of quartz, with minor lithic fragments. Fine, planar lamination.	Planar lamination suggests upper flow regime
	Sm	Massive medium sandstone	Thin to thickly bedded	Medium sand with well-sorted, subangular grains. Composed of quartz with minor lithic fragments. Bed thickness is up to 6 m. Massive.	Massive, thickly bedded well sorted sand suggests high sedimentary load and rapid deposition
	Slx	Planar and ripple cross-laminated sandstone	Thinly bedded	Fine to medium sand with well-sorted, subrounded grains. Composed of quartz with minor grey clay clasts (0.25mm). Fine, low-angle, closely spaced cross-stratification, both continuous and discontinuous. Possible trough, cross-lamination with ~2 mm-thick laminae of dark very fine sand and cream-coloured fine sand and fine ripple cross-lamination.	Planar and low-angle cross-lamination indicates upper flow regime and ripple cross-lamination ripple migration in the lower flow regime
	Sd	Deformed medium sandstone	Thickly bedded up to 40 cm	Cream-coloured, medium sand and dark green, fine sand (0.1875 – 0.25 mm) with well-sorted subrounded grains. Thin laminations extensively deformed and highly convolute, often showing vertical orientation.	Medium to thick beds show extensive soft sediment deformation with convolute lamination and vertical laminae orientation. Indicative of sediment deformation by slumping.
	Slo	Sandstone with organic laminae	Thickly bedded	Fine to medium sand with well-sorted, subangular grains. Composed of quartz with minor potassium feldspar and lithic fragments. Fine (<1 mm) laminae and beds are defined by black (~0.25 mm) organic grains. Closely spaced, planar-laminated horizons and low-angle discontinuous cross-stratification. Localized convolution and deformation of both lamination styles may be present. Bedding is planar with weak internal lamination and sharp upper and lower contacts. Bed thickness ranges from very thin (laminae thickness 2 mm) to thick (30 cm).	Planar and low-angle cross-lamination indicate upper flow regime conditions. Convolute lamination suggests soft sediment deformation due to slumping or loading of overlying sediments. Organic matter indicates terrestrial plant source.
	Sf	Fine sandstone with sand and mud lenses	Thickly bedded	Green grey, fine sand with poorly sorted, subangular grains. Composed of quartz with ~10% detrital clay. Cream-coloured, fine sand and dark grey muddy lenses present throughout. Sand lenses range from 1–2 mm thick and 4 cm long to 1 × 1 mm and mud lenses range from 1–2 mm thick and 2.5 cm long to 1 × 1 mm. Lenses are larger at depth and show a fining-up trend. Thin, 1–2 mm planar laminae of both sand and muddy material and mud drapes are present at depth where larger lenses form.	Thick, fine sands beds indicate moderate energy condition and high sediment input. Planar lamination indicates traction current activity with mud drapes, indicating suspension settling and low-energy conditions.
	Sfh	Very fine, heterolithic sandstone	Bed thickness unknown	Pale grey, very fine sand and dark grey silt. Heterolithic, lenticular bedding style, planar lamination and flaser bedding.	Fine sandstone suggests low-energy conditions. Lenticular and flaser bedding indicates alternating current energy with suspension settling of muds.
	Svf	Very fine sand	Bed thickness unknown	Very fine sand. Composed of quartz with ~10% detrital clay. Dark, very fine grained sand distributed throughout white sand. May contain ~1–2 mm thick mud drapes that are abundant and overlap each other.	Fine grain size, clay content and mud drapes indicate overall low-energy deposition, with periodic suspension settling of muds
SILTSTONE	Fhl	Heterolithic, laminated siltstone	Bed thickness unknown	Pale grey, very fine sand and dark grey silt. Heterolithic, planar and wavy lamination, ~1–2 mm thick.	Heterolithic siltstone indicates low-energy settings and weak traction current activity (e.g. Miall,1996)
	Fo	Organic siltstone	Bed thickness unknown	Green fine sand and silt. Beds comprise fine sand (80%) with silt (20%) and silt (75%) with fine sand (25%). Silt with fine sand is poorly sorted. Fossil wood is present.	Silt indicates suspension settling and low-energy conditions, possibly standing water (e.g. Miall, 1996)
	F	Siltstone	Bed thickness unknown	Dark grey silt with moderate to high clay content. Massive.	Silt and clay indicate suspension settling in very low-energy conditions
	Fl	Laminated siltstone	Bed thickness unknown	Dark green grey silt. Small mud and fine sand lenses, ~1–2 mm thick and 1–2 cm long. Large angular muddy clasts (~3 × 5 cm), containing small amounts of fine sand (~5%) also present.	Laminated siltstone indicates low-energy conditions and weak traction current activity, associated with sand deposition
	Fd	Deformed siltstone	Bed thickness unknown	Dark green silt. Large sections (20–30 cm) of massive silt and large sections with pale grey silt clasts, ranging in size from 8 × 4 cm to 1 × 1 cm. Dark mud drapes (~1–2 mm thick and 4–5 cm long) are sparsely distributed. Regions of ~3 mm-thick, dark green and pale grey laminated silt, showing deformation with convolute lamination and internal slumping on a scale of 1–2 cm. Organic fragments (3 mm long) are frequent and commonly appear aggregated as a single laminae	Silt indicates suspension settling in-low energy conditions with some weak traction current activity. Soft sediment deformation of laminated silt potentially suggests deformation by rapid loading.
	Flb	Lenticular siltstone	Bed thickness unknown	Dark grey, muddy silt and pale grey, very fine sand. Lenticular bedding style with lenses of fine sand in muddy silt. Small, 1–2 cm-long lenses of medium sand sparsely distributed throughout. Very thick laminae to very thin beds (1 cm thick) of fine sand show internal gradational structure.	Lenticular bedding suggests overall low-energy conditions with alternating weak traction current activity and supsension settling of fine sediment

MCD117 05/03/15

Appendix 3 – Composite logs from studied wells

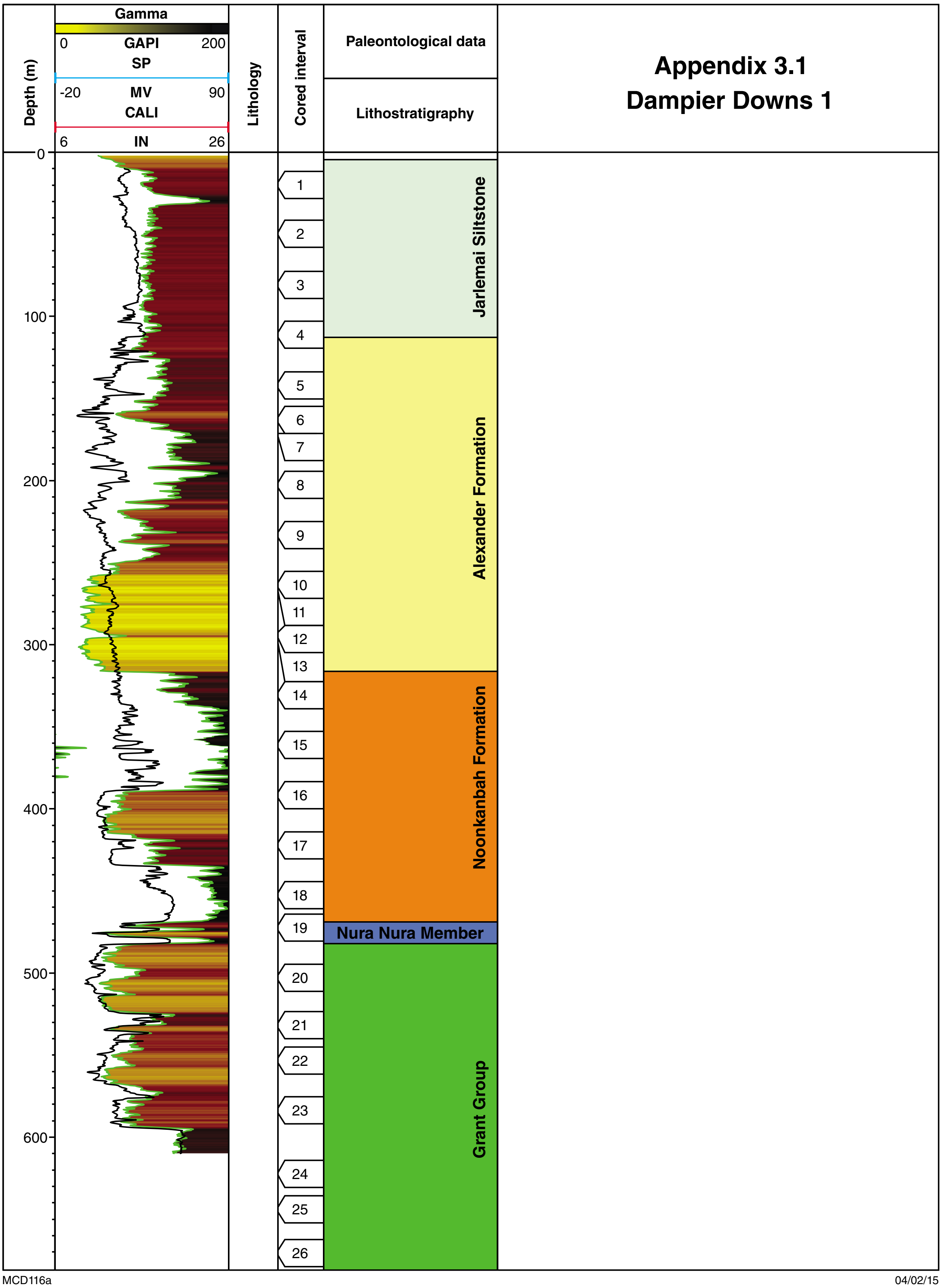

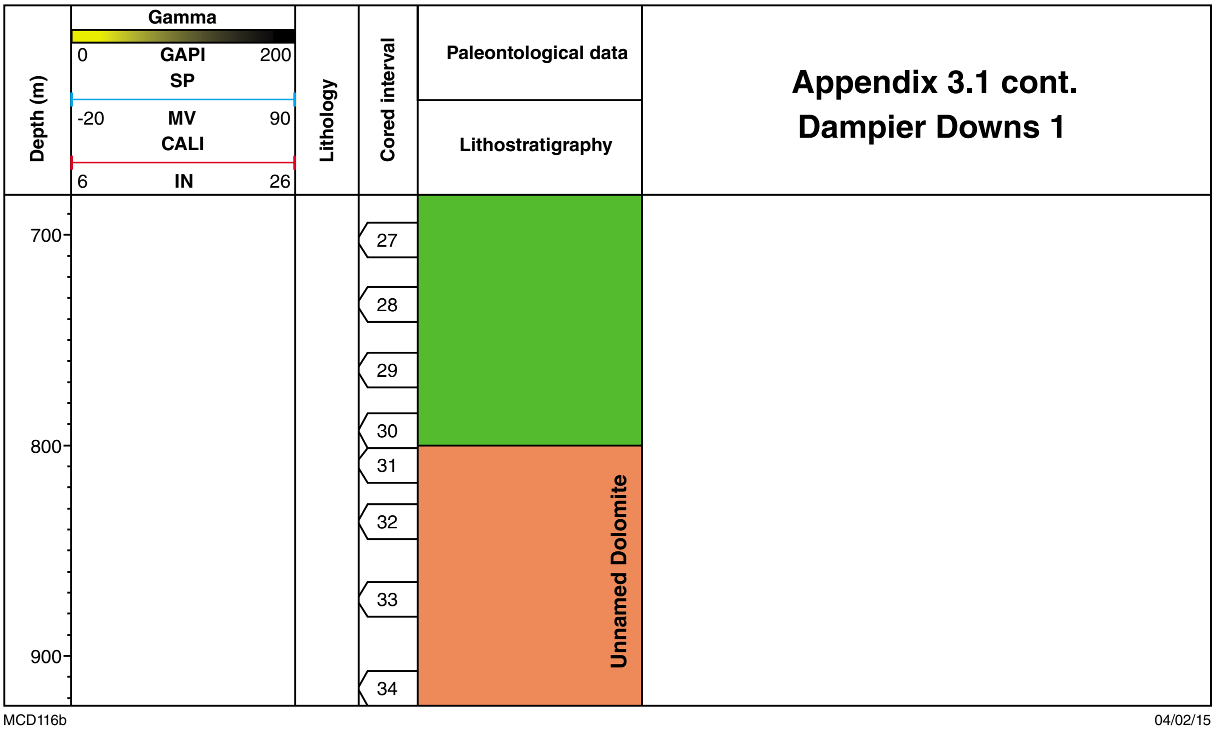
Appendix 3.1 cont.
Dampier Downs 1
Depth (m)
Gamma
0
GAPI
200
SP
-20
MV
90
CALI
6
IN
26
Lithology
Cored interval
Paleontological data
Lithostratigraphy
700
800
900
27
28
29
30
31
32
33
34
Unnamed Dolomite
MCD116b
04/02/15

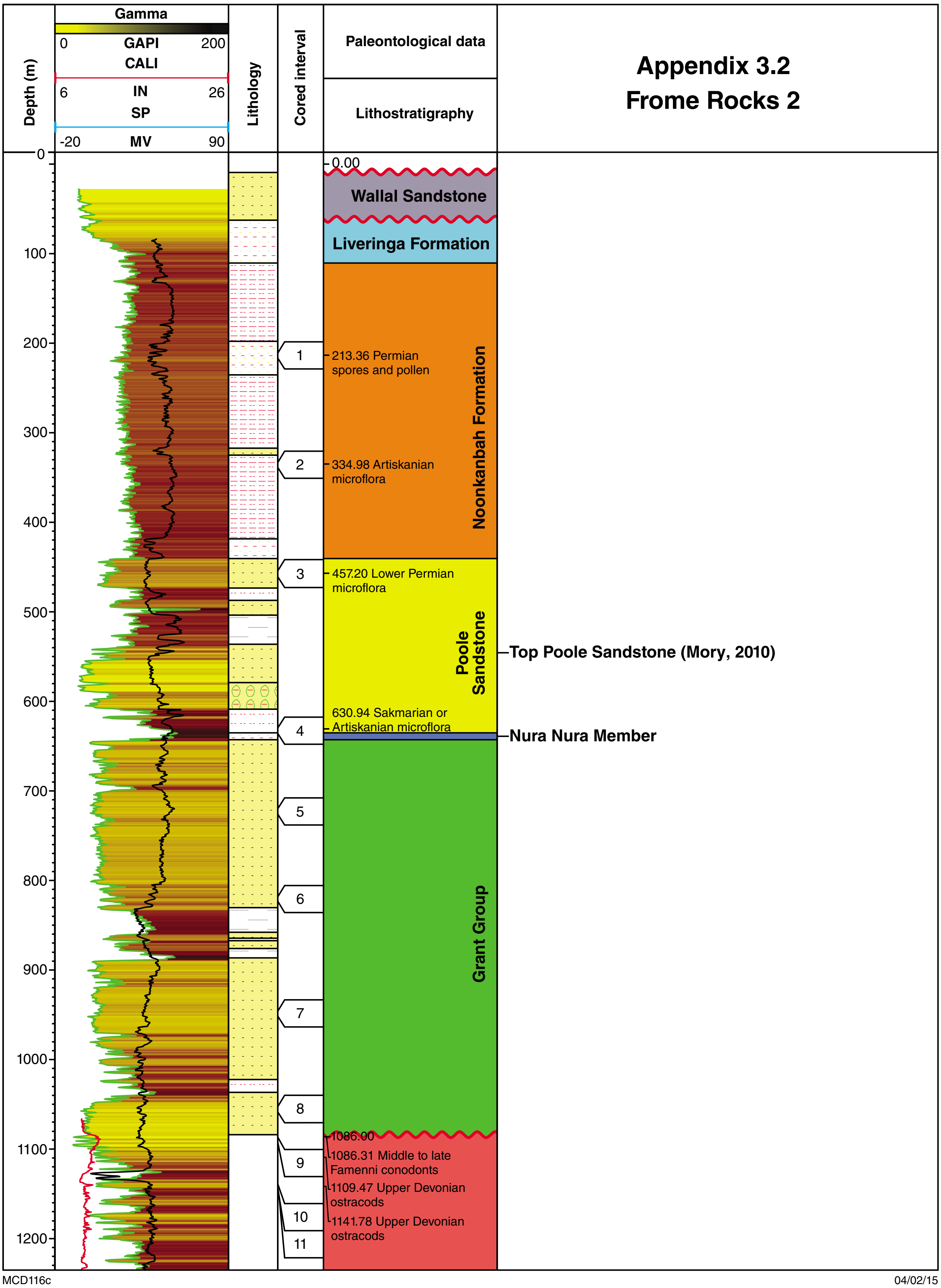
Appendix 3.2
Frome Rocks 2
Depth (m)
Gamma
0 GAPI 200
CALI
6 IN 26
SP
-20 MV 90
Lithology
Cored interval
Paleontological data
Lithostratigraphy
0.00
Wallal Sandstone
Liveringa Formation
Noonkanbah Formation
213.36 Permian spores and pollen
334.98 Artiskanian microflora
457.20 Lower Permian microflora
Poole Sandstone
Top Poole Sandstone (Mory, 2010)
630.94 Sakmarian or Artiskanian microflora
Nura Nura Member
Grant Group
1086.00
1086.31 Middle to late Famenni conodonts
1109.47 Upper Devonian ostracods
1141.78 Upper Devonian ostracods
0
100
200
300
400
500
600
700
800
900
1000
1100
1200
1
2
3
4
5
6
7
8
9
10
11
MCD116c
04/02/15

Appendix 3.2 cont.
Frome Rocks 2

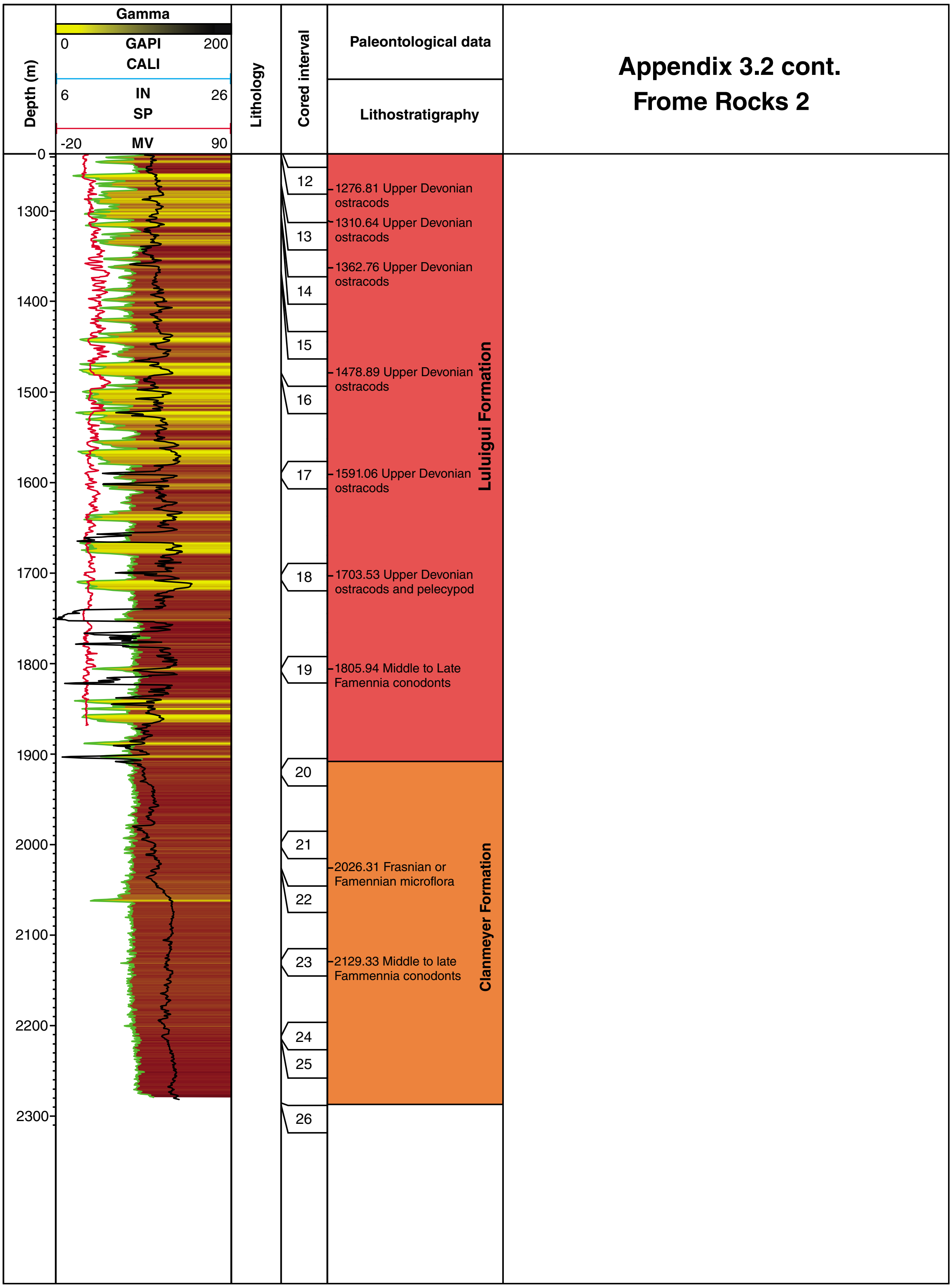

MCD116d 24/02/15

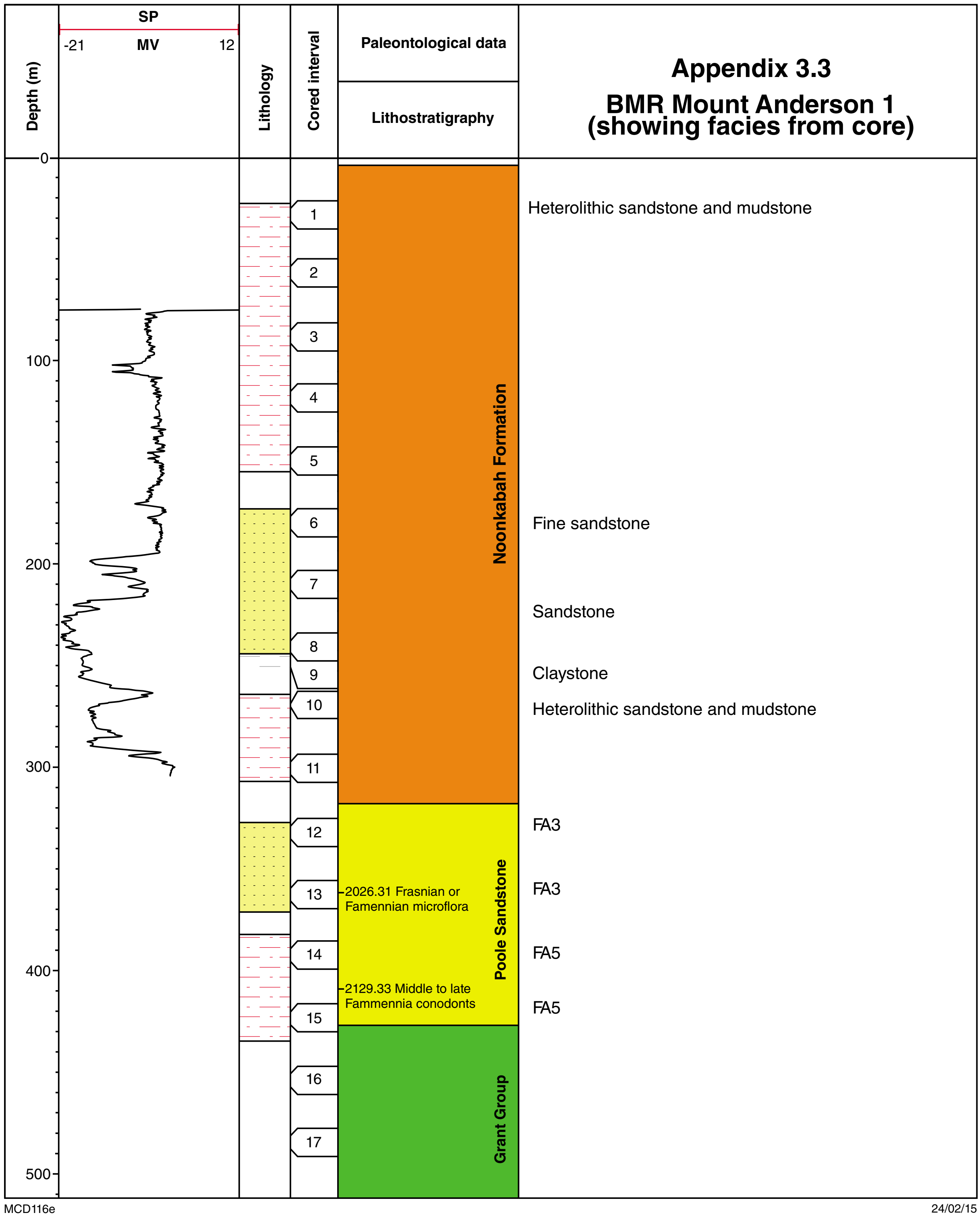
Appendix 3.3
BMR Mount Anderson 1
(showing facies from core)
Depth (m)
SP
-21
MV
12
Lithology
Cored interval
Paleontological data
Lithostratigraphy
0
100
200
300
400
500
1
2
3
4
5
6
7
8
9
10
11
12
13
14
15
16
17
Noonkabah Formation
Poole Sandstone
Grant Group
2026.31 Frasnian or Famennian microflora
2129.33 Middle to late Fammennia conodonts
Heterolithic sandstone and mudstone
Fine sandstone
Sandstone
Claystone
Heterolithic sandstone and mudstone
FA3
FA3
FA5
FA5
MCD116e
24/02/15

Appendix 3.4
Perindi 1

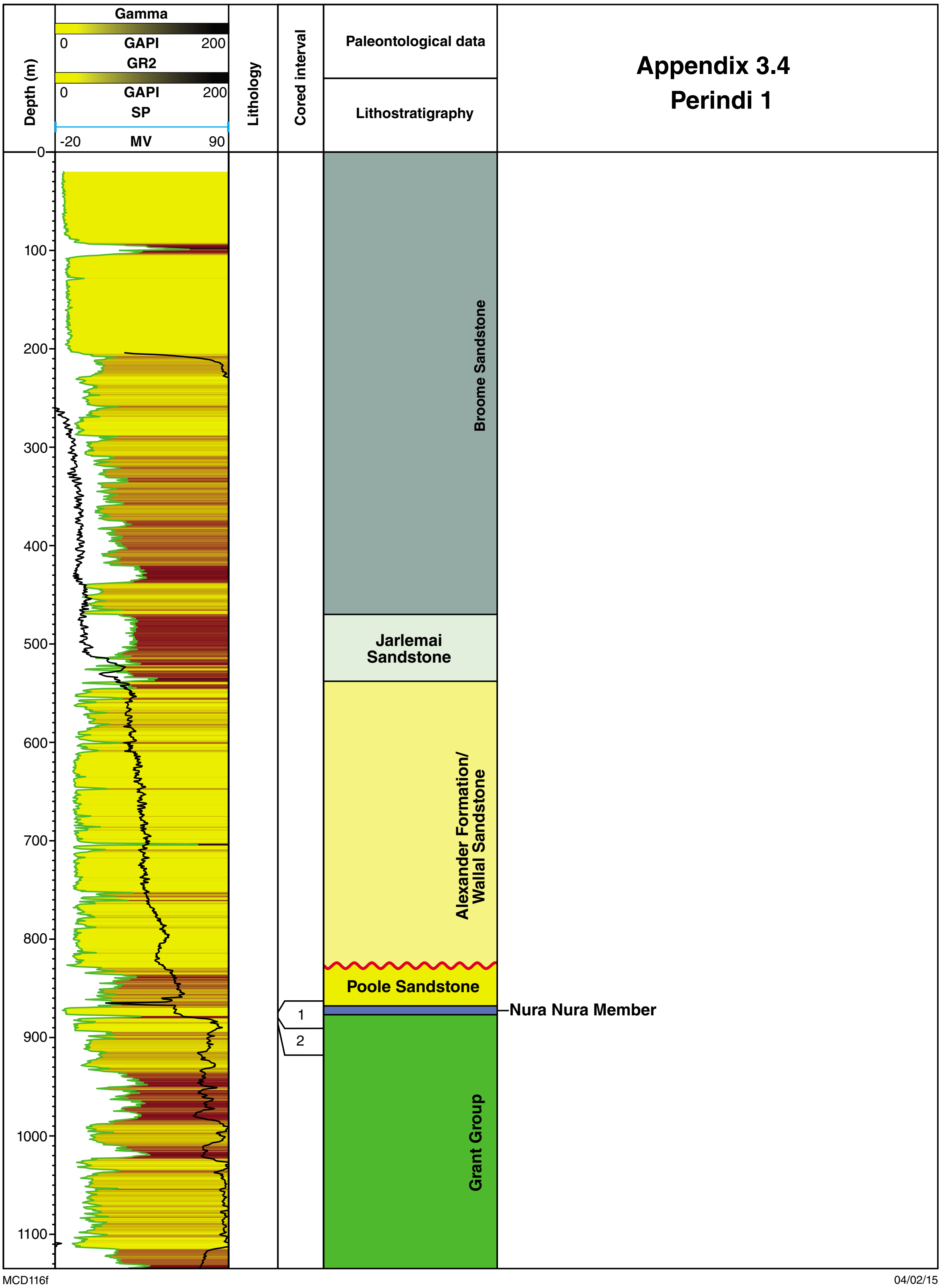

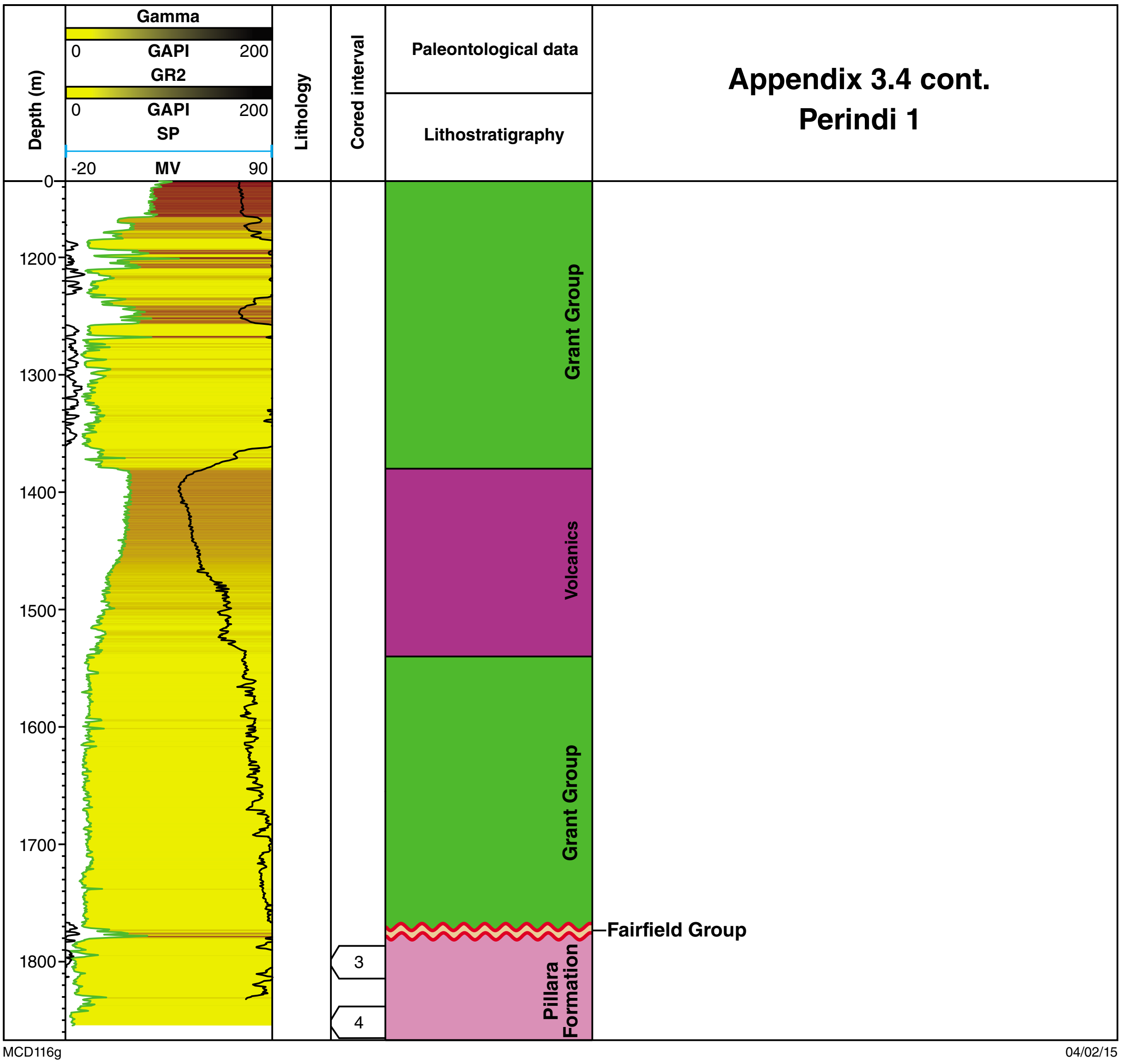
Depth (m)
Gamma
0 GAPI 200
GR2
0 GAPI 200
SP
-20 MV 90
Lithology
Cored interval
Paleontological data
Lithostratigraphy
Appendix 3.4 cont.
Perindi 1
0
1200
1300
1400
1500
1600
1700
1800
Grant Group
Volcanics
Grant Group
Fairfield Group
Pillara Formation
3
4
MCD116g
04/02/15

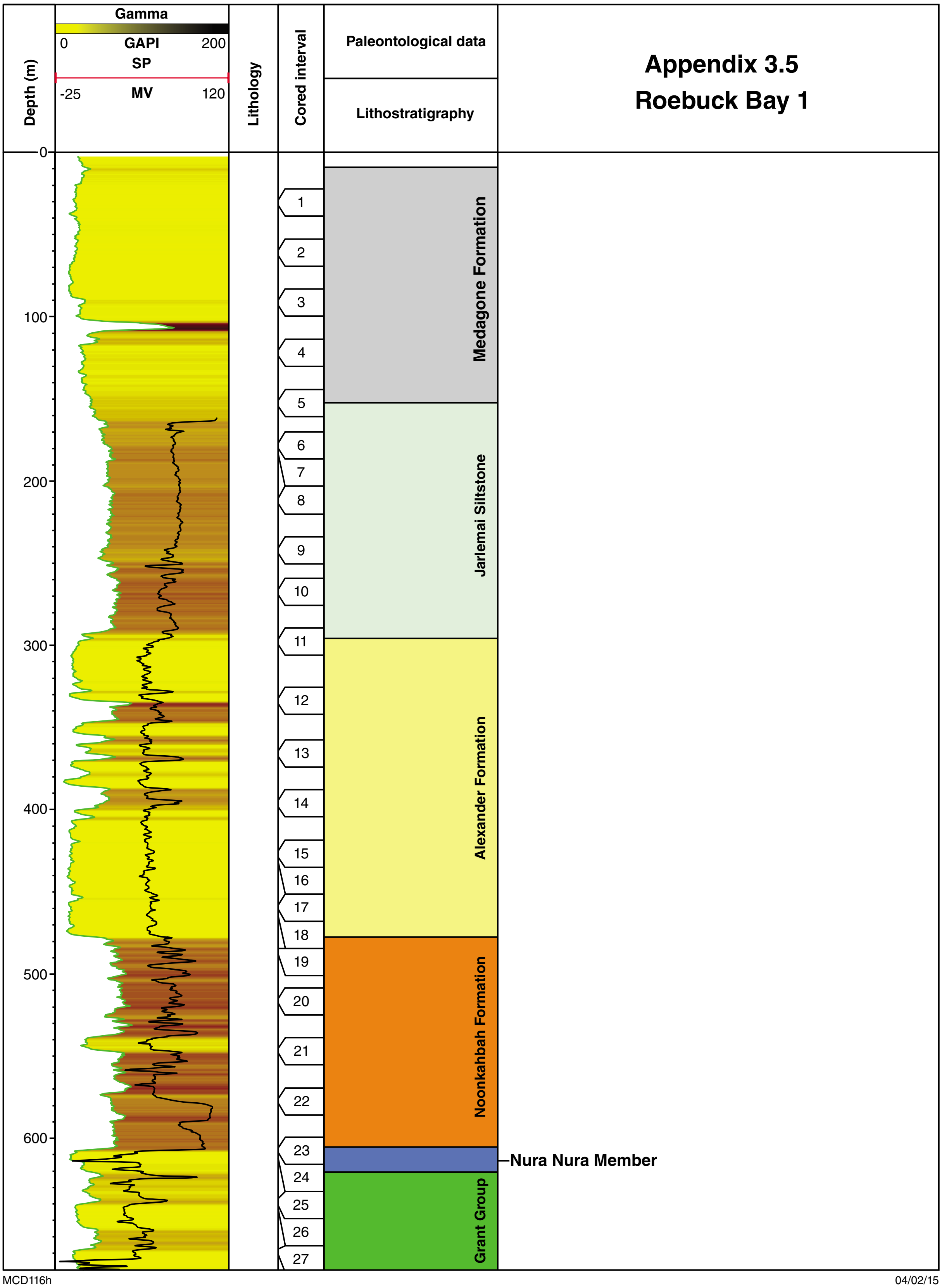
Appendix 3.5
Roebuck Bay 1
Depth (m)
Gamma
0 GAPI 200
SP
-25 MV 120
Lithology
Cored interval
Paleontological data
Lithostratigraphy
0
100
200
300
400
500
600
1
2
3
4
5
6
7
8
9
10
11
12
13
14
15
16
17
18
19
20
21
22
23
24
25
26
27
Medagone Formation
Jarlemai Siltstone
Alexander Formation
Noonkahbah Formation
Nura Nura Member
Grant Group
MCD116h
04/02/15

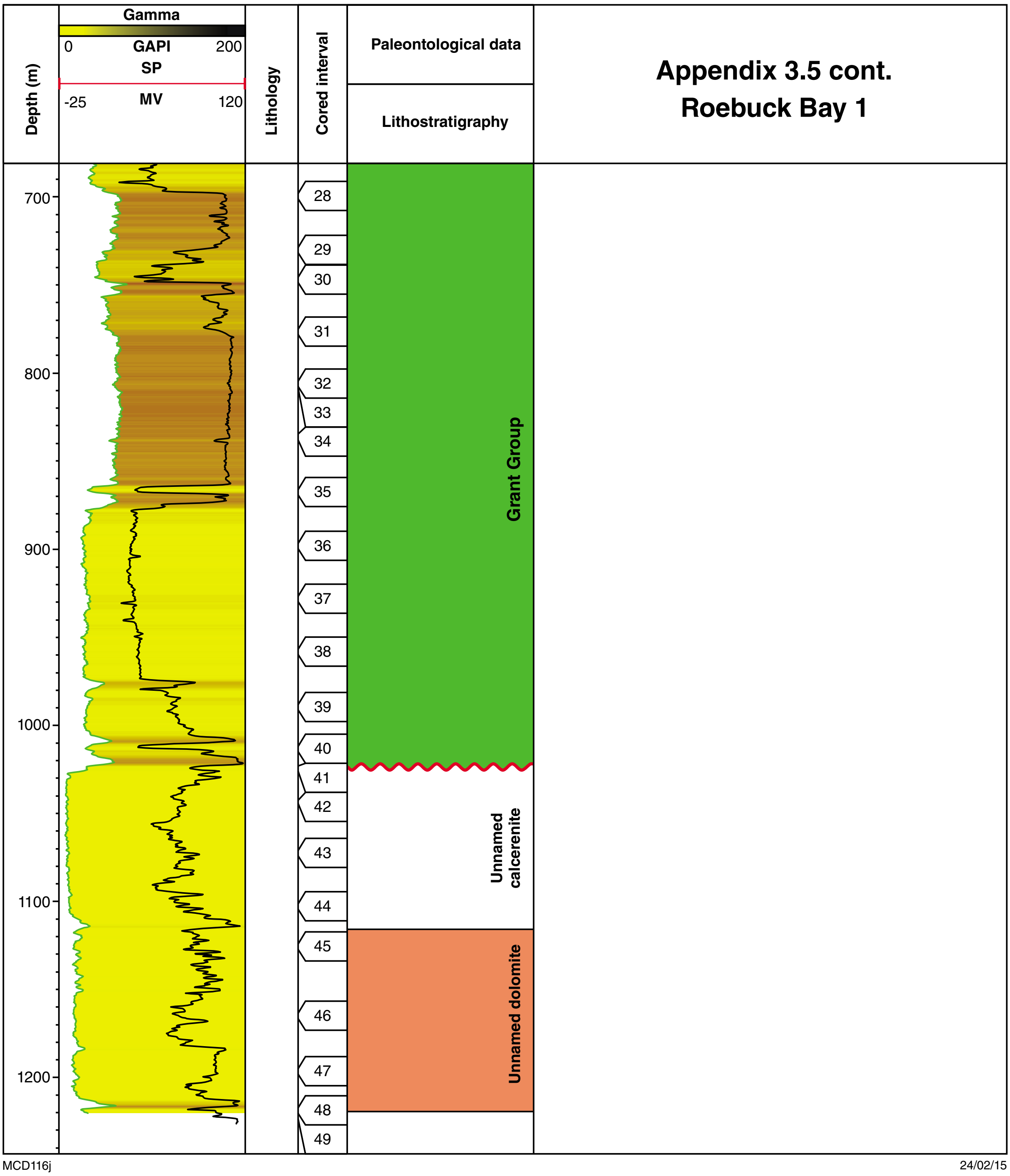
Depth (m)
Gamma
0
GAPI
200
SP
-25
MV
120
Lithology
Cored interval
Paleontological data
Lithostratigraphy
Appendix 3.5 cont.
Roebuck Bay 1
700
800
900
1000
1100
1200
28
29
30
31
32
33
34
35
36
37
38
39
40
41
42
43
44
45
46
47
48
49
Grant Group
Unnamed calcerenite
Unnamed dolomite
MCD116j
24/02/15

Appendix 3.6
Scarpia 1

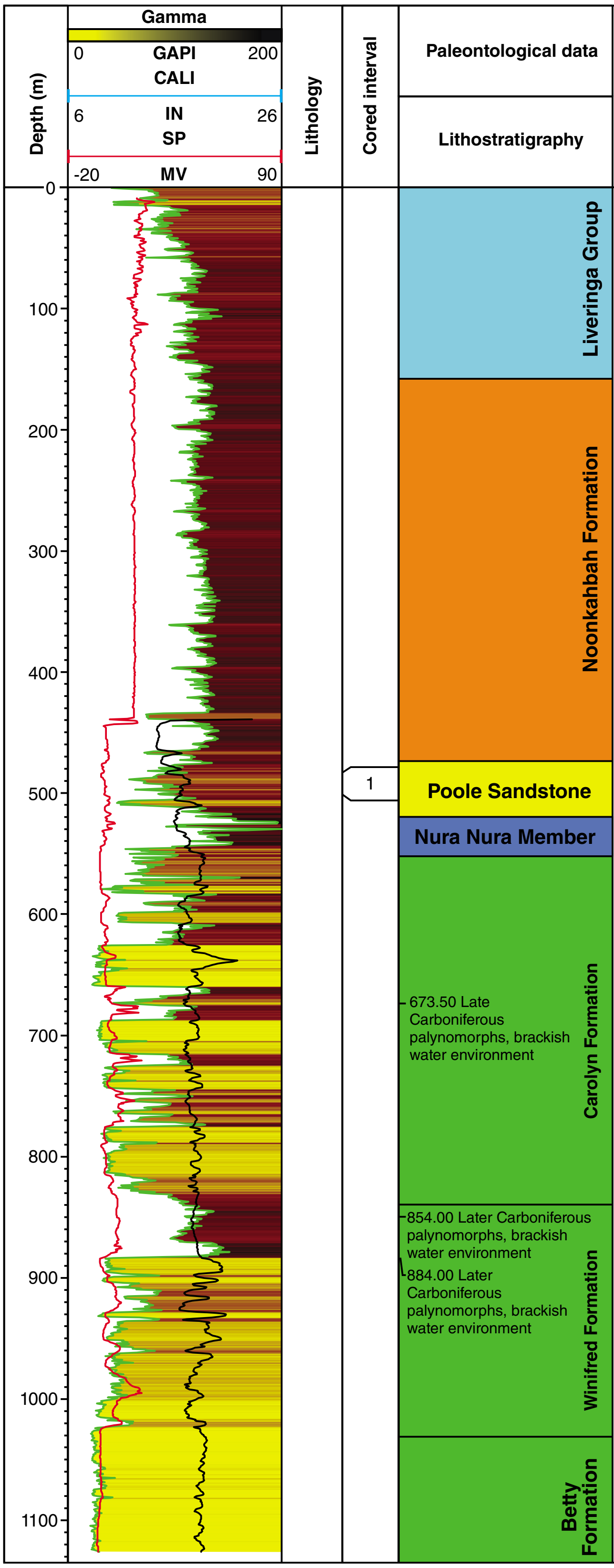

MCD116k 24/02/15

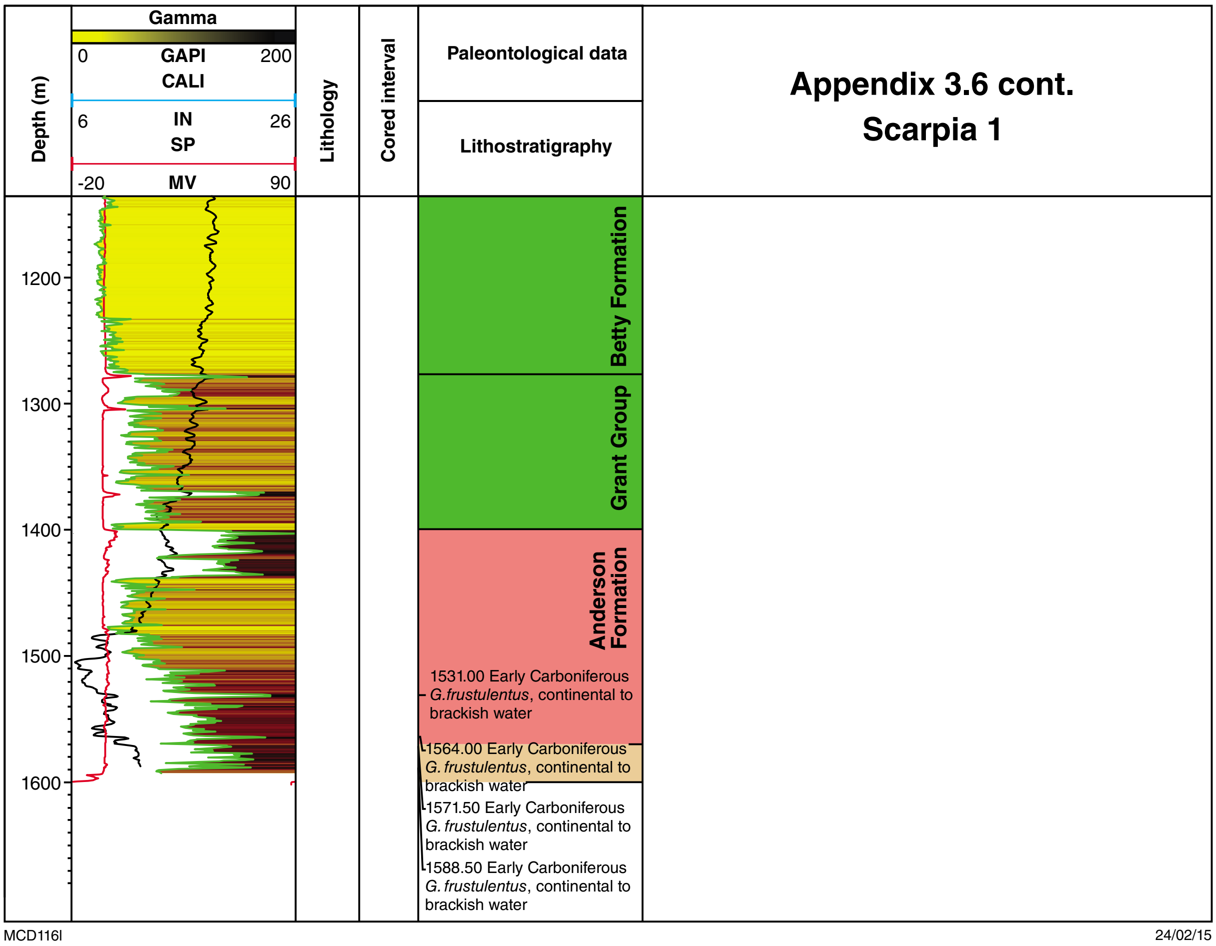
Depth (m)
Gamma
0
GAPI
200
CALI
6
IN
26
SP
-20
MV
90
Lithology
Cored interval
Paleontological data
Lithostratigraphy
Appendix 3.6 cont.
Scarpia 1
1200
1300
1400
1500
1600
Betty Formation
Grant Group
Anderson Formation
1531.00 Early Carboniferous G.frustulentus, continental to brackish water
1564.00 Early Carboniferous G. frustulentus, continental to brackish water
1571.50 Early Carboniferous G. frustulentus, continental to brackish water
1588.50 Early Carboniferous G. frustulentus, continental to brackish water
MCD116I
24/02/15

Appendix 3.7
Sundown 3

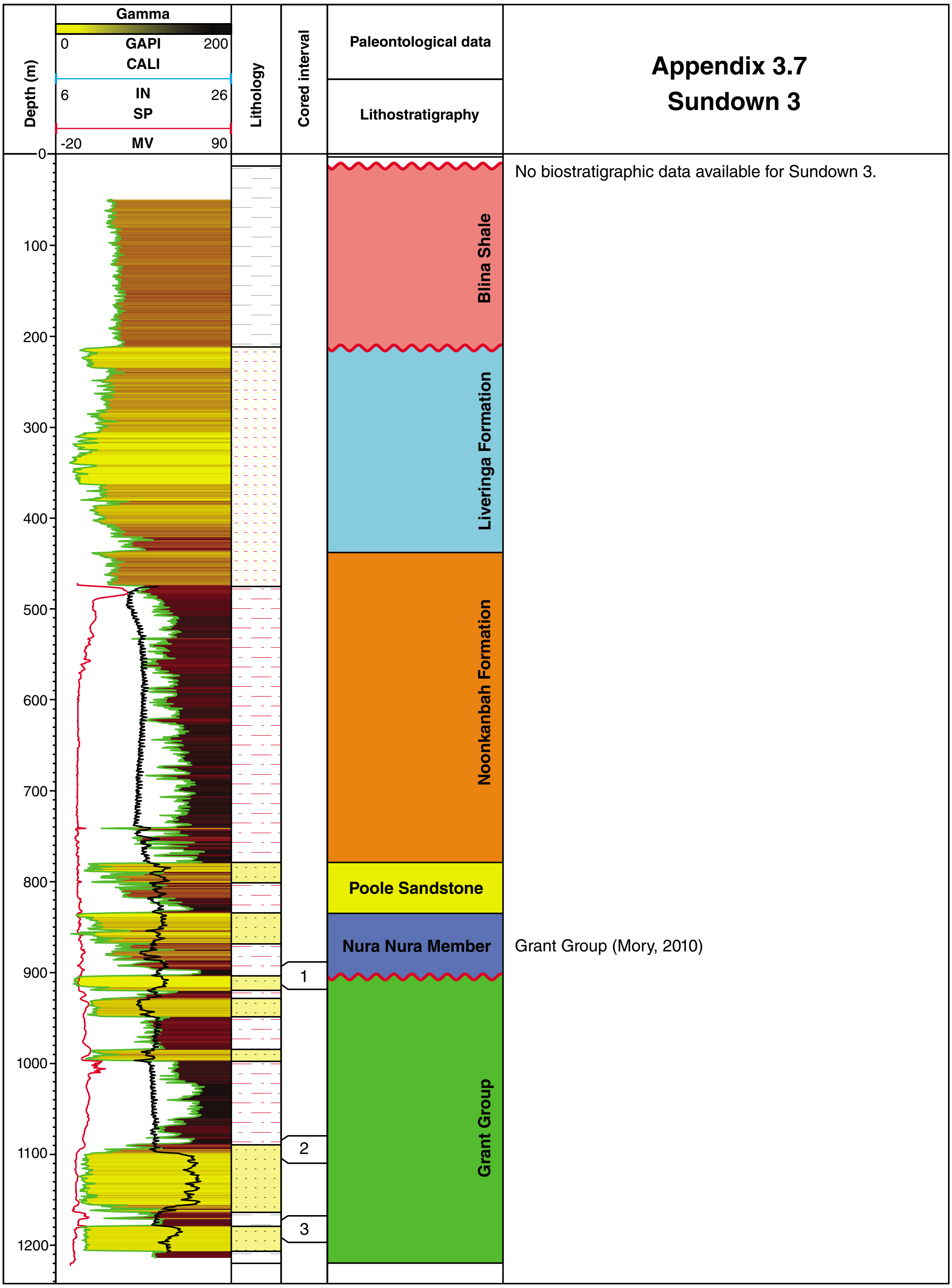

No biostratigraphic data available for Sundown 3.

Grant Group (Mory, 2010)

MCD116m 04/02/15

Appendix 3.8
The Sisters 1

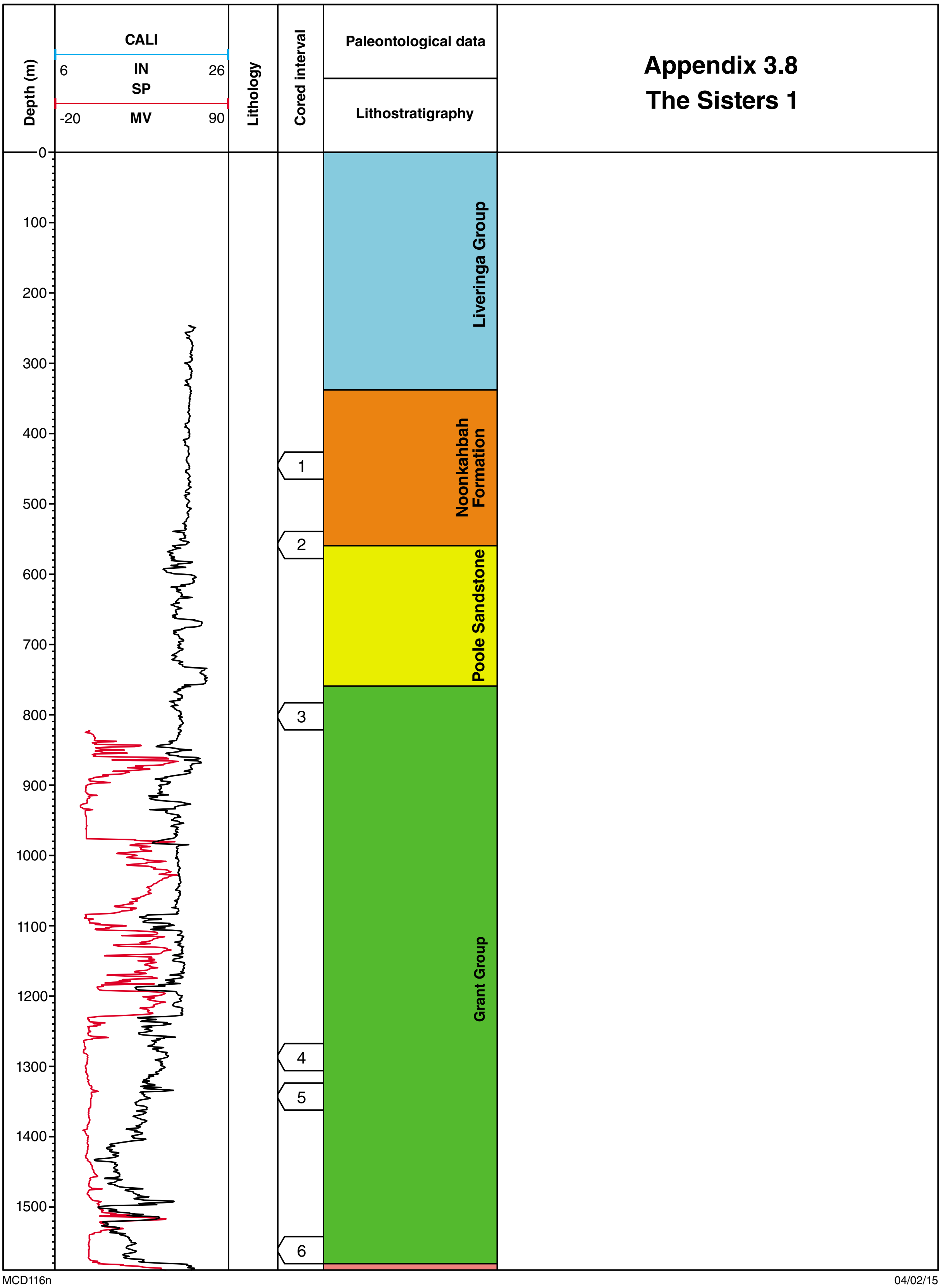

Appendix 3.8 cont.
The Sisters 1

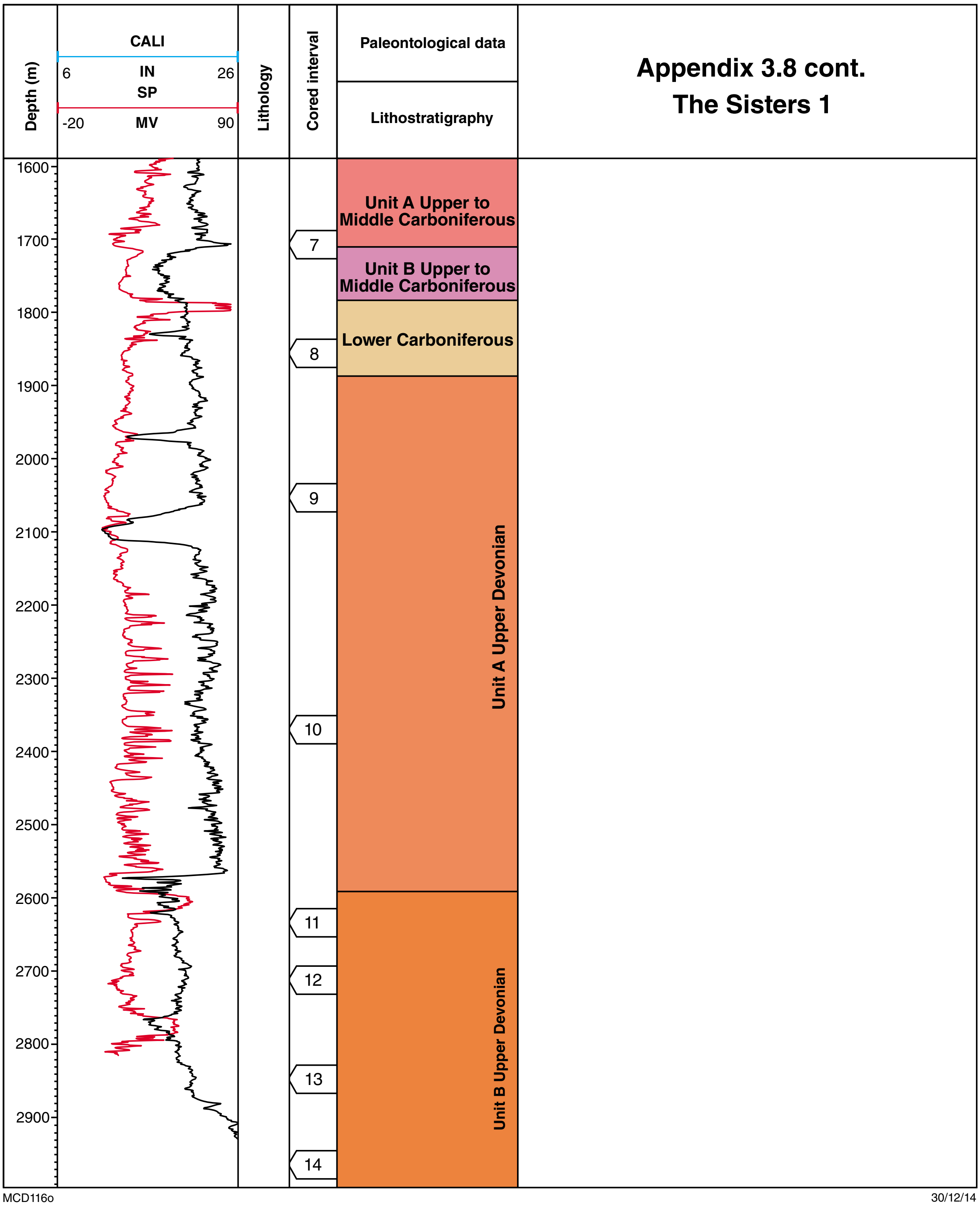

Appendix 4 – Facies scheme for Poole Sandstone, Noonkanbah Formation and Grant Group

APPENDIX 4: Facies scheme for Grant Group, Poole Sandstone and Noonkanbah Formation

	Facies	Code	Bed thickness	Description (texture and fabric)	Fossils and bioturbation index	Depositional processes and/or conditions
CONGLOMERATE	Massive, clast-supported conglomerate	Gm	N/A	Massive clast-supported conglomerate. Some clasts are brown, rounded carbonate spheres with a core of angular mudstone. Other clasts are dark grey, angular mudstone with lamination. Clasts are up to 2 mm long. Matrix is fine sandstone.	None	Coarse grain size indicates high-energy and rapid deposition
CONGLOMERATE	Pebbly sandstone	Gs	Thin	Pebbly sandstone with rounded or elongated mud rip-up clasts in medium sandstone	None	Rapid deposition in high-energy conditions
SANDSTONE	Planar-laminated, medium sandstone	Smh	Laminated	Pale grey, planar-laminated medium sandstone	None	Planar lamination in medium sandstone indicates upper flow regime condition
SANDSTONE	Thinly bedded sandstone	Sm	Thinly bedded	Thinly bedded, fine to medium sandstone with some 20 mm-long black organic matter, possibly wood fragments. Locally lenticular bedded. Sandstone is moderately sorted with subrounded to subangular quartz grains. Micaceous.	None	Massive fabric suggests rapid deposition and local fluctuating conditions to form lenticular bedding
SANDSTONE	Medium to thick, cross-bedded sandstone	Sxo	Medium to thick (0.3 to 0.5 m)	Pale grey, cross-bedded medium sandstone with scattered carbonaceous flakes. Beds have sharp bases. Locally structureless.	Mottled at the top	Cross-bedding indicates migration of 2D and 3D bars and dunes. Sharp bases with local pebbly layers suggest bars and dunes migrated over scoured surfaces.
SANDSTONE	Thick, cross-bedded	Sxm	Thick (0.5 to 1 m)	Pale grey cross-bedded medium, locally coarse, sandstone. Sharp-based beds and local pebbly bases. Local mud drapes.	None	Cross-bedded indicates migration of 2D and 3D bars and dunes. Sharp bases with local pebbly layers suggests bars and dunes migrated over scoured surfaces
SANDSTONE	Interbedded, ripple cross-laminated fine sandstone and bioturbated mudstone	Sfr	Laminated to very thin bedded	Ripple cross-laminated fine sandstone and bioturbated mudstone. Sharp contacts truncating convolute laminae or bioturbated mudstone. Mud drapes preserved in the ripple cross-laminated intervals.	Local moderate bioturbation (2) with *Teichichnus* and *Planolites*	Ripple cross-lamination indicates deposition in lower flow regime. Bioturbation suggests marine conditions. Sharp contacts from scouring by higher energy currents.

MCD118a 26/02/15

APPENDIX 4 continued: Facies scheme for Grant Group, Poole Sandstone and Noonkanbah Formation

	Facies	Code	Bed thickness	Description (texture and fabric)	Fossils and bioturbation index	Depositional processes and/or conditions
SANDSTONE	Convolute-laminated fine sandstone	Sfc	Laminated to very thin bedded	Convolute-laminated fine sandstone, locally truncated sharply	None	Convolute lamination shows rapid deposition and soft sediments deformation. Synsedimentary faults are interpreted as soft sediment deformation. Sharp contacts from scouring by higher energy currents.
	Planar-laminated fine sandstone	Sfh	Thinly to thickly laminated	Pale grey planar laminated fine sandstone	None	Planar-lamination in sandstone indicates deposition in upper flow regime
	Bioturbated sandstone with vertical burrows	Sfv	Medium (0.1 – 0.15 m)	Pale grey, fine bioturbated sandstone with up to 0.15 m vertical burrows	Moderate (2–3) with *Ophiomorpha* and *Planolites*	Presence of trace fossils, especially *Ophiomorpha* indicates marine environments. Limited number of trace fossils suggests restricted conditions.
	Sandstone with mud drapes	Sfm	Thin to medium	Fine sandstone with sharp bed bases and local mud drapes. Local lenticular bedding.	Rare horizontal burrows	Migration of 2D and 3D ripples in lower flow regime. Mud drapes indicate marine influence.
	Hummocky-swaley cross-laminated sandstone	Sfs	Laminated to thin	Fine sandstone with thin intervals (up to 10 mm) of mudstone. Laminated to hummocky–swaley cross-lamination.	None	Hummocky–swaley cross-lamination indicates influence of storm waves below fair weather wave base and above storm wave base
	Bioturbated sandstone with horizontal burrows	Sfb	Thin to medium	Pale grey, fine sandstone with scattered rounded mudstone clasts. Subangular to subrounded, well-sorted quartz grains.	Moderate (2–3)	Bioturbation indicates marine influence
	Sandstone with mud laminae	Sff	Laminated to very thin	Pale, cream-coloured fine sandstone with some mud laminae, local ripple cross-laminated or cross-bedded and some thick intervals of mud	None	Migration of 2D and 3D ripples in lower flow regime
	Wavy-laminated to lenticular-bedded sandstone	Hw	Thinly bedded (10–30 mm)	Mud-dominated, heterolithic, fine sandstone and siltstone with wavy-laminated to lenticular bedding. Intervals of mud rip-up clasts in fine sandstone matrix.	None	Deposition in fluctuating energy conditions

MCD118b 26/02/15

APPENDIX 4 continued: Facies scheme for Grant Group, Poole Sandstone and Noonkanbah Formation

	Facies	Code	Bed thickness	Description (texture and fabric)	Fossils and bioturbation index	Depositional processes and/or conditions
Heterolithic sandstone–mudstone	Lenticular-bedded, heterolithic sandstone–siltstone	Hm	Thinly bedded	Mud-dominated, heterolithic sandstone–siltstone with lenticular bedding and local ripple cross-lamination	None	Deposition in low-energy conditions with episodic higher energy conditions
	Thinly bedded, heterolithic sandstone–siltstone	Hh	Thinly bedded	Thinly bedded heterolithic sandstone–siltstone	None	Deposition in fluctuating, overall low-energy conditions
	Locally bioturbated, heterolithic sandstone–siltstone	Hl	Laminated to thinly bedded	Heterolithic sandstone–mudstone with local bioturbation, local lenticular bedding	Locally weak bioturbation	Deposition from suspension in low-energy conditions
	Bioturbated, heterolithic sandstone–siltstone	Hb	Thinly bedded (10–30 mm)	Bioturbated, heterolithic mudstone and fine sandstone	Intense (3–4) with horizontal burrows and *Chondrites*	Deposition in fluctuating energy conditions. Bioturbation suggests marine conditions. Dominance of horizontal trace fossils indicates deeper water.
Mudstone	Bioturbated mudstone	Mhb	Laminated to thinly bedded	Planar-laminated to thinly bedded dark grey mudstone	Moderate (2–3) with *Planolites* and *Teichichnus*	Fine sediment indicates deposition in low-energy conditions or stressed environment
	Mudstone	Mh	Laminated to thinly bedded	Planar-laminated to thinly bedded dark grey mudstone	None	Deposition from suspension in low-energy conditions with weak traction current activity
Limestone	Skeletal rudstone–grainstone	Lgs	Very thin to thinly bedded (20–60 mm)	Light grey, very thinly to thinly bedded skeletal rudstone–grainstone with various skeletal grains. Intervals of carbonate mudstone and siltstone with sharp contacts. Some beds are normally graded with skeletal base and siltstone tops. Skeletal grains are subhorizontally aligned. Local clasts of skeletal packstone–wackestone.	Crinoids, fusulinids, and fragmented bryozoans, brachiopods, and bivalves	Presence of marine fauna indicates deposition in marine environment. Abraded shells suggest transportation and high-energy conditions. Graded bedding indicates reworking of skeletal material.

MCD118c 26/02/15

APPENDIX 4: Summary of facies associations recognised in cored intervals in Grant Group, Poole Sandstone and Noonkanbah Formation

Unit	Facies asssociation	Bed thickness Description (texture and fabric)	Major facies	Minor facies	Trends	Well examples
Grant Group	FA1	Cross-bedded sandstone	Sxo, Sxm			Sundown 3 C1
	FA2	Lenticular-bedded heterolithic sandstone–siltstone and mudstone	Sfr, Hm, Mh	Smh, Zh	FU	Sundown 3 C1
	FA3	Ripple cross-laminated heterolithic sandstone–mudstone	Sfr	Sfc	CU	Sundown 3 C1
Poole Sandstone	FA4	Medium to fine sandstone	Sm	Gs, Sff?	FU	Mt Anderson C7–C8; Dampier Downs 1 C14 and C17 (and C16?); Frome Rocks 2 C3; Mt Anderson C12?–C13
	FA5	Heterolithic sandstone–mudstone with minor conglomerate	Sff, Hw	Sfv, Sfh, Gm	FU	The Sisters 1 C2; Mt Anderson 1 C14?–C15?; Scarpia 1 C1
	FA6	Heterolithic sandstone–mudstone with hummocky–swaley cross-stratification and mudstone	Sfs, Sfm	Hl	FU	Frome Rocks 2 C4; Mt Anderson C15?
	FA7	Skeletal rudstone–grainstone and mudstone	Lgs, Mh			Perindi 1 C1; Dampier Downs 1 C19; Roebuck Bay 1 C23–C24
Noonkanbah Formation	FA8	Heterolithic sandstone–mudstone	Hh	Mh	FU	The Sisters 1 C1; Frome Rocks 2 C2; Dampier Downs 1 C15 and C18
	FA9	Bioturbated, heterolithic sandstone–mudstone	Hb, Hm	Sfb, Sff	FU	Frome Rocks 2 C1; Roebuck Bay 1 C19–C20; Mt Anderson C6?; Roebuck Bay 1 C22. Sisters 1 C2

MCD118d 25/02/15

This report assesses the potential of Carboniferous–Permian formations (Grant Group and Poole Sandstone) in the northwestern Fitzroy Trough, onshore Canning Basin for CO_2 sequestration. Three major sequestration sites have been identified within 200 km of James Price Point, following examination of broadly distributed open-file data to identify suitable traps with porous and permeable reservoir, thick seals, and likely sealing faults. Sedimentological analysis indicates that the sandstone-dominated Grant Group has good reservoir quality and a thick intraformational seal in the Fitzroy Trough. Although sandy facies are well known in the Poole Sandstone outcrop to the southeast, and the overlying Noonkanbah Formation is a good-quality seal, these facies are restricted in the study area and overall reservoir quality is lowered by dominance of heterolithic, fluvial to shallow-marine facies.

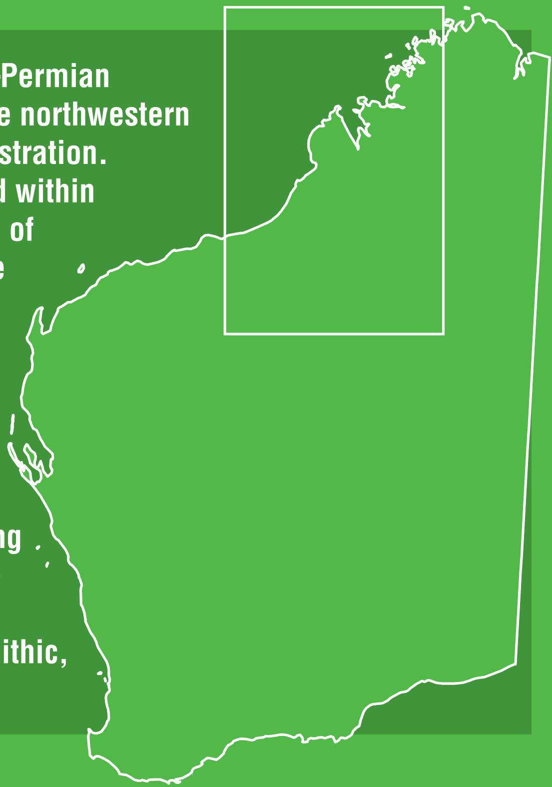

Further details of geological products and maps produced by the Geological Survey of Western Australia are available from:

Information Centre
Department of Mines and Petroleum
100 Plain Street
EAST PERTH WA 6004
Phone: (08) 9222 3459   Fax: (08) 9222 3444

www.dmp.wa.gov.au/GSWApublications